**Vysoké učení technické v Brně**

**Fakulta stavební**

**Ústav kovových a dřevěných konstrukcí**

Veveří 331/95, 602 00 Brno
TEL/FAX: +420 549 245 212
E-mail: kdk@fce.vutbr.cz

# VERIFIKACE NUMERICKÉHO MODELU I-PROFILU V IDEA STATICA STEEL

**Objednatel:**
IDEA Statica s.r.o.
Šumavská 519/35, 602 00 Brno-střed

**Řešitelé:**
Ing. Ondřej Pešek, Ph.D.
Ing. Ivan Balázs, Ph.D.
Ing. Martin Horáček, Ph.D.

**Číslo zakázky:**
SR122257017
SR122257092

**Brno, říjen 2022**

# VERIFICATION OF NUMERICAL MODEL OF I-BEAM IN IDEA STATICA STEEL

WRITTEN BY:

Ing. Ondřej Pešek, Ph.D.
Ing. Ivan Balázs, Ph.D.
Ing. Martin Horáček, Ph.D.

Institute of Metal and Timber Structures
Faculty of Civil Engineering
Brno University of Technology

**Brno, October 2022**

## CONTENT

# 1. Introduction

Object of the final report is verification of resistance of steel members of double symmetrical cross-sections subjected to transverse compression which may arise e.g. due to effect of connection of adjacent transverse members or transverse loads applied on the member. Typical examples of members (columns) subjected to transverse compression are in Fig. 1.

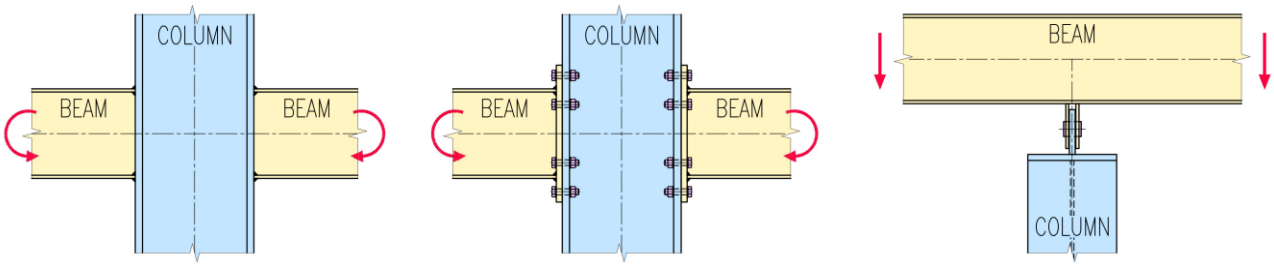


*Fig. 1 Columns subjected to transverse compression*

Members in transverse compression may exhibit several possible failure modes including yielding, buckling or crippling of the web or column-sway buckling. The latter one should normally be constructively prevented and is not a subject of this investigation. Failure modes are in Fig. 2.

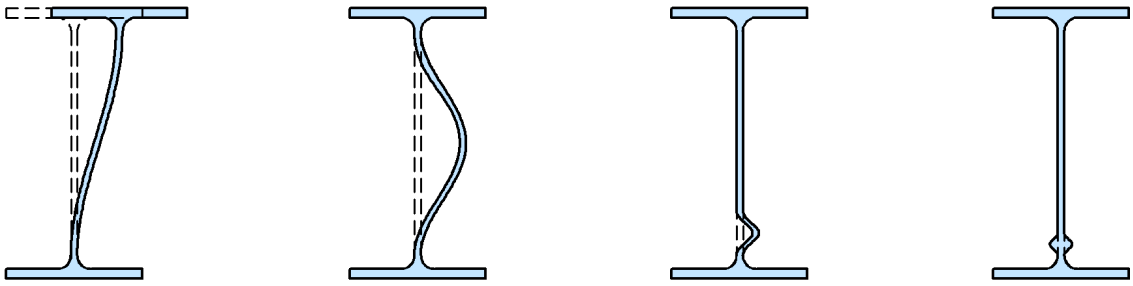

(a) (b) (c) (d)

*Fig. 2 Failure modes of members in transverse compression: (a) column-sway buckling, (b) buckling, (c) crippling and (d) yielding of the member web*

The verification is performed using numerical analysis based on finite element models. The models represented series of members of rolled or welded cross-sections usually used in steel structures. For rolled members, primarily IPE cross-sections were used, for broadening in some cases also HEA, HEB and American W cross-sections were used to cover wider range of web slenderness and geometric properties.

# 2. Methodology

## 2.1. Assumptions

### 2.1.1. Material model

Nonlinear material model (elastic-plastic with linear strain hardening) was used within the numerical analysis. Young's modulus of the elastic part of $\sigma$-$\varepsilon$ diagram was 210 GPa, in plastic part of the $\sigma$-$\varepsilon$ diagram the modulus was considered to be 210 MPa (1000 times lower).

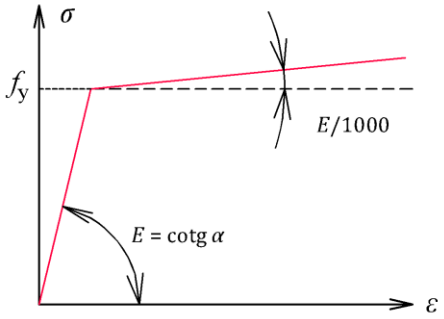


*Fig. 3 Material model*

### 2.1.2. Initial geometrical imperfections

In compliance with EN 1993-1-5 [2], initial local equivalent geometric imperfection in the shape of the first relevant buckling mode was used for the web of investigated members with magnitude $e_0$ being $d_w/200$ where $d_w$ was depth of the member web without rounded corners of rolled cross-sections or fillet welds of the welded cross-sections. The shape of the initial geometric imperfection is in Fig. 4.

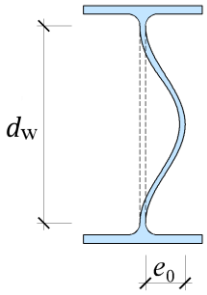


*Fig. 4 Initial geometrical imperfection*

## 2.2. Numerical solution in IDEA StatiCa Steel

The analysis of transverse compression resistance of steel members of open double-symmetrical cross-sections was performed in the Member module in IDEA StatiCa Steel software [7]. The cross-sections were selected from the library of profiles included in the software (welded cross-sections were specified by their dimensions using tools in the Cross-Section Navigator). To introduce transverse compression to the web of the analysed member, adjacent transverse member(s) was (were) added and interaction with the analysed member was achieved using mutual connection whose parameters were set in the Connection module of IDEA StatiCa Steel.

Investigated cases:

- transverse load applied at both flanges
- transverse load applied at one flange
- transverse load applied at both flanges through bolted end-plates
- transverse load applied close to the free end of the member
- combination of transverse load and axial load in the analysed member

### 2.2.1. General properties of numerical models

General calculation settings which were identical for all investigated cases are listed below. In general, default settings of the program related to the analysis and finite element mesh was retained for most of parameters.

- limit plastic strain 5%
- number of elements on biggest member web or flange: 16 (it does not necessary mean that it was in all cases related to the analysed member as adjacent members might have had bigger web or flanges, respectively)
- minimal size of element: 10 mm
- maximal size of element: 50 mm

Boundary conditions differed depending on which parameter or what geometry of the member was being investigated (detailed description is below). The assessment was performed for the analysed member (AM1, orange colour in the figures). On its both ends related members (RM) were attached. When investigating the influence of the transverse load applied close to the free end of the analysed member, related member was attached at one end of the analysed member only. Other related members represented transverse structural elements introducing transverse compression in the web of the analysed member.

Strength class of steel S355 was assigned to all members. The material was taken from the material library of the software.

### 2.2.2. Boundary conditions and loads

**Transverse load applied at both flanges of the analysed member**

The transverse load was assigned to the transverse related member and applied through a short plate attached to the end plate of one of the transverse related members (RM2). The thickness of the plate was identical with the thickness of the flange of the analysed member. Related members RM4 and RM5 were supported at their ends with boundary conditions preventing all the degrees of freedom except vertical displacement. Boundary conditions at RM3 prevented all degrees of freedom, at RM2 vertical displacement was not prevented. Suitable cross-sections from the library were assigned to the transverse related members.

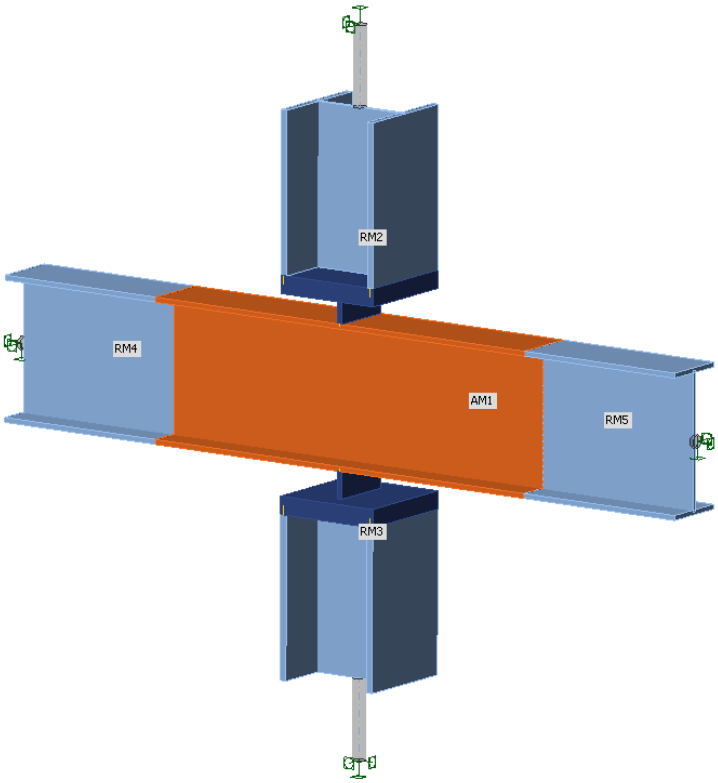


*Fig. 5 Concentrated transverse load applied at both flanges*

**Transverse load applied at one flange of the analysed member**

The transverse load was assigned to the transverse related member and applied through a short plate attached to the end plate of the transverse related member of suitable cross-section. To ensure that only effect of the transverse force applies and no effects of bending moment in the investigated web of the analysed member occurs, at the ends of the related members RM4 and RM5 balancing moments were assigned. The thickness of the plate was identical with the thickness of the flange of the analysed member. Vertical displacement of the ends of the related members RM4 and RM5 was prevented while rotation about horizontal axis was allowed. Vertical displacement of the transverse related member RM2 was not prevented.

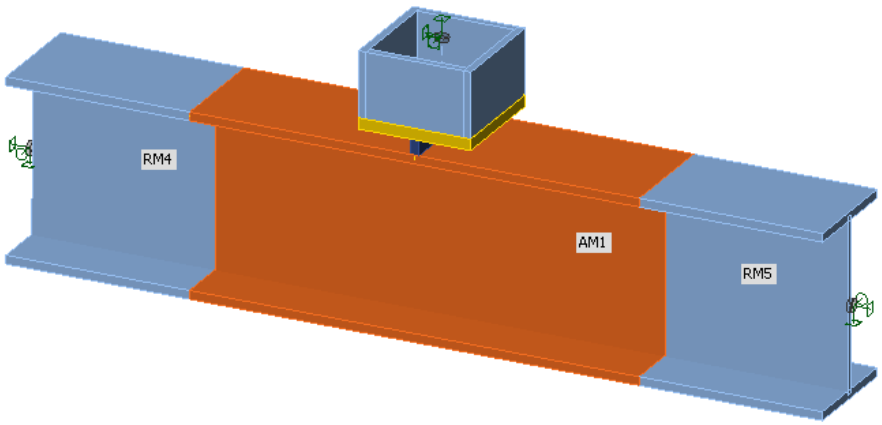


*Fig. 6 Concentrated transverse load applied at one flange*

**Transverse load applied at both flanges of the analysed member through bolted end-plates**

The transverse load was applied through one of the bolted end-plates that were attached at both flanges of the analysed member. The thickness of the transverse plates were identical with the thickness of the flange of the analysed member. Thickness of the end-plate was in all cases specified as 1.5 times the thickness of the flange of the analysed member. Related members RM4 and RM5 were supported at their ends with boundary conditions preventing all the degrees of freedom except vertical displacement. Boundary conditions at RM3 (lower end-plate) prevented all degrees of freedom, at RM2 (upper end-plate) vertical displacement was not prevented.

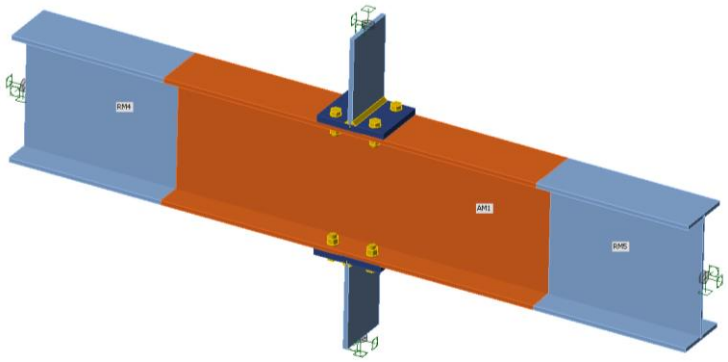


*Fig. 7 Concentrated transverse load applied through bolted end-plates*

**Transverse load applied close to the end of the analysed member**

To investigate the effect of the transverse load applied close to the free end of the analysed member, four positions of the transverse load related to the end of the analysed member were considered and numerically assessed: transverse load in the distances from the end 0.1×*h*, 0.3×*h*, 0.5×*h* and 1×*h* where *h* was the depth of the analysed member.

There was related member RM2 attached to the analysed member with boundary conditions at its end allowing only vertical displacement. The load was applied through transverse related member RM4. Boundary conditions at RM3 prevented all degrees of freedom, at RM2 vertical displacement was not prevented.

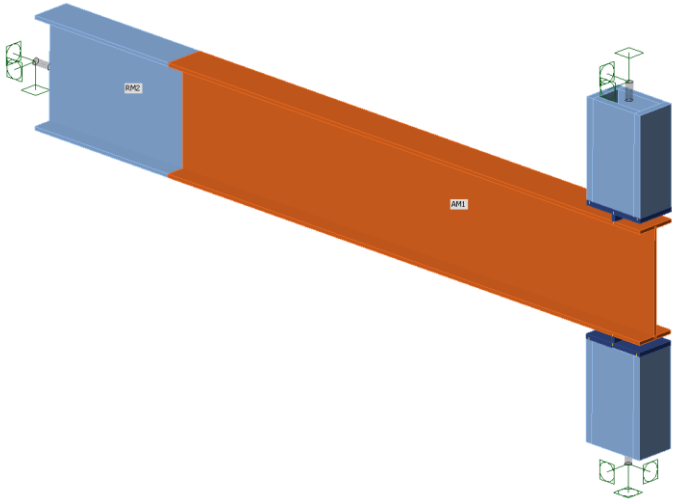


*Fig. 8 Concentrated transverse load applied close to the end of the analysed member*

### 2.2.3. Analysis

Three phases of the analysis were performed:

1. ***Materially nonlinear analysis (MNA)***
   - percentage expression of the applied load was obtained as a result of the analysis and used to determine the resistance given as the load necessary to reach 5% of plastic strain in the web of the analysed member
   - geometrical imperfections not considered
   - results comparable with yielding resistance $F_{c,wc,Rd}$ in terms of EN 1993-1-8

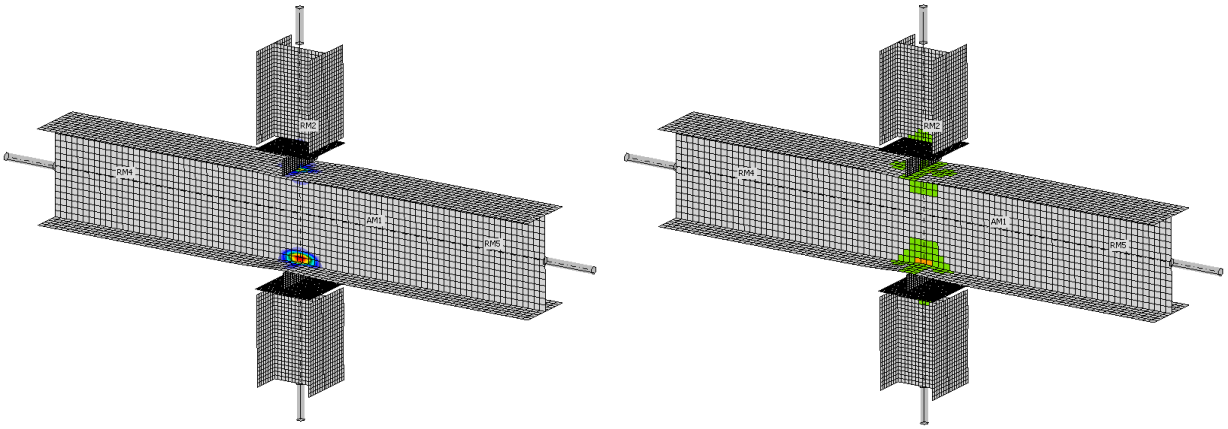

*Fig. 9 Example of results of MNA: Plastic strain and highlighting of critical regions*

2. ***Linear buckling analysis***
   - buckling modes and load amplifiers obtained as results of the analysis

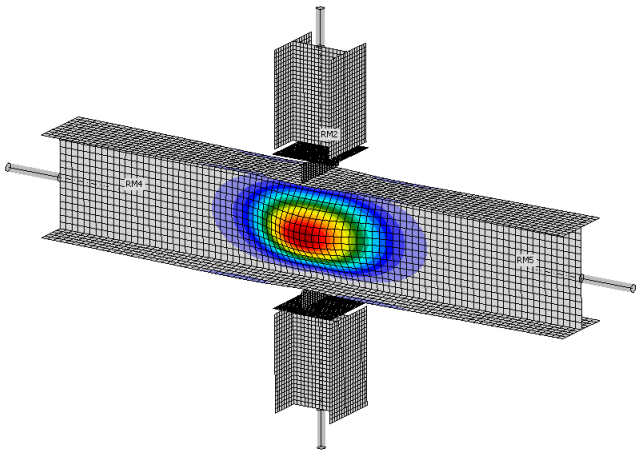

*Fig. 10 Example of results of LBA: buckling mode*

3. ***Geometrically and materially nonlinear analysis with imperfections (GMNIA)***
   - the geometry of the member was modified according to the buckling mode relevant for the local buckling of the web of the related member
   - imperfection amplitude specified as $d_w/200$ where $d_w$ was the depth of the web of the analysed member (without rounded corners of rolled cross-sections of fillet welds of the welded cross-sections, respectively)

- percentage expression of the applied load was obtained and used to determine the resistance given as the load necessary to reach 5% of plastic strain in the web of the analysed member
- results comparable with buckling resistance $F_{c,wc,Rd}$ in terms of EN 1993-1-8

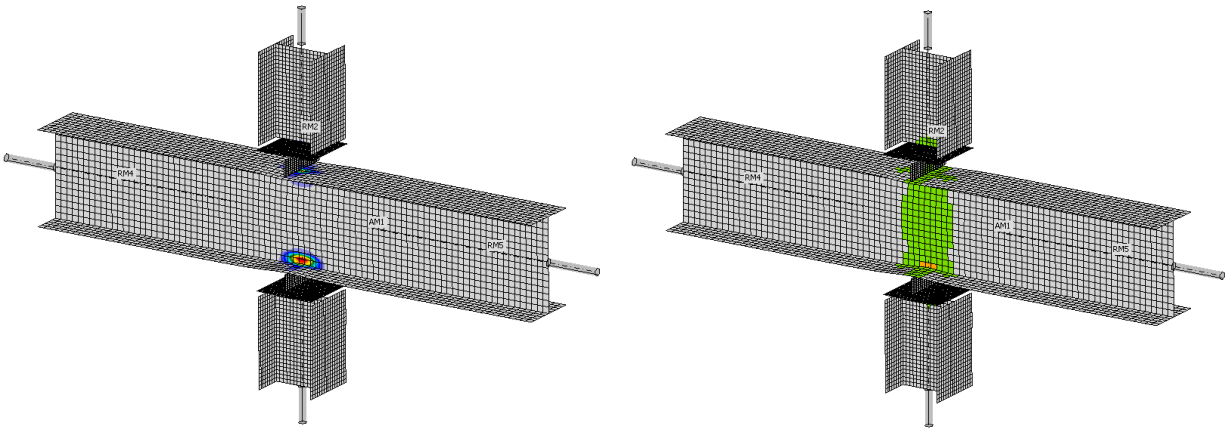

*Fig. 11 Example of results of GMNIA: Plastic strain and highlighting of critical regions*

## 2.3. Numerical solution in ANSYS Workbench

ANSYS Workbench [8] is software which allows to perform numerical simulations of structures using finite element method.

### 2.3.1. General properties of numerical models

The goal was to create all the models in the same way to obtain reasonable results comparison. In next subchapters the basic numerical models set-up is described, but in specific cases there are differences in mesh or boundary conditions or geometry.

**Geometry**

In general case the beam length is 4 times higher than cross section height. Cross section of the beam is hot rolled (European IPE, HEA/HEB or American W) or welded – in each case of double symmetrical cross section. "Loading plates" have the same thickness and width as thickness and width of beam flanges. The basic geometry is shown in Fig. 12.

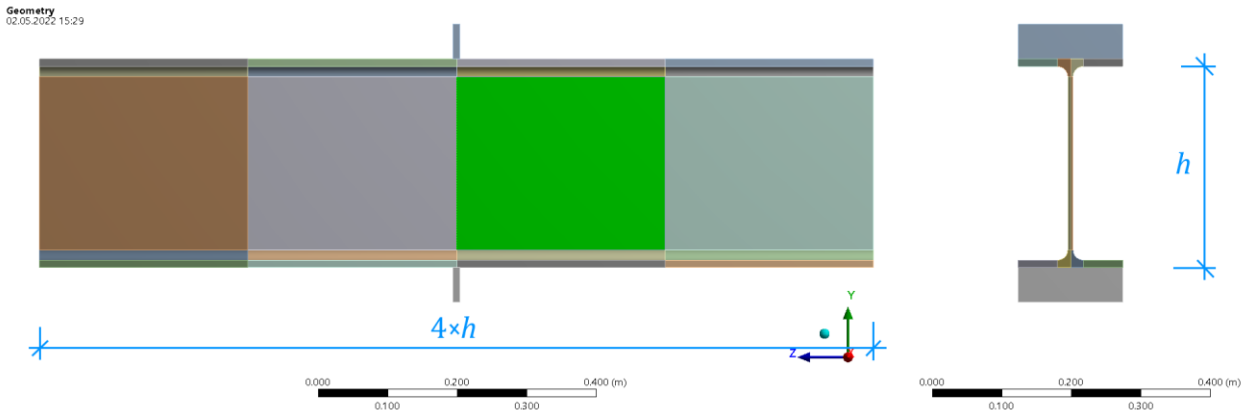


*Fig. 12 Basic case – geometry*

**Mesh**

Finite element mesh was performed in the same way at all models. In longitudinal direction the area between "loading" plates were meshed with smaller elements than in outer area (length of elements is 1/50 or 1/10 of beam height in inner or outer area respectively). Beam web and flanges are divided into 4 elements through thickness. Flanges are divided into 8 elements along them and beam web is divided into 32 elements along web height. Meshed model is shown in Fig. 13.

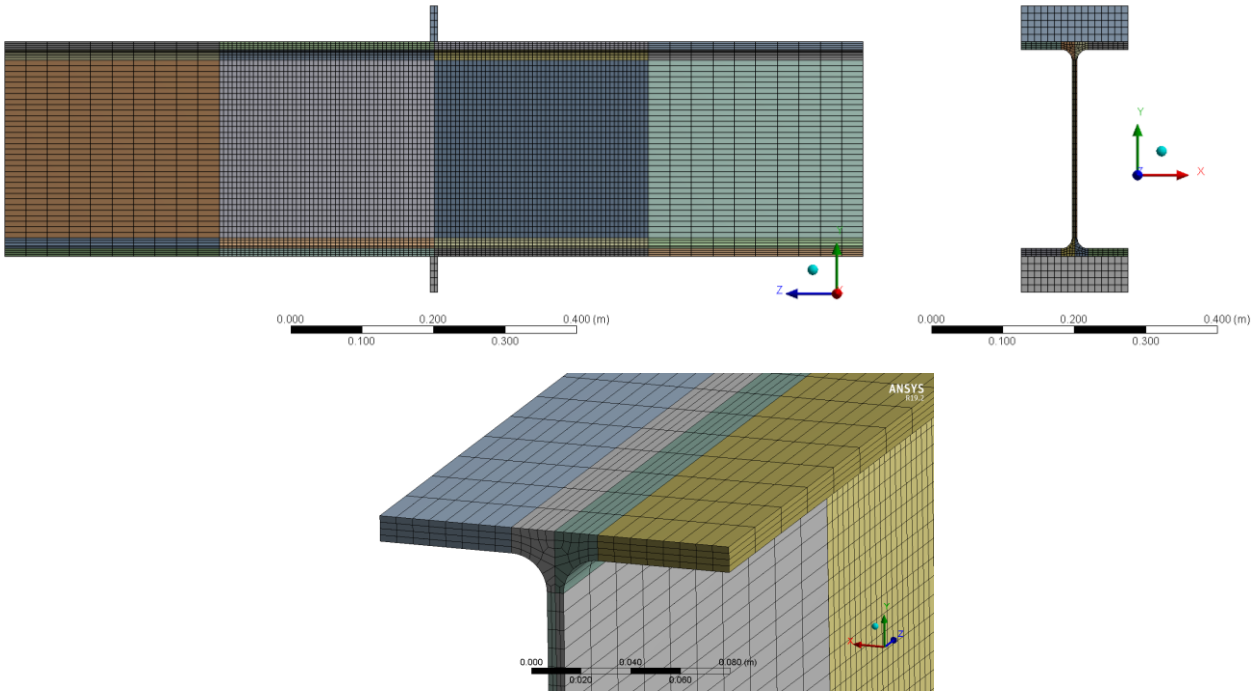


*Fig. 13 Basic case – finite element meshing*

**Boundary conditions**

The boundary conditions were set to respect actual behaviour of modelled member. Both "loading" plates were supported in lateral direction, the upper "loading" plate was supported against vertical movements, on the upper "loading" plate the load (force or displacement) was applied. The ends of beam were generally supported in longitudinal direction (but not in some specific cases as described further).

### 2.3.2. Type of analysis and analysis settings

Each model was analysed three times using different analysis type. The first analysis was MNA analysis (Materially Nonlinear Analysis without imperfections) which provided load-carrying capacity with consideration of influence of material nonlinearity but without consideration of influence of geometric imperfections. This load-carrying capacity is comparable to web yielding capacity according to the EN 1993-1-8. The next one analysis was LBA (Linear Buckling Analysis) which provided Eigen buckling shapes (and thus respective critical load factors $\alpha_{cr}$). LBA was performed with loads corresponding to 10% of load-carrying capacity from MNA analysis. The last analysis was GMNIA (Geometrically and Materially Nonlinear Analysis with Imperfections) that takes into account nonlinear material behaviour and initial geometric

imperfections from LBA solution. The first Eigen value shapes were taken as the imperfect initial geometry.

The analyses were performed with 20 loading substeps.

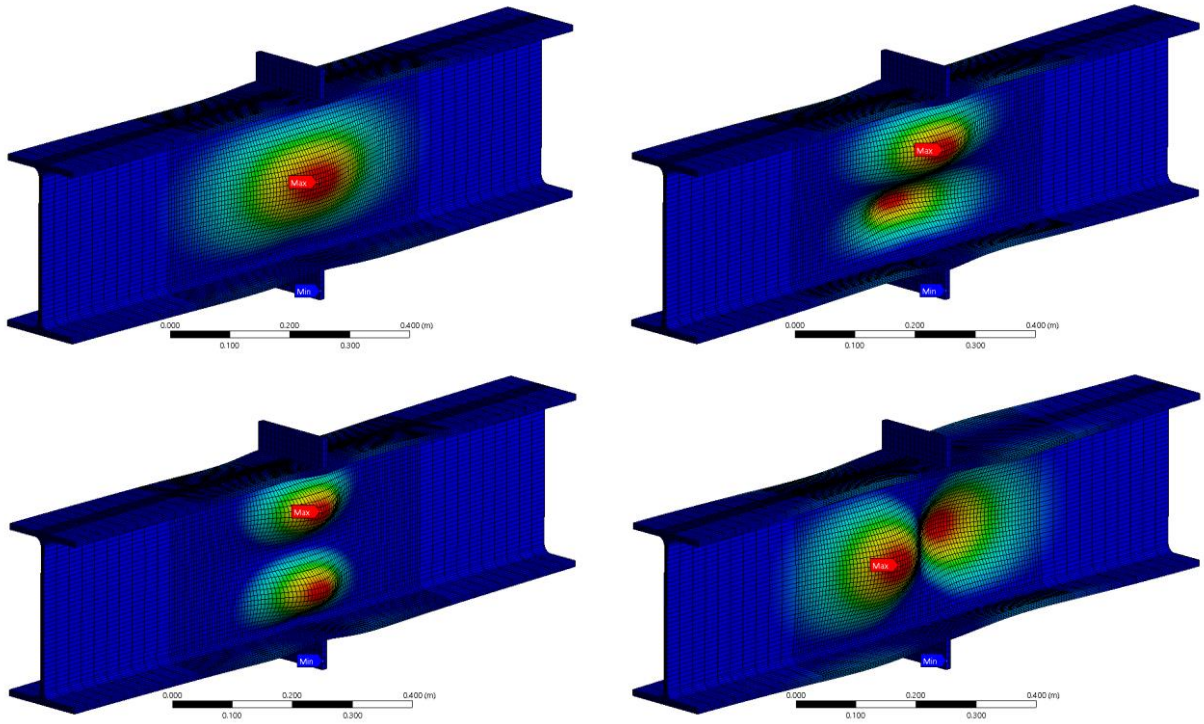


*Fig. 14 Basic case LBA – Eigen buckling shapes*

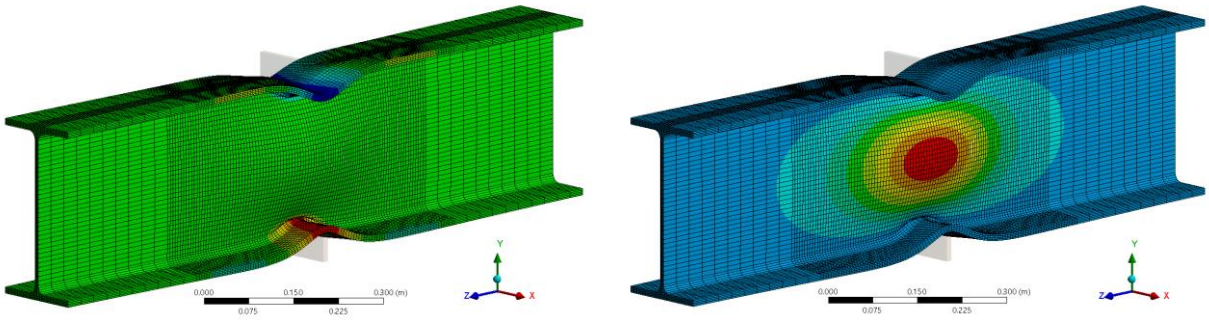


*Fig. 15 Basic case GMNIA – vertical deformation (left), lateral deformation (right)*

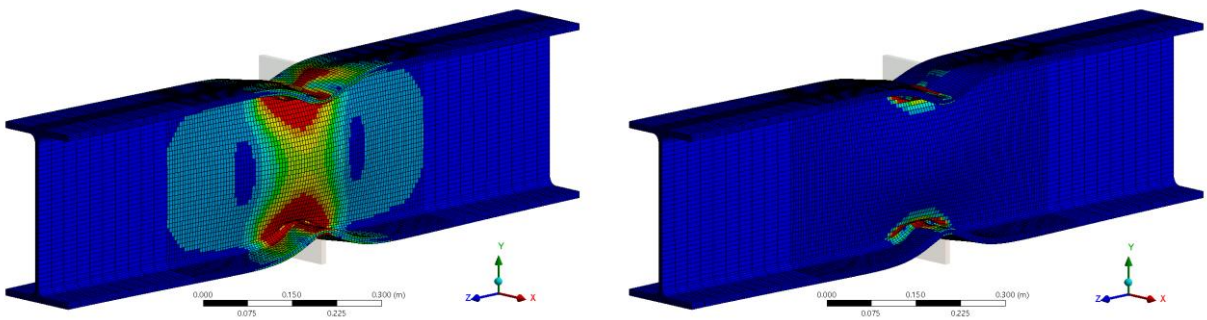


*Fig. 16 Basic case GMNIA – equivalent stress (left), plastic strain (right)*

### 2.3.3. Results evaluation

The basic results of numerical solutions taken into account are deformations (vertical and lateral), relative deformation (strain) and stresses (maximal equivalent stresses in whole beam or equivalent stress in the middle of beam web height between loading plates). According to the EN 1993-1-5 the load-carrying capacity is either the load at plastic strain equal to 5% or the maximum achieved load – the value which is achieved first (see Fig. 17).

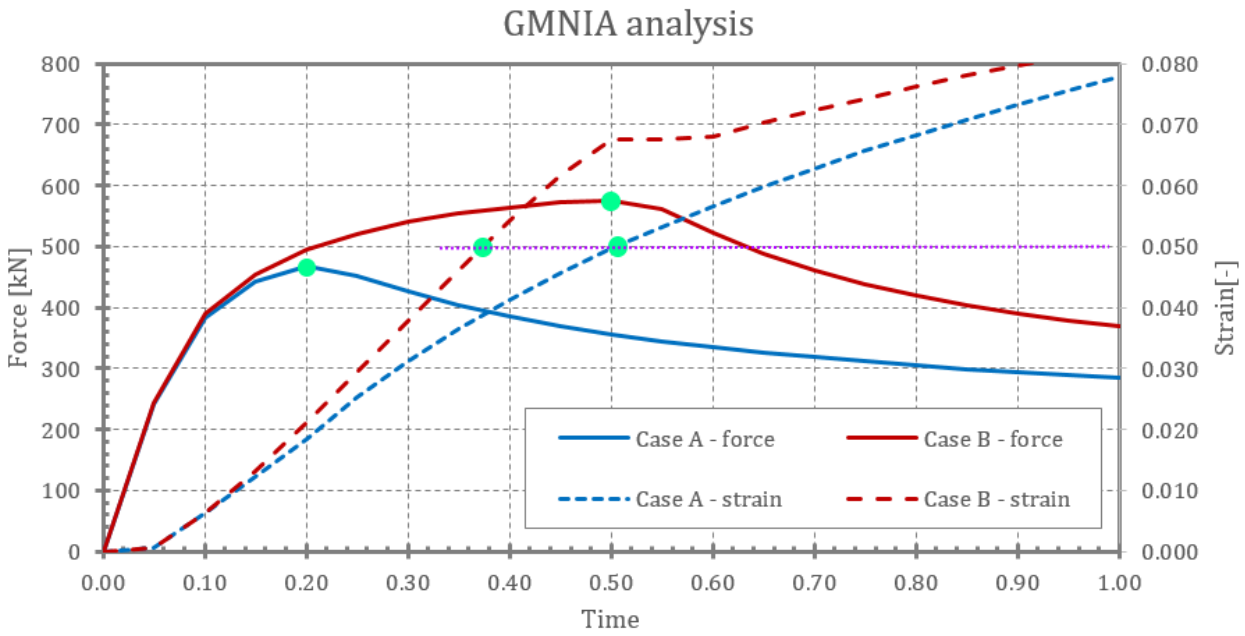


*Fig. 17 Load-carrying capacity evaluation*

## 2.4. Solution by design codes

Load-carrying capacity was calculated according to the common standards for structural steel designing – European EN 1993-1-8 [3], EN 1993-1-5 [2] and American AISC 360-16 [5].

### 2.4.1. EN 1993-1-8 (Design of joints)

In terms of the European standard for design of joints in steel structures [3], the resistance of the web in transverse compression is given as minimum of yielding or buckling resistance given by following equations (first one for yielding, second one for buckling):

$$F_{c,wc,Rd} = \frac{\omega \cdot k_{wc} \cdot b_{eff,c,wc} \cdot t_{wc} \cdot f_{y,wc}}{\gamma_{M0}} \quad (1)$$

$$F_{c,wc,Rd} = \frac{\omega \cdot k_{wc} \cdot \rho \cdot b_{eff,c,wc} \cdot t_{wc} \cdot f_{y,wc}}{\gamma_{M1}} \quad (2)$$

In these equations $f_{y,wc}$ is yield strength of the web, $t_{wc}$ is thickness of the web, $b_{eff,c,wc}$ is effective breadth (on which the transverse load is distributed to the web), $\rho$ is reduction factor for plate buckling, $k_{wc}$ is factor taking into account influence of axial load in the member, $\omega$ is factor for interaction with shear and $\gamma_{M0}$ and $\gamma_{M1}$ are partial safety factors for steel.

The effective breadth $b_{eff,c,wc}$ is defined by the standard depending on structural solution of the joint:

- welded joint: $b_{\mathrm{eff,c,wc}} = t_{\mathrm{fb}} + 2 \cdot \sqrt{2} \cdot a_{\mathrm{b}} + 5 \cdot (t_{\mathrm{fc}} + s)$
- bolted joint with end-plates: $b_{\mathrm{eff,c,wc}} = t_{\mathrm{fb}} + 2 \cdot \sqrt{2} \cdot a_{\mathrm{p}} + 5 \cdot (t_{\mathrm{fc}} + s) + s_{\mathrm{p}}$
  - for columns of rolled cross-sections (I, H): $s = r_{\mathrm{c}}$
  - for columns of welded cross-sections (I, H): $s = \sqrt{2} \cdot a_{\mathrm{c}}$
  - $s_{\mathrm{p}}$ – length obtained by distribution of stress in the end plate at angle of 45° (minimum $t_{\mathrm{p}}$ and up to $2 \cdot t_{\mathrm{p}}$ provided overlap of the end-plate below the flange is sufficient)
  - for other symbols see figures Fig. 18 and Fig. 19.

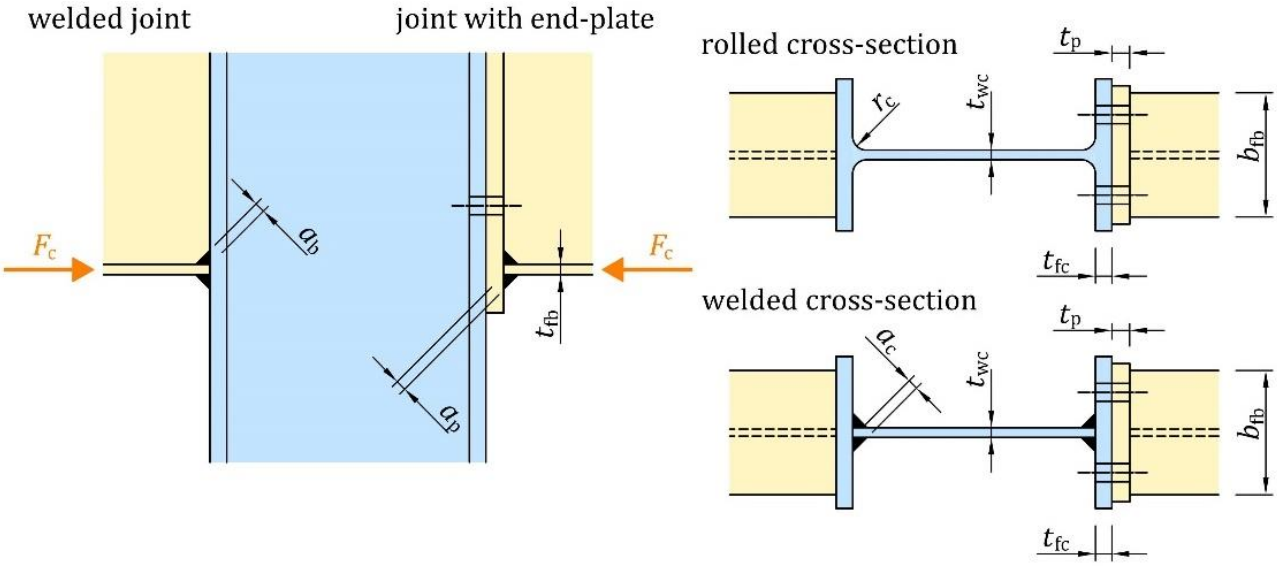


*Fig. 18 EN 1993-1-8: Transverse compression – welded joint and joint with end-plate*

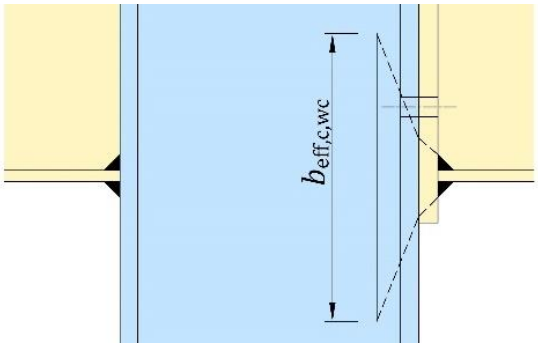


*Fig. 19 EN 1993-1-8: Effective breadth*

The reduction factor for plate buckling $\rho$ depends on the value of plate relative slenderness $\bar{\lambda}_p$:

$$\bar{\lambda}_{\mathrm{p}} = 0.932 \cdot \sqrt{\frac{b_{\mathrm{eff,c,wc}} \cdot d_{\mathrm{wc}} \cdot f_{\mathrm{y,wc}}}{E \cdot t_{\mathrm{wc}}^2}} \tag{3}$$

- if $\bar{\lambda}_{\mathrm{p}} \leq 0.72$ than $\rho = 1$
- if $\bar{\lambda}_{\mathrm{p}} > 0.72$ than $\rho = \frac{\bar{\lambda}_{\mathrm{p}} - 0.2}{\bar{\lambda}_{\mathrm{p}}^2}$
  - for columns of rolled cross-sections (I, H): $d_{\mathrm{wc}} = h_{\mathrm{c}} - 2 \cdot (t_{\mathrm{fc}} + r_{\mathrm{c}})$

- for columns of welded cross-sections (I, H): $d_{wc} = h_c - 2 \cdot \left(t_{fc} + \sqrt{2} \cdot a_c\right)$

The factor $k_{wc}$ is considered as 1.00 provided maximum compression stress $\sigma_{com,Ed}$ caused by axial load or bending moment in the member is less than $0.7 \cdot f_{y,wc}$, otherwise it is defined by the following expression:

$$k_{wc} = 1.7 - \frac{\sigma_{com,Ed}}{f_{y,wc}} \tag{4}$$

### 2.4.2. EN 1993-1-5 (Plated structural elements)

In terms of the European standard for design of plated structures [2], the resistance of the web in transverse compression is given by the following expression where $f_{yw}$ is yield strength of the web, $L_{eff}$ is effective length defined as $L_{eff} = \chi_F \times l_y$, $t_w$ is thickness of the web and $\gamma_{M1}$ is partial safety factor for steel.

$$F_{Rd} = \frac{f_{yw} \cdot L_{eff} \cdot t_w}{\gamma_{M1}} \tag{5}$$

The effective length $L_{eff}$ is calculated using reduction factor for local buckling $\chi_F$ and effective loaded length $l_y$ appropriate to the length of stiff bearing $s_s$ which is taken as the distance over which the applied load is effectively distributed at a slope of 1:1 (not larger than clear distance between flanges $h_w$).

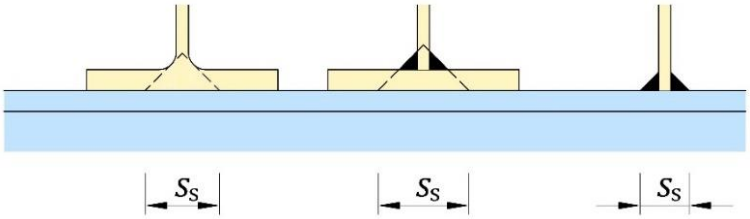


*Fig. 20 EN 1993-1-5: Length of stiff bearing*

Reduction factor for local buckling $\chi_F$ is obtained from the following formula with relative slenderness $\bar{\lambda}_f$ calculated using critical force $F_{cr}$.

$$\chi_F = \frac{0.5}{\bar{\lambda}_F} \leq 1.0 \tag{6}$$

$$\bar{\lambda}_F = \sqrt{\frac{l_y \cdot t_w \cdot f_{yw}}{F_{cr}}} \tag{7}$$

$$F_{cr} = 0.9 \cdot k_F \cdot E \cdot \frac{t_w^3}{h_w} \tag{8}$$

Factor $k_F$ (for webs without longitudinal stiffeners) should be taken from the following figure depending on type of load application.

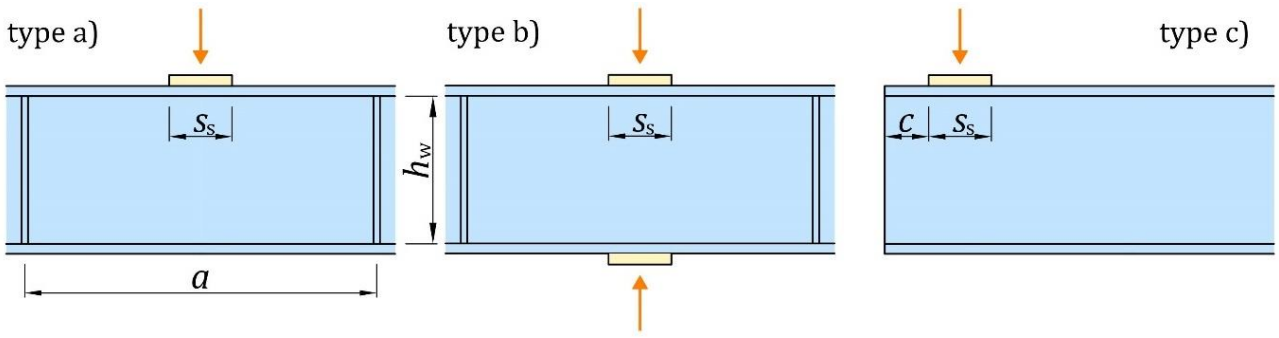


$$k_F = 6 + 2 \cdot \left( \frac{h_w}{a} \right)^2 \qquad k_F = 3.5 + 2 \cdot \left( \frac{h_w}{a} \right)^2 \qquad k_F = 2 + 6 \cdot \left( \frac{s_s + c}{h_w} \right)^2 \leq 6$$

*Fig. 21 EN 1993-1-5: Buckling coefficients*

The effective loaded length $l_y$ is calculated using factors $m_1$ and $m_2$:

$$m_1 = \frac{f_{yf} \cdot b_f}{f_{yw} \cdot t_w} \tag{9}$$

$$m_2 = 0.02 \cdot \left( \frac{h_w}{t_f} \right)^2 \quad \text{if} \quad \bar{\lambda}_F > 0.5 \tag{10}$$

$$m_2 = 0 \quad \text{if} \quad \bar{\lambda}_F \leq 0.5 \tag{11}$$

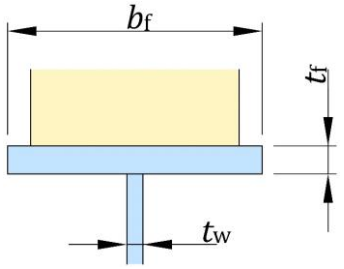


*Fig. 22 EN 1993-1-5: Dimensions of the cross-section*

Effective loaded length $l_y$ is calculated using following figure for types (a) and (b) in the figure above. It is not considered larger than distance between transversal stiffeners $a$.

$$l_y = s_s + 2 \cdot t_f \cdot \left( 1 + \sqrt{m_1 + m_2} \right) \tag{12}$$

For type (c) – load applied close to the unstiffened end through one flange, the effective loaded length is a minimum of the following values: $l_y$, $l_{y1}$ or $l_{y2}$.

$$l_{y1} = l_e + t_f \cdot \sqrt{\frac{m_1}{2} + \left( \frac{l_e}{t_f} \right)^2 + m_2} \tag{13}$$

$$l_{y2} = l_e + t_f \cdot \sqrt{m_1 + m_2} \tag{14}$$

In these expressions, value of $l_e$ should be calculated as follows:

$$l_e = \frac{k_F \cdot E \cdot t_w^2}{2 \cdot f_{yw} \cdot h_w} \leq s_s + c \tag{15}$$

### 2.4.3. EN 1993-6 (Crane supporting structures)

European standard for design of crane supporting structures [4] do not propose unique calculation procedure of resistance in transversal compression of beam. This standard refers to EN 1993-1-5 with use of different value of effective length $l_{eff}$ where the effect of crane rail may be included.

### 2.4.4. AISC 360-16 (Specification for structural steel buildings)

According to American National Standard AISC 360-16 (Specification for Structural Steel Buildings) [5], the provisions for calculation the design resistance in transverse compression due to the yielding of a web provide same results as the provisions listed in European standards. The yielding resistance is given as in equation (16) for the case when the concentrated force to be resisted is applied at a distance from the member end that is greater than the full nominal depth of the member *d*. When the concentrated force to be resisted is applied at a distance from the member end that is less than or equal to the full nominal depth of the member *d*, web local yielding resistance shall be determined by equation (17). In equations $F_{yw}$ is yield strength of steel, $t_w$ is web thickness, $l_b$ is length of bearing and *k* is distance from outer face of the flange to the web toe of the fillet.

$$\phi \cdot R_n = \phi \cdot F_{yw} \cdot t_w \cdot \left(5 \cdot k + l_b\right) \tag{16}$$

$$\phi \cdot R_n = \phi \cdot F_{yw} \cdot t_w \cdot \left(2.5 \cdot k + l_b\right) \tag{17}$$

The American standard differs in its approach to determining the design resistance in transverse compression due to the buckling of a web and crippling of a web. The web buckling resistance is given as in equation (18). In the American standard approach there is no effective loaded length considered, the geometric parameters inputs of the beam are only the web height *h* (clear distance between flanges less the fillet or corner radius for rolled shapes) and web thickness $t_w$. This equation is applicable to a pair of moment connections and to other pairs of compressive forces applied at both flanges of a member, for which $l_b/d$ is approximately less than 1, where $l_b$ is the length of bearing and *d* is the depth of the member. When $l_b/d$ is not small, the member web should be designed as a compression member in accordance with Chapter E of AISC 360-16. It should be noted that equation (18) is predicated on an interior member loading condition - the compressive force is at the distance least *c* (measured to member end) equal to half time beam depth *d* ($c \geq 0.5 \times d$). In the absence of applicable research, a 50% reduction has been introduced for cases wherein the compressive forces are close to the member end [6]. Coefficient $Q_f$ is equal to 1.0 for wide-flange sections.

$$\phi \cdot R_n = \phi \cdot \left( \frac{24 \cdot t_w^3 \cdot \sqrt{E \cdot F_{yw}}}{h} \right) \cdot Q_f \tag{18}$$

Web crippling resistance is given in equation (19) when the concentrated compressive force to be resisted is applied at a distance from the member end that is greater than or equal to $d/2$. In other case the resistance is reduced.

$$\phi \cdot R_n = \phi \cdot 0.8 \cdot t_w^2 \cdot \left[1 + 3 \cdot \left(\frac{l_b}{d}\right) \cdot \left(\frac{t_w}{t_f}\right)^{1.5}\right] \cdot \sqrt{\frac{E \cdot F_{yw} \cdot t_f}{t_w}} \cdot Q_f \quad (19)$$

AISC 360-16 provides calculations of strength in web sidesway buckling (see Fig. 2a), but when this buckling mode is forbidden in Eurocode (the structure have to be resisted against this buckling mode), web sidesway is not considered in this study.

For the LRFD design the resistance factor $\Phi$ = 1.00 should be applied to the equation (16) and (17), $\Phi$ = 0.90 to the equation (18) and $\Phi$ = 0.75 to the equation (19).

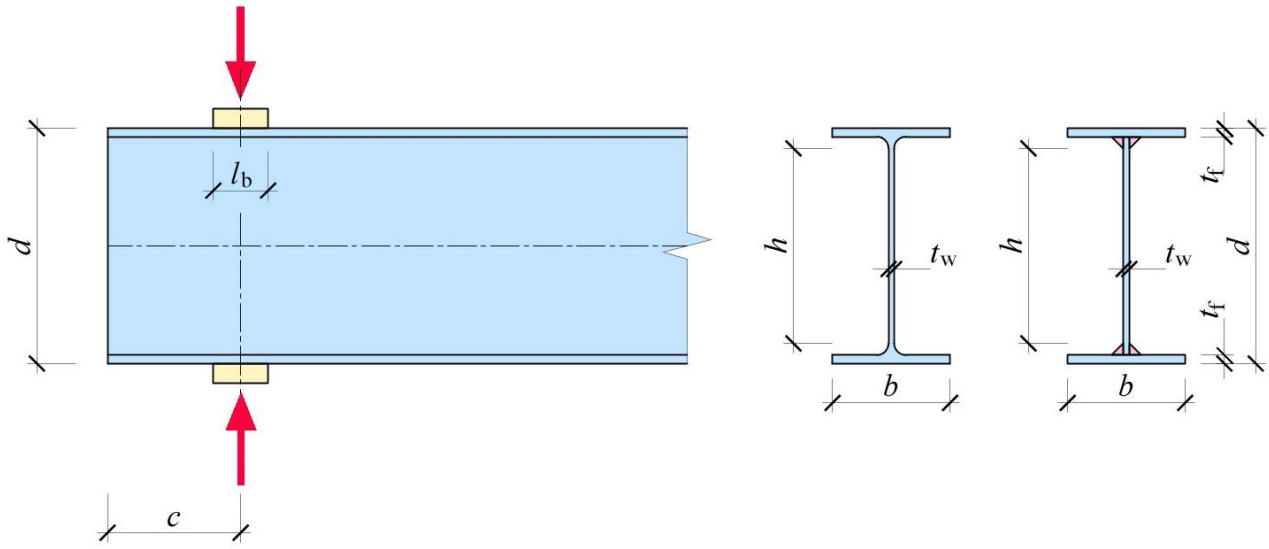


*Fig. 23 AISC 360-16: (a) loading near the end of member, (b) rolled section, (c) welded section*

# 3. Sensitivity analysis ANSYS and IDEA numerical models

ANSYS models were subjected to sensitivity analysis to ensure that they give correct results to make comparison with results of IDEA StatiCa software and codes calculations. Sensitivity analysis was carried out to determine influence of transversally loaded member length and used boundary conditions. After that influence of yield strength of used structural steel is observed, because all other simulations were performed with structural steel S355.

## 3.1. Influence of length of transversally compressed member

### 3.1.1. Methodology

In this part of study, the influence of beam length on results is observed. The goal is to determine modelled length of transversally loaded member which gives correct results and at the same time is effective from the point of view of computing time.

The study was performed on transversally loaded member of cross-section IPE 400 made of structural steel S355. The overall length of member was $L$ = 8×$h$; 6×$h$; 4×$h$; 2×$h$ and 1×$h$, where $h$ is cross section height. These six members were analysed using MNA, LBA and GMNIA. Measured parameters were deformations (vertical and lateral), equivalent stress, plastic strain, critical force and factor of critical load. Analysed member is illustrated in Fig. 24.

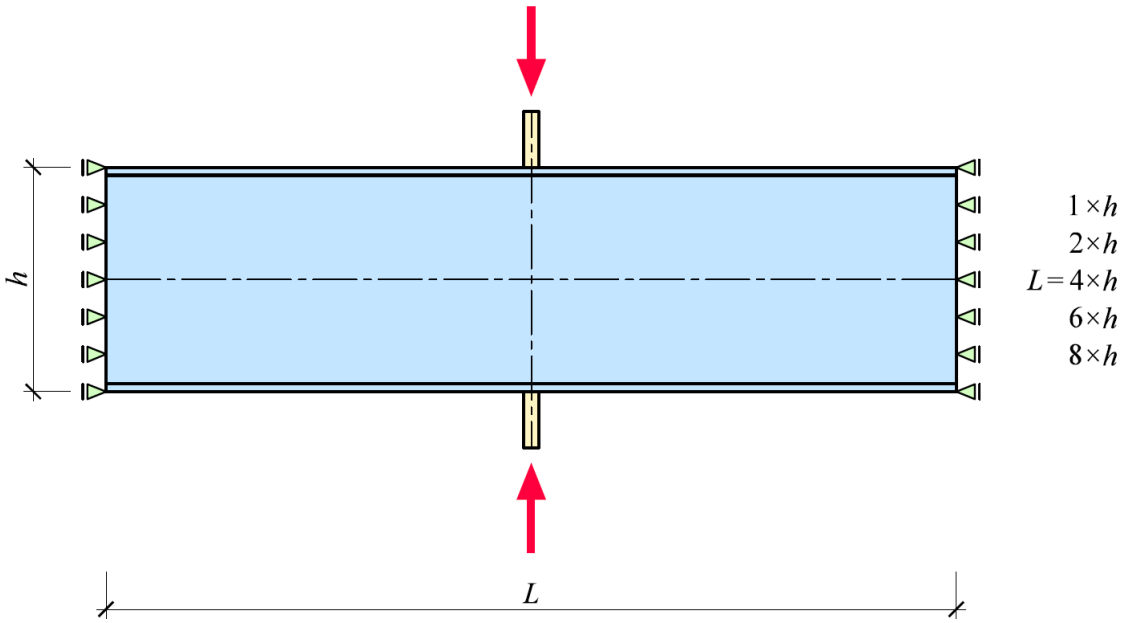


*Fig. 24 Influence of member length – geometry and boundary conditions*

### 3.1.2. Results

Calculated load-carrying capacities are listed in Tab. 1.

*Tab. 1 Influence of member length - Load-carrying capacity [kN]*

| | ANSYS | |
|---|---|---|
| | MNA | GMNIA |
| $L = 8\times H$ | 579.636 | 578.219 |
| $L = 6\times H$ | 579.534 | 578.067 |
| $L = 4\times H$ | 579.330 | 577.789 |
| $L = 2\times H$ | 578.607 | 578.226 |
| $L = 1\times H$ | 578.010 | 550.160 |

Load-carrying capacities of members with different length are plotted in Fig. 25. On the left absolute values are plotted, on the right relative values are plotted (ratio of absolute value for any member length to value of beam with length $L = 8\times h$). From chart on the right it is obvious that for $L = 1\times h$ there is 5% decrease of load-carrying capacity in compare to the $L = 8\times h$ (considering GMNIA), but for longer members the decrease is negligible.

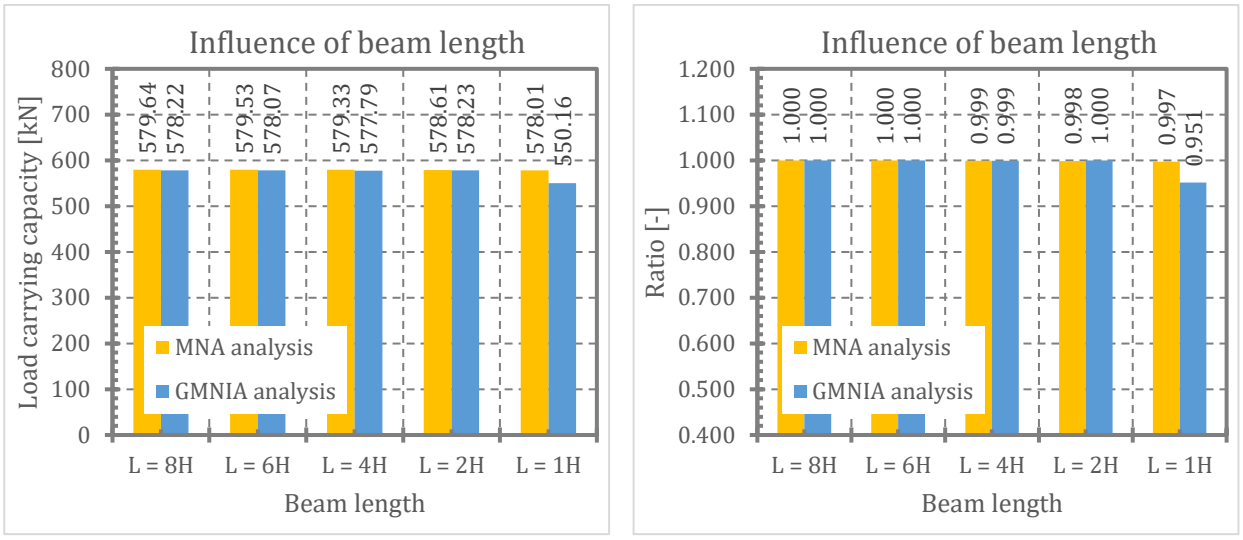


*Fig. 25 Influence of member length – load-carrying capacity*

Selected results are listed in charts in figures below. Fig. 26 shows results of linear buckling analysis – critical forces $F_{cr}$ and factors of critical force $\alpha_{cr}$. Both, $F_{cr}$ and $\alpha_{cr}$ are decreasing with member length $L$ decreasing.

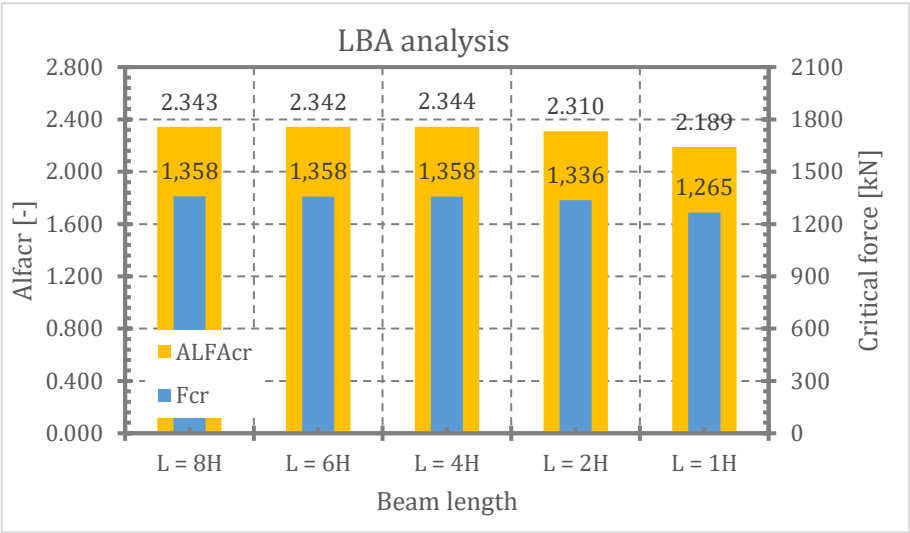


*Fig. 26 Influence of member length – LBA results*

The relationships of vertical deformations, lateral deformations, equivalent stresses and plastic strains to the lateral force are plotted in Fig. 27, Fig. 28, Fig. 29, Fig. 30 and Fig. 31. From curves valid for MNA and GMNIA it is obvious that only $L = 1 \times h$ curves are significantly deviated from reference case $L = 8 \times h$.

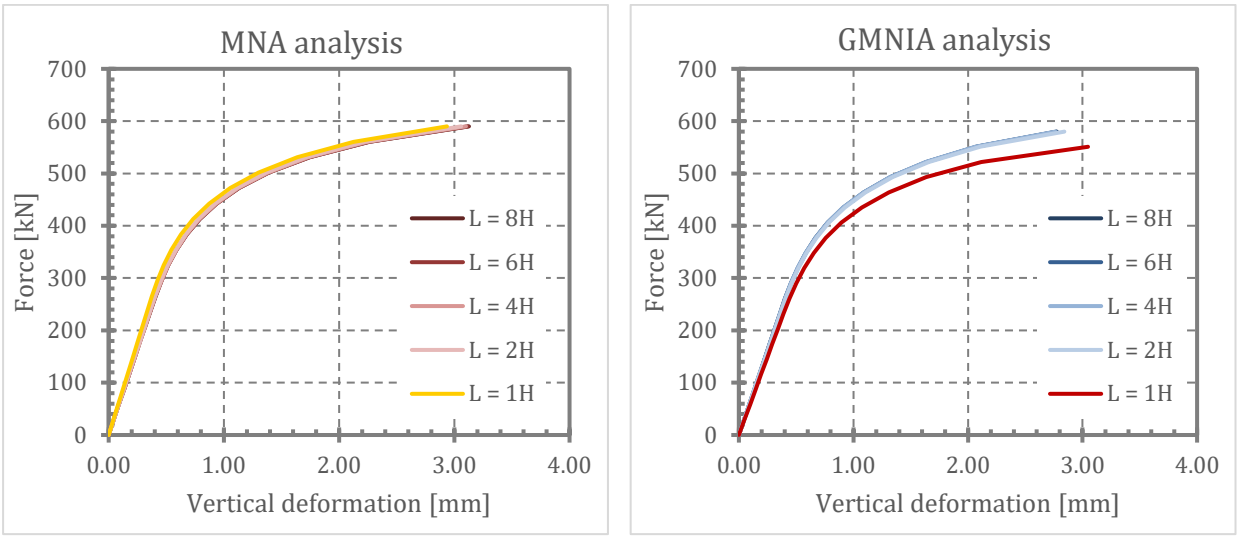


*Fig. 27 Influence of member length – vertical deformation-force relationship*

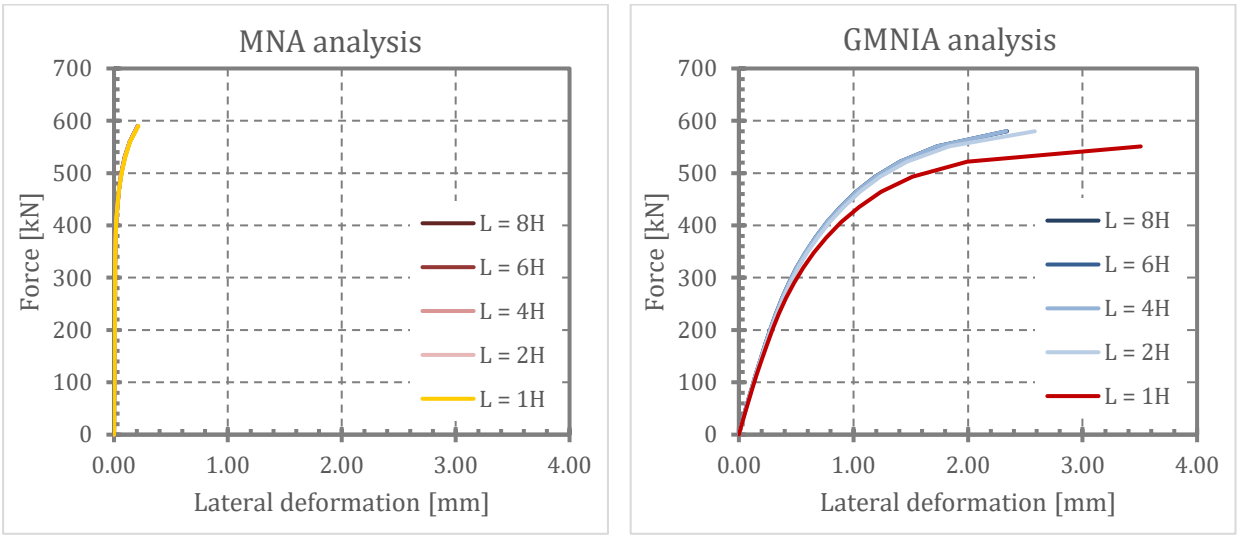


*Fig. 28 Influence of member length – lateral deformation-force relationship*

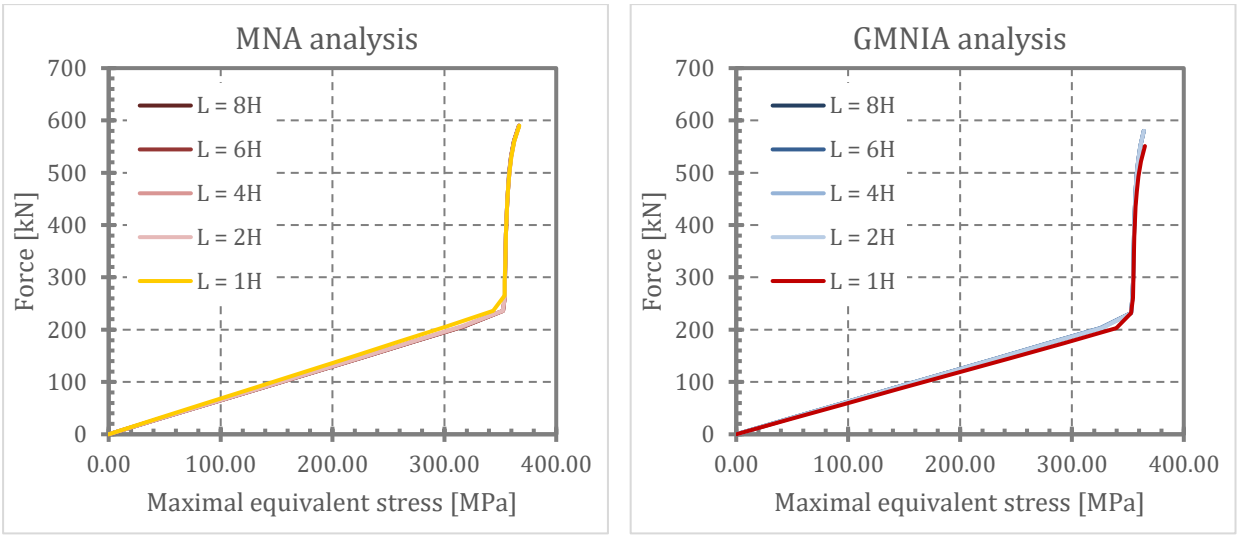


*Fig. 29 Influence of member length – maximal equivalent stress-force relationship*

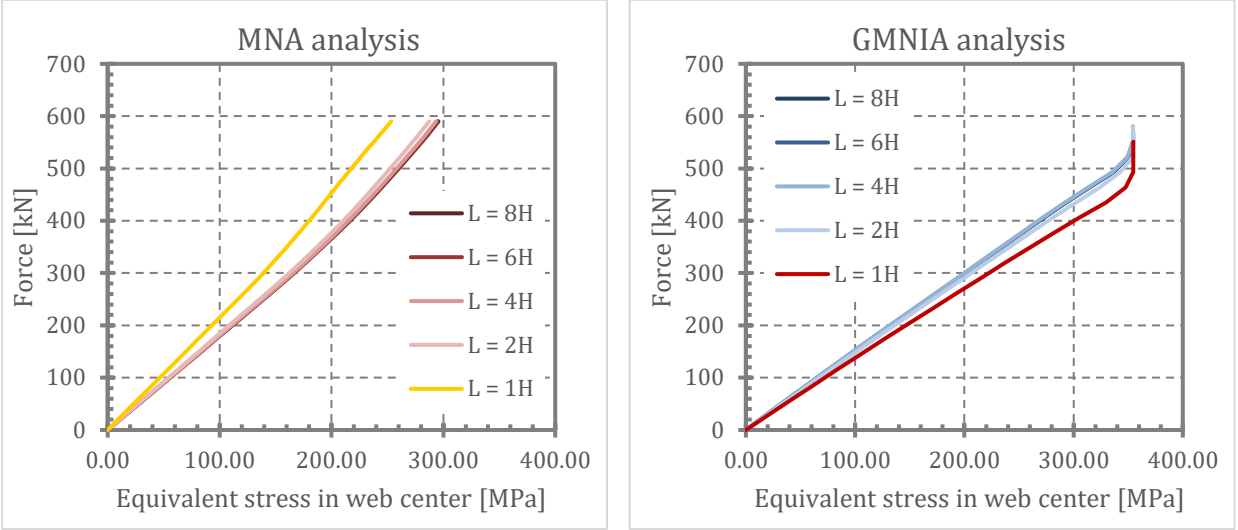


*Fig. 30 Influence of member length – equivalent stress in web center-force relationship*

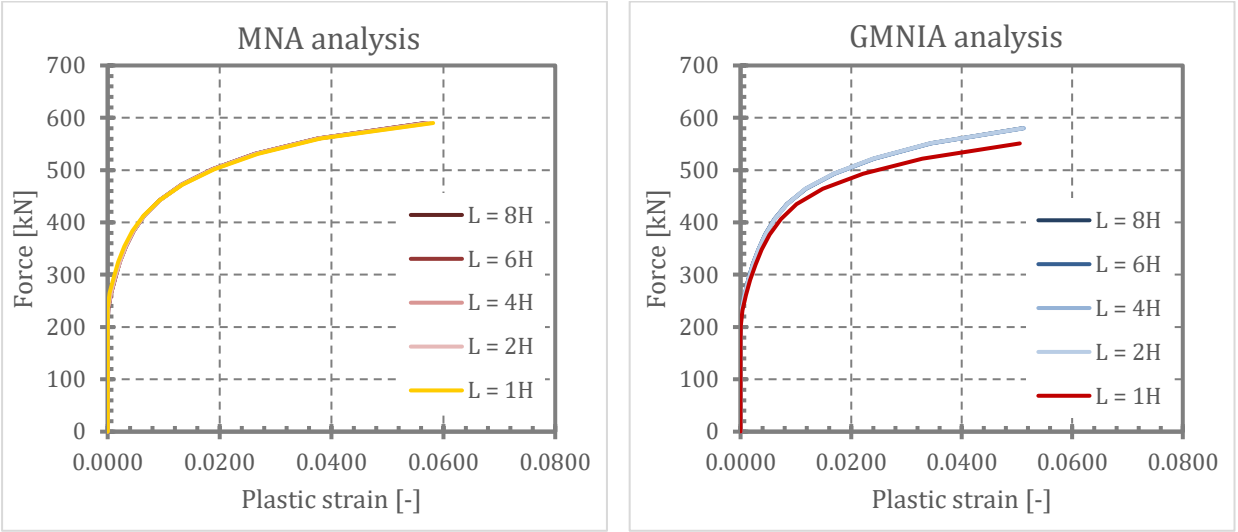


*Fig. 31 Influence of beam length – plastic strain-force relationship*

### 3.1.3. Conclusion

Presented results indicate that basically considered models of member length $L = 4 \times h$ gives correct results ad it is possible to use them on other studies (except the influence of unrestrained end).

## 3.2. Influence of boundary conditions

In this part of study, the influence of boundary conditions applied on the ends of transversally compressed member on results is observed. The goal is to verify applied boundary conditions are correct and eliminate their influence on the results.

### 3.2.1. Methodology

The study was performed on transversally loaded member of cross-section IPE 400 made of structural steel S355. The overall length of member was $L = 4 \times h$. Tested boundary conditions were: (i) beam ends restrained in longitudinal direction, (ii) beam ends unrestrained in longitudinal direction. These two transversally loaded members were analysed using MNA, LBA

and GMNIA. Measured parameters were deformations (vertical and lateral), equivalent stresses, plastic strain, critical force and factors of critical load. Analysed member is illustrated in Fig. 32.

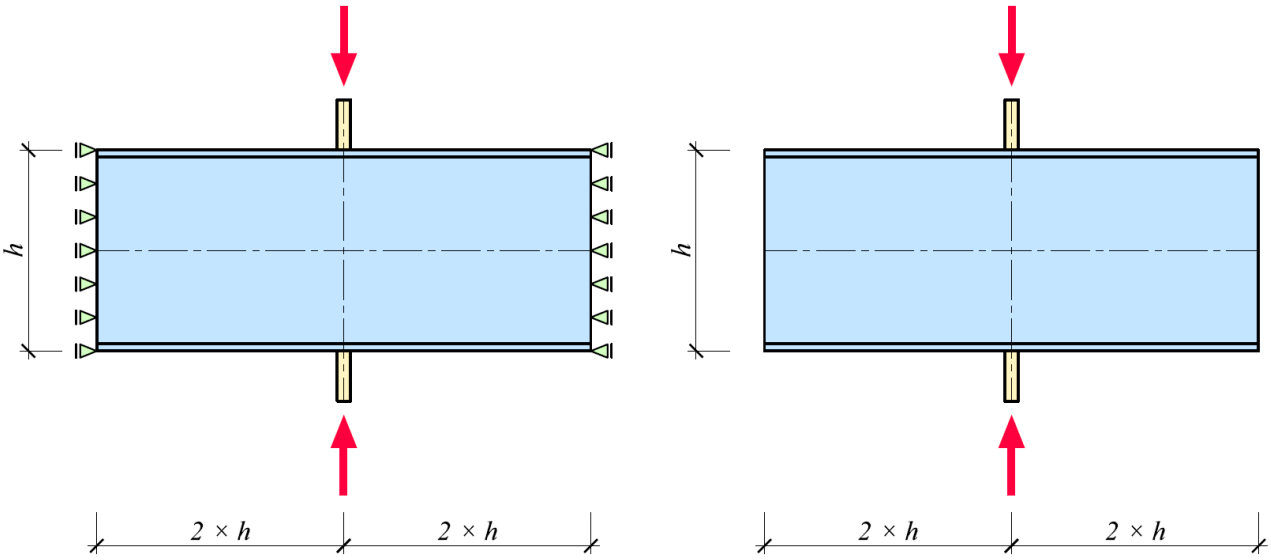


*Fig. 32 Influence of boundary conditions – geometry and boundary conditons*

### 3.2.2. Results

Calculated load-carrying capacities are listed in Tab. 2.

*Tab. 2 Influence of boundary conditions - Load-carrying capacity [kN]*

| | ANSYS | |
|---|---|---|
| | MNA | GMNIA |
| Restrained ends | 579.330 | 577.789 |
| Unrestrained ends | 579.926 | 578.648 |

Load-carrying capacities of members with different boundary conditions are plotted in Fig. 33. On the left absolute values are plotted, on the right relative values are plotted (ratio of absolute value for any boundary condition to value of beam with restrained ends). From charts it is obvious that the results are almost the same for both boundary conditions.

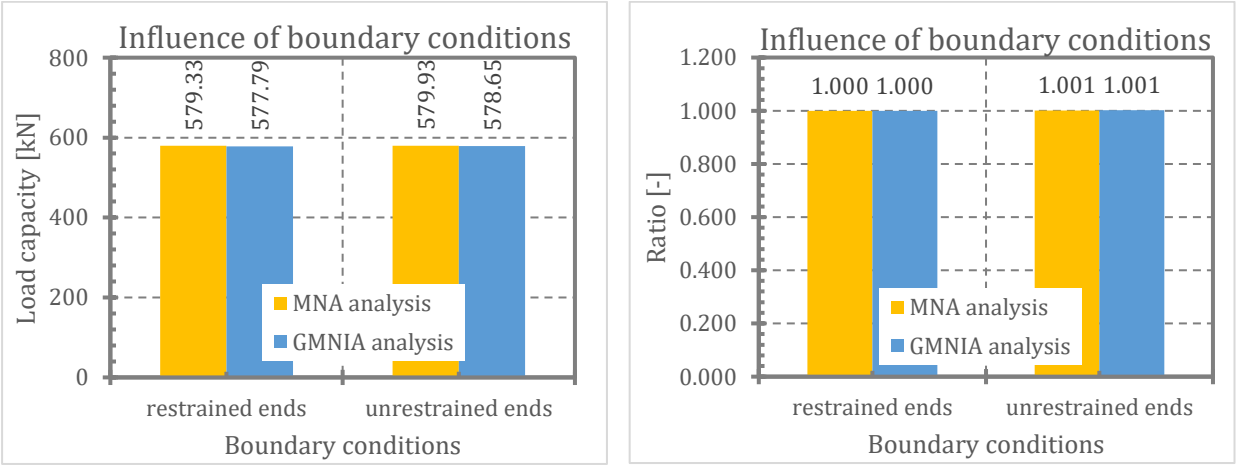


*Fig. 33 Influence of boundary condition – load-carrying capacity*

Selected results are listed in charts in figures below. Fig. 34 shows results of linear buckling analysis – critical forces $F_{cr}$ and factors of critical force $\alpha_{cr}$. Both, $F_{cr}$ and $\alpha_{cr}$ are of the same value for both boundary conditions.

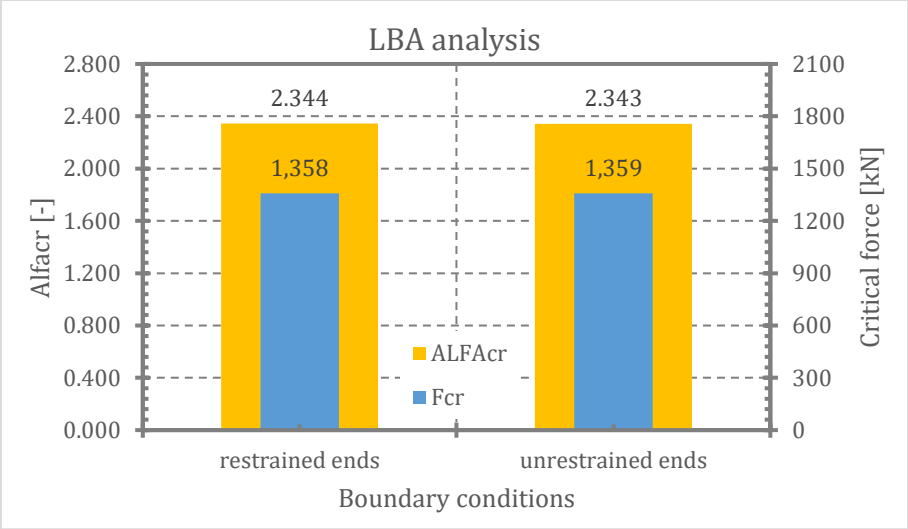


*Fig. 34 Influence of boundary condition – LBA results*

The relationships of vertical deformations, lateral deformations, equivalent stresses and plastic strains to the lateral force are plotted in Fig. 35, Fig. 27, Fig. 36, Fig. 37, Fig. 38 and Fig. 39. From curves valid for MNA and GMNIA it is obvious that different boundary conditions give the same results.

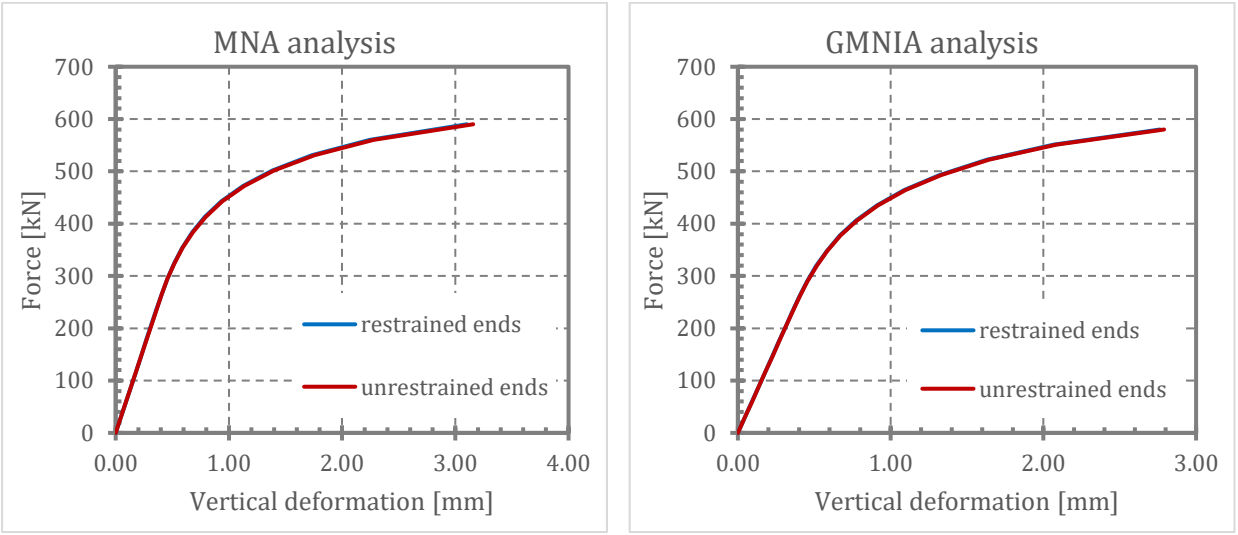


*Fig. 35 Influence of boundary condition – vertical deformation-force relationship*

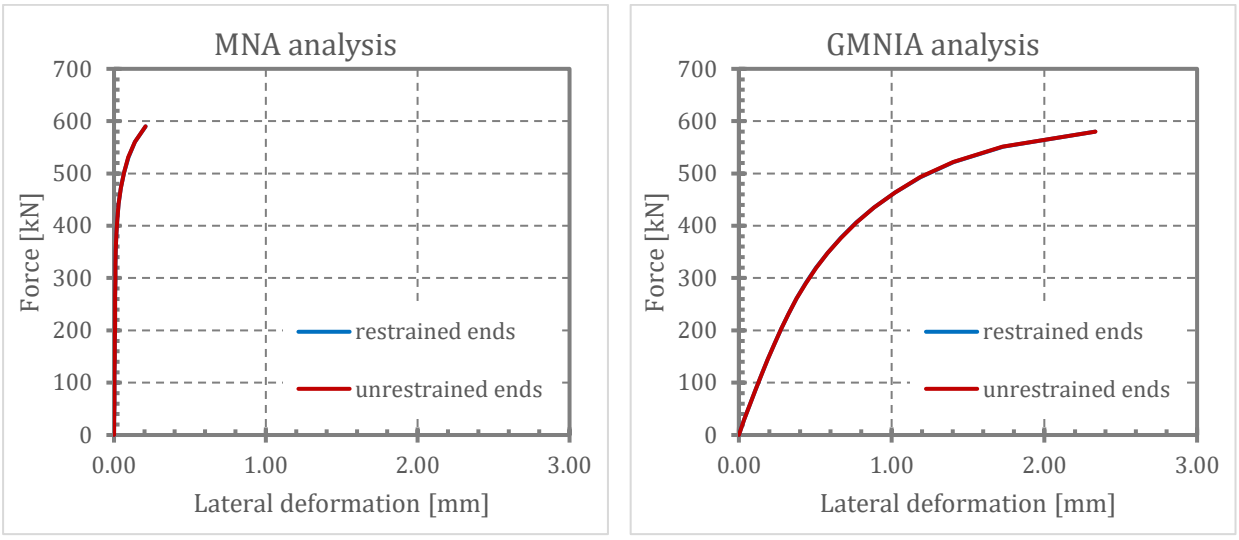


*Fig. 36 Influence of boundary condition – lateral deformation-force relationship*

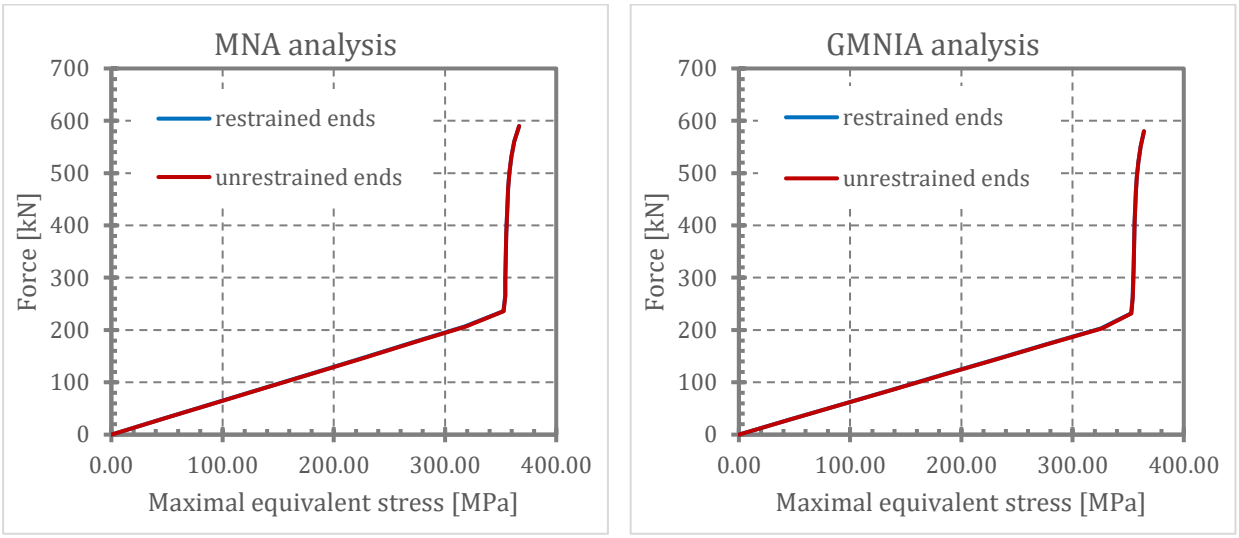


*Fig. 37 Influence of boundary condition – maximal equivalent stress-force relationship*

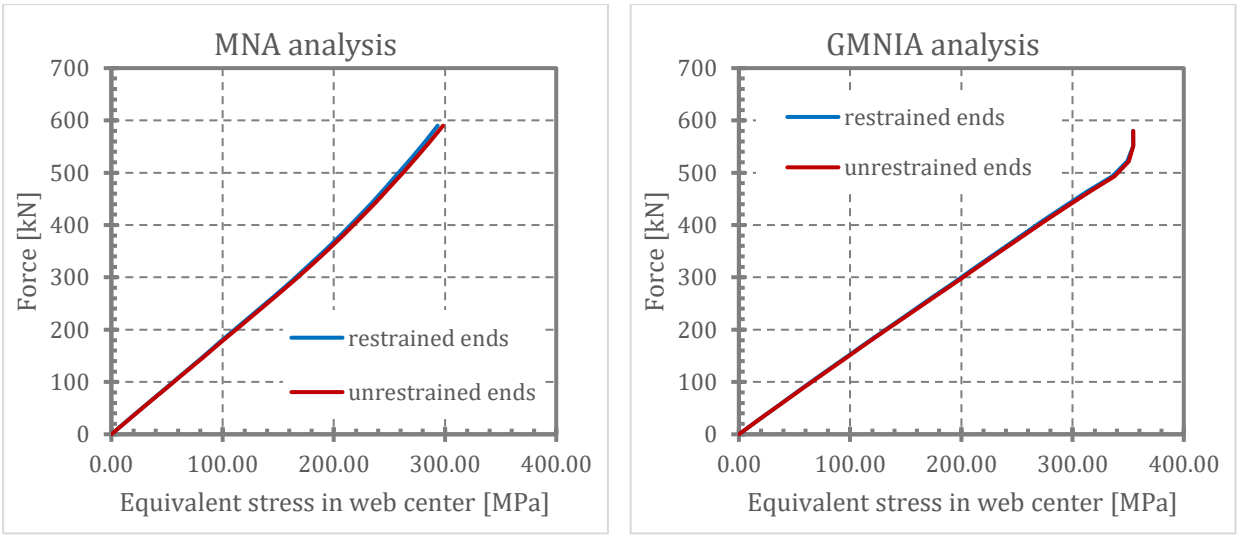


*Fig. 38 Influence of boundary condition – equivalent stress in web center-force relationship*

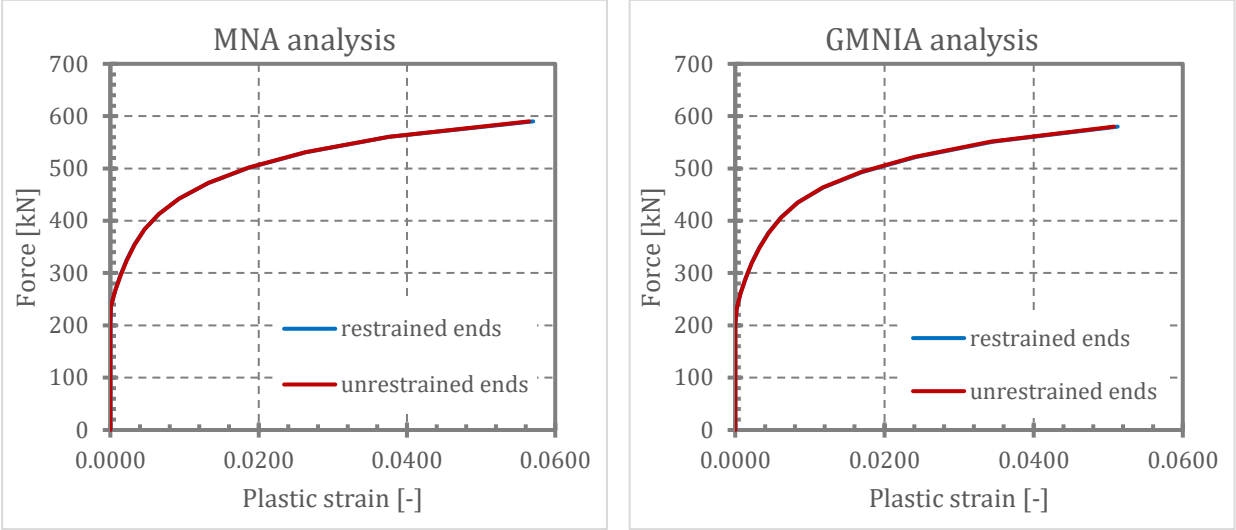


*Fig. 39 Influence of boundary condition – plastic strain-force relationship*

### 3.2.3. Conclusion

Presented results show that basically considered boundary conditions (restrained ends) give correct results and it is possible to use them on other studies (except the influence of unstiffened end).

## 3.3. Influence of finite element mesh in IDEA StatiCa

The aim of this part of study is to verify influence of finite element mesh applied on web of the transversally compressed member on results (load-carrying capacity of that member) for finite element analysis carried out in IDEA StatiCa.

### 3.3.1. Methodology

The study was performed on transversally loaded member of various cross-sections (IPE 100, 200, 300, 400, 500 and 600) with overall length of member $L = 4 \times h$. Member is made of structural steel S355. The imperfection amplitude was $d_w/200$. Finite element analysis was performed in ANSYS software and IDEA StatiCa. In IDEA StatiCa four finite element mesh were analysed (where the number of shell finite elements in vertical direction of the web of the transversally compressed member was 8, 16, 24 and 32). As reference numerical model ANSYS precise finite element model (made of 3D brick elements) was taken with member web divided into 32 finite elements in vertical direction. These transversally loaded members were analysed using MNA, LBA and GMNIA. Analysed member is illustrated in Fig. 40.

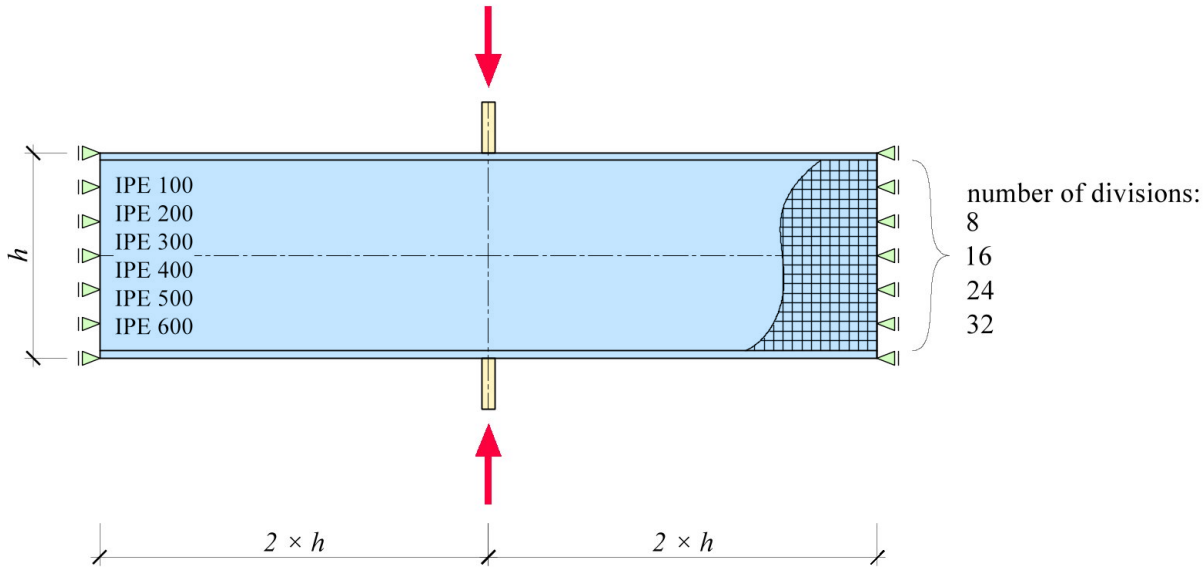


*Fig. 40 Influence of finite element mesh – geometry and boundary conditions*

### 3.3.2. Results

Load-carrying capacities resulting from numerical simulations are listed in Tab. 3. The same values are plotted in chart in Fig. 42 from which it could be concluded that IDEA StatiCa numerical models with 8 finite elements along the web give unsafe results, models with 16 elements along the web give good agreement with results of ANSYS models and IDEA models with 24 and 32 elements along the web give very low values of resistance in comparison with ANSYS.

Fig. 41 shows dependency of load-carrying capacity on number of finite element along the transversally compressed member web in IDEA StatiCa.

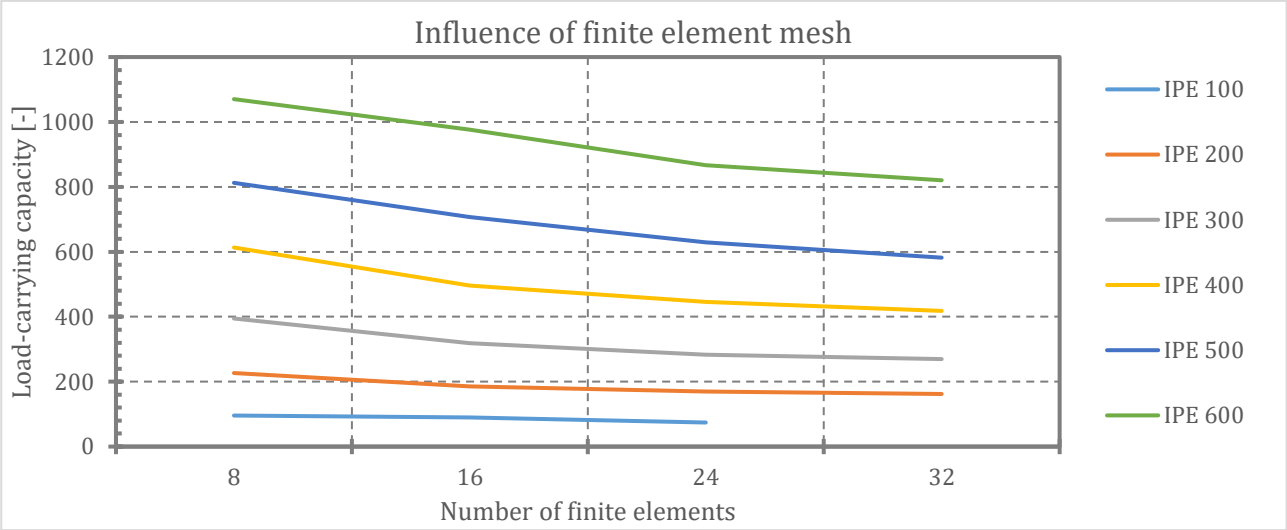


*Fig. 41 Influence of finite element mesh – influence of number of elements on load-carrying capacity*

*Tab. 3 Influence of finite element mesh - Load-carrying capacity [kN]*

| Cross section | Number of elements | IDEA StatiCa | | ANSYS | |
|---|---|---|---|---|---|
| | | MNA | GMNIA | MNA | GMNIA |
| IPE 100 | 8 | 95.508 | 95.703 | - | - |
| | 16 | 89.844 | 89.844 | - | - |
| | 24 | 74.219 | 74.169 | - | - |
| | 32 | 72.266 | - | 90.379 | 90.966 |
| IPE 200 | 8 | 228.516 | 226.563 | - | - |
| | 16 | 187.500 | 185.547 | - | - |
| | 24 | 169.922 | 169.922 | - | - |
| | 32 | 162.110 | 162.110 | 205.683 | 209.599 |
| IPE 300 | 8 | 398.438 | 394.532 | - | - |
| | 16 | 320.313 | 318.360 | - | - |
| | 24 | 285.157 | 283.203 | - | - |
| | 32 | 269.532 | 269.532 | 348.543 | 348.182 |
| IPE 400 | 8 | 621.094 | 613.281 | - | - |
| | 16 | 500.000 | 496.094 | - | - |
| | 24 | 445.313 | 445.313 | - | - |
| | 32 | 417.969 | 417.969 | 561.442 | 559.203 |
| IPE 500 | 8 | 820.313 | 812.500 | - | - |
| | 16 | 710.938 | 707.031 | - | - |
| | 24 | 632.813 | 628.906 | - | - |
| | 32 | 585.938 | 582.031 | 741.919 | 736.679 |
| IPE 600 | 8 | 1078.126 | 1070.312 | - | - |
| | 16 | 984.376 | 976.562 | - | - |
| | 24 | 875.000 | 867.188 | - | - |
| | 32 | 820.312 | 820.312 | 1013.987 | 1007.422 |

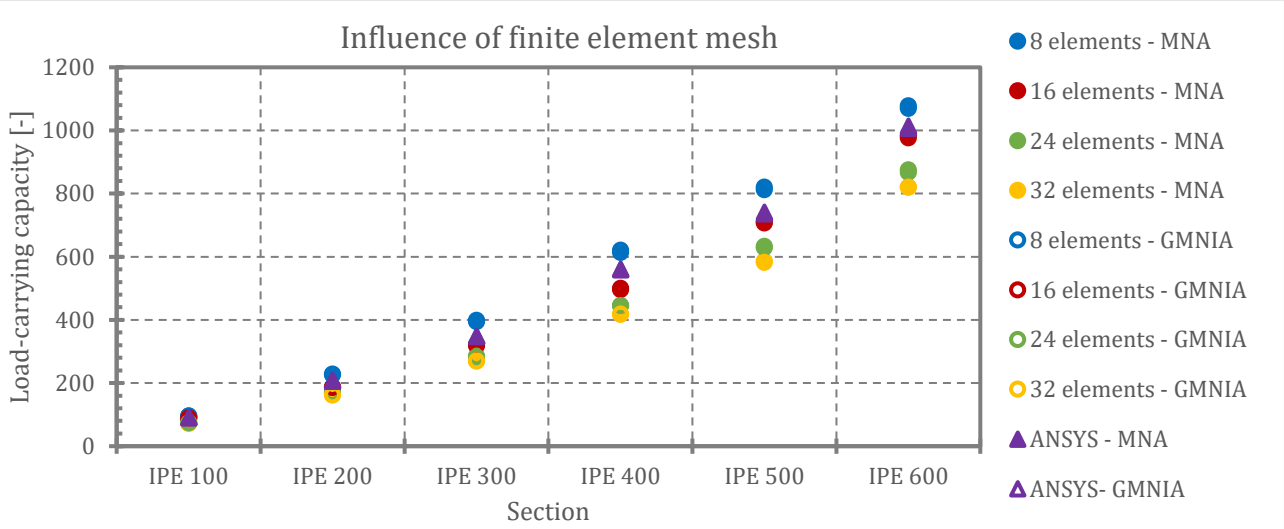


*Fig. 42 Influence of finite element mesh – comparison of IDEA and ANSYS results*

### 3.3.3. Conclusions

As it was mentioned above, the best agreement of results between IDEA StatiCa and ANSYS software was achieved with dividing of transversally compressed member web into 16 finite elements. Thus all finite element analyses carried out in IDEA StatiCa in the frame of this study were performed with 16 elements along the web.

## 4. Influence of input parameters on load-carrying capacity

In this part of study influence of some input parameters is observed. Problem solution was carried out using ANSYS software, IDEA StatiCa software and design codes calculations. Observed input parameters are:

- Yield strength of steel
- Imperfection amplitude
- Thickness of loading plates
- Rounded corners at rolled sections and throat welds of welded sections
- Unstiffened and unrestrained end
- Normal force in column

### 4.1. Influence of yield strength

This part of study shows the influence of steel grade represented by yield strength $f_y$ of structural steel on load-carrying capacity and other results. The goal is to evaluate linear and nonlinear dependency of load-carrying capacity on yield strength for yielding/MNA and buckling/GMNIA.

#### 4.1.1. Methodology

The study was performed on transversally loaded member of cross-section IPE 400 with overall length of member $L = 4 \times h$. Member is made of structural steel S235, S275, S355, S420 and S460. The imperfection amplitude was $d_w/200$. These five transversally loaded members were analysed using MNA, LBA and GMNIA in IDEA and ANSYS. Load-carrying capacity was calculated according to the codes EN 1993-1-8, EN 1993-1-5 and AISC 360-16 for "Yielding" and "Buckling" failure modes. Analysed member is illustrated in Fig. 43.

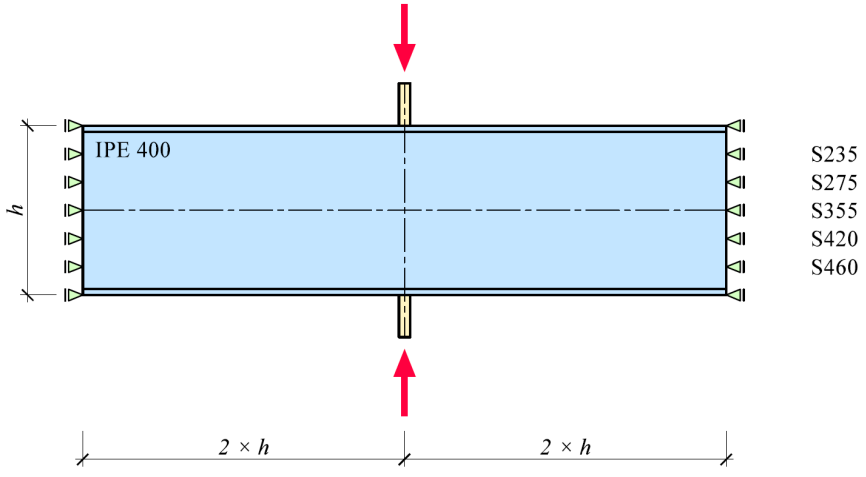


*Fig. 43 Influence of yield strength – geometry and boundary conditions*

### 4.1.2. Results

Calculated load-carrying capacities are listed in Tab. 4 for all used methods for all structural steel grades on transversally compressed members of cross section IPE 400.

*Tab. 4 Influence of yield strength - Load-carrying capacity [kN]*

| Struct. steel | EN 1993-1-8 | | EN 1993-1-5 | AISC 360-16 | | IDEA Statica | | ANSYS | |
|---|---|---|---|---|---|---|---|---|---|
| | Yielding | Buckling | Buckling | Yielding | Buckling | MNA | GMNIA | MNA | GMNIA |
| S235 | 375.91 | 324.98 | 345.34 | 375.91 | 323.98 | 343.75 | 343.75 | 401.36 | 401.70 |
| S275 | 439.89 | 359.15 | 373.57 | 439.89 | 350.47 | 398.44 | 394.53 | 461.93 | 461.31 |
| S355 | 567.86 | 420.71 | 424.45 | 567.86 | 398.20 | 500.00 | 496.09 | 579.65 | 576.31 |
| S420 | 671.83 | 465.76 | 461.67 | 671.83 | 433.13 | 578.13 | 574.22 | 673.18 | 665.08 |
| S460 | 735.82 | 491.76 | 483.16 | 735.82 | 453.28 | 605.47 | 601.56 | 727.75 | 717.33 |

Load –carrying capacities are graphically displayed in Fig. 44 for all used methods for transversally compressed members of cross section IPE 400.

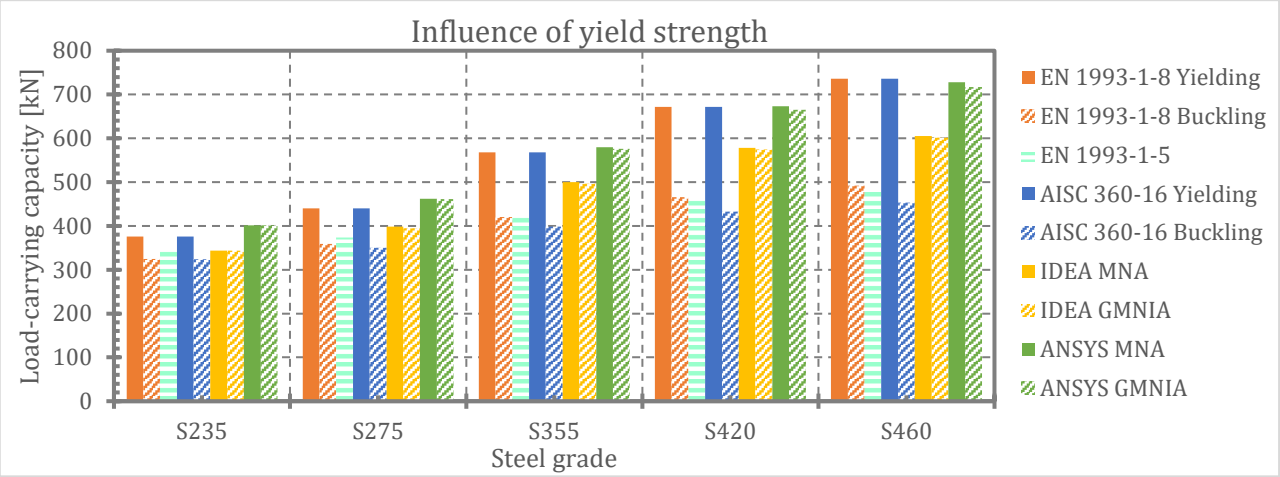


*Fig. 44 Influence of yield strength – load-carrying capacity*

Influence of yield strength $f_y$ on transversal load-carrying capacity is clearly shown in Fig. 45 where ratio of load-carrying capacities related to structural steel S235 ($f_y$ = 235 MPa) is on vertical axis.

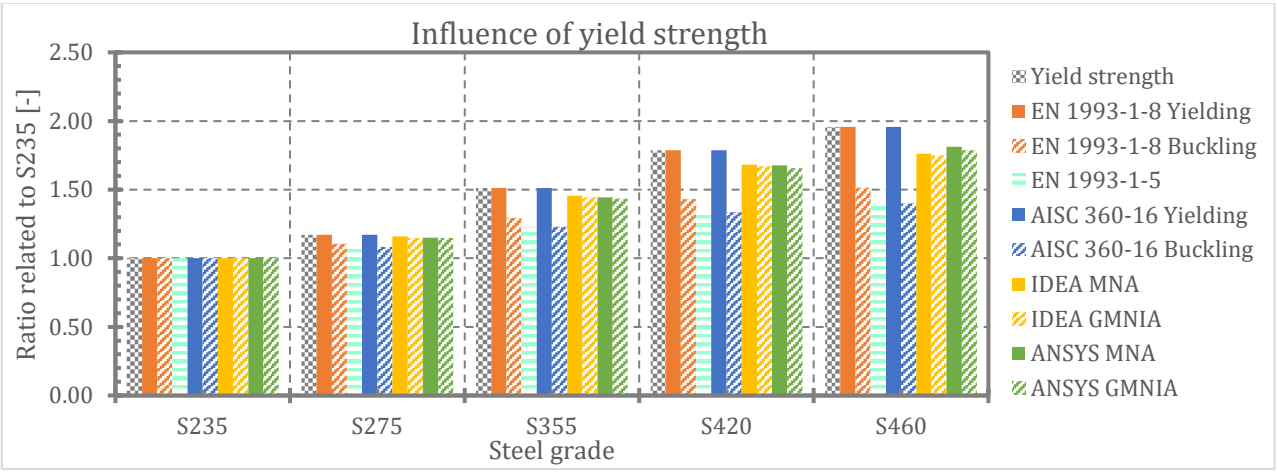


*Fig. 45 Influence of yield strength – relative influence of yield strength on load-carrying capacity*

Influence of buckling on transversal load-carrying capacity is clearly shown in Fig. 46 where ratio of load-carrying capacities resulting from Buckling/Yielding resistances according to the EN 1993-1-8 and AISC 360-16 or GMNIA/MNA resulting from numerical analysis performed in IDEA StatiCa and ANSYS is on vertical axis. Reduction factor according to the EN 1993-1-5 is directly calculated using equation (6).

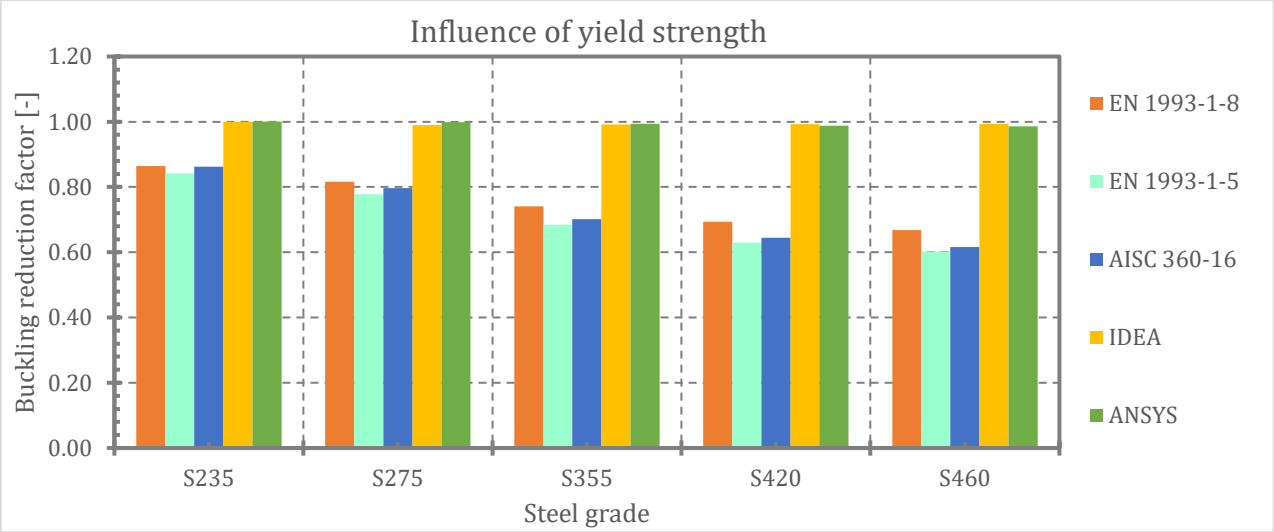


*Fig. 46 Influence of yield strength – reduction buckling factor*

Actual behaviour of axially and transversally compressed member is described in Fig. 47 to Fig. 52 for illustration for member of cross section IPE 400.

Fig. 47 shows results of linear buckling analysis – critical forces $F_{cr}$ [kN] and critical load factor $\alpha_{cr}$ [-]. For increasing yield strength of steel from which the transversally compressed member is made critical load factor decreasing and the critical force is (approximately) constant that corresponds to the theory of stability.

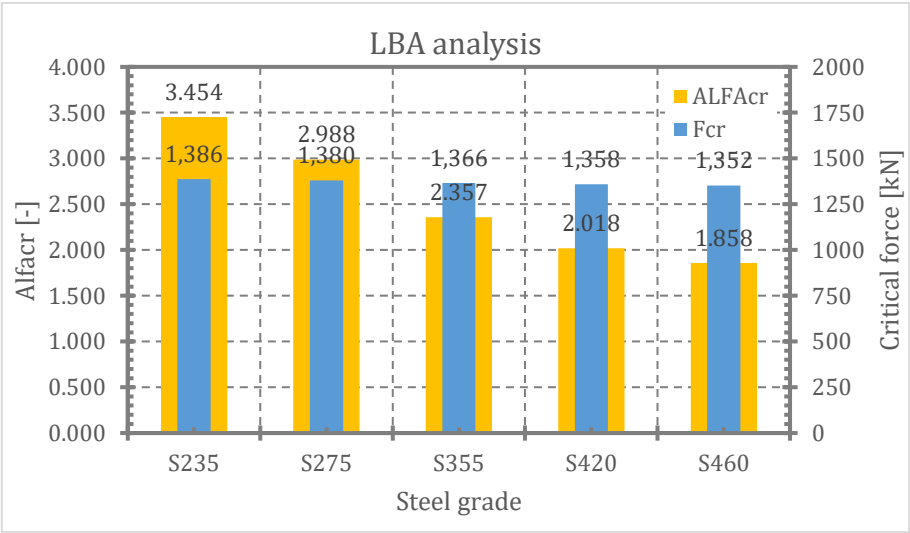


*Fig. 47 Influence of yield strength – LBA results*

Fig. 48 illustrates relationship of vertical deformation and loading force for MNA and GMNIA. Fig. 49 describes dependency of lateral deformation in the middle of beam web on loading force for MNA and GMNIA. Dependency of maximum equivalent stress and equivalent stress in the

middle of member web on loading force is plotted in Fig. 50 and Fig. 51. Fig. 52 shows developing of plastic strain with increasing loading.

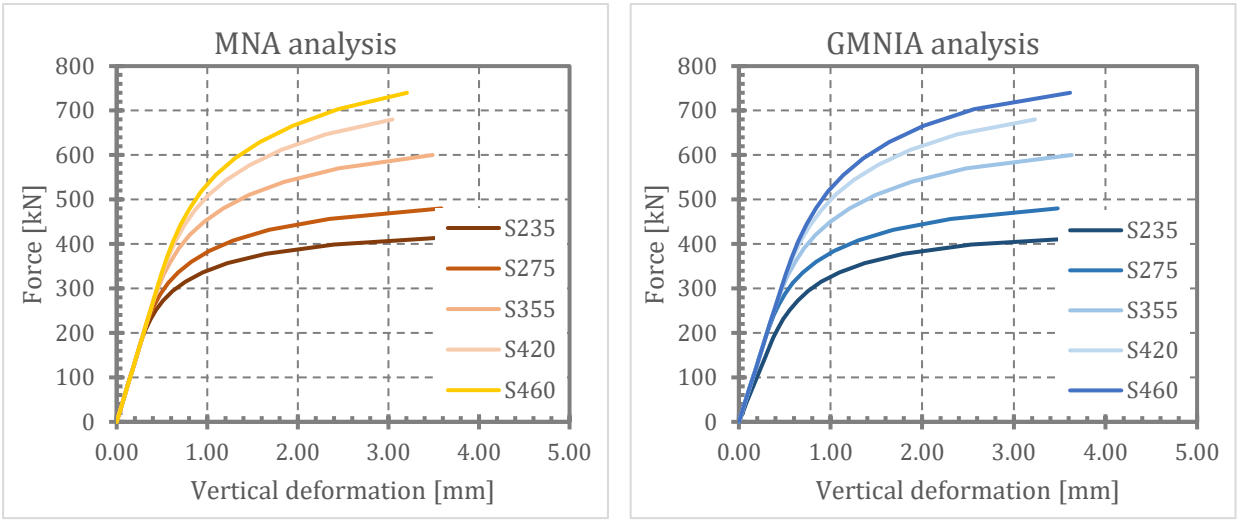


*Fig. 48 Influence of yield strength – vertical deformation-force relationship*

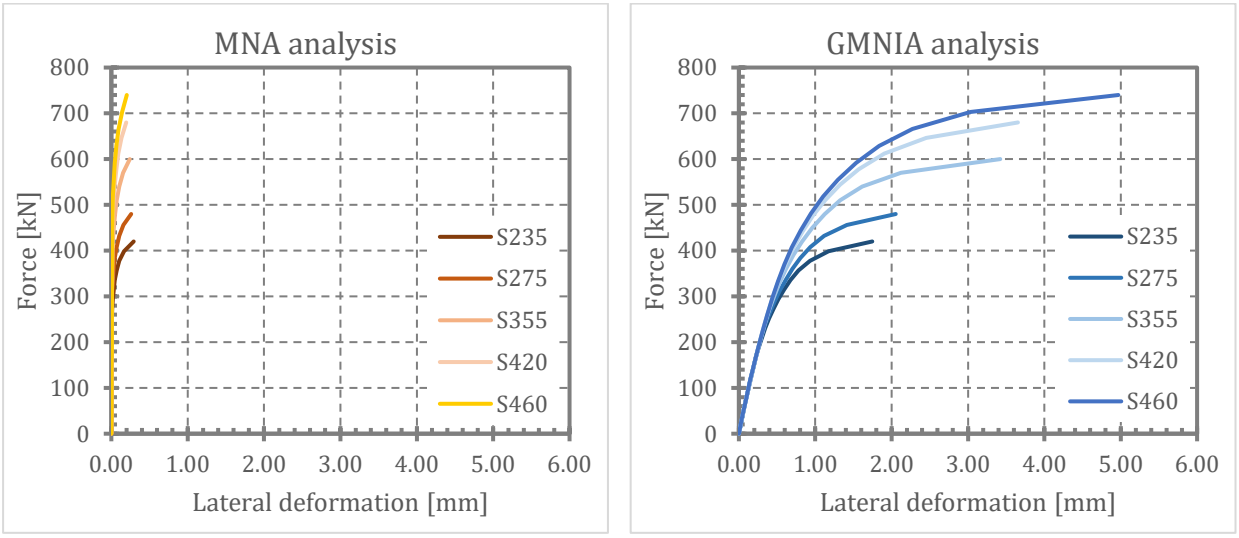


*Fig. 49 Influence of yield strength – lateral deformation-force relationship*

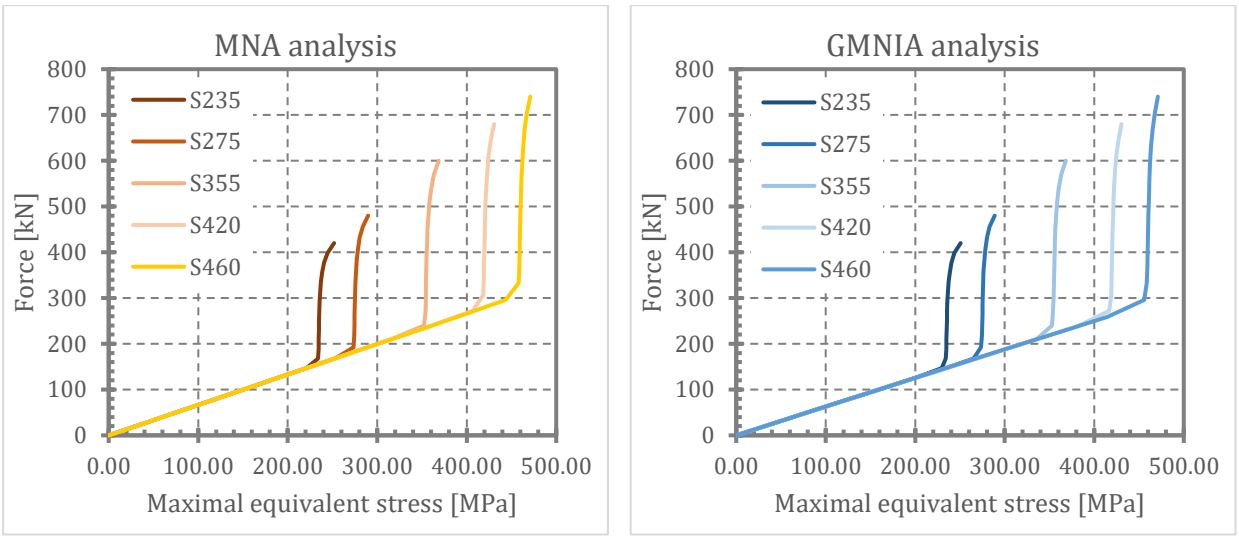


*Fig. 50 Influence of yield strength – maximal equivalent stress-force relationship*

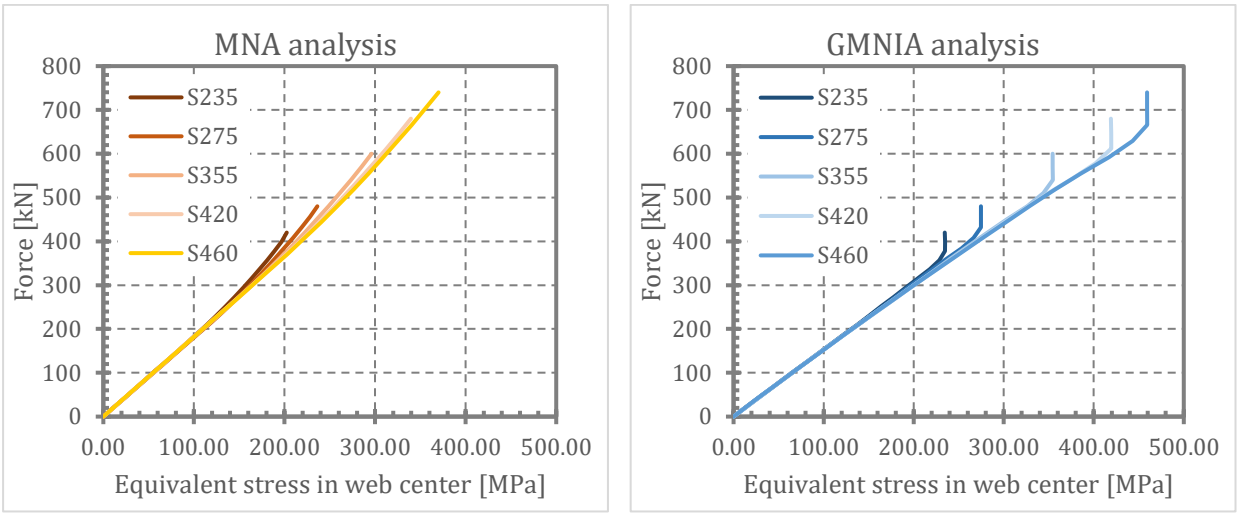


*Fig. 51 Influence of yield strength – equivalent stress in web center-force relationship*

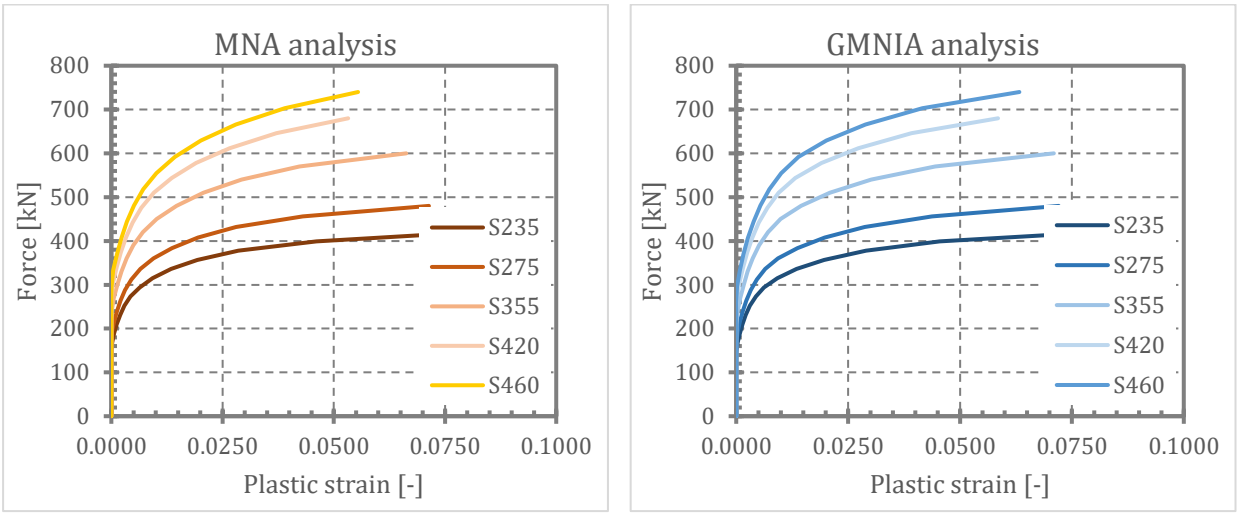


*Fig. 52 Influence of yield strength – plastic strain-force relationship*

Fig. 53 shows comparison of load-carrying capacities obtained from all investigated cases and by all used methods related to the ANSYS results (thus all ANSYS results are equal to 1.0). Design codes yielding resistances and IDEA MNA are related to ANSYS MNA, buckling resistances and IDEA GMNIA are related to ANSYS GMNIA.

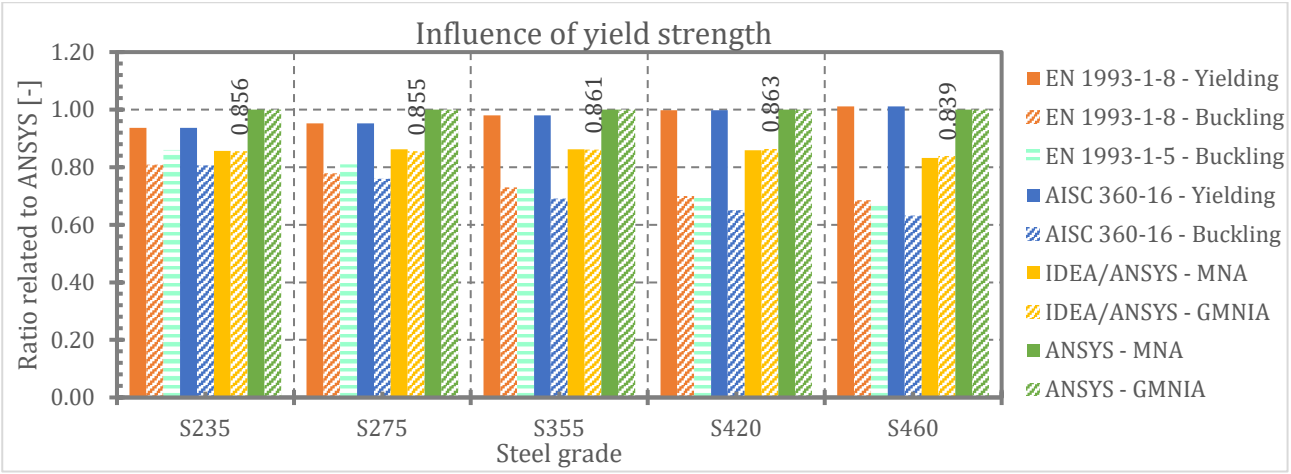


*Fig. 53 Influence of yield strength – comparison of Load-carrying capacity related to the ANSYS results*

### 4.1.3. Conclusion

Presented results show that yield strength of structural steel from which transversally compressed member is made have influence on load-carrying capacity (resistance), but according to the numerical analysis performed in IDEA StatiCa and ANSYS the increase of resistance is lower than increase of yield strength. Design codes EN 1993-1-8 and AISC 360-16 give resistance increase the same as increase of yield strength is. Design code EN 1993-1-5 gives relatively conservative results and load-carrying capacities resulting from this standard are similar to resistances resulting from EN 1993-1-8 and AISC 360-16 for buckling mode.

IDEA StatiCa provides very good agreement with ANSYS software results (load-carrying capacity of transversally compressed member) and is slightly on the safe side – there is approximately difference of 15% for both MNA and GMNIA analysis.

Buckling effect of transversally compressed members made of steel with higher yield strength is greater than for members made of steel with lower yield strength but the buckling effect is not very significant in case standard hot-rolled sections.

## 4.2. Influence of imperfection amplitude

This part of study shows the influence of initial geometric imperfection amplitude on load-carrying capacity and other results. The goal is to evaluate how much the imperfection amplitude influences the behaviour of transversally compressed member.

### 4.2.1. Methodology

The study was performed on transversally compressed member of cross-section IPE 400 with overall length of member $L = 4 \times h$. Member is made of structural steel S355. The imperfection amplitude was $d_w/200$; $d_w/150$; $d_w/100$; $d_w/50$ and $d_w/25$, where $d_w$ is web height without rounded corners - see Fig. 4. These five transversally compressed members were analysed using MNA, LBA and GMNIA in IDEA StatiCa and ANSYS. Load-carrying capacities were calculated according to the codes EN 1993-1-8, EN 1993-1-5 and AISC 360-16 for “Yielding” and “Buckling” failure modes. Analysed member is illustrated in Fig. 54.

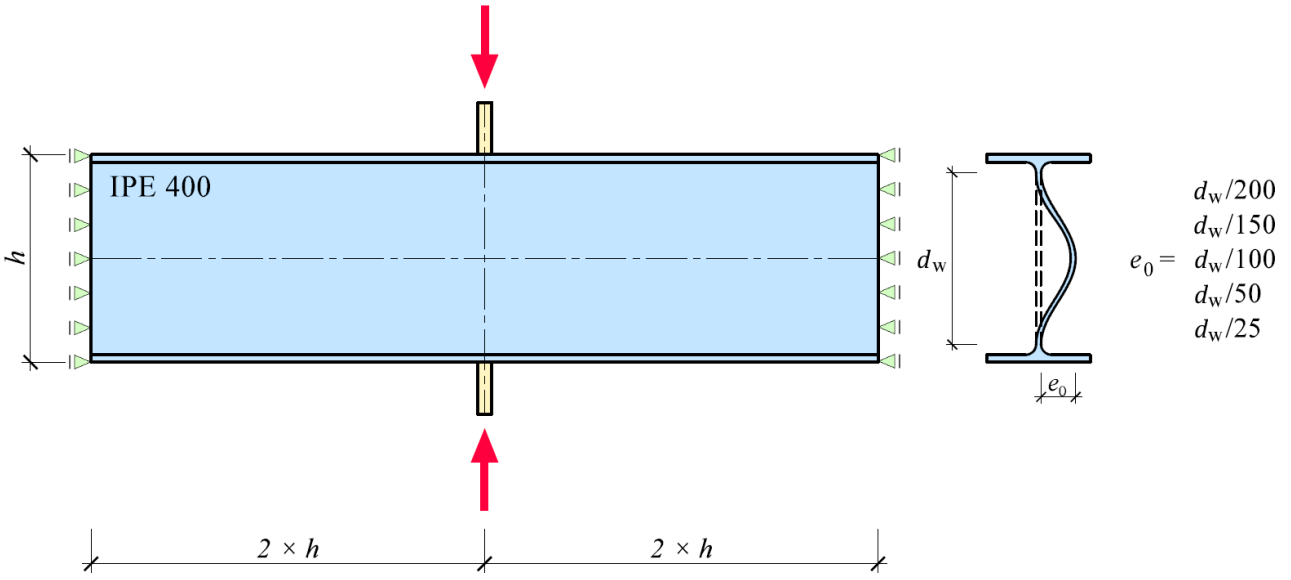


*Fig. 54 Influence of imperfection amplitude – geometry and boundary conditions*

### 4.2.2. Results

Calculated load-carrying capacities are listed in Tab. 5 for all used methods for all amplitudes of initial geometric imperfections on transversally compressed members of cross section IPE 400. Materially nonlinear analysis is not influenced by imperfections, so only geometrically and materially nonlinear analysis with imperfections gives different results. Solution according to the standards EN 1993-1-8, EN 1993-1-5 and AISC 360-16 does not offer direct input of initial geometrical imperfection amplitude, then resistances are the same for all considered amplitudes.

*Tab. 5 Influence of imperfection amplitude - Load-carrying capacity [kN]*

| Imperfection amplitude | EN 1993-1-8 | | EN 1993-1-5 | AISC 360-16 | | IDEA Statica | | ANSYS | |
|---|---|---|---|---|---|---|---|---|---|
| | Yielding | Buckling | Buckling | Yielding | Buckling | MNA | GMNIA | MNA | GMNIA |
| $d_w/200$ | 576.86 | 420.71 | 424.45 | 576.86 | 398.20 | 500.00 | 496.09 | 579.65 | 576.31 |
| $d_w/150$ | | | | | | | 496.09 | | 573.49 |
| $d_w/100$ | | | | | | | 492.19 | | 566.76 |
| $d_w/50$ | | | | | | | 488.28 | | 531.06 |
| $d_w/25$ | | | | | | | 484.38 | | 519.70 |

Load-carrying capacities are graphically displayed in Fig. 55 for all used methods and all considered amplitudes of imperfection for transversally compressed members of cross section IPE 400.

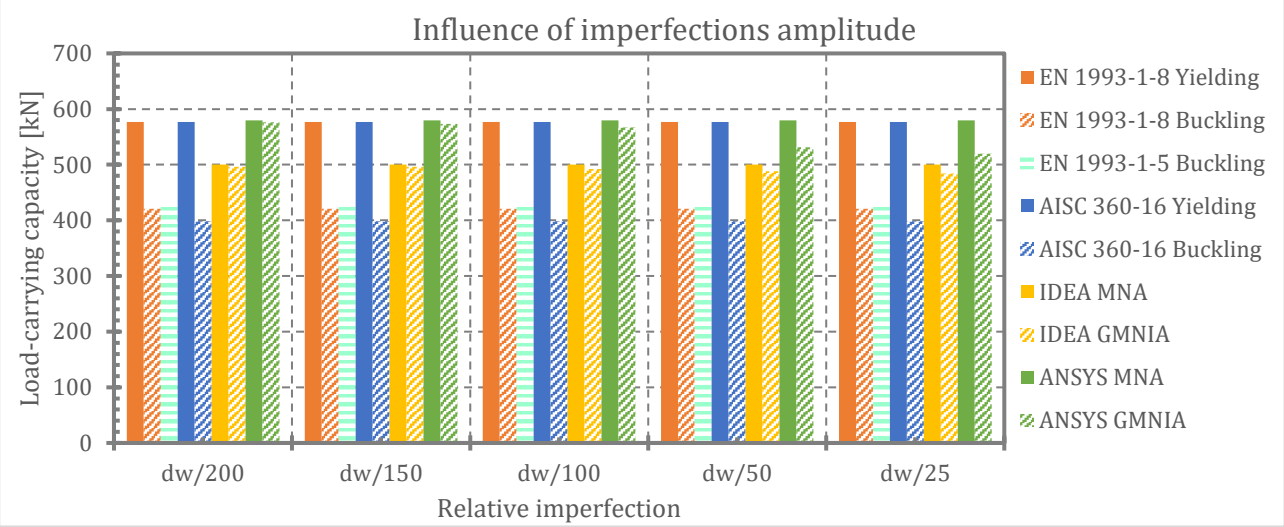


*Fig. 55 Influence of imperfection amplitude – Load-carrying capacity*

Influence of amplitude of initial geometric imperfection $e_0$ on transversal load-carrying capacity is clearly shown in Fig. 56 where ratio of load-carrying capacities related to basic value of initial imperfection $e_0 = d_w/200$ is on vertical axis. In the chart only values resulting from GMNIA performed in IDEA StatiCa and ANSYS are plotted, because all other values are equal to 1.0.

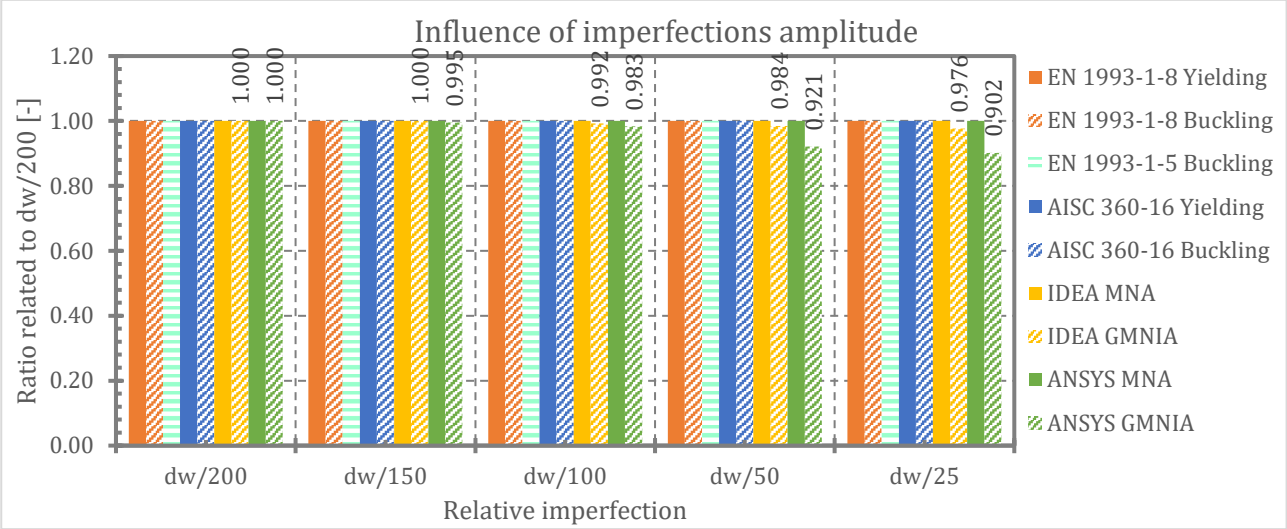


*Fig. 56 Influence of imperfection amplitude – relative influence of imperfection amplitude on load-carrying capacity*

Influence of buckling on transversal load-carrying capacity is clearly shown in Fig. 57 where ratio of load-carrying capacities resulting from Buckling/Yielding resistances according to the EN 1993-1-8 and AISC 360-16 or GMNIA/MNA resulting from numerical analysis performed in IDEA StatiCa and ANSYS are on vertical axis. Results for EN 1993-1-5 are not plotted, because there is no calculation of load-carrying capacity for "Buckling" and "Yielding" modes.

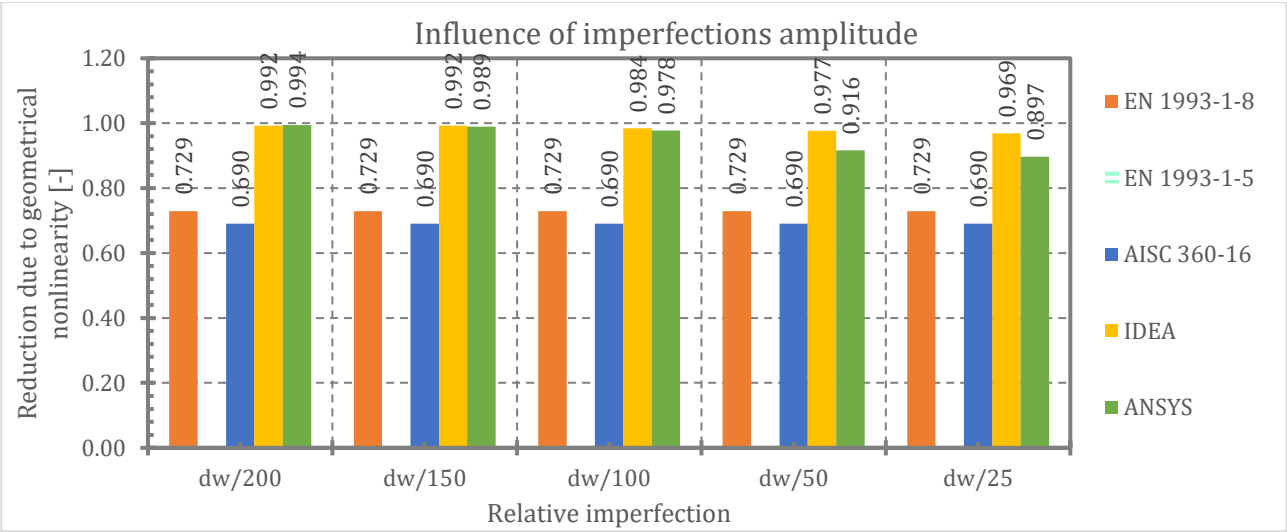


*Fig. 57 Influence of imperfection amplitude – reduction due to geometrical nonlinearity*

Actual behaviour of axially and transversally compressed member is described in Fig. 58 to Fig. 60 for illustration for member of cross section IPE 400.

Fig. 58 shows dependency of vertical deformation and lateral deformation on loading transversal force resulting from MNA and GMNIA with different initial amplitudes of imperfection.

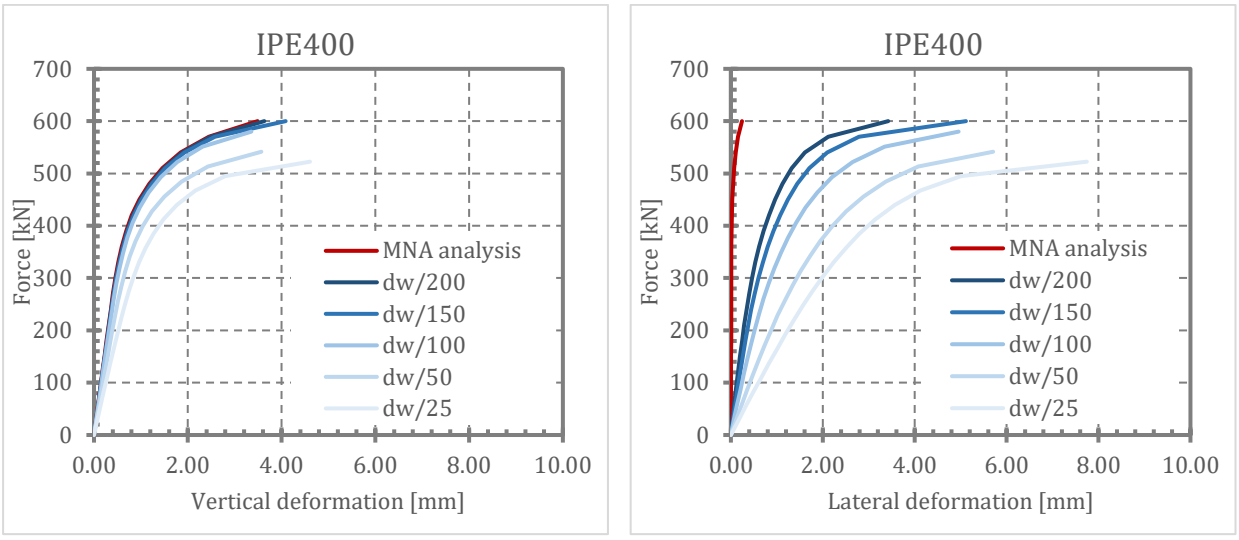


*Fig. 58 Influence of imperfection amplitude – vertical/lateral deformation-force relationship*

Similar comparison is shown in Fig. 59 for maximal equivalent stress and equivalent stress in the middle of member web.

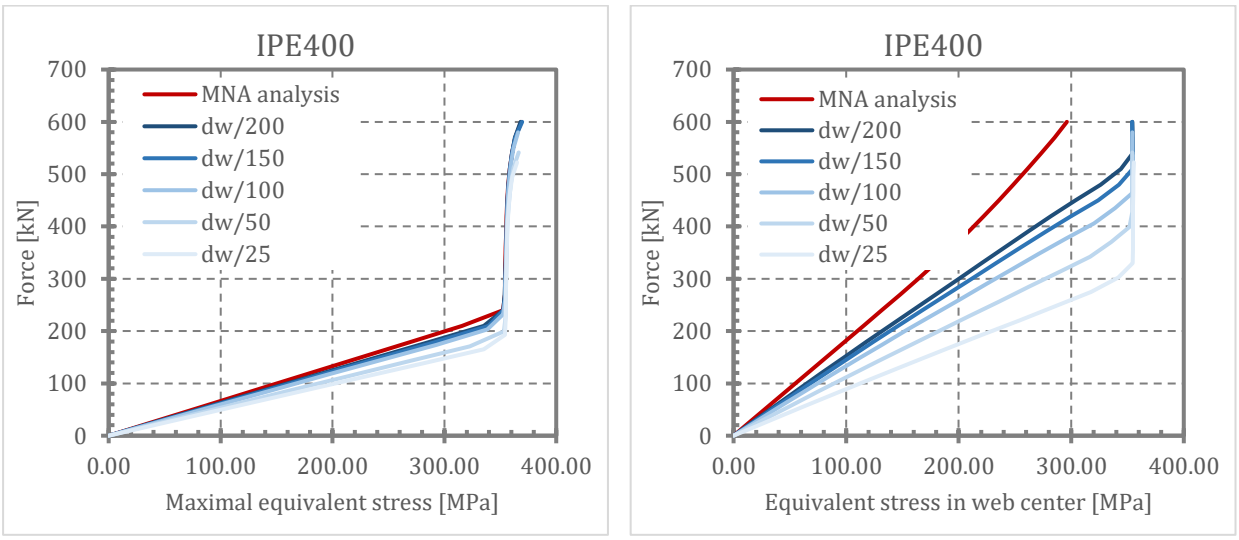


*Fig. 59 Influence of imperfection amplitude – stress-force relationship*

Fig. 60 shows developing of plastic strain with load increasing.

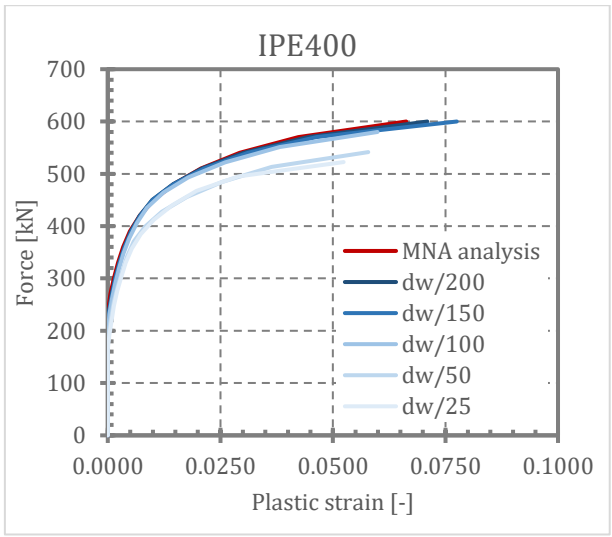


*Fig. 60 Influence of imperfection amplitude – plastic strain-force relationship*

Fig. 61 shows comparison of load-carrying capacities obtained from all investigated cases and by all used methods related to the ANSYS results (thus all ANSYS results are equal to 1.0).

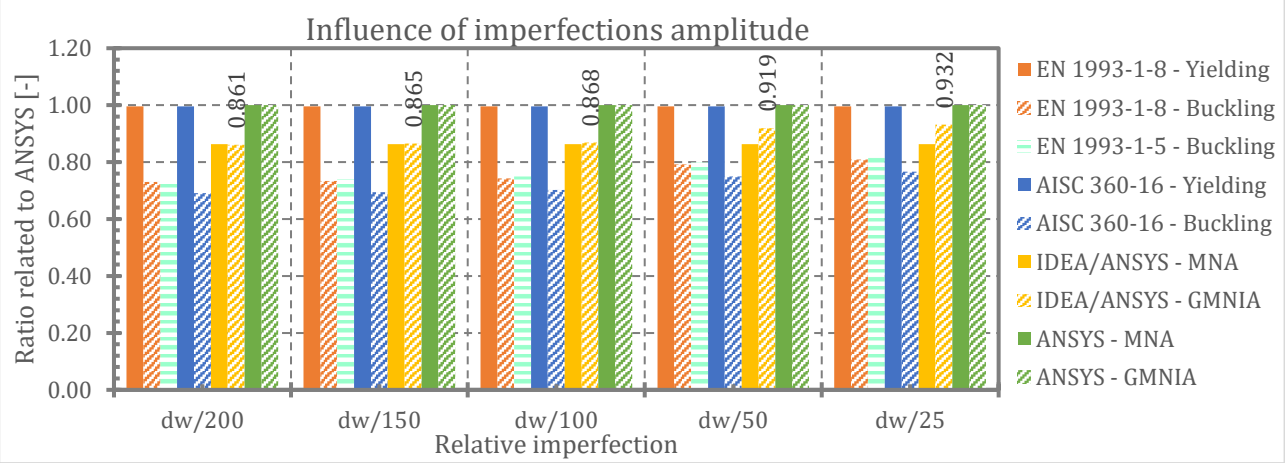


*Fig. 61 Influence of imperfection amplitude – comparison of Load-carrying capacity related to the ANSYS results*

### 4.2.3. Conclusion

As the decisive point (from the point of view of design resistance) is situated in flange-web transition, the amplitude of initial geometrical imperfection has not so strong influence as it might seem. As the amplitude is two times higher than basic value (therefore $e_0 = d_w/100$) the load-carrying resistance is lower only about 1 % or 2 % according to the IDEA StatiCa or ANSYS simulation. When amplitude is four times higher (therefore $e_0 = d_w/50$) the load-carrying resistance is lower only about 2 % or 8 % according to the IDEA StatiCa or ANSYS simulation and for extremely large imperfection (therefore $e_0 = d_w/25$) load-carrying resistance decrease only about 3 % and 10 %.

IDEA StatiCa provides good agreement with ANSYS software results (load-carrying capacity of transversally compressed member) and is slightly on the safe side – there is approximately difference of 14% for both MNA analysis and in the case of GMNIA analysis the difference vary from 14% to 7% while lower difference is for more slender members.

All other analysed models considered basic value of initial geometric imperfection $d_w/200$ according to the standard EN1993-1-5 [2].

## 4.3. Influence of loading plates thickness

This part of study shows the influence of loading plate thickness on load-carrying capacity and other results. The goal is to evaluate how much the loading plates thickness influences the behaviour of transversally loaded member.

### 4.3.1. Methodology

The study was performed on transversally compressed member of cross-section IPE 100 and IPE 600 with overall length of member $L = 4\times h$. Member is made of structural steel S355. The imperfection amplitude was $d_w/200$, where $d_w$ is web height without rounded corners. Loading plate thickness $t_p$ was related to the transversally loaded member flange thickness $t_f$: $t_p = 0.50\times t_f$; $0.75\times t_f$; $1.00\times t_f$; $1.50\times t_f$ and $2.00\times t_f$ – see Fig. 62. These five transversally loaded

members were analysed using MNA, LBA and GMNIA in IDEA StatiCa and ANSYS. Load-carrying capacity was calculated according to the codes EN 1993-1-8, EN 1993-1-5 and AISC 360-16 for "Yielding" and "Buckling" failure modes. Analysed member is illustrated in Fig. 62.

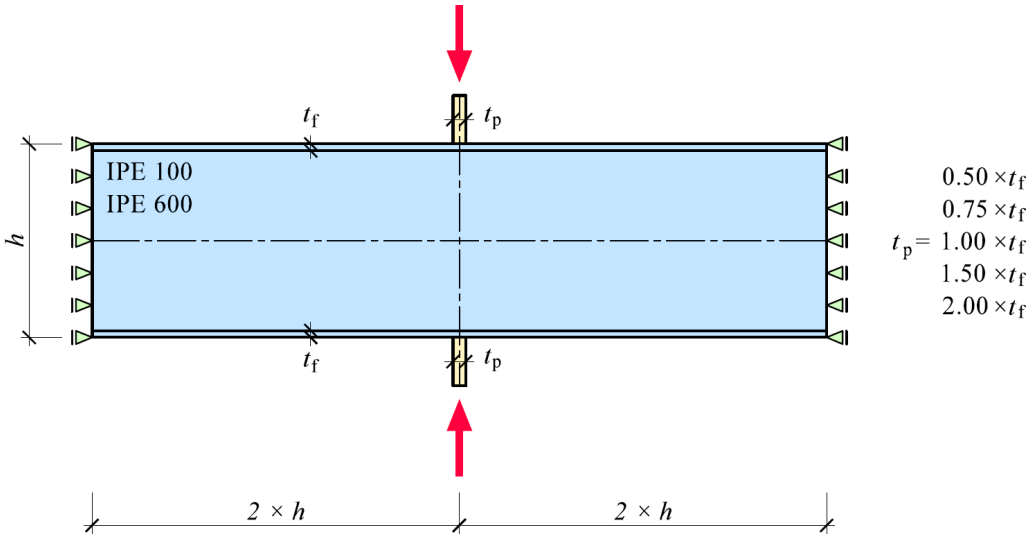


*Fig. 62 Influence of thickness of loading plates – geometry and boundary conditions*

### 4.3.2. Results

Calculated load-carrying capacities are listed in Tab. 6 and Tab. 7 for all used methods for transversally compressed members of cross sections IPE 100 and IPE 600 respectively. It is interesting that load-carrying capacity is not influenced by loading plate thickness according to the American standard AISC 360-16 for buckling failure mode.

*Tab. 6 Influence of loading plates thickness at IPE 100 - Load-carrying capacity [kN]*

| Loading plate thickness | EN 1993-1-8 | | EN 1993-1-5 | AISC 360-16 | | IDEA Statica | | ANSYS | |
|---|---|---|---|---|---|---|---|---|---|
| | Yielding | Buckling | Buckling | Yielding | Buckling | MNA | GMNIA | MNA | GMNIA |
| $0.50 \times t_f$ | 96.57 | 96.57 | 81.51 | 96.57 | 191.45 | 88.67 | 88.67 | 78.95 | 81.55 |
| $0.75 \times t_f$ | 98.65 | 98.65 | 83.59 | 98.65 | 191.45 | 90.63 | 90.63 | 88.12 | 89.06 |
| $1.00 \times t_f$ | 100.72 | 100.72 | 85.66 | 100.72 | 191.45 | 91.41 | 91.41 | 90.38 | 90.97 |
| $1.50 \times t_f$ | 104.87 | 104.87 | 89.81 | 104.87 | 191.45 | 92.97 | 92.97 | 94.21 | 95.18 |
| $2.00 \times t_f$ | 109.02 | 109.02 | 93.96 | 109.02 | 191.45 | 95.70 | 95.31 | 99.96 | 101.16 |

*Tab. 7 Influence of loading plates thickness at IPE 600 - Load-carrying capacity [kN]*

| Loading plate thickness | EN 1993-1-8 | | EN 1993-1-5 | AISC 360-16 | | IDEA Statica | | ANSYS | |
|---|---|---|---|---|---|---|---|---|---|
| | Yielding | Buckling | Buckling | Yielding | Buckling | MNA | GMNIA | MNA | GMNIA |
| $0.50 \times t_f$ | 956.37 | 719.10 | 783.76 | 956.37 | 696.65 | 953.13 | 945.31 | 954.76 | 954.98 |
| $0.75 \times t_f$ | 976.61 | 728.38 | 790.50 | 976.61 | 696.65 | 968.75 | 960.94 | 953.28 | 983.43 |
| $1.00 \times t_f$ | 996.84 | 737.56 | 797.18 | 996.84 | 696.65 | 984.38 | 976.56 | 1013.99 | 1007.42 |
| $1.50 \times t_f$ | 1037.31 | 755.65 | 810.39 | 1037.31 | 696.65 | 1000.00 | 992.19 | 1016.07 | 1034.42 |
| $2.00 \times t_f$ | 1077.78 | 773.39 | 823.38 | 1077.78 | 696.65 | 1023.44 | 1015.63 | 1054.06 | 1047.26 |

Load –carrying capacities are graphically displayed in Fig. 63 and Fig. 64 for all used methods for transversally compressed members of cross section IPE 100 and IPE 600.

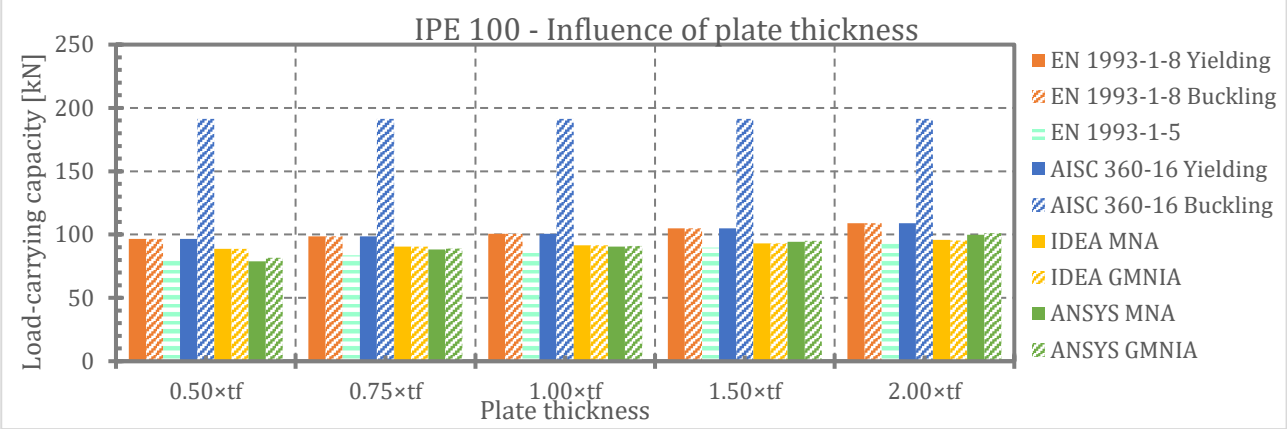


*Fig. 63 Influence of loading plates thickness at IPE 100 – Load-carrying capacity*

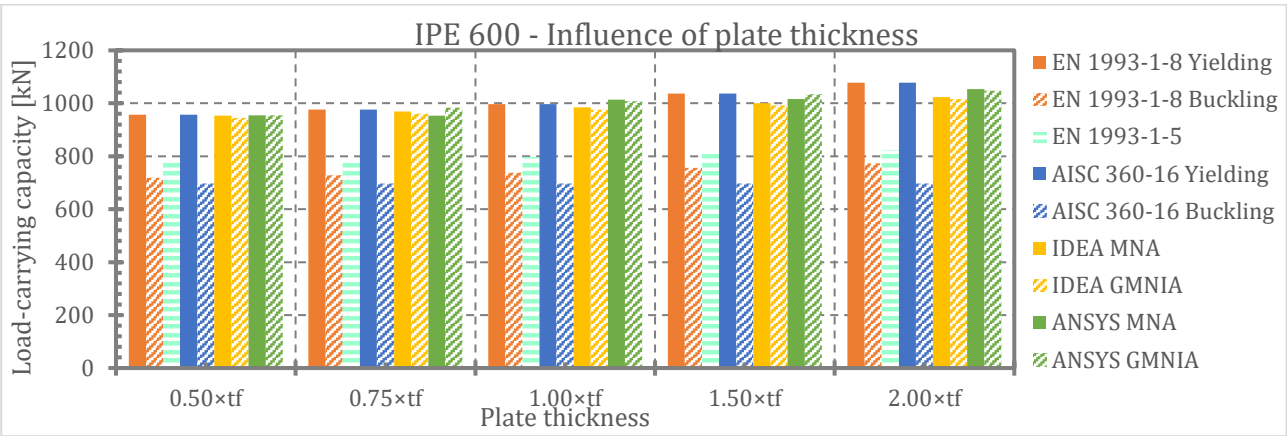


*Fig. 64 Influence of loading plates thickness at IPE 600 – Load-carrying capacity*

Influence of loading plates thickness $t_p$ on transversal load-carrying capacity is clearly shown in Fig. 65 and Fig. 66 where ratio of load-carrying capacities related to basic value of loading plate thickness $t_p = 1.0 \times t_f$ is on vertical axis. It should be mentioned, that according to the AISC 360-16 the loading plate thickness does not influence load-carrying resistance.

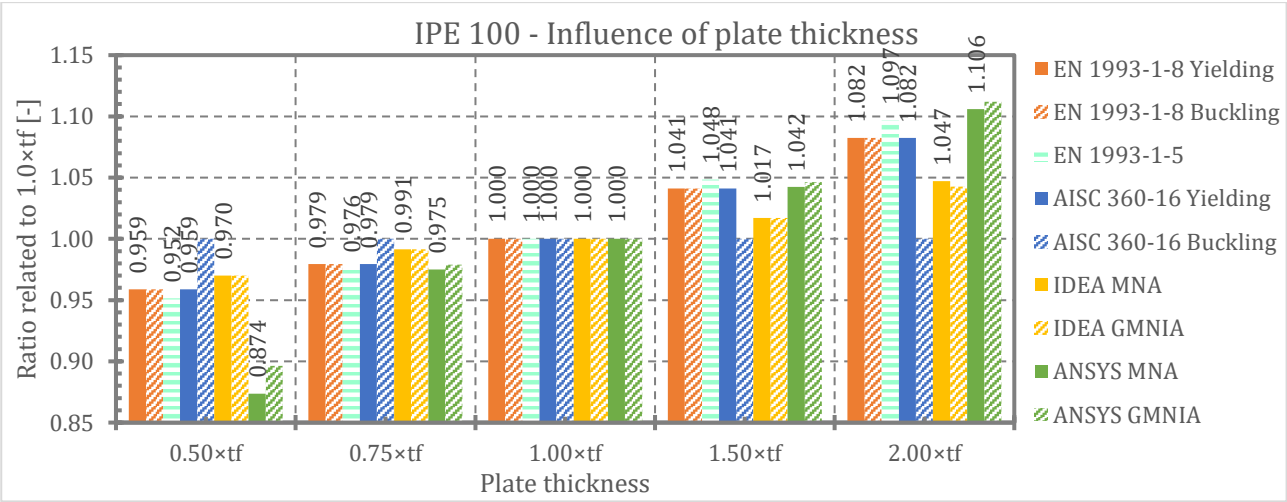


*Fig. 65 Influence of loading plates thickness at IPE 100 – relative influence of loading plates thickness on load-carrying capacity*

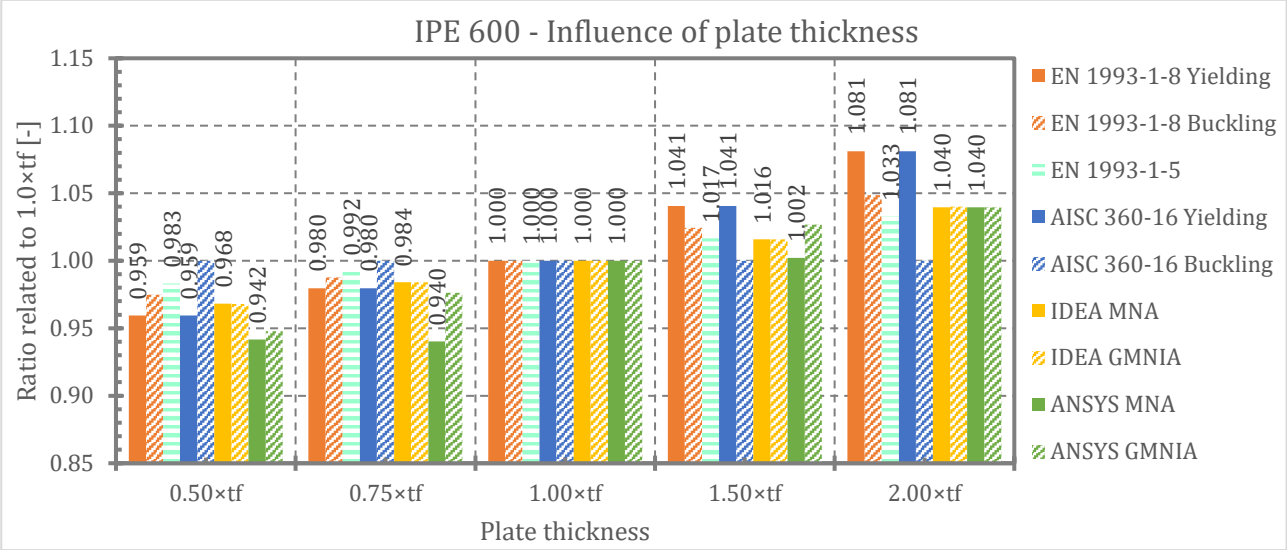


*Fig. 66 Influence of loading plates thickness at IPE 600 – relative influence of loading plates thickness on load-carrying capacity*

Influence of buckling on transversal load-carrying capacity is clearly shown in Fig. 67 and Fig. 68 where ratio of load-carrying capacities resulting from Buckling/Yielding resistances according to the EN 1993-1-8 and AISC 360-16 or GMNIA/MNA resulting from numerical analysis performed in IDEA StatiCa and ANSYS are on vertical axis. "Buckling factor" for EN 1993-1-5 is directly calculated according to the equation (6). Results shows that American standard gives very different results in comparison from all other methods. In the case of IPE 100 GMNIA analysis give resistance almost two times higher than for MNA analysis and on the other hand in the case of IPE 600 the reduction due to buckling is highest of all used methods.

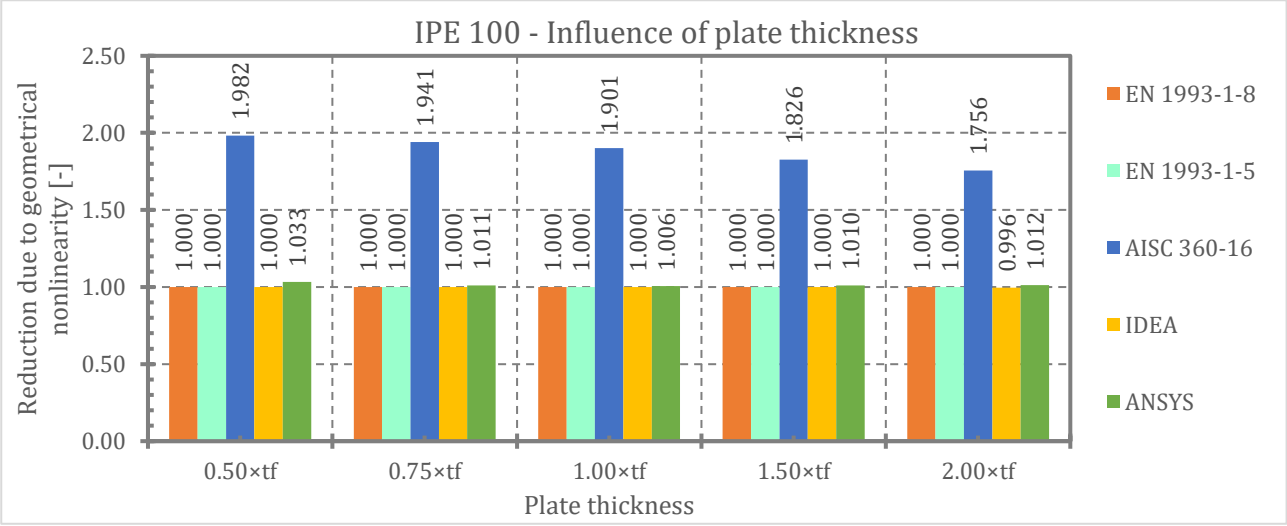


*Fig. 67 Influence of loading plates thickness at IPE 100 – reduction due to geometrical nonlinearity*

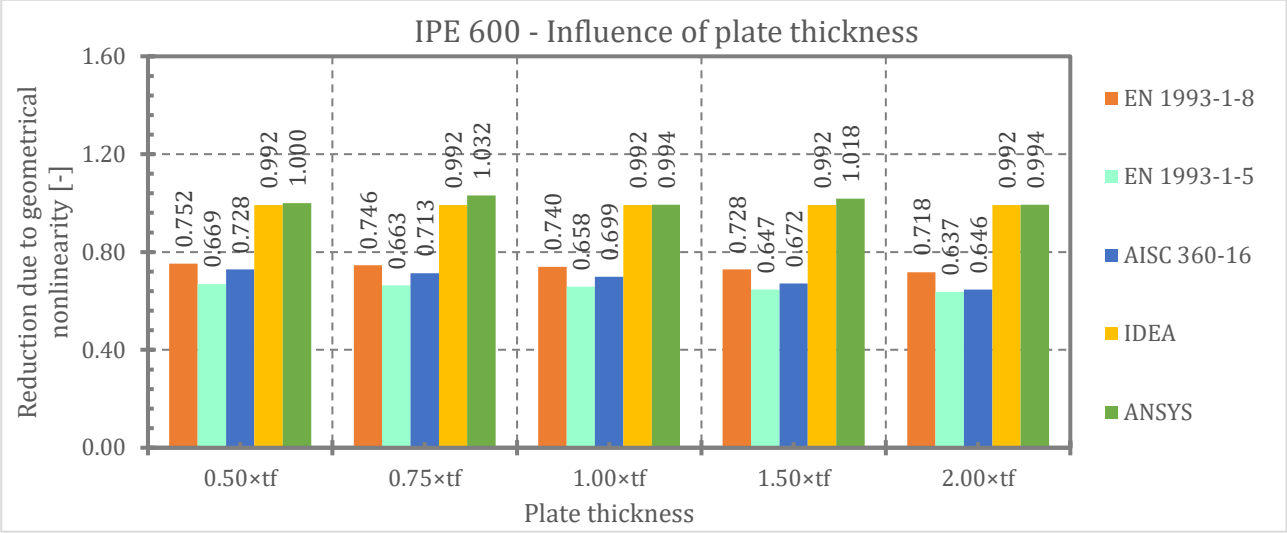


*Fig. 68 Influence of loading plates thickness at IPE 600 – reduction due to geometrical nonlinearity*

Actual behaviour of axially and transversally compressed member is described in Fig. 69 to Fig. 74 for illustration for member of cross section IPE 100.

Fig. 69 shows results of linear buckling analysis – critical forces $F_{cr}$ [kN] and critical load factor $\alpha_{cr}$ [-]. For increasing loading plate thickness critical force increasing abut critical load factor decreasing.

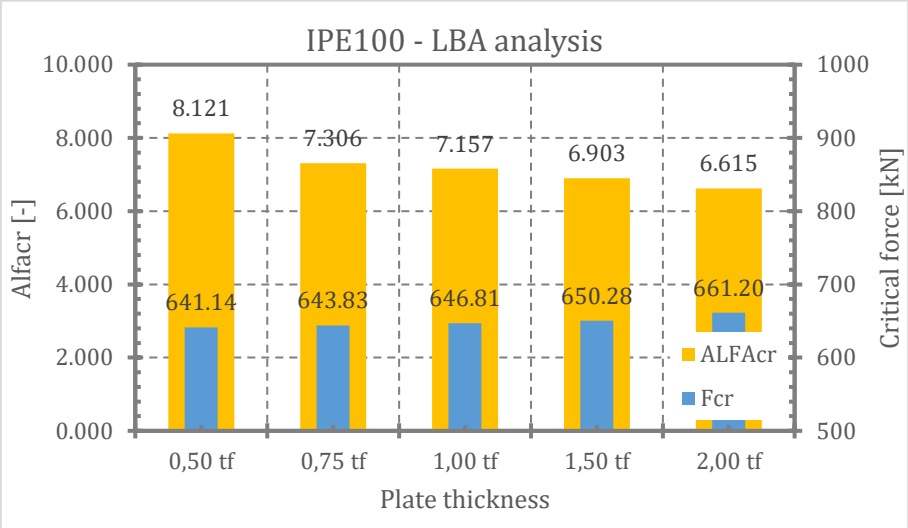


*Fig. 69 Influence of loading plates thickness – LBA results*

Fig. 70 illustrates relationship of vertical deformation and loading force for MNA and GMNIA. Fig. 71 describes dependency of lateral deformation in the middle of beam web on loading force for MNA and GMNIA. Dependency of maximal equivalent stress and equivalent stress in the middle of member web on loading force is plotted in Fig. 72 and Fig. 73. Fig. 74 shows developing of plastic strain with loading increasing.

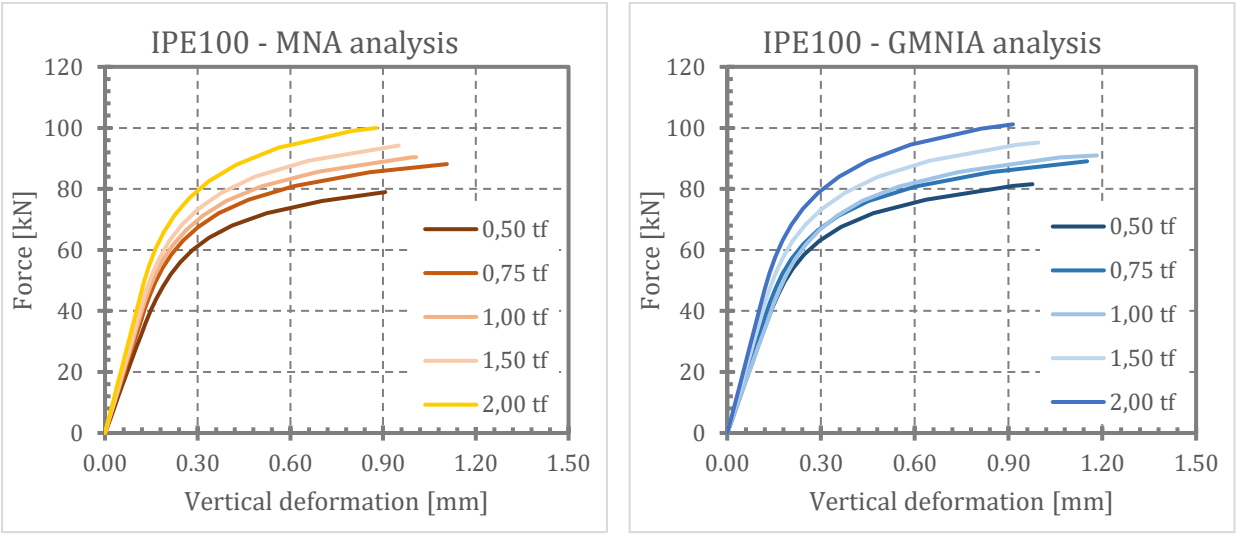


*Fig. 70 Influence of loading plates thickness – vertical deformation-force relationship*

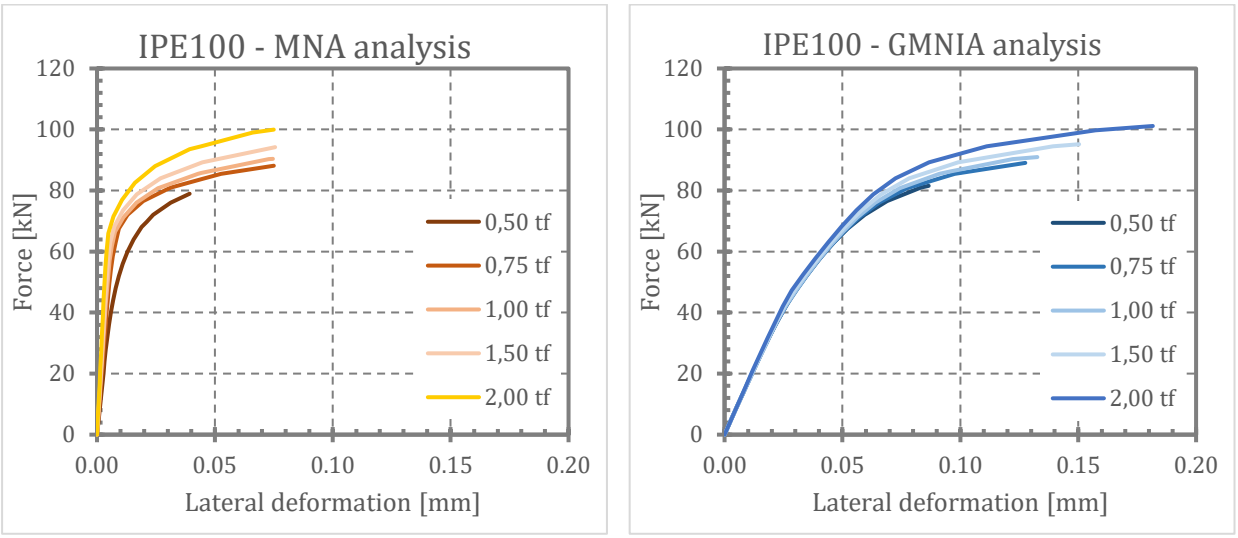


*Fig. 71 Influence of loading plates thickness – lateral deformation-force relationship*

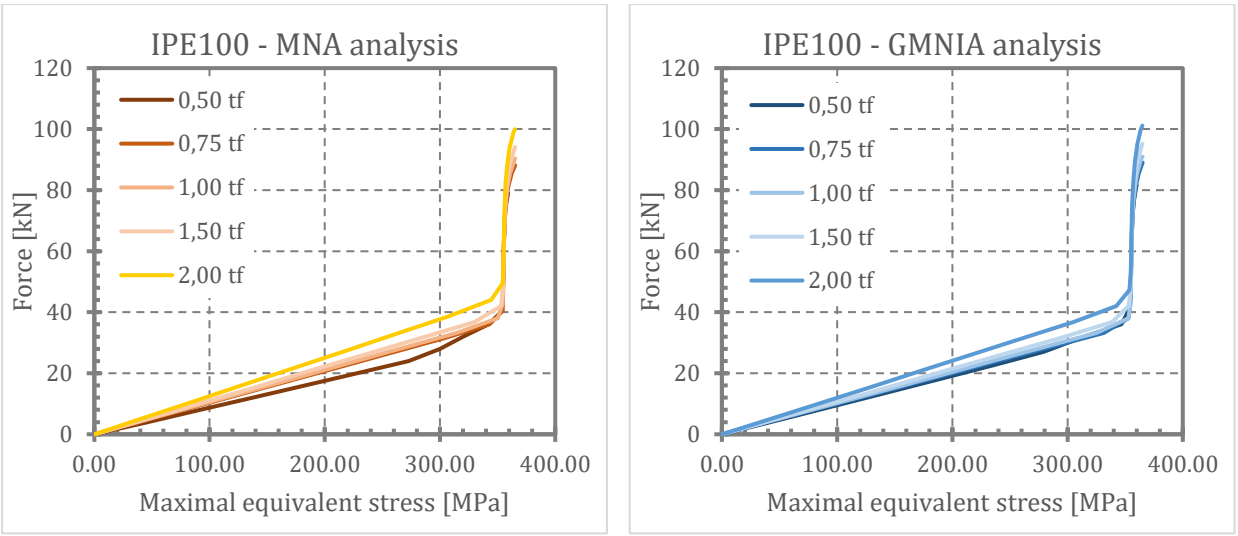


*Fig. 72 Influence of loading plates thickness – maximal equivalent stress-force relationship*

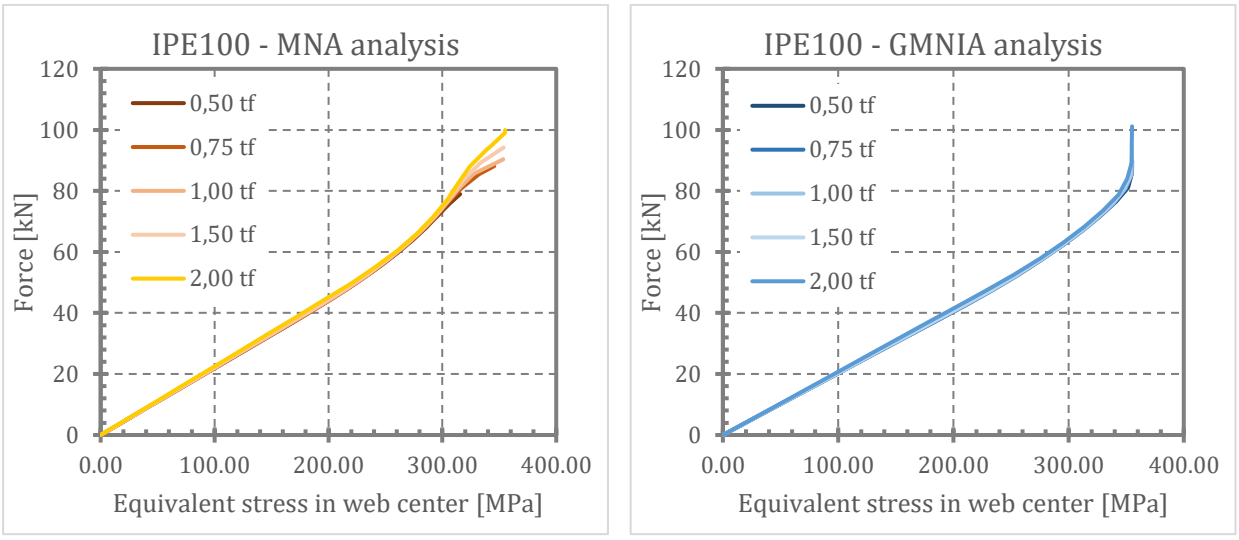


*Fig. 73 Influence of loading plates thickness – equivalent stress in web center-force relationship*

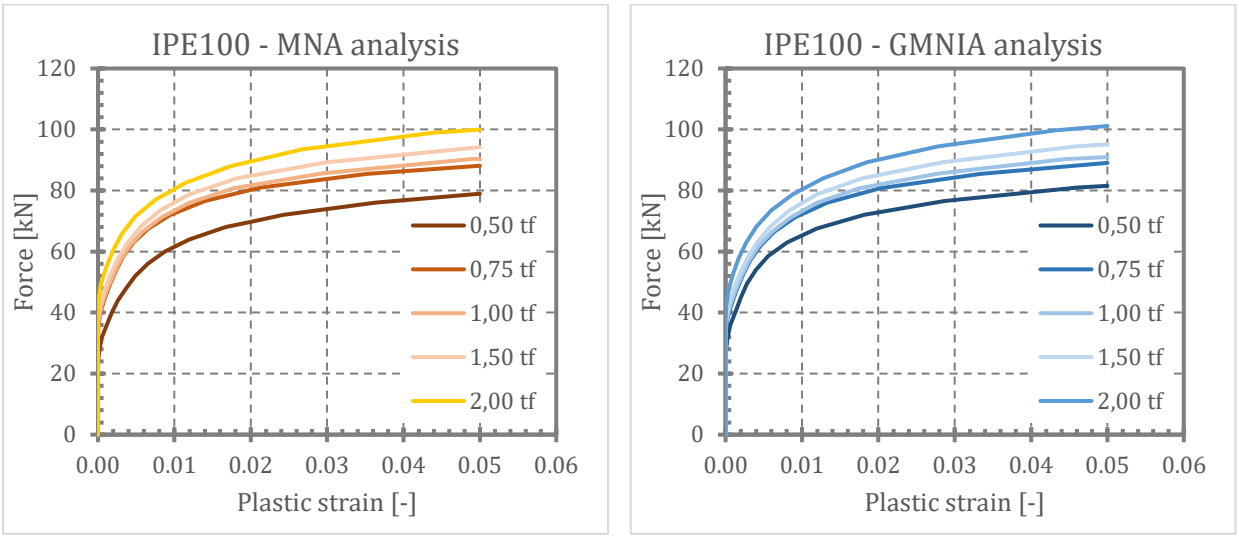


*Fig. 74 Influence of loading plates thickness – plastic strain-force relationship*

Fig. 75 and Fig. 76 show comparison of load-carrying capacities obtained from all investigated cases and by all used methods related to the ANSYS results (i.e. ANSYS results are equal to 1.0).

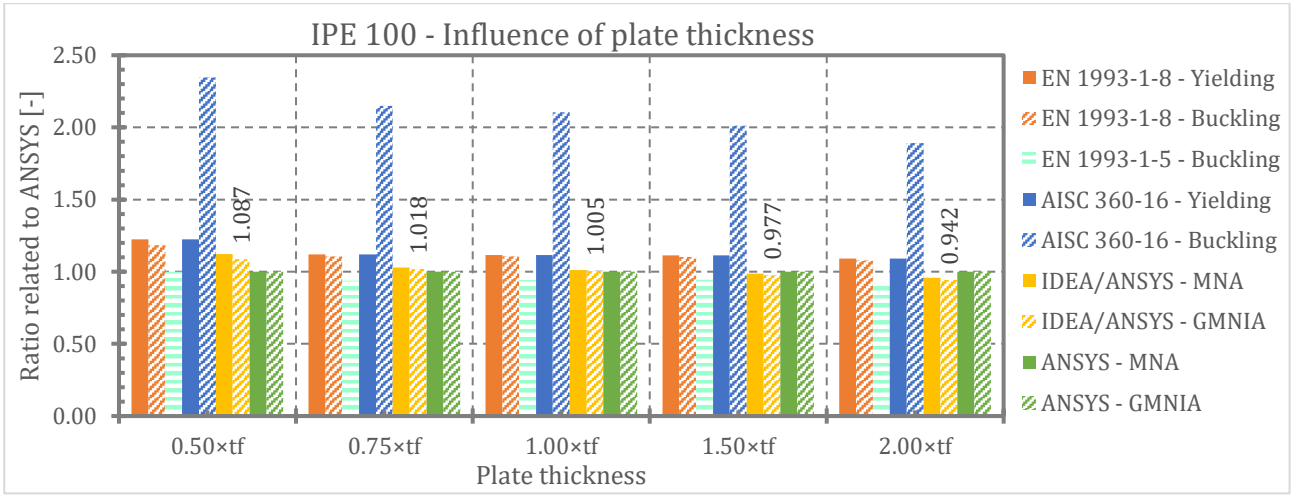


*Fig. 75 Influence of loading plates thickness – comparison of Load-carrying capacity related to the ANSYS results*

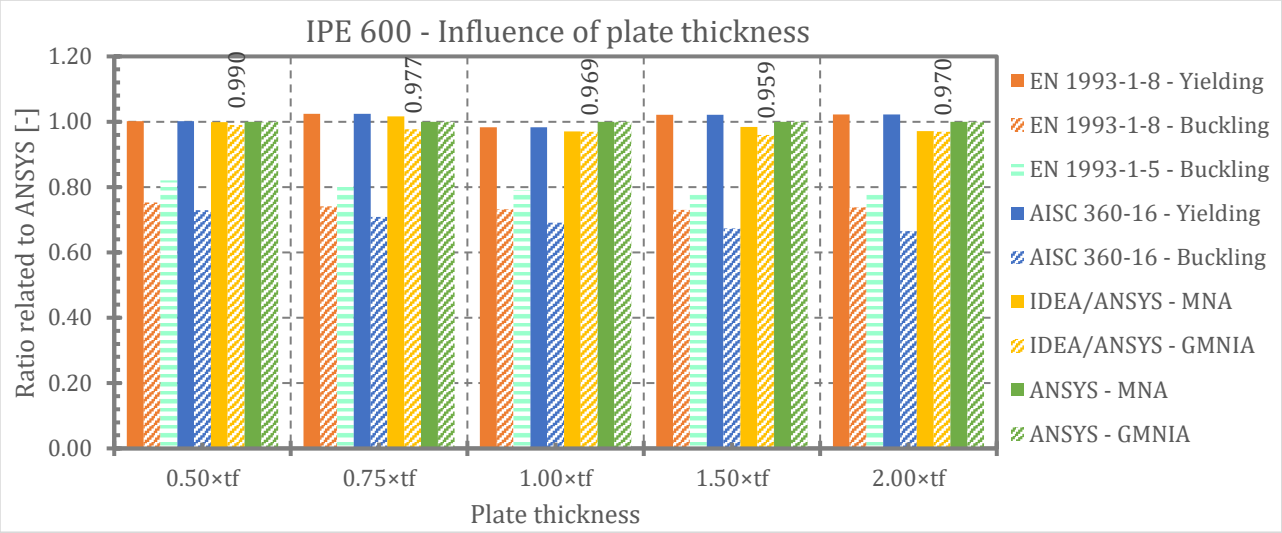


*Fig. 76 Influence of loading plates thickness – comparison of Load-carrying capacity related to the ANSYS results*

### 4.3.3. Conclusion

Loading plates thickness influences load-carrying capacity of transversally compressed member. Load-carrying capacity is increasing with increasing thickness. But this effect has not the same relative value – change of plate thickness stronger influences smaller members than greater members, it is caused by ratio of transversally compressed member flange thickness, radius and section height. For example, at transversally compressed member IPE 100 load-carrying capacity for loading plate thickness $t_p = 2.0 \times t_f$ increase is about 5% according to the IDEA StatiCa or 10% according to the ANSYS, at transversally compressed member IPE 600 load-carrying capacity for loading plate thickness $t_p = 2.0 \times t_f$ increase about 4% according to the both IDEA StatiCa and ANSYS.

IDEA StatiCa numerical simulations give very similar results in comparison with ANSYS software – for greater sections (in this study IPE 600) slightly on the safe side (the difference vary from 1% to 4%), but in the case of less slender sections (in this study IPE 100) the results may be slightly on the unsafe side (the difference vary from +6% to -9 %).

At all other cases in this study loading plates thickness $t_p$ is considered the same as transversally compressed member flange thickness $t_f$.

## 4.4. Influence of rounded corners of rolled sections and throat welds of welded sections

The aim of this section is to evaluate the relevance of the geometry of the web-flange transition on resistance of the web in transverse compression. It is assumed that the geometry of the web-flange transition influences the distribution of the transverse load from its position of application (on the flange) to the member web. To assess this effect, three different types of numerical models were created in ANSYS computation system: (i) precise solid models that include rounded corners of rolled sections or throat welds of welded sections, (ii) solid models without rounded corners or welds and shell models without rounded corners or welds. The comparison of the results of individual types of numerical models can be used for quantification

of this influence and secondly it might indicate the suitability of different types of models for numerical analysis of transverse compression resistance.

### 4.4.1. Methodology

The study was performed on members of selected rolled and welded cross-sections with transverse load applied through the "loading plate" and identical boundary conditions as in previous sections. Steel grade S355 was considered.

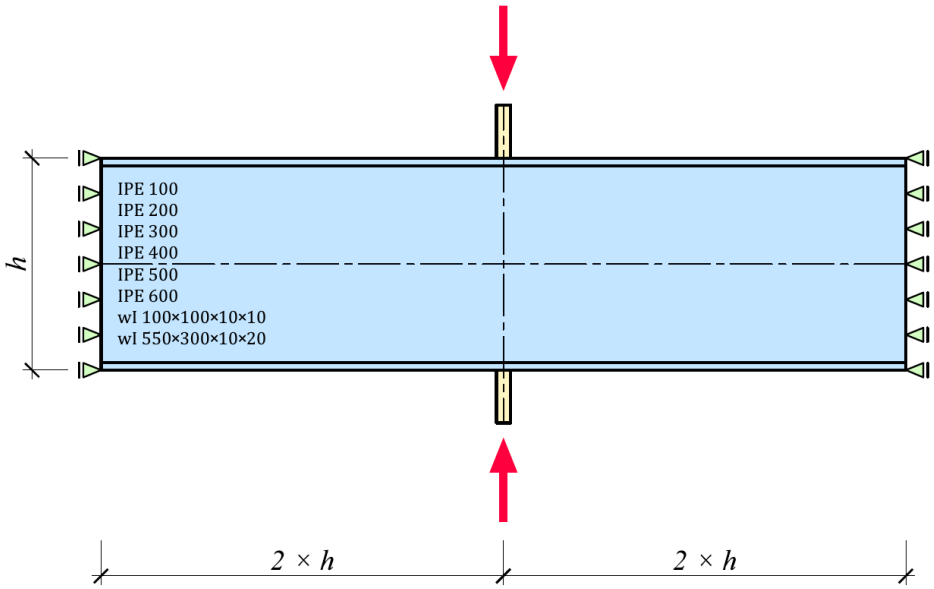


*Fig. 77 Influence of rounded corners or throat welds – geometry and boundary conditions*

In ANSYS computational system the members were modelled in three types of finite element models: (i) solid model with precise consideration of the actual geometry of the cross-section (including rounded corners of given radius or throat welds of certain throat thickness) created using volume elements, (ii) solid model with no rounded corners or throat welds at the web-flange transition (simplified model) created using volume elements and (iii) model created using shell elements with assigned thickness.

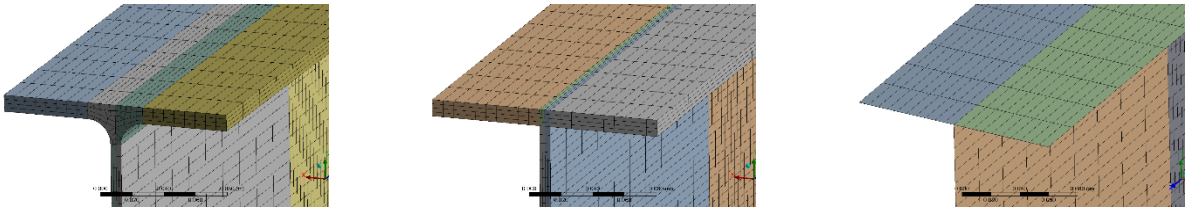

(a) (b) (c)

*Fig. 78 Types of numerical models: (a) precise solid, (b) simplified solid, (c) shell*

The models were in all cases subjected to MNA, LBA and GMNIA analysis with identical assumptions (material model, initial geometric imperfection, number of substeps etc.) and evaluation procedure as in previous sections. The analysis of the members in IDEA StatiCa followed the procedure described in section 2.2.3. Resistances according to EN 1993-1-8, EN 1993-1-5 and AISC 360-16 were calculated for yielding and buckling of the member web.

### 4.4.2. Results

The results of numerical analysis and calculation according to design codes are summarized in Tab. 8 and Tab. 9 for IPE rolled cross-sections and selected welded cross-sections.

*Tab. 8 Influence of rounded corners or throat welds – IPE and welded cross-sections – Load-carrying capacity [kN]*

| Cross-section | EN 1993-1-8 | | EN 1993-1-5 | AISC 360-16 | | IDEA StatiCa | |
|---|---|---|---|---|---|---|---|
| | Yield. | Buckl. | Buckling | Yield. | Buckl. | MNA | GMNIA |
| IPE 100 | 100.72 | 100.72 | 85.66 | 100.72 | 191.45 | 89.85 | 89.85 |
| IPE 200 | 220.67 | 189.34 | 192.50 | 220.67 | 228.88 | 187.50 | 185.55 |
| IPE 300 | 350.85 | 279.84 | 295.44 | 350.85 | 298.34 | 322.25 | 320.30 |
| IPE 400 | 567.86 | 420.71 | 424.45 | 567.86 | 398.20 | 500.00 | 496.10 |
| IPE 500 | 727.82 | 541.62 | 582.03 | 727.82 | 516.21 | 710.90 | 707.00 |
| IPE 600 | 996.84 | 737.56 | 797.18 | 996.84 | 696.65 | 984.40 | 976.60 |
| wI 100×100×10×10 | 288.31 | 288.31 | 331.02 | 288.31 | 2897.61 | 312.50 | 312.50 |
| wI 550×300×100×20 | 526.41 | 408.22 | 618.40 | 526.41 | 415.54 | 937.50 | 914.10 |

*Tab. 9 Influence of rounded corners or throat welds – IPE, welded – Load-carrying capacity [kN]*

| Cross-section | ANSYS | | | | | |
|---|---|---|---|---|---|---|
| | Solid model (with round. corners/welds) | | Solid model (without round. corners/welds) | | Shell model | |
| | MNA | GMNIA | MNA | GMNIA | MNA | GMNIA |
| IPE 100 | 90.38 | 90.97 | 68.54 | 69.21 | 58.66 | 61.30 |
| IPE 200 | 205.68 | 209.60 | 154.67 | 156.41 | 137.51 | 142.27 |
| IPE 300 | 348.54 | 348.18 | 260.89 | 263.85 | 234.30 | 240.56 |
| IPE 400 | 561.44 | 559.20 | 405.06 | 409.68 | 366.45 | 376.72 |
| IPE 500 | 741.92 | 736.68 | 564.92 | 571.50 | 515.93 | 527.97 |
| IPE 600 | 1013.99 | 1007.42 | 785.74 | 795.54 | 714.05 | 731.02 |
| wI 100×100×10×10 | 279.98 | 280.79 | 249.54 | 250.61 | 181.92 | 195.34 |
| wI 550×300×100×20 | 901.61 | 899.52 | 810.95 | 830.65 | 666.77 | 712.61 |

In Fig. 80 ratios of MNA and GMNIA resistances obtained from simplified models (solid models without rounded corners or welds and shell models) related to the precise solid models with rounded corners or welds are shown. Fig. 79 summarizes results of calculations according to design codes, IDEA StatiCa software and precise solid finite element models with rounded corners or welds.

Note: EN 1993-1-8 and AISC 360-16 provide identical yielding resistances, therefore in the respective figures the points corresponding to the yielding resistances according to these design codes coincide.

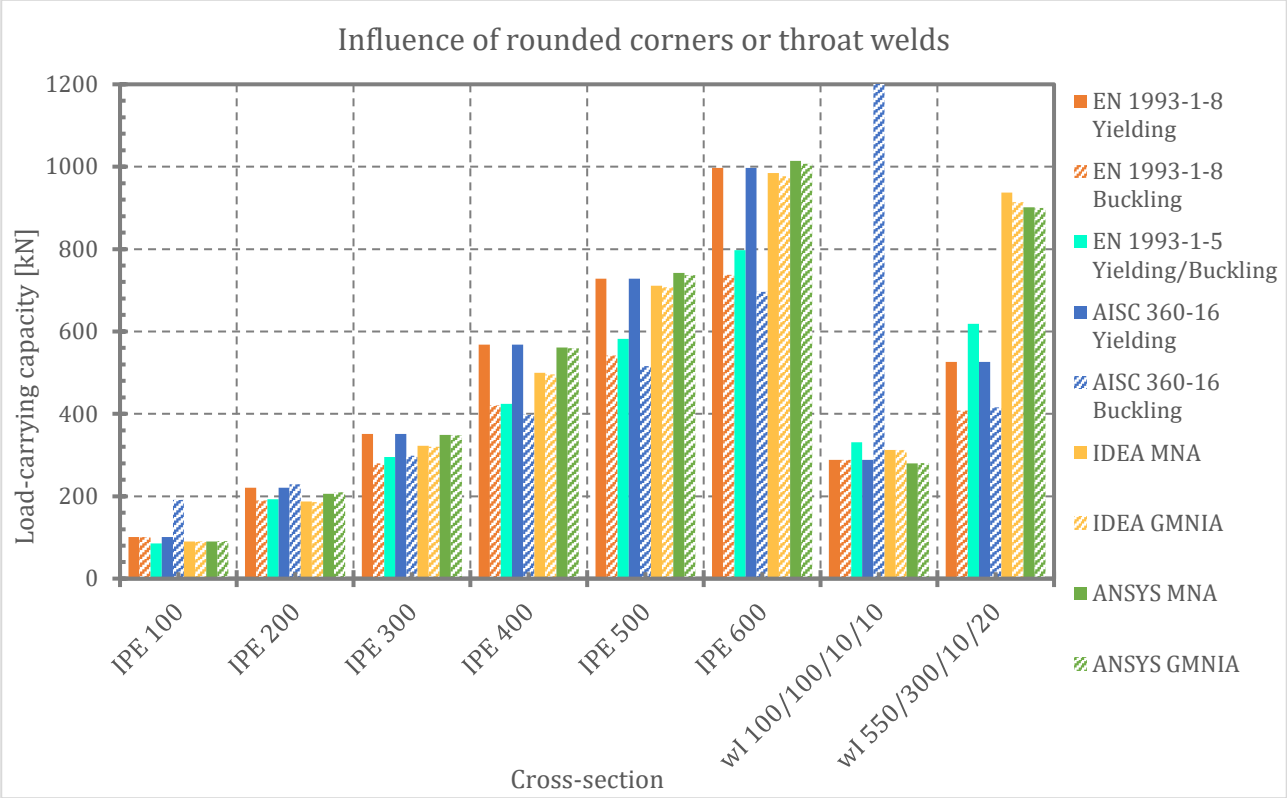


*Fig. 79 Influence of rounded corners or throat welds – IPE, welded – load-carrying capacity*

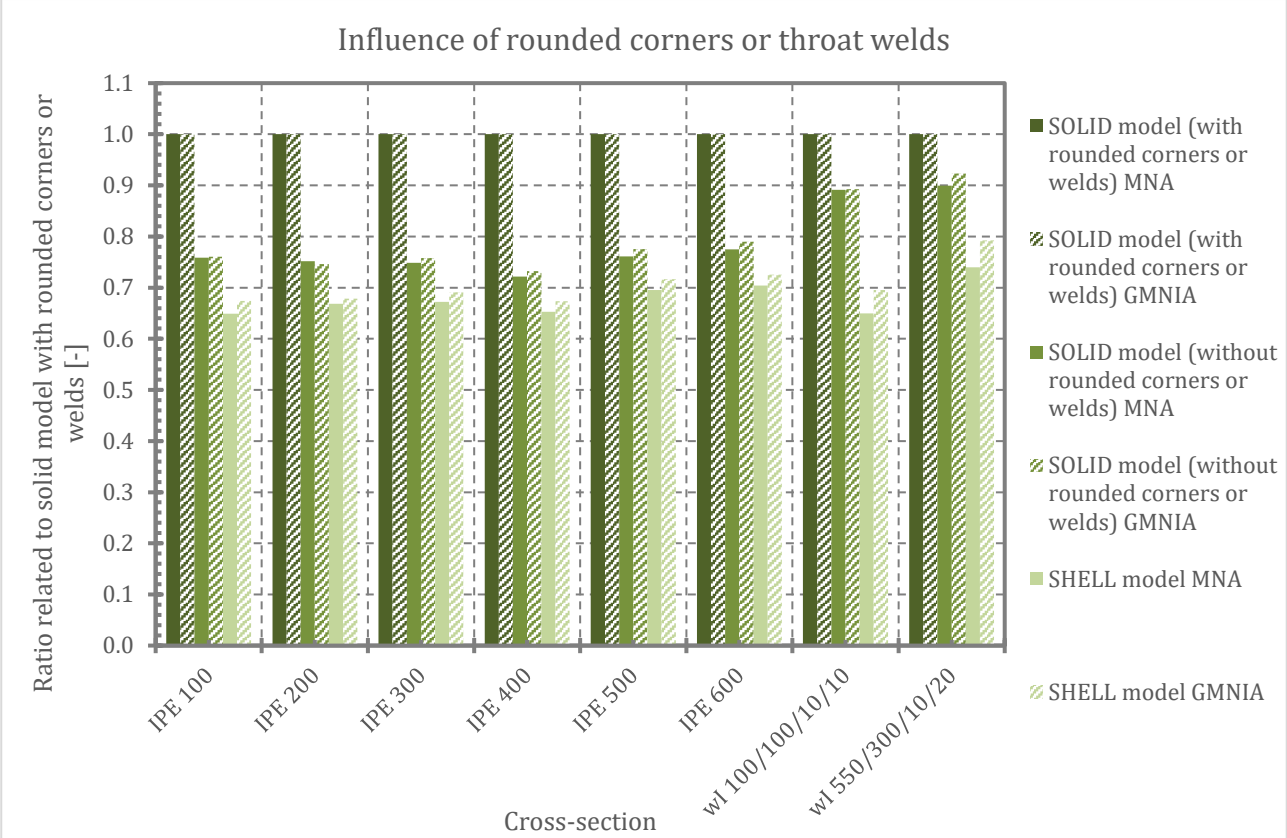


*Fig. 80 Influence of rounded corners or throat welds – resistance ratio related to precise solid models*

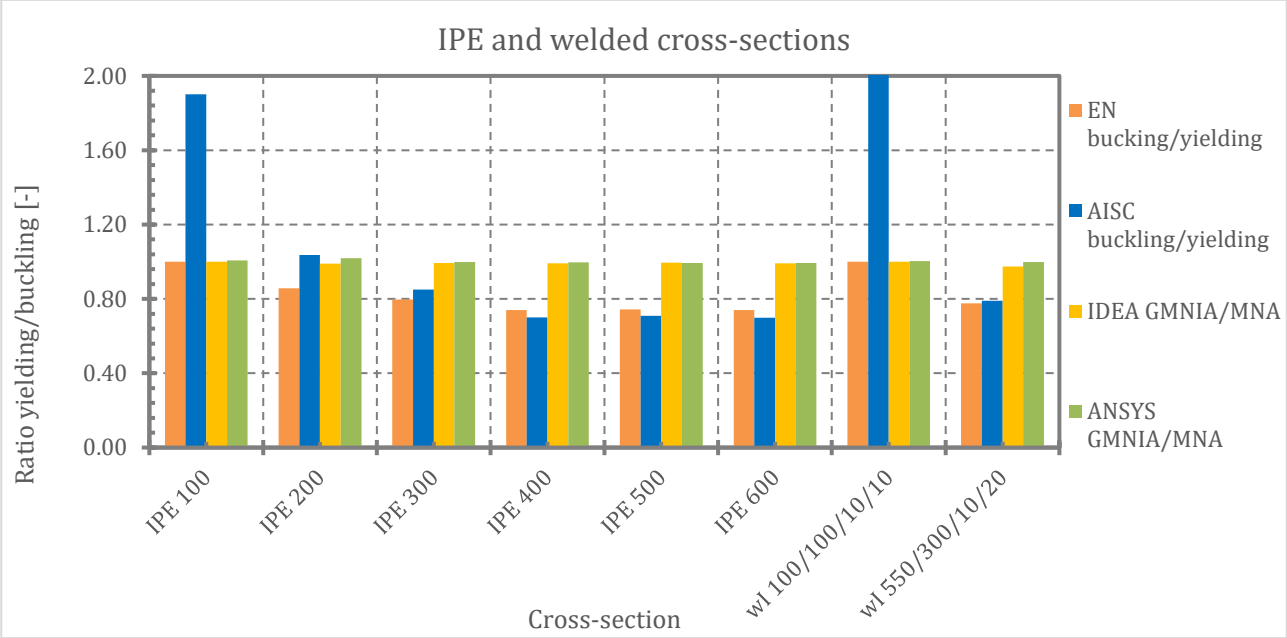


*Fig. 81 Influence of rounded corners or throat welds – IPE, welded – load-carrying capacity*

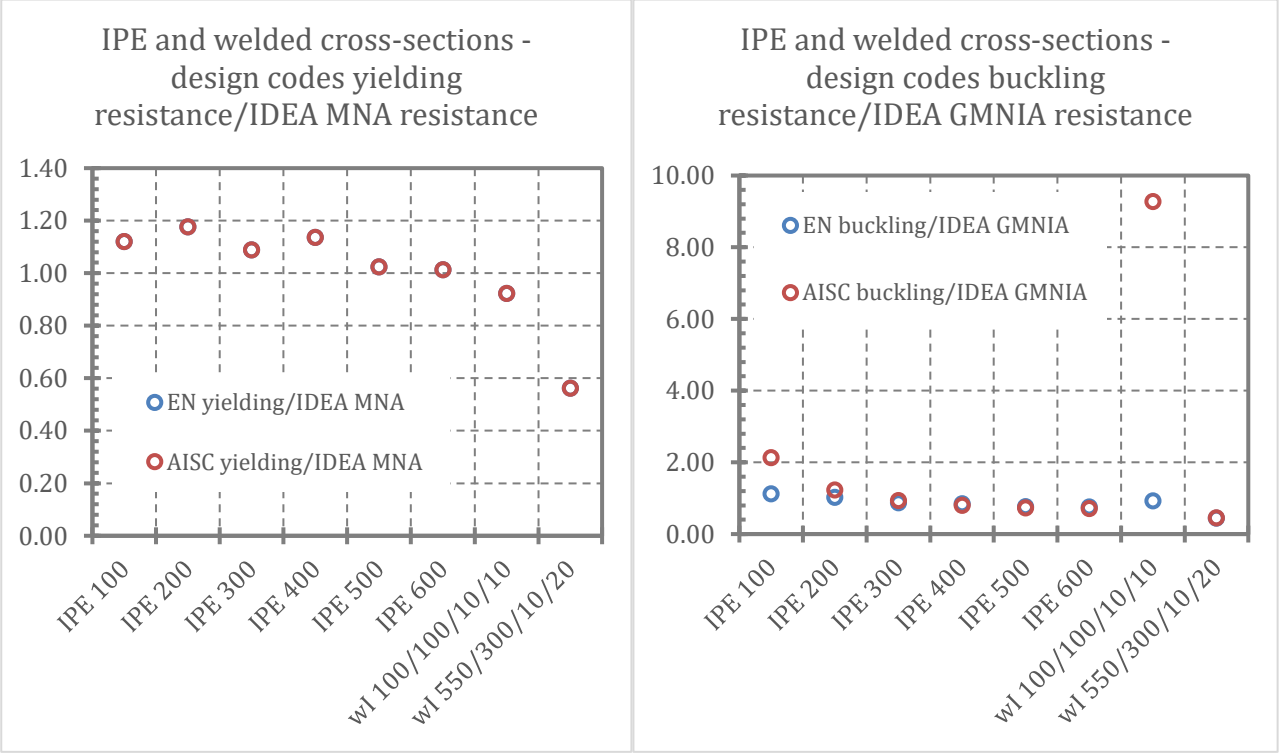


*Fig. 82 Ratio between design code resistances and FEM resistances – IPE, welded cross-sections*

In the following tables results of design code calculations and numerical analysis performed in IDEA StatiCa are presented for selected HEA, HEB and American W cross-sections. As the influence of the type of numerical model (solid models with or without rounded corners or welds, shell models) was evaluated above, for these cross-sections this investigation was not performed.

*Tab. 10 HEB cross-sections – Load-carrying capacity [kN]*

| Cross-section | EN 1993-1-8 | | EN 1993-1-5 | AISC 360-16 | | IDEA StatiCa | |
|---|---|---|---|---|---|---|---|
| | Yield. | Buckl. | Buckling | Yield. | Buckl. | MNA | GMNIA |
| HEB 100 | 255.60 | 255.60 | 237.81 | 255.60 | 799.28 | 214.80 | 214.80 |
| HEB 200 | 575.10 | 575.10 | 595.62 | 575.10 | 1127.35 | 496.10 | 496.10 |
| HEB 300 | 972.35 | 917.07 | 951.83 | 972.35 | 1326.02 | 820.30 | 816.40 |
| HEB 400 | 1337.11 | 1234.48 | 1348.05 | 1337.11 | 1710.88 | 1257.8 | 1250.0 |
| HEB 500 | 1559.69 | 1338.88 | 1487.12 | 1559.69 | 1619.85 | 1601.6 | 1593.8 |
| HEB 600 | 1733.29 | 1421.39 | 1596.94 | 1733.29 | 1587.79 | 1843.8 | 1821.6 |
| HEB 700 | 1973.45 | 1598.69 | 1824.68 | 1973.45 | 1749.28 | 2085.9 | 2074.2 |
| HEB 800 | 2161.95 | 1654.18 | 1848.46 | 2161.95 | 1647.74 | 2331.9 | 2320.2 |
| HEB 900 | 2364.30 | 1770.39 | 2007.00 | 2364.30 | 1703.96 | 2543.1 | 2519.4 |
| HEB 1000 | 2468.67 | 1789.60 | 2053.60 | 2468.67 | 1637.48 | 2648.4 | 2625.0 |

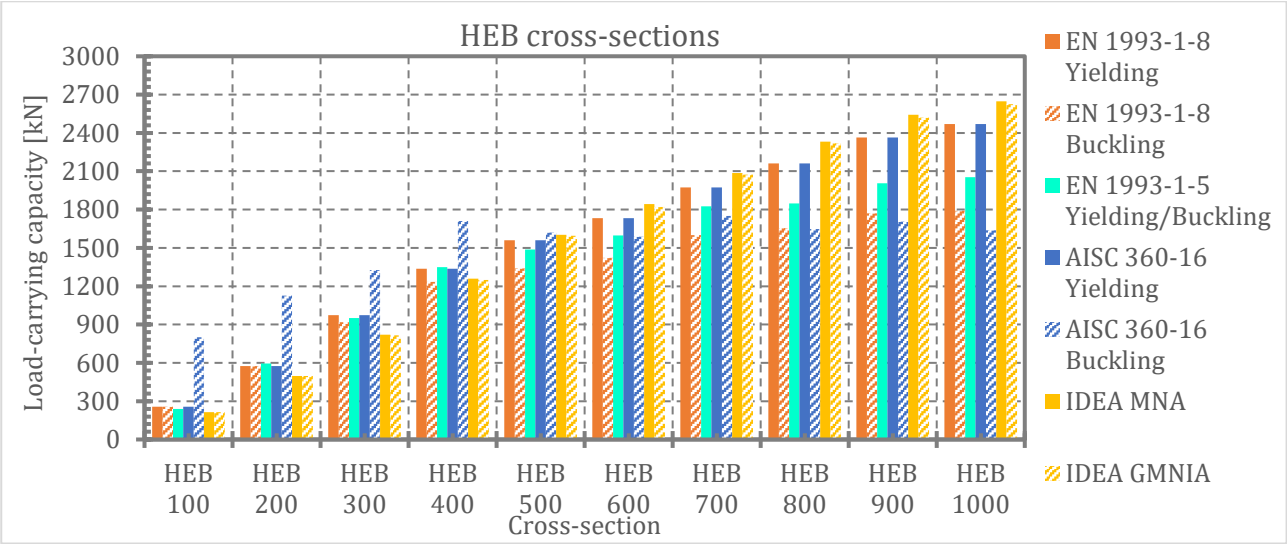


*Fig. 83 Influence of rounded corners or throat welds – HEB cross-sections – load-carrying capacity*

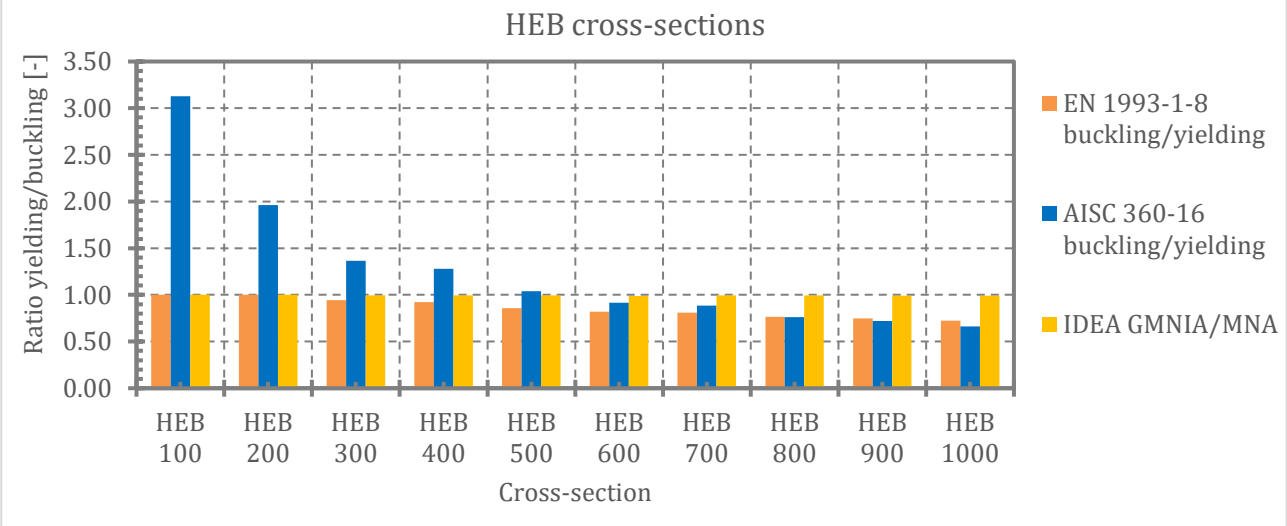


*Fig. 84 HEB cross-sections – ratio yielding resistance / buckling resistance (EN 1993-1-8 and AISC 360-16) and GMNIA/MNA resistances (IDEA StatiCa)*

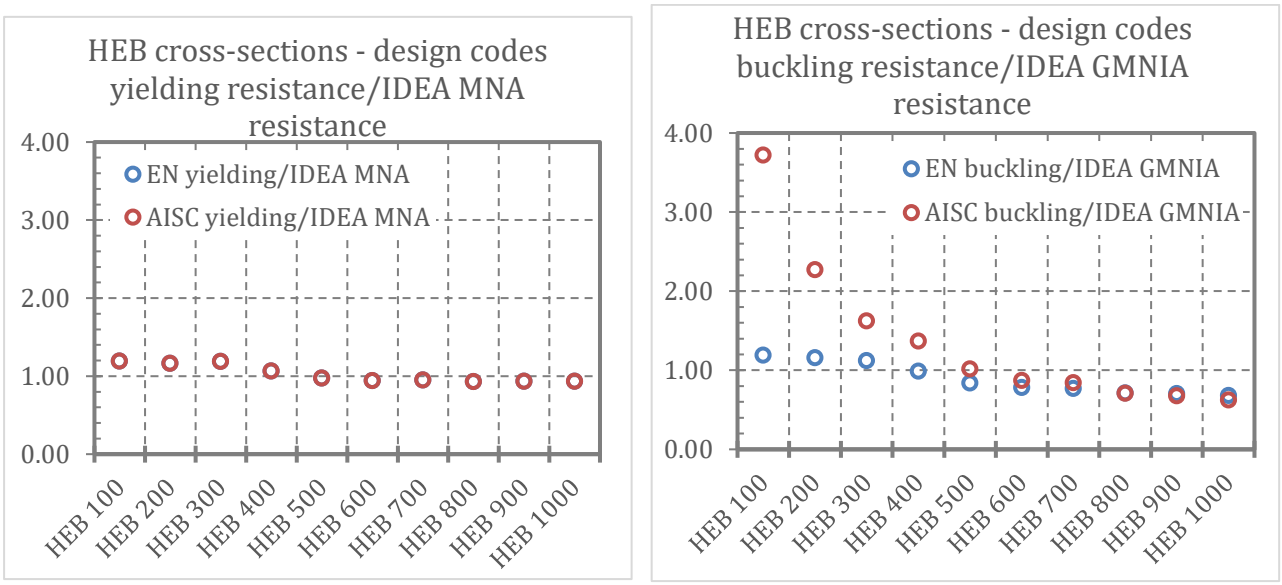


*Fig. 85 Ratio between design code resistances and FEM resistances – HEB cross-sections*

*Tab. 11 HEA cross-sections – Load-carrying capacity [kN]*

| Cross-section | EN 1993-1-8 | | EN 1993-1-5 | AISC 360-16 | | IDEA StatiCa | |
|---|---|---|---|---|---|---|---|
| | Yield. | Buckl. | Buckling | Yield. | Buckl. | MNA | GMNIA |
| HEA 100 | 191.70 | 191.70 | 169.61 | 191.70 | 462.55 | 156.30 | 156.30 |
| HEA 200 | 346.13 | 315.03 | 309.34 | 346.13 | 424.69 | 261.70 | 261.70 |
| HEA 300 | 660.83 | 544.05 | 519.40 | 660.83 | 611.83 | 503.90 | 500.00 |
| HEA 400 | 972.35 | 808.71 | 837.36 | 972.35 | 925.54 | 851.60 | 851.60 |
| HEA 500 | 1162.98 | 901.90 | 966.59 | 1162.98 | 918.15 | 1148.40 | 1140.60 |
| HEA 600 | 1315.28 | 980.36 | 1072.44 | 1315.28 | 936.76 | 1351.60 | 1343.80 |
| HEA 700 | 1528.81 | 1138.15 | 1273.01 | 1528.81 | 1085.47 | 1664.10 | 1652.40 |
| HEA 800 | 1693.35 | 1189.65 | 1307.07 | 1693.35 | 1037.65 | 1828.20 | 1804.80 |
| HEA 900 | 1874.40 | 1295.39 | 1450.43 | 1874.40 | 1102.31 | 2027.40 | 2004.00 |
| HEA 1000 | 1968.12 | 1318.99 | 1500.48 | 1968.12 | 1072.43 | 2121.00 | 2097.60 |

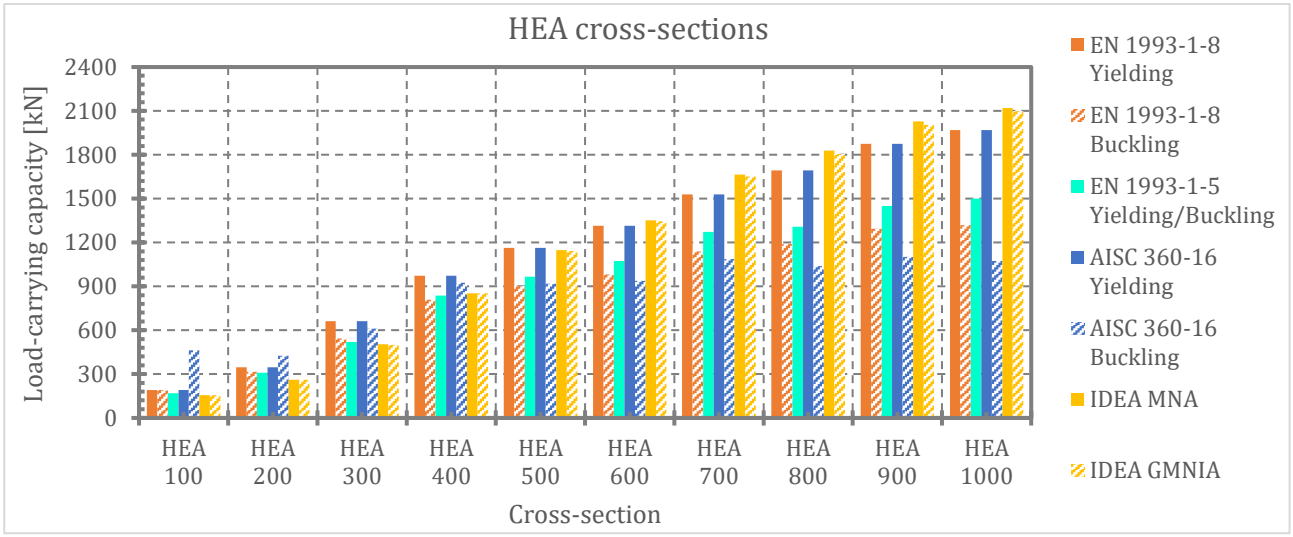


*Fig. 86 Influence of rounded corners or throat welds – HEA cross-sections – load-carrying capacity*

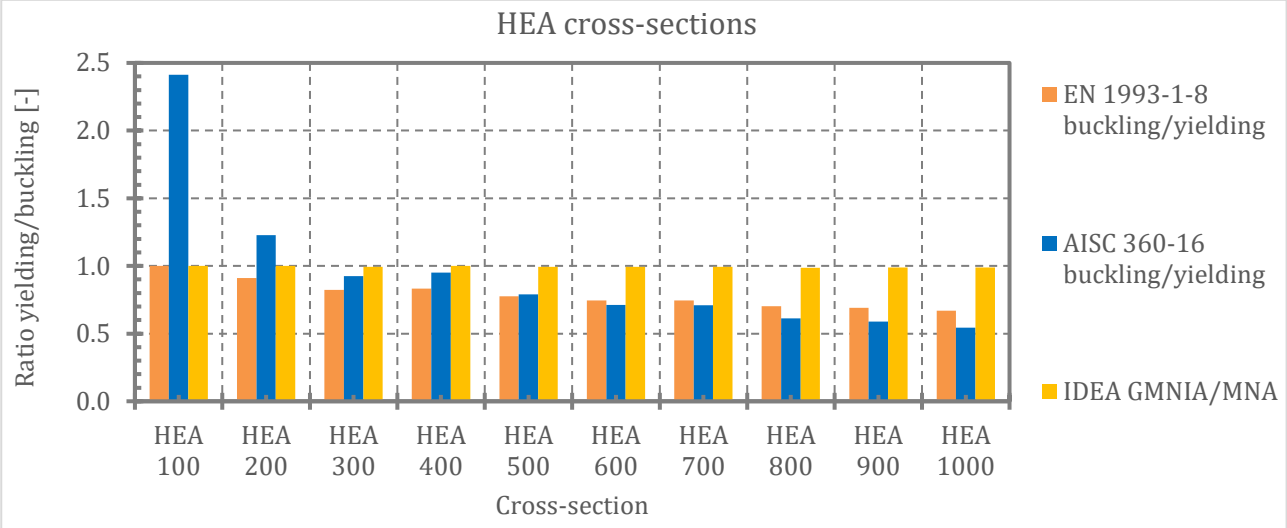


*Fig. 87 HEA cross-sections – ratio yielding resistance / buckling resistance (EN 1993-1-8 and AISC 360-16) and GMNIA/MNA resistances (IDEA StatiCa)*

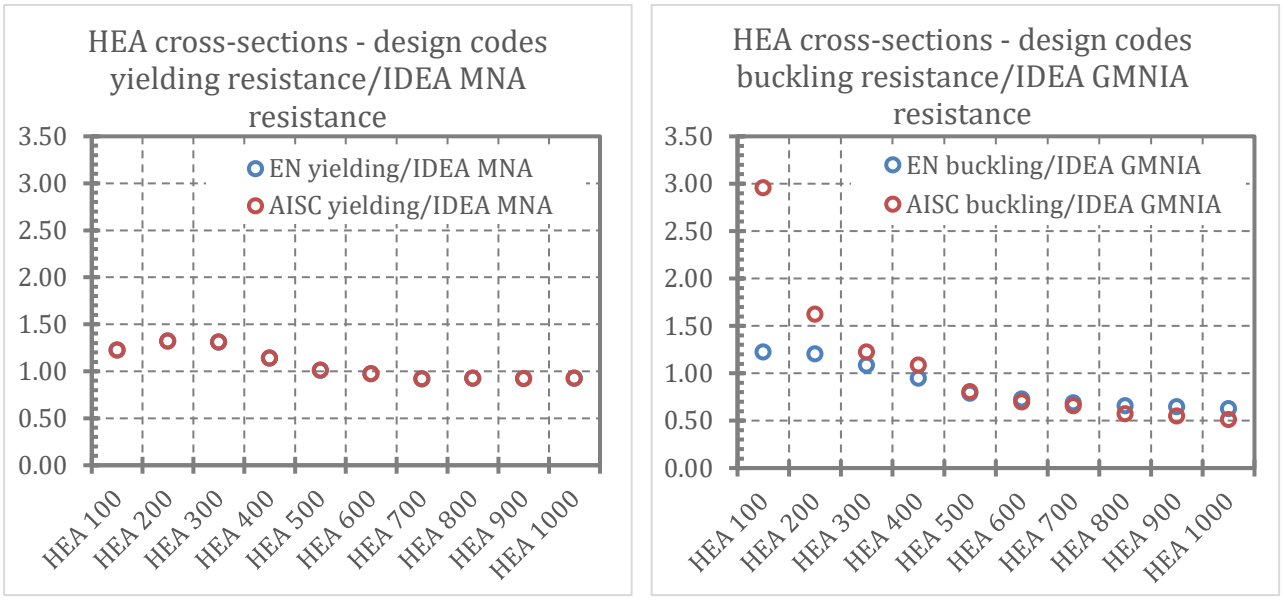


*Fig. 88 Ratio between design code resistances and FEM resistances – HEA cross-sections*

*Tab. 12 W cross-sections – Load-carrying capacity [kN]*

| Cross-section | EN 1993-1-8 | | EN 1993-1-5 | AISC 360-16 | | IDEA StatiCa | |
|---|---|---|---|---|---|---|---|
| | Yield. | Buckl. | Buckling | Yield. | Buckl. | MNA | GMNIA |
| W12X14 | 173.64 | 112.46 | 115.59 | 173.64 | 87.00 | 140.62 | 139.06 |
| W16X26 | 328.30 | 208.59 | 211.82 | 328.30 | 157.00 | 270.32 | 267.20 |
| W16X36 | 432.17 | 316.96 | 337.55 | 432.17 | 295.28 | 376.95 | 373.05 |
| W21X55 | 552.08 | 406.38 | 468.97 | 552.08 | 380.77 | 585.90 | 582.00 |
| W18X46 | 589.85 | 452.02 | 508.25 | 589.85 | 451.39 | 589.80 | 585.90 |
| W30X90 | 930.55 | 680.28 | 808.06 | 930.55 | 630.62 | 898.40 | 886.70 |
| W40X149 | 1478.29 | 1060.13 | 1196.74 | 1478.29 | 954.03 | 1101.60 | 1093.80 |
| W36X150 | 1477.73 | 1088.42 | 1326.65 | 1477.73 | 1020.79 | 1656.20 | 1640.60 |

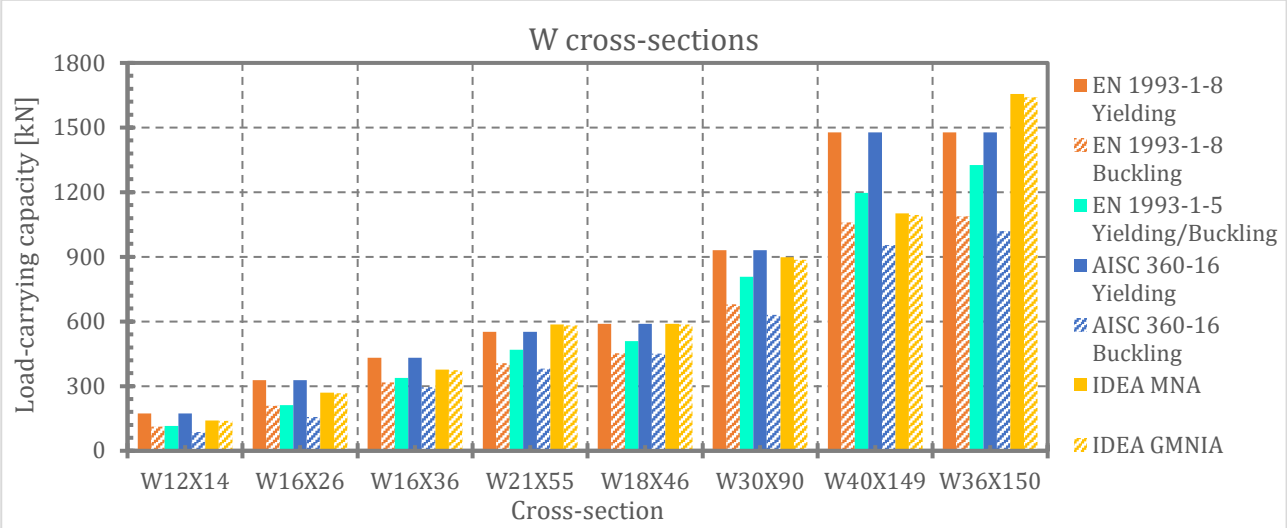


*Fig. 89 Influence of rounded corners or throat welds – W cross-sections – load-carrying capacity*

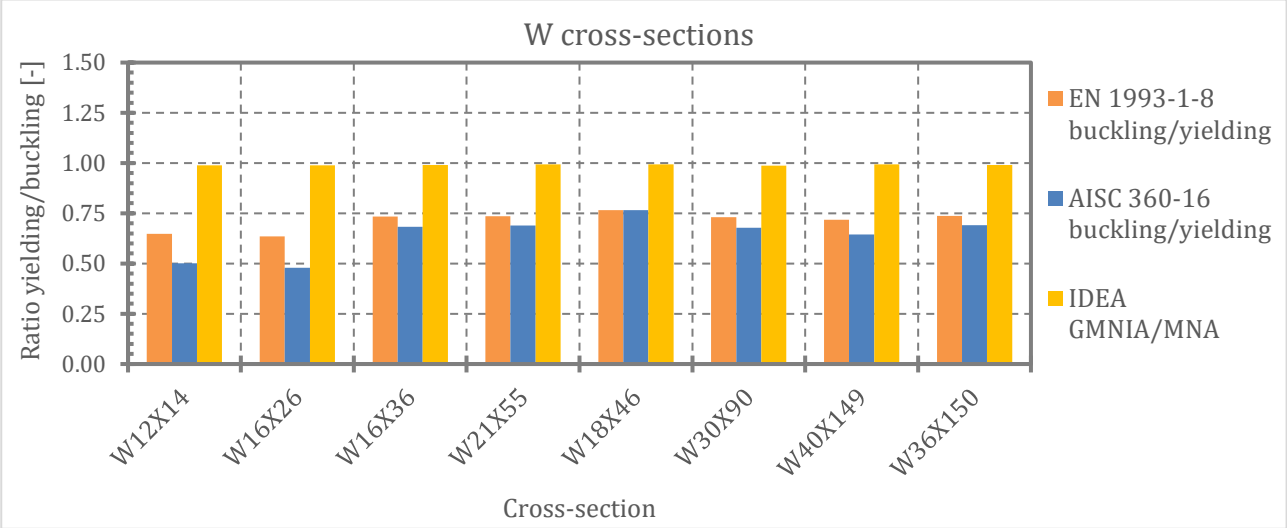


*Fig. 90 HEA cross-sections – ratio yielding resistance / buckling resistance (EN 1993-1-8 and AISC 360-16) and GMNIA/MNA resistances (IDEA StatiCa)*

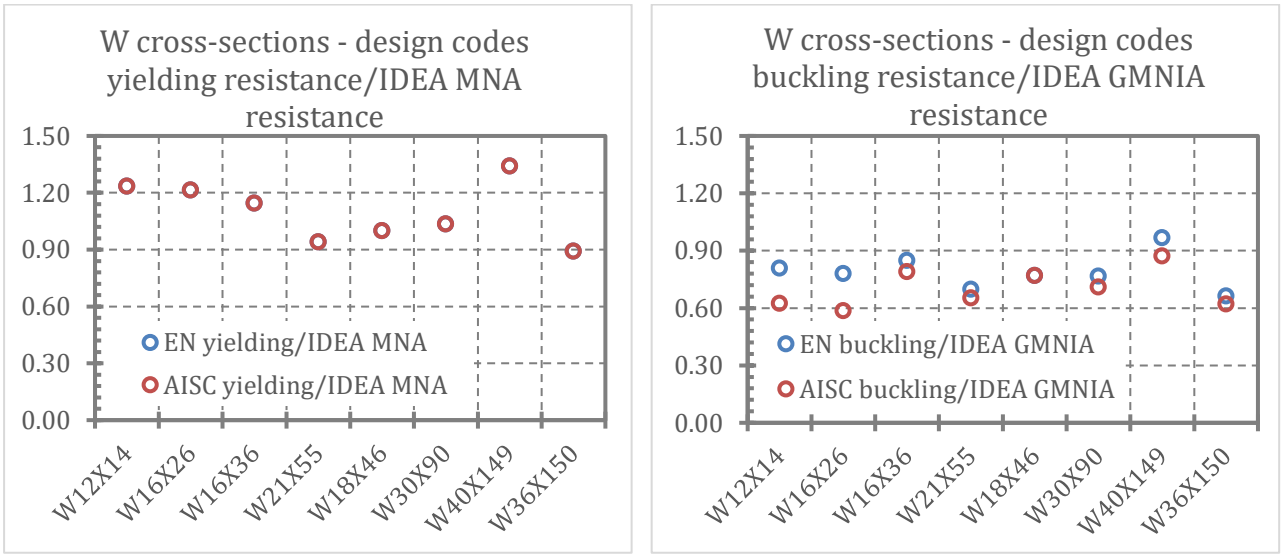


*Fig. 91 Ratio between design code resistances and FEM resistances – W cross-sections*

The results of simplified solid numerical models (with no rounded corners or fillet welds) of selected cross-sections are compared with design codes resistances calculated with the assumptions of cross-sections without rounded corners or welds (therefore the cross-sections considered for design codes calculations correspond to the simplified numerical models).

The resistances obtained from design codes and from numerical analysis are summarized in Tab. 13.

*Tab. 13 Influence of rounded corners or throat welds – IPE and welded cross-sections – Load-carrying capacity [kN] – cross-sections with no rounded corners or welds*

| Cross-section | EN 1993-1-8 (cross-sections without rounded corners/welds) | | AISC 360-16 (cross-sections without rounded corners/welds) | | ANSYS Solid model (without rounded corners/welds) | |
|---|---|---|---|---|---|---|
| | Yield. | Buckl. | Yield. | Buckl. | MNA | GMNIA |
| IPE 100 | 49.78 | 49.78 | 49.78 | 161.20 | 68.54 | 69.21 |
| IPE 200 | 101.39 | 101.39 | 101.39 | 198.86 | 154.67 | 156.41 |
| IPE 300 | 161.82 | 162.07 | 161.82 | 266.21 | 260.89 | 263.85 |
| IPE 400 | 247.29 | 236.84 | 247.29 | 353.36 | 405.06 | 409.68 |
| IPE 500 | 347.62 | 326.90 | 347.62 | 469.88 | 564.92 | 571.50 |
| IPE 600 | 485.64 | 452.16 | 485.64 | 637.15 | 785.74 | 795.54 |
| wI 100×100×10×10 | 213.00 | 213.00 | 213.00 | 2590.27 | 249.54 | 250.61 |
| wI 550×300×100×20 | 426.00 | 354.57 | 426.00 | 406.32 | 810.95 | 830.47 |

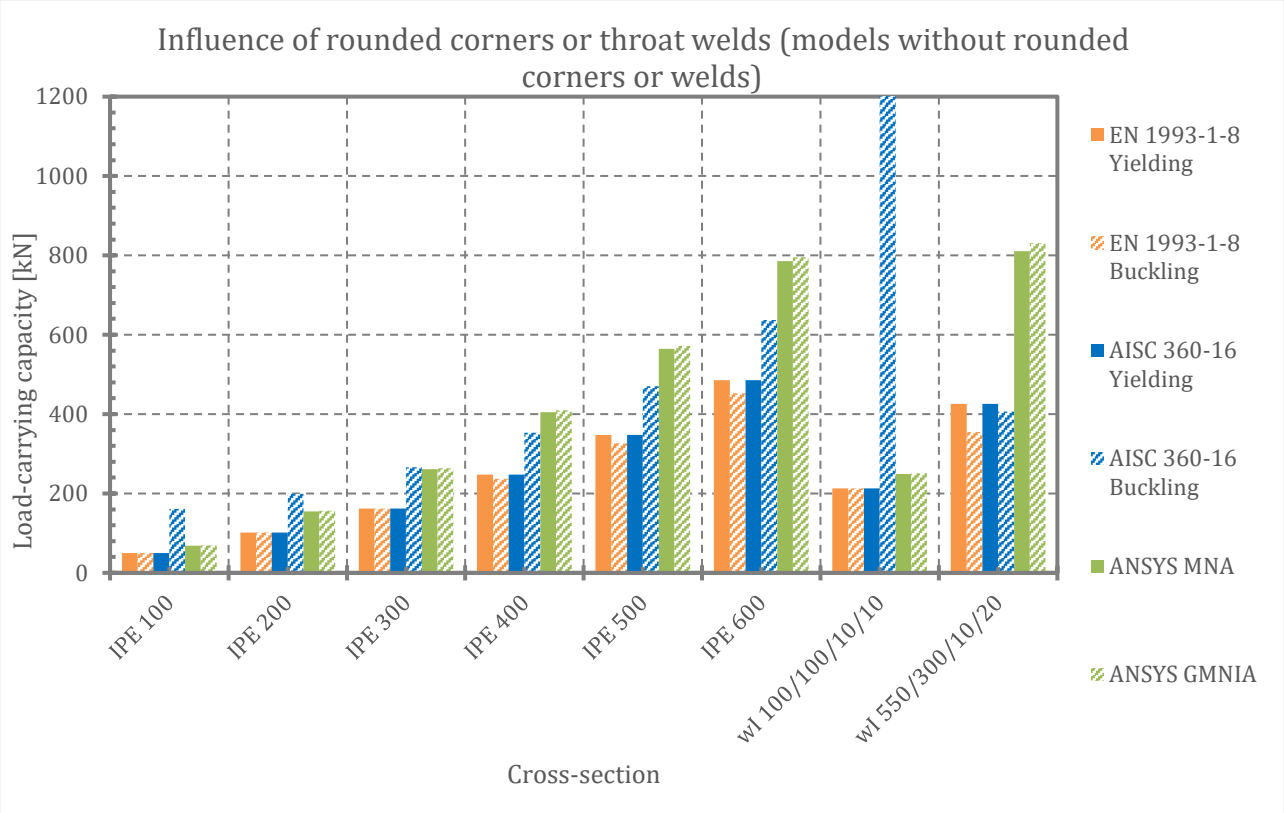


*Fig. 92 Influence of rounded corners or throat welds – IPE, welded – load-carrying capacity*

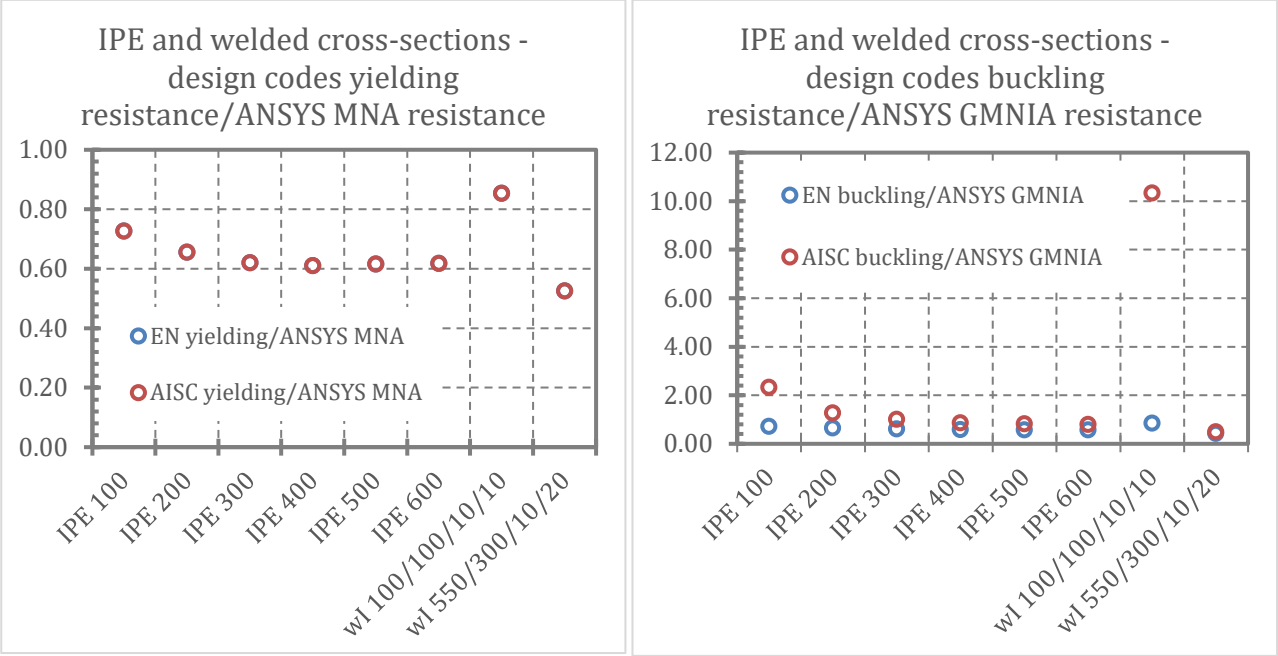


*Fig. 93 Ratio between design code resistances and FEM resistances – IPE, welded cross-sections (without rounded corners or welds)*

### 4.4.3. Conclusion

The comparison of results obtained using different types of numerical models indicate significant influence of the geometry of the web-flange transition of the cross-section on resistance in transverse compression. Neglecting of the rounded corners or throat welds in the model results in significantly lower resistances.

The results of the numerical analysis indicate that the influence of local buckling of the web of the members in terms of the design codes provisions might be overestimated (the ratio between GMNIA resistances and MNA resistances was very close to 1.00 for the investigated cross-sections with various web slenderness).

For all investigated cross-sections the resistances of their web in transverse compression obtained from numerical analysis were, for lower and medium web slenderness, lower than resistances obtained from the design code calculations (EN 1993-1-8, AISC 360-16).

## 4.5. Influence of unstiffened end

This part of study shows the influence of one unstiffened end of transversally compressed member on load-carrying capacity and other results. The goal is to evaluate actual behaviour and make comparison with design resistances according to the EN 1993 and AISC 360-16.

### 4.5.1. Methodology

The study was performed on transversally compressed member of cross-sections IPE 100, 200, 300, 400, 500 and 600 with length on one side from loading plates $L = 2\times h$ (restraining boundary conditions are applied on this end) and on the second side have length L = $0.1\times h$; $0.2\times h$; $0.3\times h$; $0.4\times h$; $0.5\times h$; $1.0\times h$ and $2.0\times h$ (unrestrained and unstiffened end). Member is made of structural steel S355. The imperfection amplitude for GMNIA was $d_w/200$, where $d_w$ is web height without rounded corners – see Fig. 4. These six transversally loaded members were

analysed using MNA, LBA and GMNIA in IDEA StatiCa and ANSYS. Load-carrying capacity was calculated according to the codes EN 1993-1-8 and AISC 360-16 for "Yielding" and "Buckling" failure modes. Analysed member is illustrated in Fig. 94.

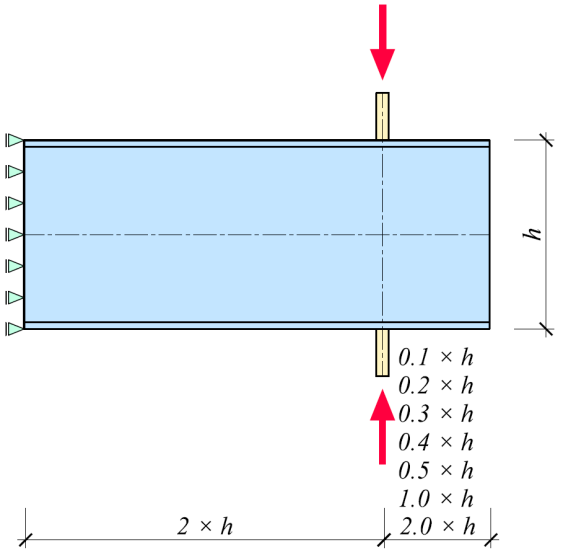


*Fig. 94 Influence of unstiffened end – geometry amd boundary conditions*

### 4.5.2. Results

Calculated load-carrying capacities are listed in Tab. 14to Tab. 19 for all used methods for axially and transversally compressed members of cross section from IPE 100 to IPE 600 respectively.

*Tab. 14 Influence of unstiffened end of IPE 100 - Load-carrying capacity [kN]*

| Length of unstiffened end | EN 1993-1-8 | | EN 1993-1-5 | AISC 360-16 | | IDEA StatiCa | | ANSYS | |
|---|---|---|---|---|---|---|---|---|---|
| | Yielding | Buckling | | Yielding | Buckling | MNA | GMNIA | MNA | GMNIA |
| LoUE=2.0×H | - | - | 85.66 | 100.72 | 191.45 | 97.66 | 95.70 | 90.38 | 90.97 |
| LoUE=1.0×H | - | - | 85.66 | 100.72 | 191.45 | 97.65 | 95.70 | 90.39 | 91.45 |
| LoUE=0.5×H | - | - | 85.66 | 100.72 | 191.45 | 95.70 | 95.70 | 89.28 | 89.93 |
| LoUE=0.4×H | - | - | 85.66 | 54.51 | 95.72 | 91.80 | 89.84 | 85.93 | 86.85 |
| LoUE=0.3×H | - | - | 85.66 | 54.51 | 95.72 | 84.00 | 84.00 | 81.26 | 81.93 |
| LoUE=0.2×H | - | - | 91.89 | 54.51 | 95.72 | 80.08 | 66.41 | 75.07 | 72.72 |
| LoUE=0.1×H | - | - | 86.51 | 54.51 | 95.72 | 56.65 | 52.75 | 59.78 | 59.60 |

*Tab. 15 Influence of unstiffened end of IPE 200 - Load-carrying capacity [kN]*

| Length of unstiffened end | EN 1993-1-8 | | EN 1993-1-5 | AISC 360-16 | | IDEA StatiCa | | ANSYS | |
|---|---|---|---|---|---|---|---|---|---|
| | Yielding | Buckling | | Yielding | Buckling | MNA | GMNIA | MNA | GMNIA |
| LoUE=2.0×H | - | - | 193.51 | 220.67 | 228.88 | 228.52 | 228.52 | 205.68 | 209.60 |
| LoUE=1.0×H | - | - | 193.51 | 220.67 | 228.88 | 228.50 | 228.50 | 208.41 | 209.78 |
| LoUE=0.5×H | - | - | 201.44 | 220.67 | 228.88 | 228.50 | 226.55 | 207.94 | 208.72 |
| LoUE=0.4×H | - | - | 183.39 | 118.78 | 114.44 | 222.66 | 214.84 | 205.76 | 205.22 |
| LoUE=0.3×H | - | - | 167.82 | 118.78 | 114.44 | 212.90 | 185.55 | 194.02 | 183.42 |
| LoUE=0.2×H | - | - | 155.46 | 118.78 | 114.44 | 195.31 | 148.44 | 180.62 | 156.32 |
| LoUE=0.1×H | - | - | 147.12 | 118.78 | 114.44 | 140.65 | 113.30 | 145.49 | 127.75 |

*Tab. 16 Influence of unstiffened end of IPE 300 - Load-carrying capacity [kN]*

| Length of unstiffened end | EN 1993-1-8 | | EN 1993-1-5 | AISC 360-16 | | IDEA StatiCa | | ANSYS | |
|---|---|---|---|---|---|---|---|---|---|
| | Yielding | Buckling | | Yielding | Buckling | MNA | GMNIA | MNA | GMNIA |
| LoUE=2.0×H | - | - | 381.00 | 350.85 | 298.34 | 396.50 | 394.53 | 348.54 | 348.18 |
| LoUE=1.0×H | - | - | 381.00 | 350.85 | 298.34 | 396.50 | 394.55 | 348.79 | 349.36 |
| LoUE=0.5×H | - | - | 305.82 | 350.85 | 298.34 | 396.50 | 390.65 | 348.96 | 346.48 |
| LoUE=0.4×H | - | - | 278.88 | 188.91 | 149.17 | 396.48 | 365.23 | 347.98 | 346.48 |
| LoUE=0.3×H | - | - | 255.72 | 188.91 | 149.17 | 386.70 | 310.55 | 337.69 | 307.17 |
| LoUE=0.2×H | - | - | 237.43 | 188.91 | 149.17 | 353.52 | 249.55 | 311.77 | 256.06 |
| LoUE=0.1×H | - | - | 225.22 | 188.91 | 149.17 | 257.80 | 191.40 | 257.81 | 209.06 |

*Tab. 17 Influence of unstiffened end of IPE 400 - Load-carrying capacity [kN]*

| Length of unstiffened end | EN 1993-1-8 | | EN 1993-1-5 | AISC 360-16 | | IDEA StatiCa | | ANSYS | |
|---|---|---|---|---|---|---|---|---|---|
| | Yielding | Buckling | | Yielding | Buckling | MNA | GMNIA | MNA | GMNIA |
| LoUE=2.0×H | - | - | 547.30 | 567.86 | 398.20 | 621.10 | 613.30 | 561.44 | 559.20 |
| LoUE=1.0×H | - | - | 547.30 | 567.86 | 398.20 | 621.10 | 613.30 | 561.33 | 561.05 |
| LoUE=0.5×H | - | - | 438.03 | 567.86 | 398.20 | 617.20 | 593.80 | 561.34 | 559.08 |
| LoUE=0.4×H | - | - | 399.63 | 304.54 | 199.10 | 625.00 | 546.88 | 560.51 | 532.36 |
| LoUE=0.3×H | - | - | 366.65 | 304.54 | 199.10 | 613.30 | 468.80 | 539.88 | 468.07 |
| LoUE=0.2×H | - | - | 340.66 | 304.54 | 199.10 | 554.69 | 375.00 | 498.99 | 387.27 |
| LoUE=0.1×H | - | - | 323.34 | 304.54 | 199.10 | 449.20 | 293.00 | 417.02 | 316.75 |

*Tab. 18 Influence of unstiffened end of IPE 500 - Load-carrying capacity [kN]*

| Length of unstiffened end | EN 1993-1-8 | | EN 1993-1-5 | AISC 360-16 | | IDEA StatiCa | | ANSYS | |
|---|---|---|---|---|---|---|---|---|---|
| | Yielding | Buckling | | Yielding | Buckling | MNA | GMNIA | MNA | GMNIA |
| LoUE=2.0×H | - | - | 750.40 | 727.82 | 516.21 | 816.41 | 804.70 | 741.92 | 736.68 |
| LoUE=1.0×H | - | - | 750.40 | 727.82 | 516.21 | 816.40 | 804.70 | 742.05 | 738.86 |
| LoUE=0.5×H | - | - | 599.03 | 727.82 | 516.21 | 812.50 | 793.00 | 742.35 | 737.12 |
| LoUE=0.4×H | - | - | 546.75 | 392.88 | 258.10 | 812.50 | 738.28 | 741.70 | 724.50 |
| LoUE=0.3×H | - | - | 501.88 | 392.88 | 258.10 | 796.90 | 632.80 | 733.82 | 641.01 |
| LoUE=0.2×H | - | - | 466.57 | 392.88 | 258.10 | 738.28 | 507.81 | 683.62 | 528.51 |
| LoUE=0.1×H | - | - | 443.11 | 392.88 | 258.10 | 550.80 | 402.30 | 578.94 | 432.25 |

*Tab. 19 Influence of unstiffened end of IPE 600 - Load-carrying capacity [kN]*

| Length of unstiffened end | EN 1993-1-8 | | EN 1993-1-5 | AISC 360-16 | | IDEA StatiCa | | ANSYS | |
|---|---|---|---|---|---|---|---|---|---|
| | Yielding | Buckling | | Yielding | Buckling | MNA | GMNIA | MNA | GMNIA |
| LoUE=2.0×H | - | - | 1027.78 | 996.84 | 696.65 | 1070.3 | 1062.5 | 1014.0 | 1007.4 |
| LoUE=1.0×H | - | - | 1027.88 | 996.84 | 696.65 | 1070.4 | 1054.6 | 1014.1 | 1011.0 |
| LoUE=0.5×H | - | - | 820.05 | 996.84 | 696.65 | 1070.4 | 1046.8 | 1015.3 | 1008.8 |
| LoUE=0.4×H | - | - | 748.54 | 538.89 | 348.33 | 1054.7 | 992.19 | 1017.5 | 995.01 |
| LoUE=0.3×H | - | - | 687.18 | 538.89 | 348.33 | 1023.4 | 859.40 | 1006.5 | 878.90 |
| LoUE=0.2×H | - | - | 638.90 | 538.89 | 348.33 | 968.75 | 695.31 | 935.51 | 726.76 |
| LoUE=0.1×H | - | - | 606.85 | 538.89 | 348.33 | 759.60 | 546.80 | 797.27 | 593.91 |

Load –carrying capacities are graphically displayed in Fig. 95to Fig. 100 for all used methods for axially and transversally compressed members of cross section for rolled IPE 100 to IPE 600 respectively.

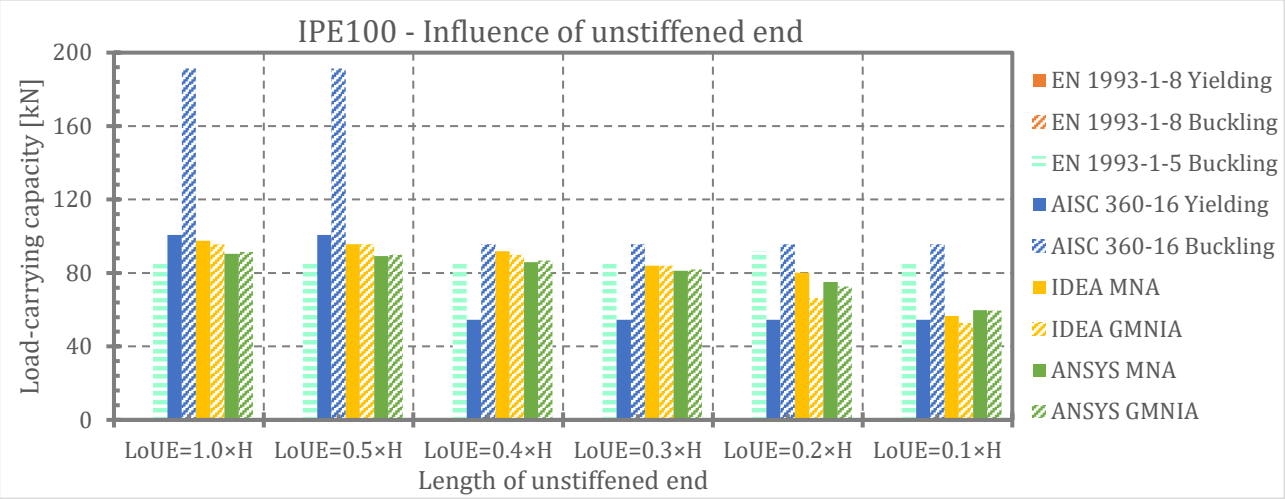


*Fig. 95 Influence of unstiffened end of IPE 100 – Load-carrying capacity*

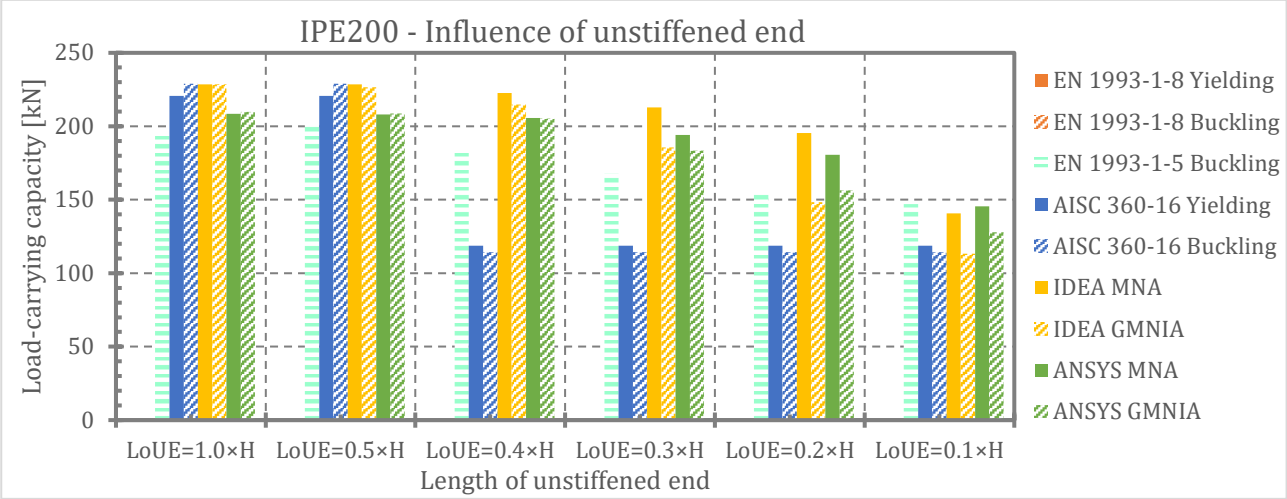


*Fig. 96 Influence of unstiffened end of IPE 200 – Load-carrying capacity*

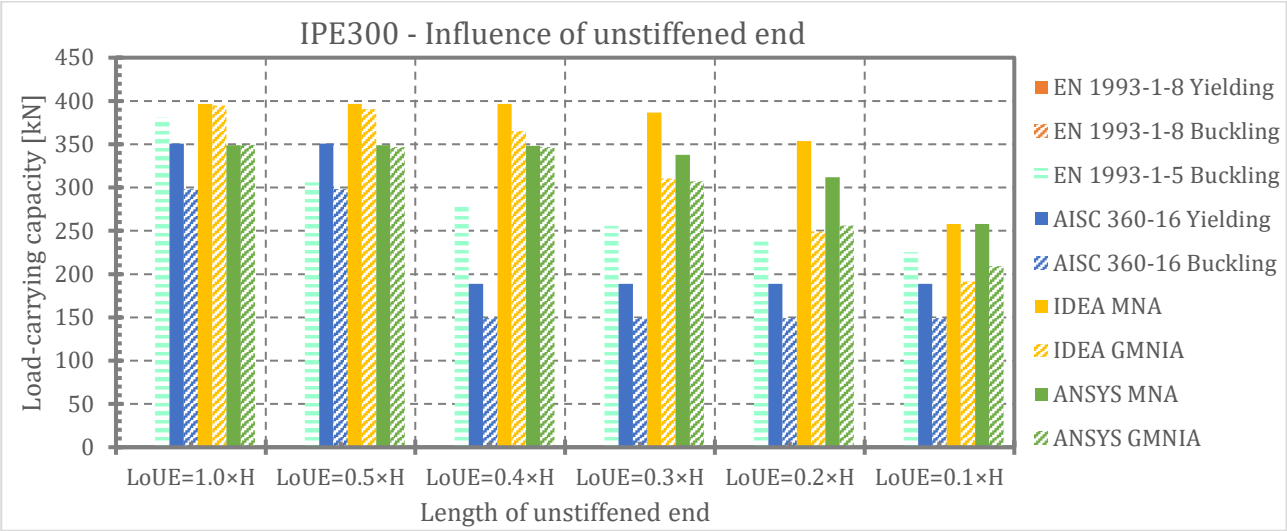


*Fig. 97 Influence of unstiffened end of IPE 300 – Load-carrying capacity*

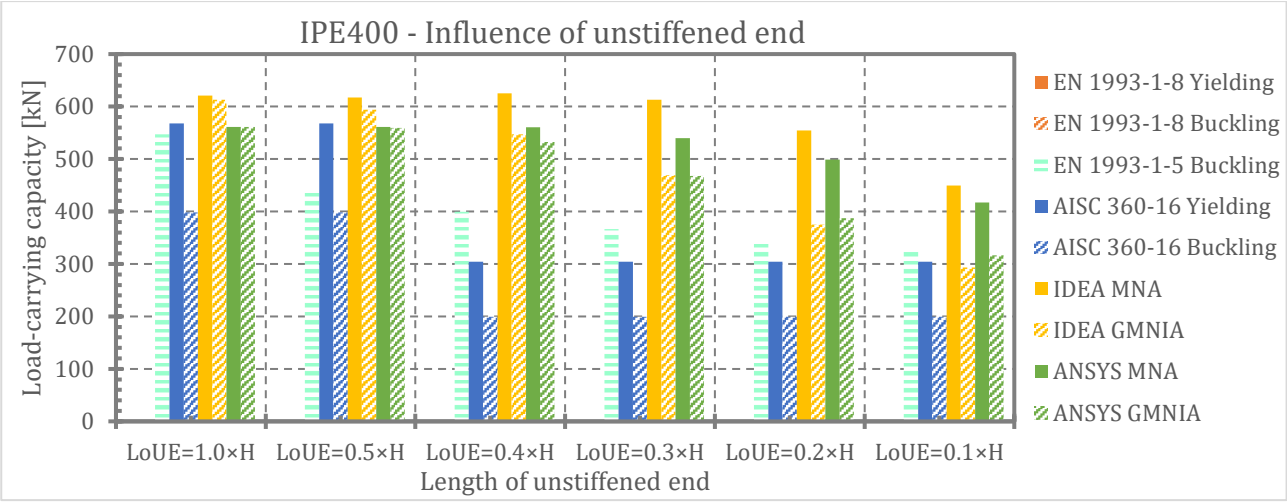


*Fig. 98 Influence of unstiffened end of IPE 400 – Load-carrying capacity*

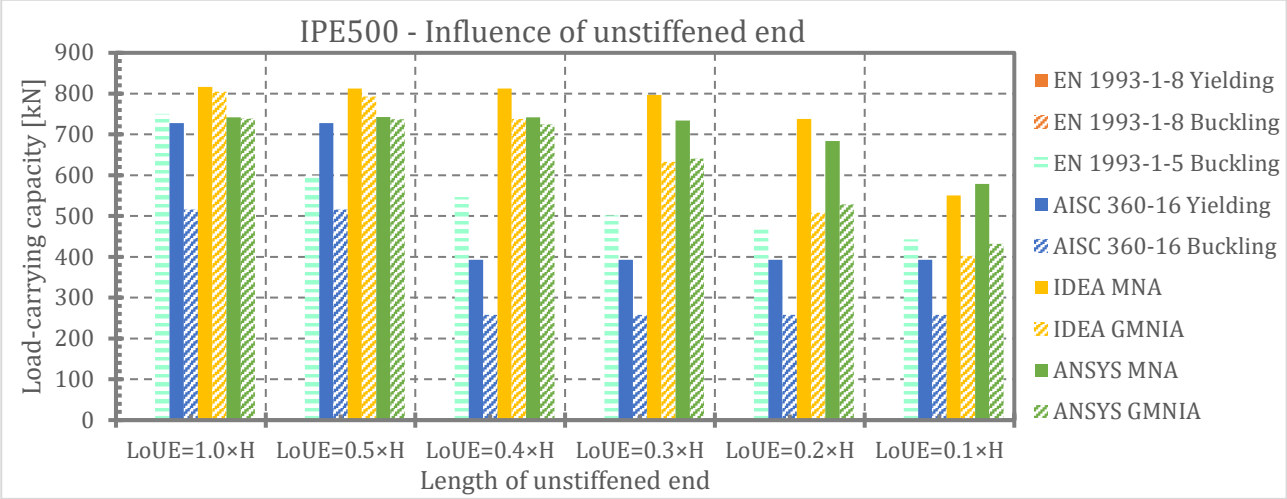


*Fig. 99 Influence of unstiffened end of IPE 500 – Load-carrying capacity*

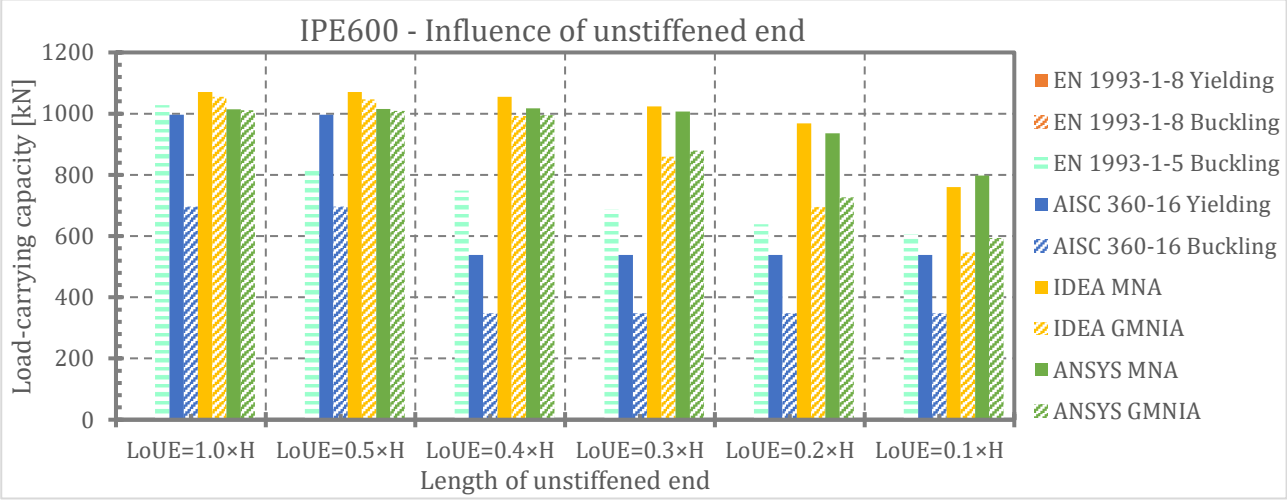


*Fig. 100 Influence of unstiffened end of IPE 600 – Load-carrying capacity*

Influence of unstiffened end on transversal load-carrying capacity is clearly shown in Fig. 101 to Fig. 106 where ratio of load-carrying capacities related to "noninfluencing" length of unstiffened end (LoUE = 2.0×*H*) is on vertical axis.

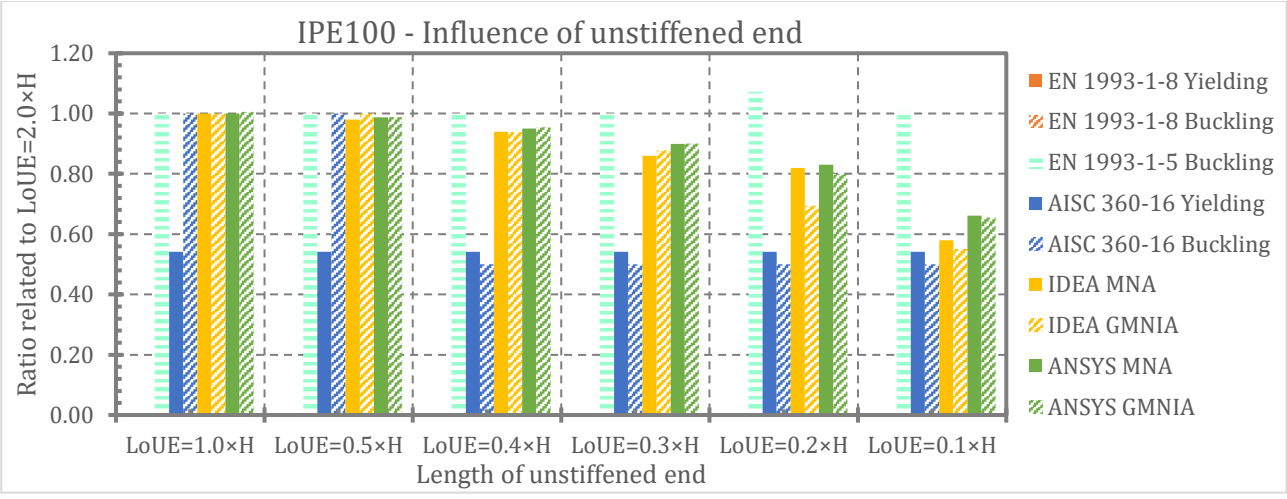


*Fig. 101 Influence of unstiffened end of IPE 100 – relative influence of unstif. end on load-carrying capacity*

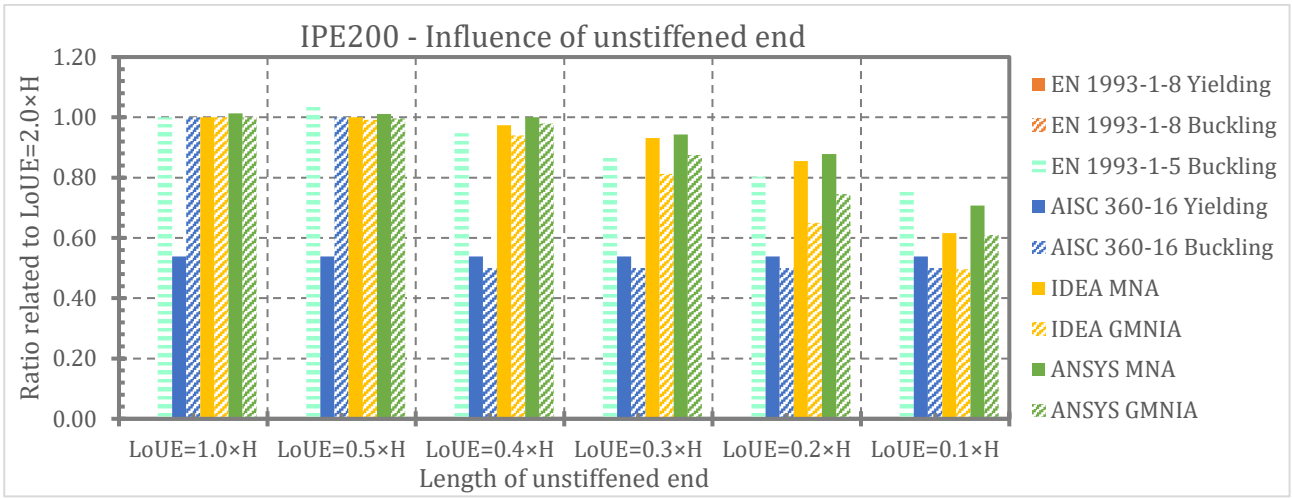


*Fig. 102 Influence of unstiffened end of IPE 200 – relative influence of unstif. end on load-carrying capacity*

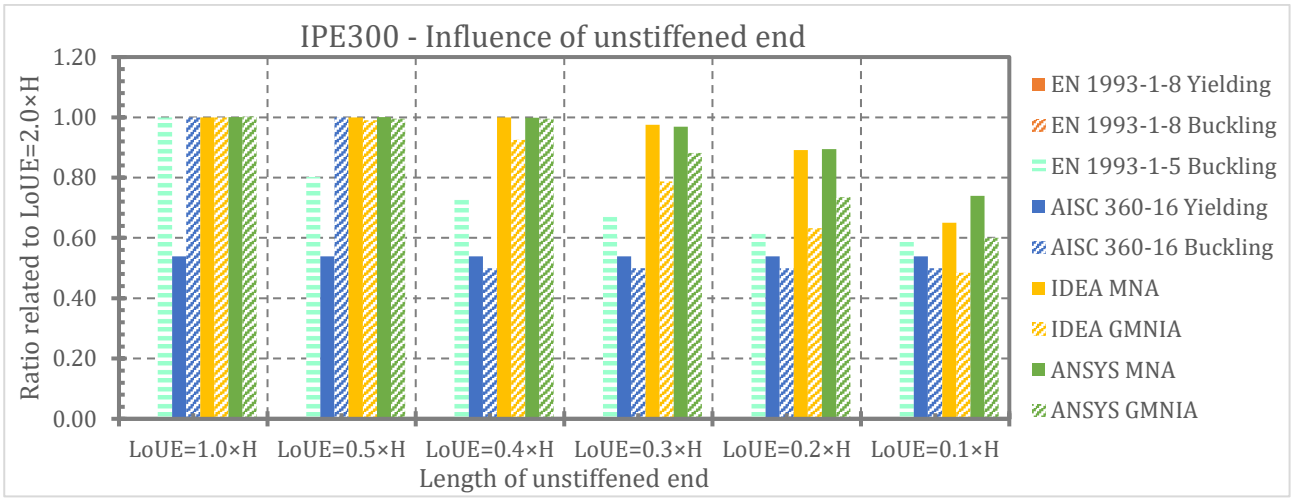


*Fig. 103 Influence of unstiffened end of IPE 300 – relative influence of unstif. end on load-carrying capacity*

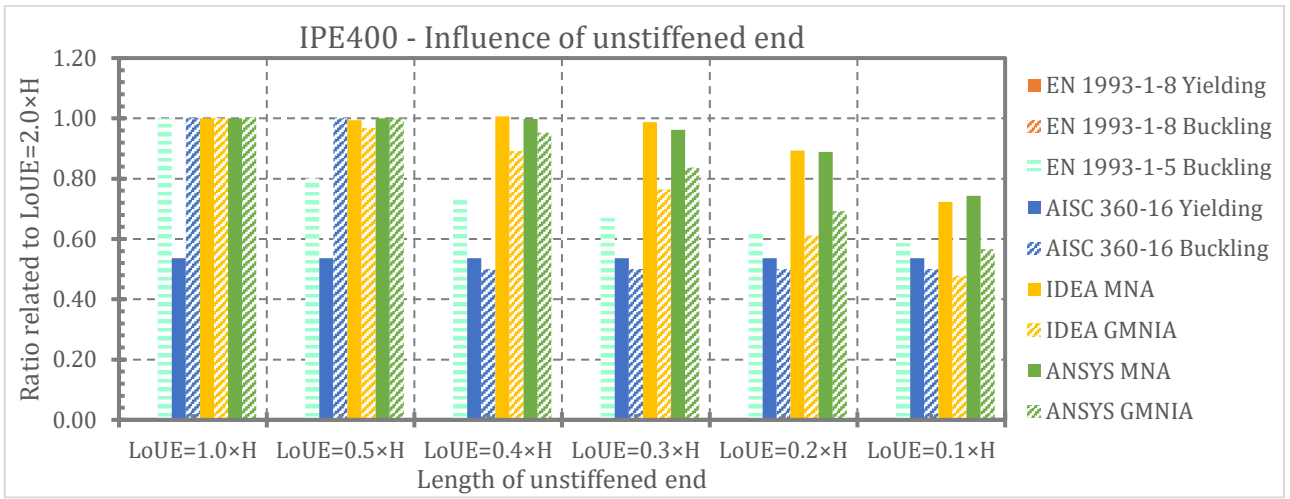


*Fig. 104 Influence of unstiffened end of IPE 400 – relative influence of unstif. end on load-carrying capacity*

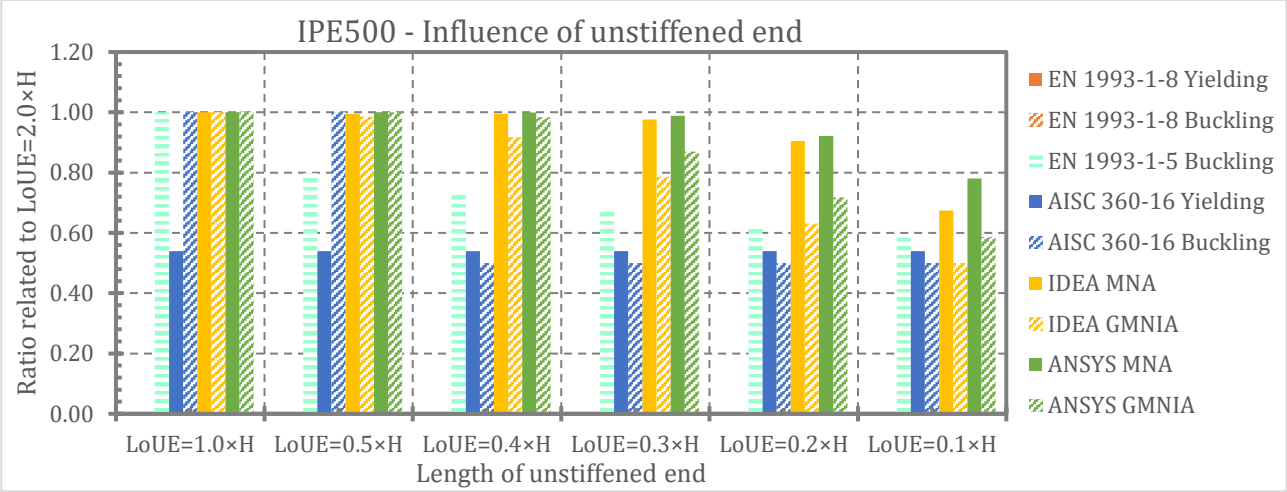


*Fig. 105 Influence of unstiffened end of IPE 500 – relative influence of unstif. end on load-carrying capacity*

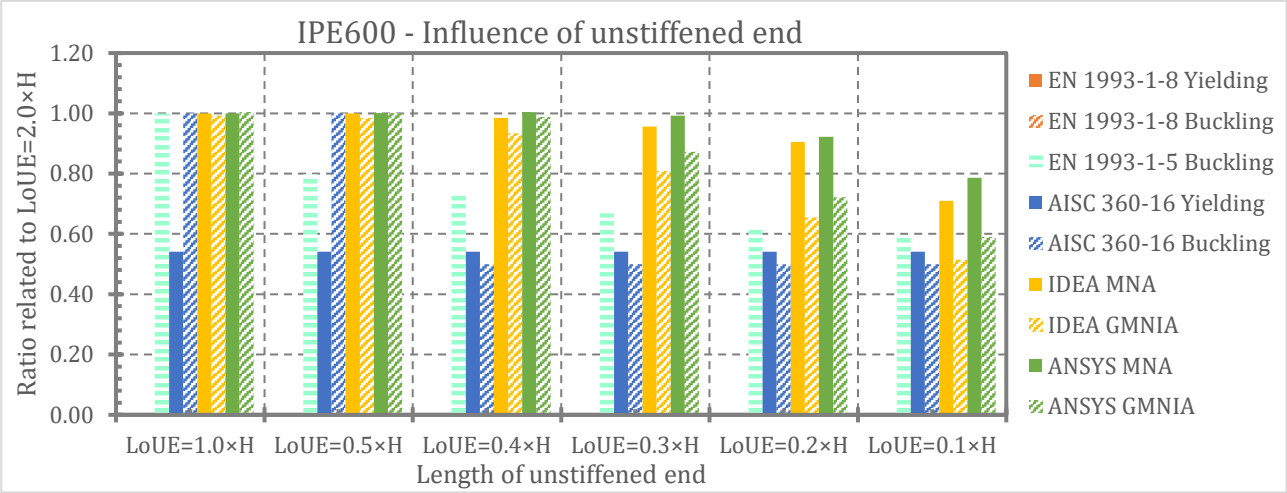


*Fig. 106 Influence of unstiffened end of IPE 600 – relative influence of unstif. end on load-carrying capacity*

Influence of buckling on load-carrying capacity is clearly shown in Fig. 107 to Fig. 112 where ratio of load-carrying capacities resulting from Buckling/Yielding resistances according to the AISC 360-16 or GMNIA/MNA resulting from numerical analysis performed in IDEA StatiCa and ANSYS are on vertical axis. Buckling factor according to the EN 1993-1-5 takes into account web buckling and influence of close member end since the results are only illustrative.

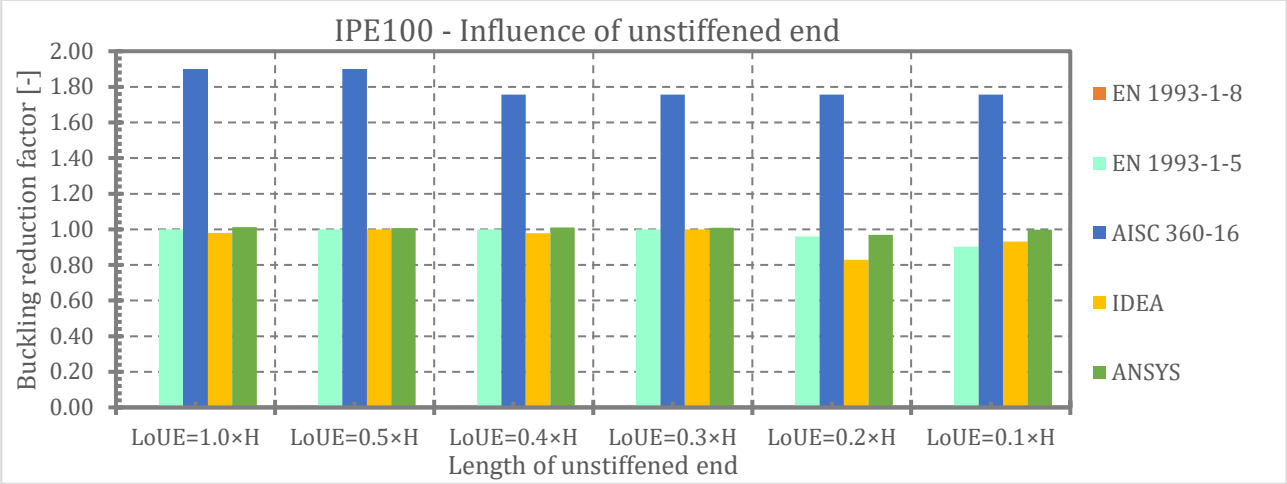


*Fig. 107 Influence of unstiffened end of IPE 100 – reduction due to geometrical nonlinearity*

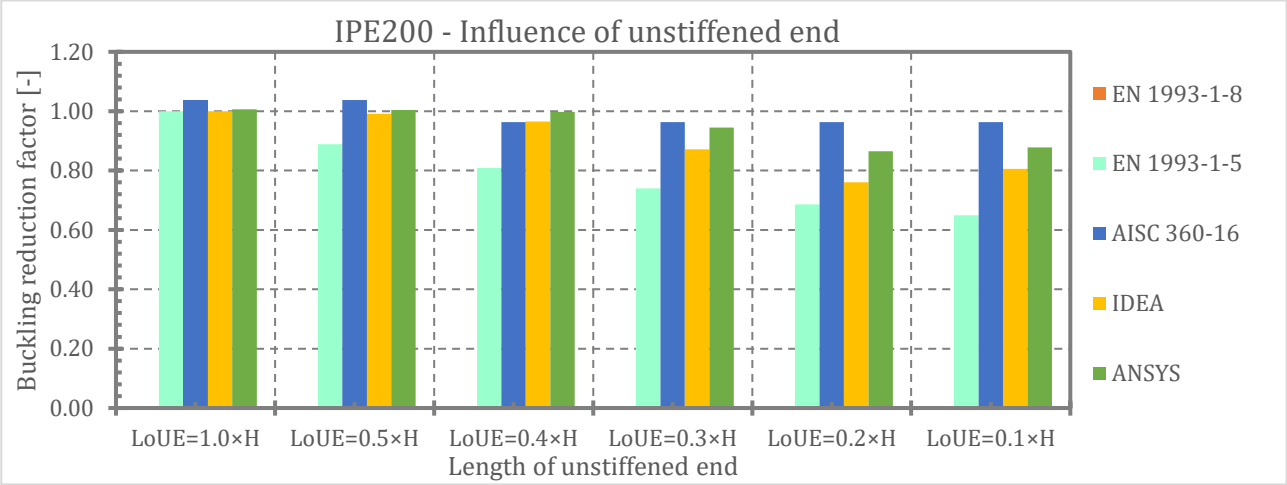


*Fig. 108 Influence of unstiffened end of IPE 200 – reduction due to geometrical nonlinearity*

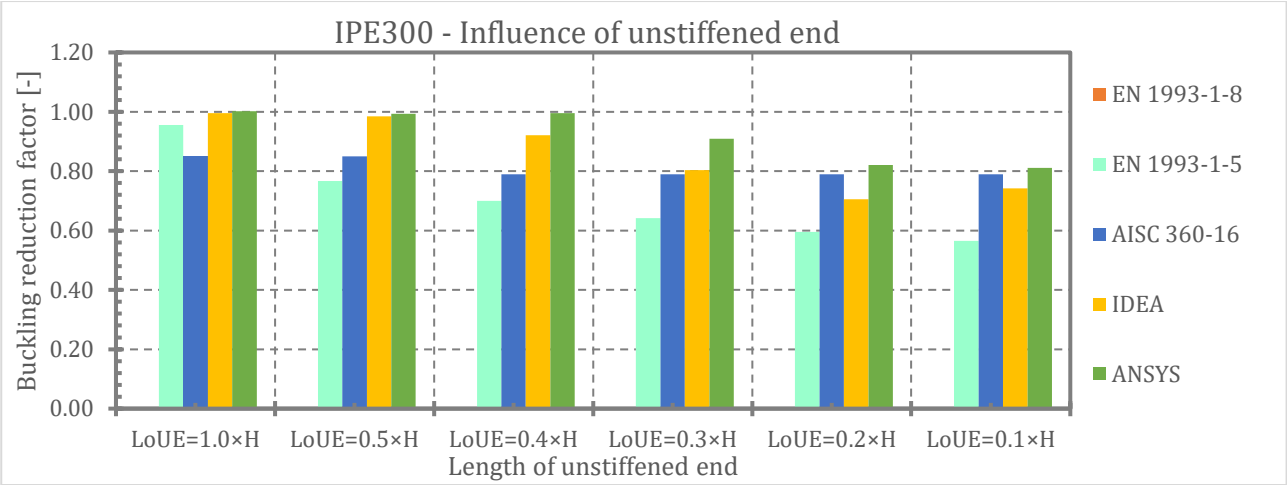


*Fig. 109 Influence of unstiffened end of IPE 300 – reduction due to geometrical nonlinearity*

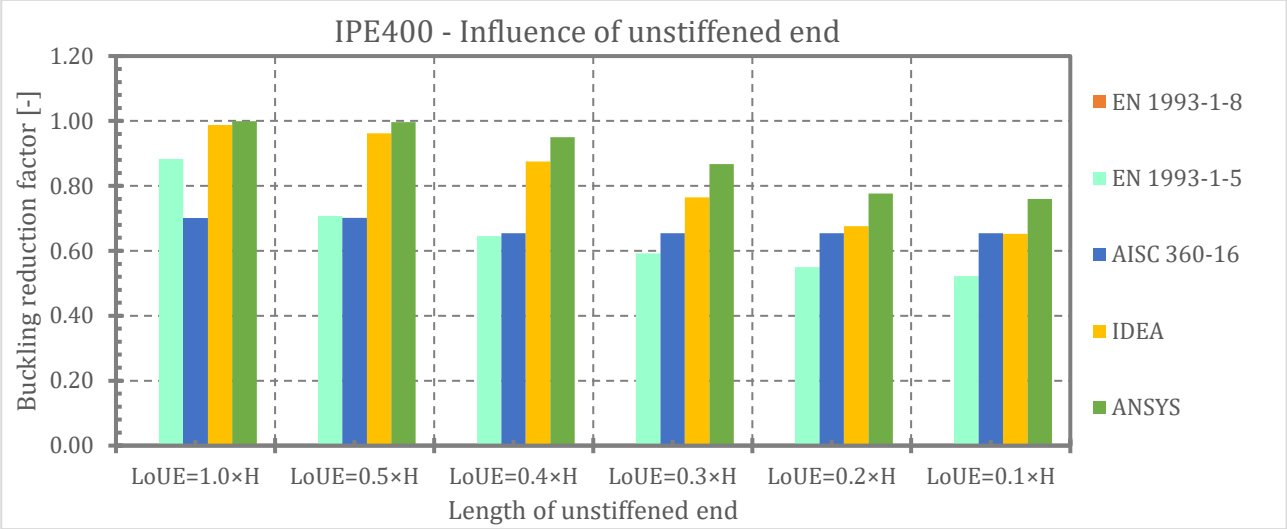


*Fig. 110 Influence of unstiffened end of IPE 400 – reduction due to geometrical nonlinearity*

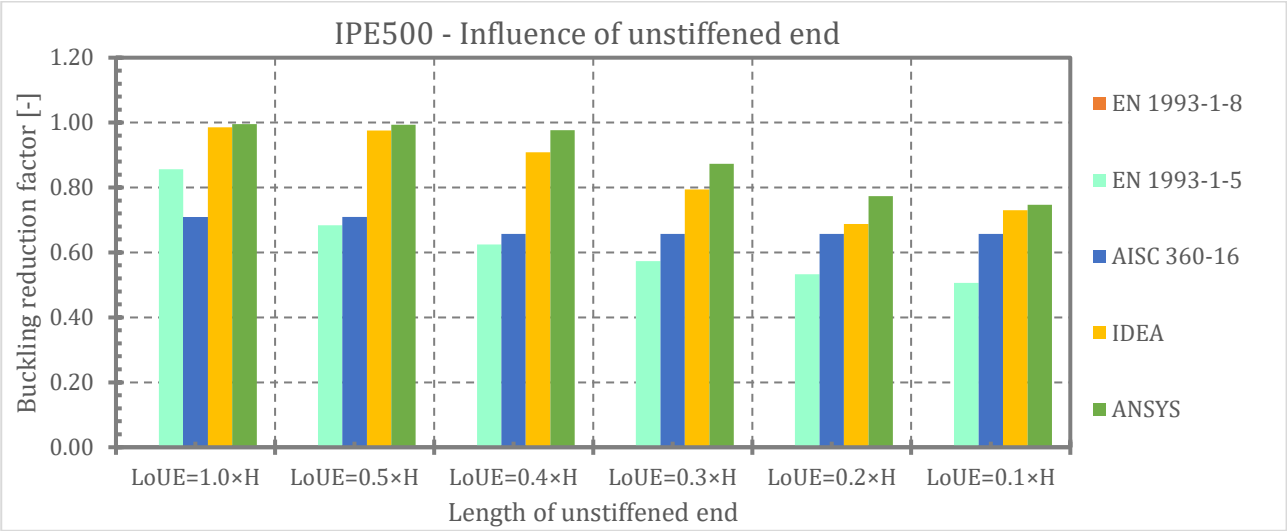


*Fig. 111 Influence of unstiffened end of IPE 500 – reduction due to geometrical nonlinearity*

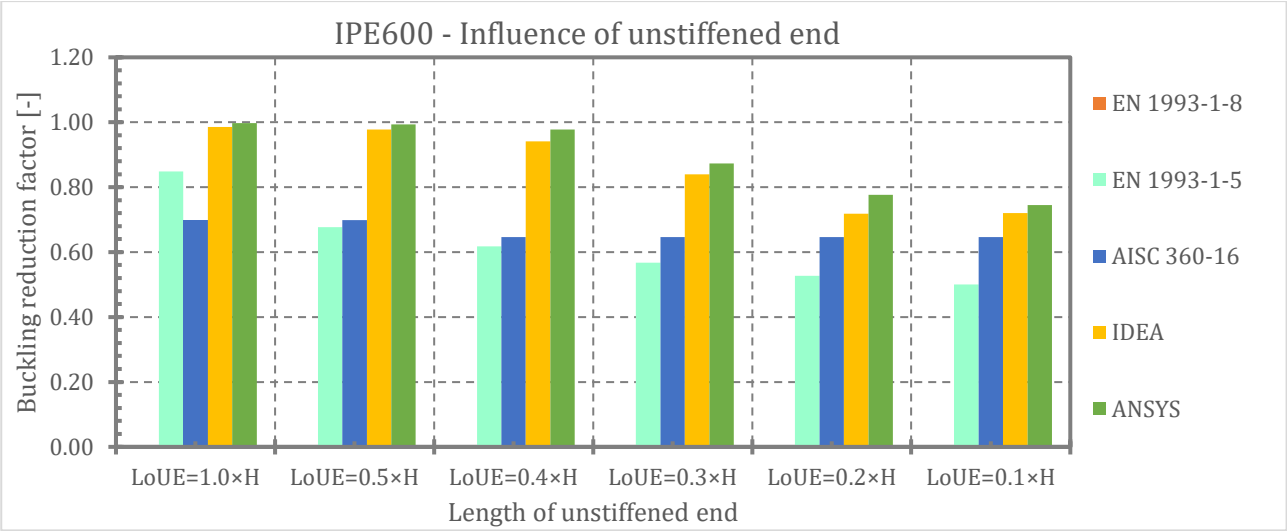


*Fig. 112 Influence of unstiffened end of IPE 600 – reduction due to geometrical nonlinearity*

Synthesis of all obtained data is plotted in Fig. 113 to Fig. 116, where level of reduction is on vertical axis for AISC 360-16 (for yielding and buckling mode) or as ratio of load-carrying capacities for any length of unstiffened end related to the member depth. Level of reduction resulting from EN 1993-1-5 is plotted by cross marks for each section separately, because there is not one value. All results put together are plotted in Fig. 117.

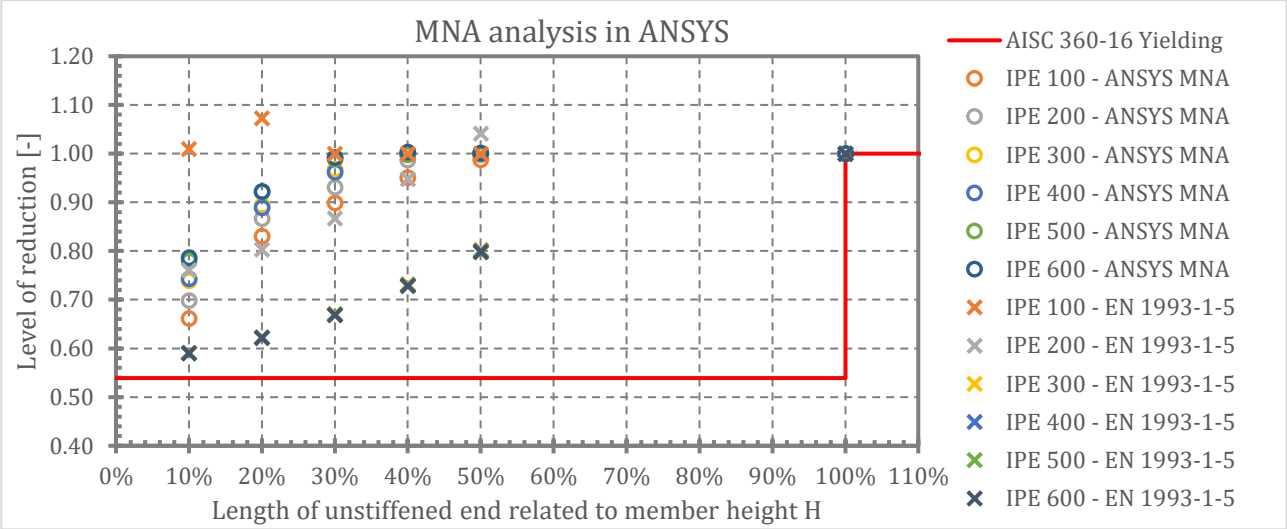


*Fig. 113 Influence of unstiffened end on load-carrying capacity*

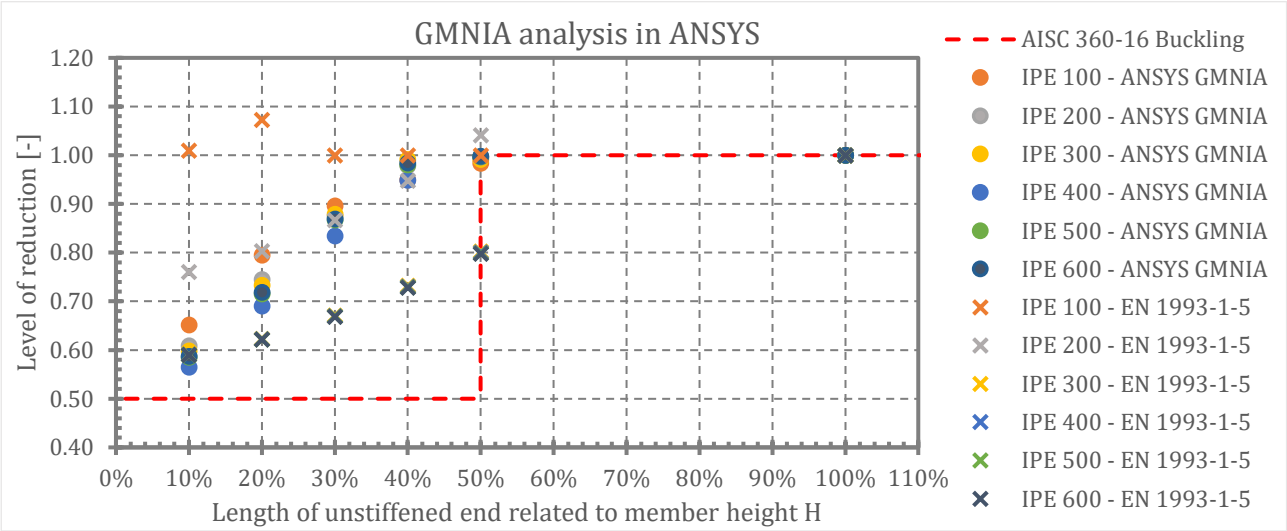


*Fig. 114 Influence of unstiffened end on load-carrying capacity*

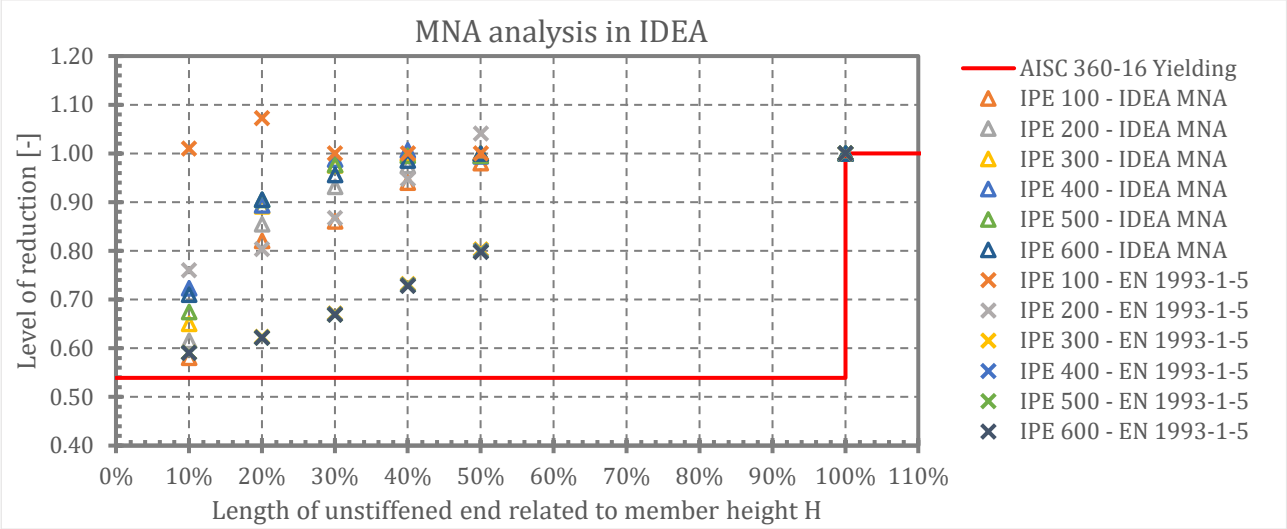


*Fig. 115 Influence of unstiffened end on load-carrying capacity*

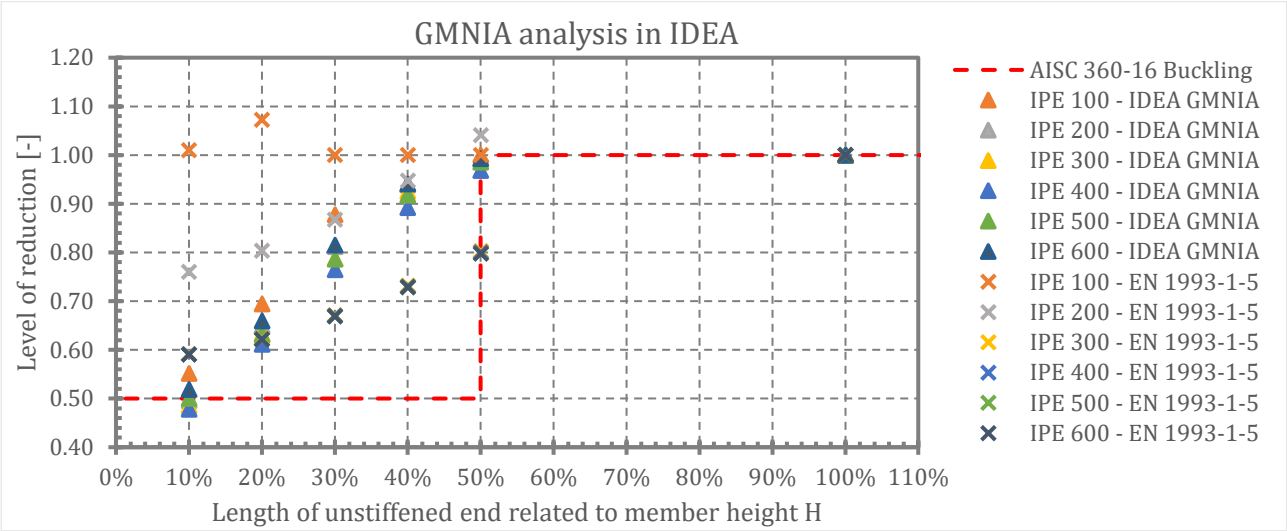


*Fig. 116 Influence of unstiffened end on load-carrying capacity*

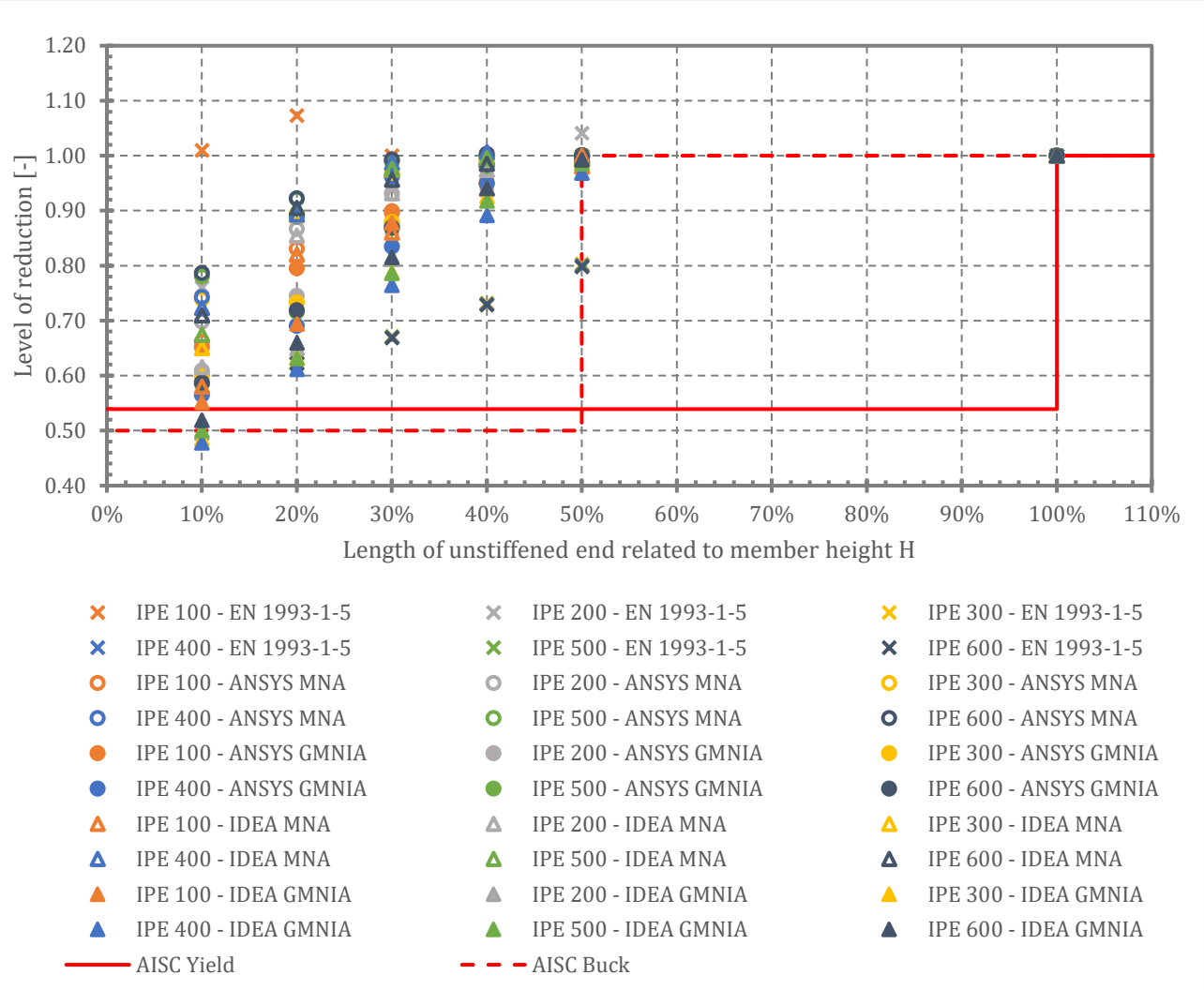


*Fig. 117 Influence of unstiffened end on load-carrying capacity*

Actual behaviour of transversally compressed member with one unstiffened and unrestrained end is described in Fig. 118 to Fig. 123 for illustration for member of cross section IPE 400. For other analysed cross sections, the charts are similar.

Fig. 118 shows results of linear buckling analysis – critical forces $F_{cr}$ [kN] and critical load factor $\alpha_{cr}$ [-]. For decreasing length of unstiffened end of transversally compressed member both critical force and critical load factor are decreasing.

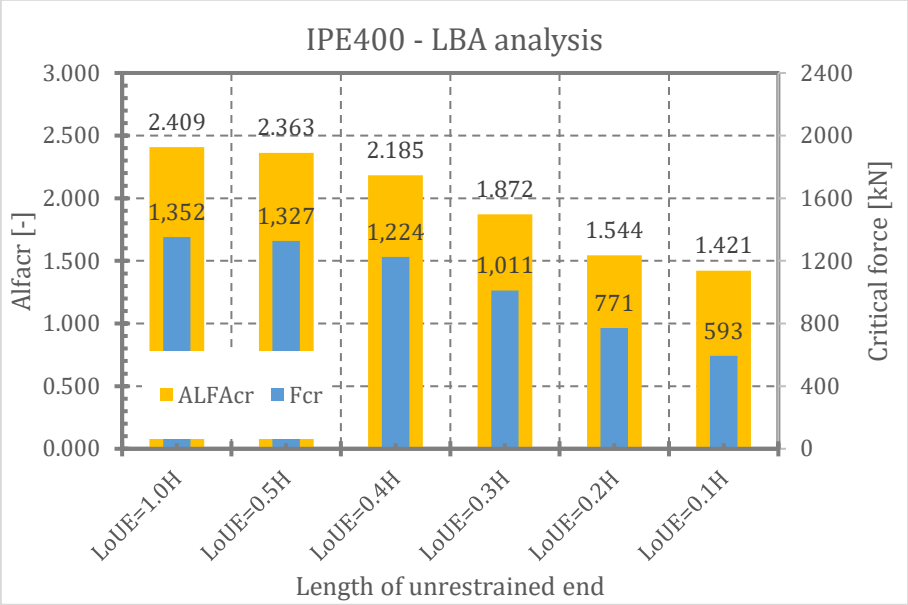


*Fig. 118 Influence of unstiffened end – LBA results*

Fig. 119 illustrates relationship of vertical deformation and loading force for MNA and GMNIA. Fig. 120 describes dependency of lateral deformation in the middle of beam web on loading force for MNA and GMNIA. Dependency of maximal equivalent stress and equivalent stress in the middle of member web on loading force is plotted in Fig. 121 and Fig. 122. Fig. 123 shows developing of plastic strain with loading increasing.

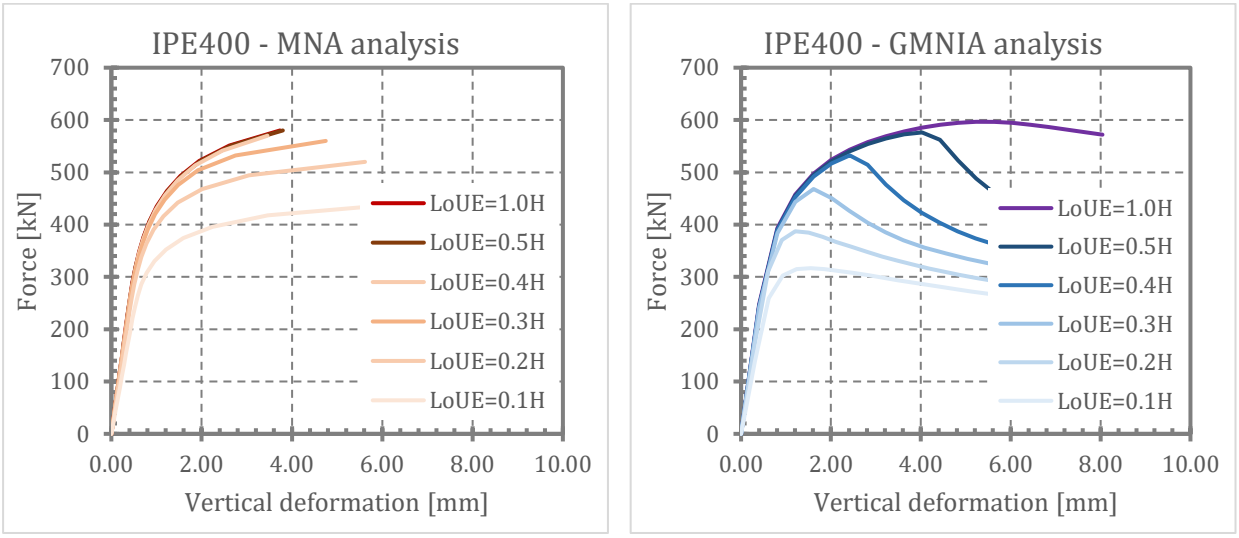


*Fig. 119 Influence of unstiffened end – vertical deformation-force relationship*

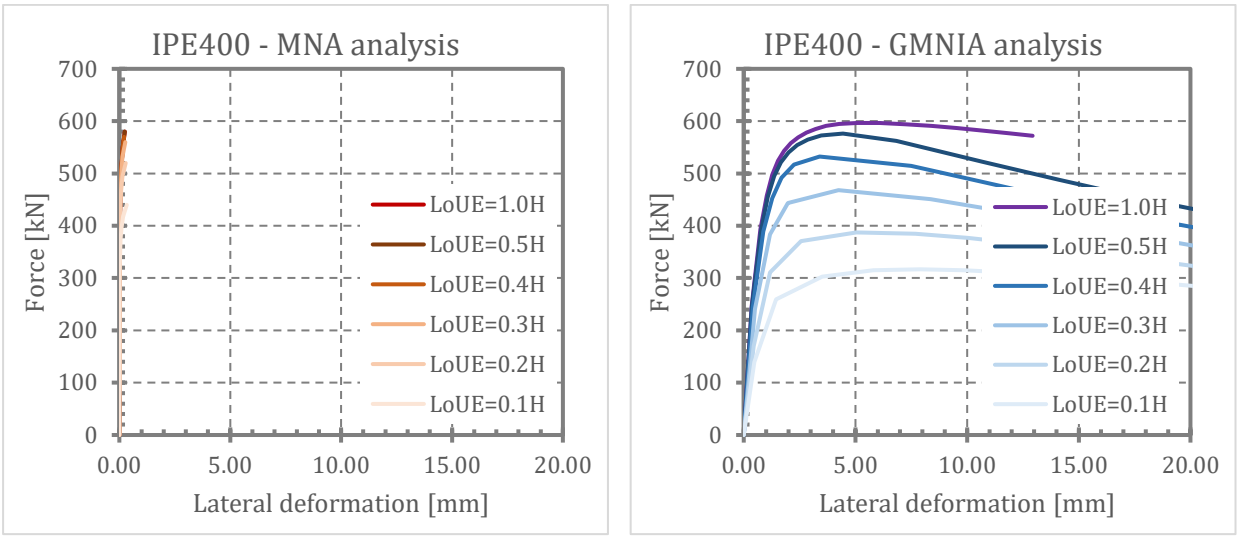


*Fig. 120 Influence of unstiffened end – lateral deformation-force relationship*

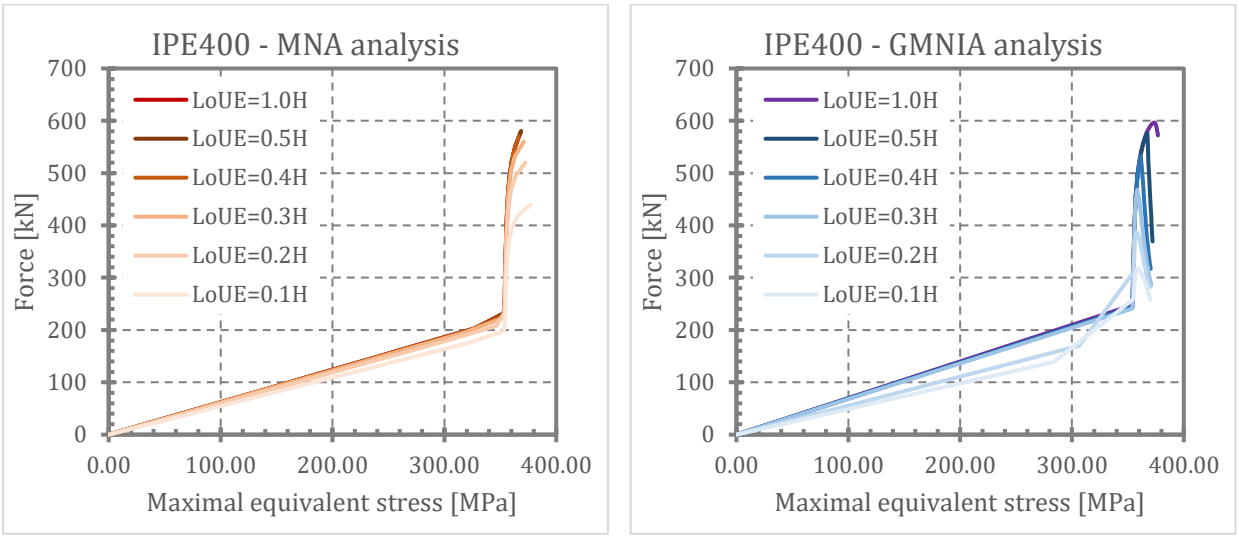


*Fig. 121 Influence of unstiffened end – maximal equivalent stress-force relationship*

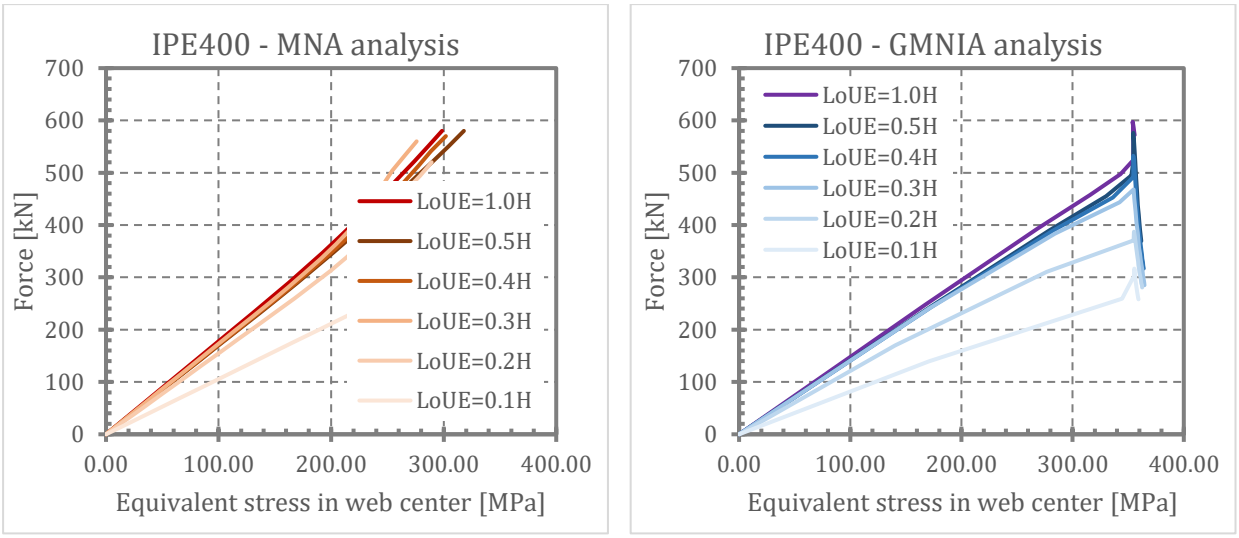


*Fig. 122 Influence of unstiffened end – equivalent stress in web center-force relationship*

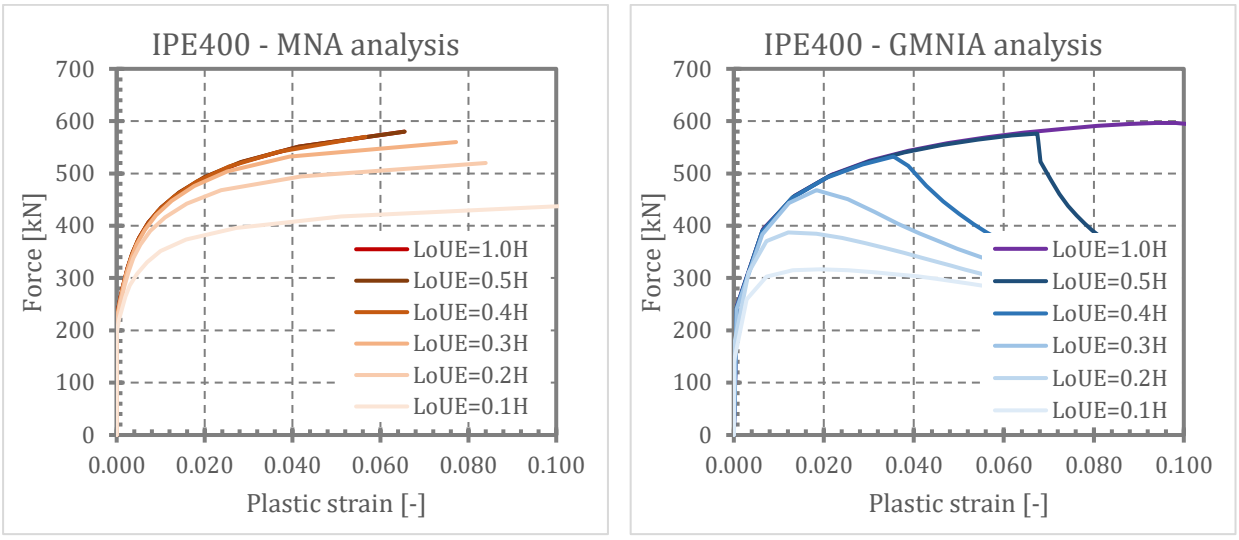


*Fig. 123 Influence of unstiffened end – plastic strain-force relationship*

Fig. 124 to Fig. 129 shows comparison of load-carrying capacities obtained from all investigated cases and by all used methods related to the ANSYS results (i.e. ANSYS results are equal to 1.0).

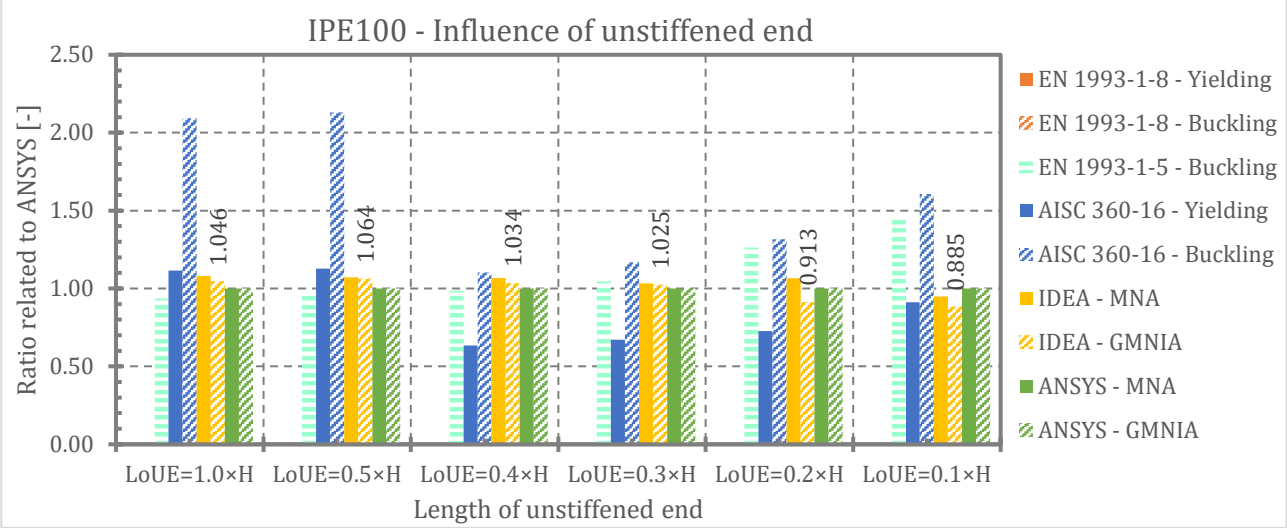


*Fig. 124 Influence of unstiffened end – comparison of load-carrying capacity related to the ANSYS results*

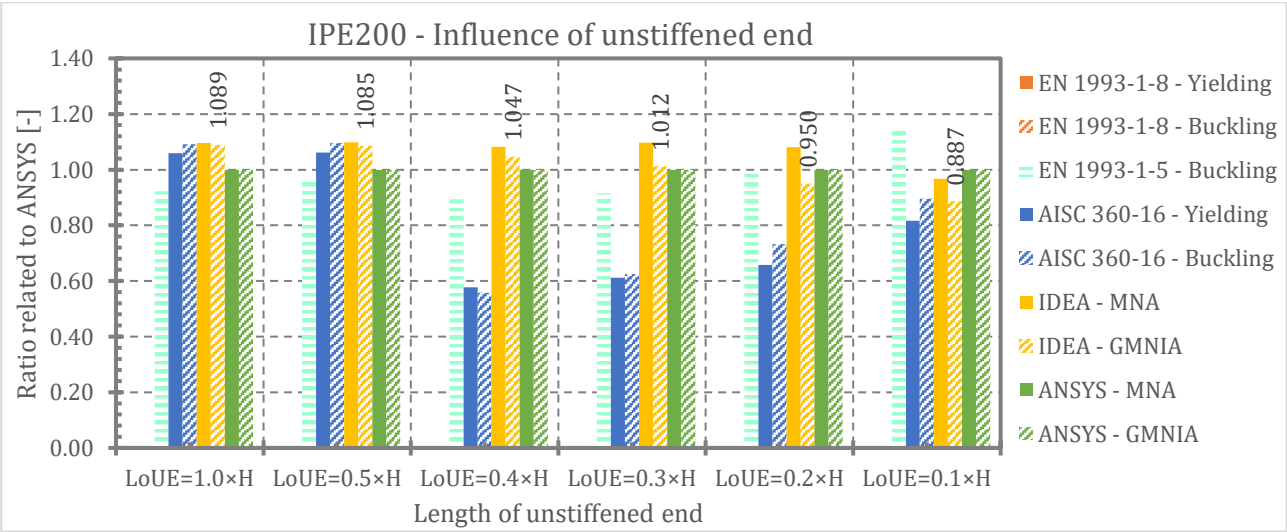


*Fig. 125 Influence of unstiffened end – comparison of load-carrying capacity related to the ANSYS results*

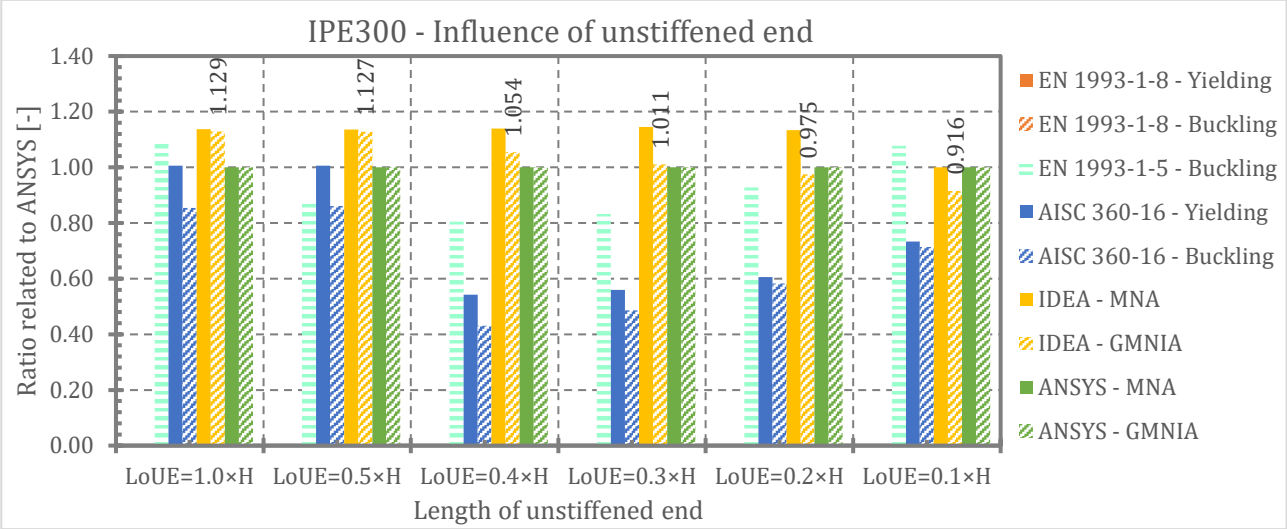


*Fig. 126 Influence of unstiffened end – comparison of load-carrying capacity related to the ANSYS results*

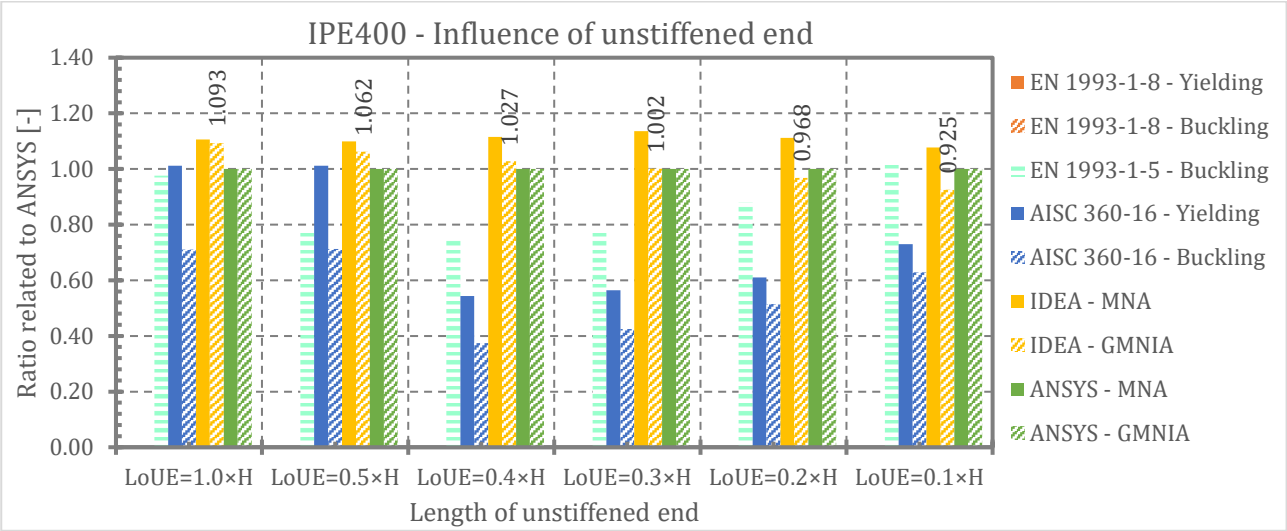


*Fig. 127 Influence of unstiffened end – comparison of load-carrying capacity related to the ANSYS results*

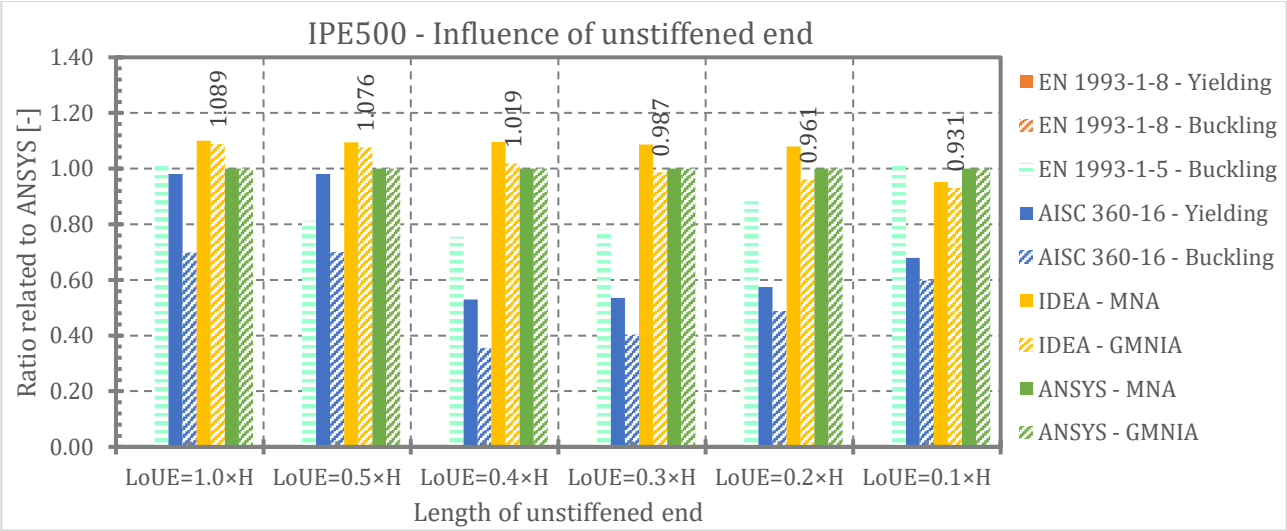


*Fig. 128 Influence of unstiffened end – comparison of load-carrying capacity related to the ANSYS results*

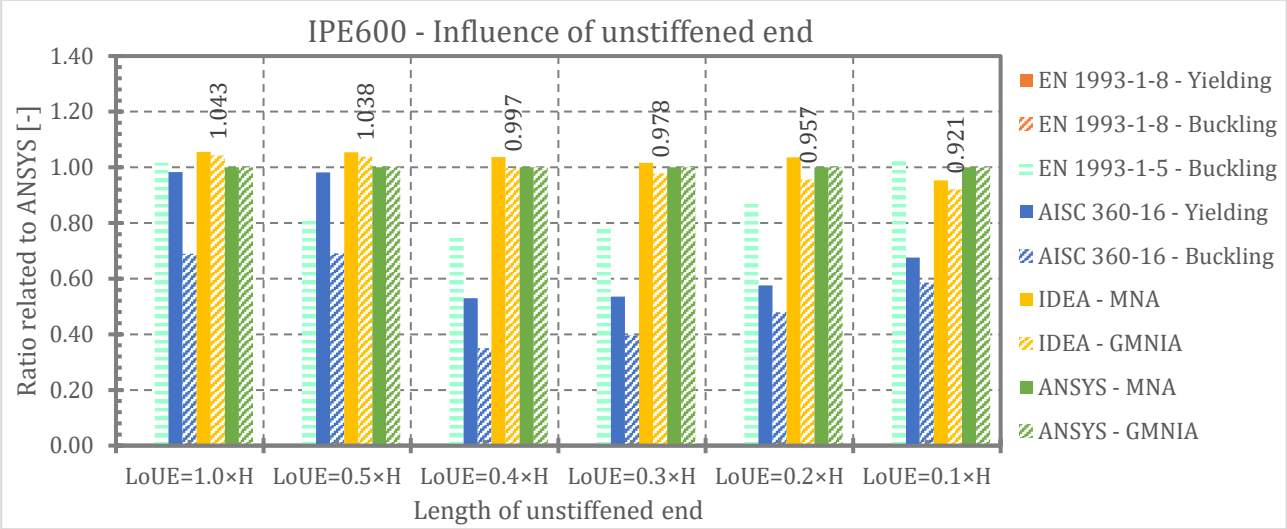


*Fig. 129 Influence of unstiffened end – comparison of load-carrying capacity related to the ANSYS results*

### 4.5.3. Conclusion

As results of numerical simulations performed in IDEA StatiCa and ANSYS show, transversal force applied on the member close to the unrestrained and unstiffened end of that member influences their resistance. The influence is stronger for decreasing distance from unstiffened end of member to acting transversal forces. The reduction of transversal strength due to unstiffened end is negligible for distances of 100% and 50% of member depth *h*, for shorter distances (40%, 30%, 20% and 10%) it is approximately 5%, 10%, 30% and 40% according to the MNA and GMNIA carried out in ANSYS software. Comparison of ANSYS results and IDEA StatiCa results shows very good agreement between results. Load-carrying capacities calculated according to the American standard AISC 360-16 give very conservative results when there is no reduction up to distance from unstiffened end of member to acting transversal force is equal to 50% of member depth, for smaller distance there is reduction 50% for web buckling and approximately 50% for web yielding. On the other hand, for smallest considered distance (10%) the calculated resistance according to the AISC 360-16 correspond to the MNA and GMNIA results obtained from IDEA StatiCa and ANSYS numerical simulations. Calculation according to the EN 1993-1-5 is more complex in comparison to the AISC 360-16 and gives relatively exact values of resistances for relatively great and small distances from unstiffened end of member to the acting forces (100%, 50% and 10%), for intermediate distances (from 40% to 20%) there is relatively great difference but always on the safe side.

From comparison of IDEA StatiCa results and ANSYS software results it may be concluded that it is always (at all investigated cross sections in the frame of this study) on the unsafe side in the case of materially nonlinear analysis MNA, but on the other hand in the case of geometrically and material nonlinear analysis with imperfections GMNIA IDEA StatiCa results are on the unsafe side for only longer unstiffened end of the member (for LoUE = 1×*h*, 0.5×*h* and 0.4×*h*), for length equal to 30% of member height the results are practically the same and for shorter unstiffened end (for LoUE = 0.2×*h* and 0.1×*h*) IDEA gives results slightly on the safe side.

## 4.6. Influence of normal force in transversally compressed member

This part of study shows the influence of normal compression force in transversally compressed member on load-carrying capacity and other results. The goal is to evaluate actual behaviour and make comparison with design resistances according to the EN 1993-1-8.

### 4.6.1. Methodology

The study was performed on transversally compressed member of rolled cross-sections IPE 100, 200, 300, 400, 500 and 600 and welded cross-section wI 100×100×10×10 and wI 550×300×10×20 (section height × flange width × web thickness × flange thickness) with length on both side from loading plates $L = 2\times h$ (overall length is $L = 4\times h$). Member is made of structural steel S355. The imperfection amplitude for GMNIA was $d_w/200$, where $d_w$ is web height without rounded corners – see Fig. 4. Normal compression force is variable in range from 10% to 90% in the steps of 20% of resistance in pure compression: $F_x = 0.1\times N_{Rk}$; $0.3\times N_{Rk}$; $0.5\times N_{Rk}$; $0.7\times N_{Rk}$ and $0.9\times N_{Rk}$, where $N_{Rk} = A\times f_y$. Coefficients 0.1; 0.3 etc. correspond to the ratio $\sigma_{com,Ed}/f_{y,wc}$ in equation (4). These five transversally loaded members were analysed using MNA, LBA and GMNIA in IDEA StatiCa and ANSYS. Load-carrying capacity was calculated according to the codes EN 1993-1-8 for "Yielding" and "Buckling" failure modes. EN 1993-1-5 and AISC 360-16 does not specify a calculation procedure applicable for this problem. Results are compared with basic case with no normal force $F_x = 0$. Analysed member is illustrated in Fig. 130.

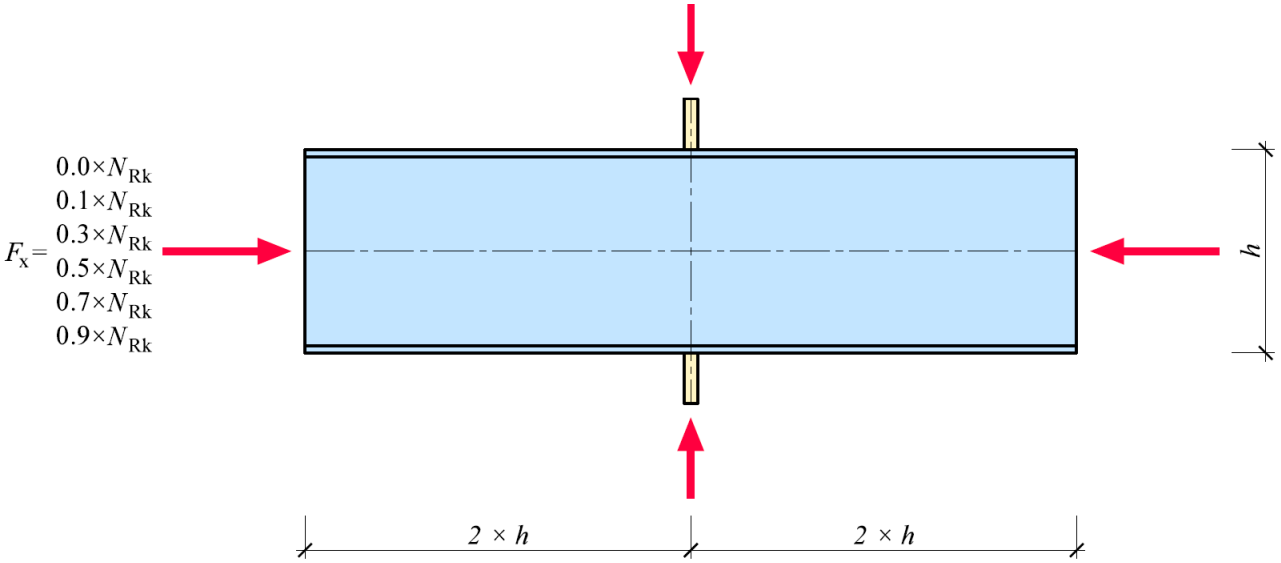


*Fig. 130 Influence of normal force in member – geometry amd boundary conditions*

### 4.6.2. Results

Calculated load-carrying capacities are listed in Tab. 20 to Tab. 25 and Tab. 26 and Tab. 27 for all used methods for axially and transversally compressed members of cross section from IPE 100 to IPE 600 and welded sections respectively.

*Tab. 20 Influence of normal force in IPE 100 - Load-carrying capacity [kN]*

| Normal force $F_x$ | EN 1993-1-8 | | EN 1993-1-5 | AISC 360-16 | | IDEA StatiCa | | ANSYS | |
|---|---|---|---|---|---|---|---|---|---|
| | Yielding | Buckling | | Yielding | Buckling | MNA | GMNIA | MNA | GMNIA |
| $0\times N_{Rk}$ | 100.72 | 100.72 | - | - | - | 89.85 | 89.85 | 90.57 | 91.55 |
| $0.1\times N_{Rk}$ | 100.72 | 100.72 | - | - | - | 89.85 | 89.85 | 90.34 | 91.10 |
| $0.3\times N_{Rk}$ | 100.72 | 100.72 | - | - | - | 89.85 | 87.90 | 88.96 | 89.15 |
| $0.5\times N_{Rk}$ | 100.72 | 100.72 | - | - | - | 87.90 | 85.95 | 86.73 | 86.28 |
| $0.7\times N_{Rk}$ | 100.72 | 100.72 | - | - | - | 82.05 | 78.15 | 82.16 | 81.03 |
| $0.9\times N_{Rk}$ | 80.58 | 80.58 | - | - | - | 70.50 | 66.40 | 72.21 | 68.85 |

*Tab. 21 Influence of normal force in IPE 200 - Load-carrying capacity [kN]*

| Normal force $F_x$ | EN 1993-1-8 | | EN 1993-1-5 | AISC 360-16 | | IDEA StatiCa | | ANSYS | |
|---|---|---|---|---|---|---|---|---|---|
| | Yielding | Buckling | | Yielding | Buckling | MNA | GMNIA | MNA | GMNIA |
| $0\times N_{Rk}$ | 220.67 | 189.34 | - | - | - | 187.50 | 185.55 | 208.83 | 210.26 |
| $0.1\times N_{Rk}$ | 220.67 | 189.34 | - | - | - | 185.50 | 183.50 | 208.44 | 209.17 |
| $0.3\times N_{Rk}$ | 220.67 | 189.34 | - | - | - | 183.50 | 179.50 | 204.58 | 204.26 |
| $0.5\times N_{Rk}$ | 220.67 | 189.34 | - | - | - | 177.50 | 174.00 | 199.11 | 197.11 |
| $0.7\times N_{Rk}$ | 220.67 | 189.34 | - | - | - | 166.00 | 160.00 | 188.87 | 183.33 |
| $0.9\times N_{Rk}$ | 176.53 | 151.47 | - | - | - | 142.50 | 131.00 | 167.91 | 144.92 |

*Tab. 22 Influence of normal force in IPE 300 - Load-carrying capacity [kN]*

| Normal force $F_x$ | EN 1993-1-8 | | EN 1993-1-5 | AISC 360-16 | | IDEA StatiCa | | ANSYS | |
|---|---|---|---|---|---|---|---|---|---|
| | Yielding | Buckling | | Yielding | Buckling | MNA | GMNIA | MNA | GMNIA |
| $0\times N_{Rk}$ | 350.85 | 279.84 | - | - | - | 322.25 | 320.30 | 350.17 | 350.04 |
| $0.1\times N_{Rk}$ | 350.85 | 279.84 | - | - | - | 318.35 | 318.35 | 349.39 | 348.19 |
| $0.3\times N_{Rk}$ | 350.85 | 279.84 | - | - | - | 314.45 | 314.45 | 343.72 | 340.83 |
| $0.5\times N_{Rk}$ | 350.85 | 279.84 | - | - | - | 306.65 | 306.65 | 333.65 | 329.04 |
| $0.7\times N_{Rk}$ | 350.85 | 279.84 | - | - | - | 289.05 | 289.05 | 317.24 | 299.83 |
| $0.9\times N_{Rk}$ | 280.68 | 223.88 | - | - | - | 250.00 | 250.00 | 285.15 | 200.13 |

*Tab. 23 Influence of normal force in IPE 400 - Load-carrying capacity [kN]*

| Normal force $F_x$ | EN 1993-1-8 | | EN 1993-1-5 | AISC 360-16 | | IDEA StatiCa | | ANSYS | |
|---|---|---|---|---|---|---|---|---|---|
| | Yielding | Buckling | | Yielding | Buckling | MNA | GMNIA | MNA | GMNIA |
| $0\times N_{Rk}$ | 567.86 | 420.71 | - | - | - | 500.00 | 496.10 | 564.42 | 562.61 |
| $0.1\times N_{Rk}$ | 567.86 | 420.71 | - | - | - | 498.05 | 490.25 | 561.45 | 560.01 |
| $0.3\times N_{Rk}$ | 567.86 | 420.71 | - | - | - | 492.20 | 480.45 | 552.60 | 546.55 |
| $0.5\times N_{Rk}$ | 567.86 | 420.71 | - | - | - | 478.50 | 459.00 | 539.15 | 519.02 |
| $0.7\times N_{Rk}$ | 567.86 | 420.71 | - | - | - | 447.25 | 408.20 | 512.42 | 459.80 |
| $0.9\times N_{Rk}$ | 454.29 | 336.57 | - | - | - | 380.85 | 330.10 | 460.27 | 343.94 |

*Tab. 24 Influence of normal force in IPE 500 - Load-carrying capacity [kN]*

| Normal force $F_x$ | EN 1993-1-8 | | EN 1993-1-5 | AISC 360-16 | | IDEA StatiCa | | ANSYS | |
|---|---|---|---|---|---|---|---|---|---|
| | Yielding | Buckling | | Yielding | Buckling | MNA | GMNIA | MNA | GMNIA |
| $0\times N_{Rk}$ | 727.82 | 541.62 | - | - | - | 710.90 | 707.00 | 745.00 | 741.46 |
| $0.1\times N_{Rk}$ | 727.82 | 541.62 | - | - | - | 707.00 | 695.30 | 742.19 | 735.28 |
| $0.3\times N_{Rk}$ | 727.82 | 541.62 | - | - | - | 699.20 | 679.70 | 731.33 | 719.38 |
| $0.5\times N_{Rk}$ | 727.82 | 541.62 | - | - | - | 679.70 | 644.50 | 711.12 | 689.68 |
| $0.7\times N_{Rk}$ | 727.82 | 541.62 | - | - | - | 640.60 | 578.10 | 675.85 | 600.34 |
| $0.9\times N_{Rk}$ | 582.26 | 433.29 | - | - | - | 554.70 | 472.70 | 610.72 | 422.93 |

*Tab. 25 Influence of normal force in IPE 600 - Load-carrying capacity [kN]*

| Normal force $F_x$ | EN 1993-1-8 | | EN 1993-1-5 | AISC 360-16 | | IDEA StatiCa | | ANSYS | |
|---|---|---|---|---|---|---|---|---|---|
| | Yielding | Buckling | | Yielding | Buckling | MNA | GMNIA | MNA | GMNIA |
| $0\times N_{Rk}$ | 996.84 | 737.56 | - | - | - | 984.40 | 976.60 | 1018.20 | 1013.84 |
| $0.1\times N_{Rk}$ | 996.84 | 737.56 | - | - | - | 976.60 | 964.80 | 1014.72 | 1005.88 |
| $0.3\times N_{Rk}$ | 996.84 | 737.56 | - | - | - | 968.80 | 941.40 | 1001.21 | 985.22 |
| $0.5\times N_{Rk}$ | 996.84 | 737.56 | - | - | - | 941.40 | 894.50 | 974.19 | 943.74 |
| $0.7\times N_{Rk}$ | 996.84 | 737.56 | - | - | - | 882.80 | 789.10 | 926.58 | 800.91 |
| $0.9\times N_{Rk}$ | 797.47 | 590.05 | - | - | - | 769.50 | 652.30 | 841.64 | 565.28 |

*Tab. 26 Influence of normal force in wI100×100×10×10 - Load-carrying capacity [kN]*

| Normal force $F_x$ | EN 1993-1-8 | | EN 1993-1-5 | AISC 360-16 | | IDEA StatiCa | | ANSYS | |
|---|---|---|---|---|---|---|---|---|---|
| | Yielding | Buckling | | Yielding | Buckling | MNA | GMNIA | MNA | GMNIA |
| $0\times N_{Rk}$ | 288.31 | 288.31 | - | - | - | 314.45 | 314.45 | 279.98 | 280.79 |
| $0.1\times N_{Rk}$ | 288.31 | 288.31 | - | - | - | 312.50 | 310.55 | 281.34 | 282.41 |
| $0.3\times N_{Rk}$ | 288.31 | 288.31 | - | - | - | 306.65 | 302.75 | 283.56 | 283.74 |
| $0.5\times N_{Rk}$ | 288.31 | 288.31 | - | - | - | 294.90 | 291.00 | 279.01 | 278.38 |
| $0.7\times N_{Rk}$ | 288.31 | 288.31 | - | - | - | 271.50 | 265.65 | 267.45 | 265.77 |
| $0.9\times N_{Rk}$ | 230.65 | 230.65 | - | - | - | 228.50 | 222.65 | 235.74 | 225.41 |

*Tab. 27 Influence of normal force in wI550×300×10×20 - Load-carrying capacity [kN]*

| Normal force $F_x$ | EN 1993-1-8 | | EN 1993-1-5 | AISC 360-16 | | IDEA StatiCa | | ANSYS | |
|---|---|---|---|---|---|---|---|---|---|
| | Yielding | Buckling | | Yielding | Buckling | MNA | GMNIA | MNA | GMNIA |
| $0\times N_{Rk}$ | 526.41 | 408.22 | - | - | - | 937.50 | 914.06 | 901.61 | 899.52 |
| $0.1\times N_{Rk}$ | 526.41 | 408.22 | - | - | - | 933.59 | 898.44 | 897.59 | 886.02 |
| $0.3\times N_{Rk}$ | 526.41 | 408.22 | - | - | - | 921.88 | 871.09 | 880.56 | 844.43 |
| $0.5\times N_{Rk}$ | 526.41 | 408.22 | - | - | - | 898.44 | 816.41 | 854.98 | 778.95 |
| $0.7\times N_{Rk}$ | 526.41 | 408.22 | - | - | - | 843.75 | 738.28 | 810.31 | 670.87 |
| $0.9\times N_{Rk}$ | 421.13 | 326.57 | - | - | - | 753.91 | 632.81 | 723.59 | 452.17 |

Hot-rolled sections HEA 100 and HEA 1000 and welded section wI 550×300×5×20 were analysed only in IDEA StatiCa and resulting resistances are listed in Tab. 28 together with load-carrying capacities according to the EN 19993-1-8.

*Tab. 28 Influence of normal force – other sections - Load-carrying capacity [kN]*

| Section | Normal force $F_x$ $\sigma_{com}/f_y$ | EN 1993-1-8 | | IDEA StatiCa | |
|---|---|---|---|---|---|
| | | Yielding | Buckling | MNA | GMNIA |
| HEA 100 | 0.00 | 191.70 | 191.70 | 156.30 | 156.30 |
| | 0.10 | 191.70 | 191.70 | 152.30 | 152.30 |
| | 0.20 | 191.70 | 191.70 | 152.30 | 148.40 |
| | 0.30 | 191.70 | 191.70 | 148.40 | 144.50 |
| | 0.38 | 191.70 | 191.70 | 144.50 | 144.50 |
| HEA 1000 | 0.00 | 1968.12 | 1318.99 | 2109.30 | 2085.90 |
| | 0.22 | 1968.12 | 1318.99 | 2062.50 | 2004.00 |
| | 0.43 | 1968.12 | 1318.99 | 1968.90 | 1863.30 |
| | 0.59 | 1968.12 | 1318.99 | 1828.20 | 1687.50 |
| | 0.73 | 1917.03 | 1284.75 | 1675.80 | 1511.70 |
| | 0.83 | 1709.78 | 1145.86 | 1535.10 | 1335.90 |
| | 0.91 | 1547.22 | 1036.91 | 1406.40 | 1171.80 |
| wI 550×300×5×20 | 0.00 | 263.20 | 114.17 | 596.12 | 308.98 |
| | 0.32 | 263.20 | 114.17 | 579.67 | 300.79 |
| | 0.67 | 263.20 | 114.17 | 609.91 | 287.14 |
| | 0.82 | 231.29 | 100.33 | 494.90 | 273.42 |
| | 0.95 | 197.43 | 85.64 | 429.31 | 262.50 |
| | 1.01 | 182.73 | 79.26 | 363.65 | 248.85 |

Load–carrying capacities are graphically displayed in Fig. 131 to Fig. 136 and Fig. 137 to Fig. 138 for all used methods for axially and transversally compressed members of cross section for rolled IPE 100 to IPE 600 and welded wI100×100×10×10 and wI550×300×10×20, respectively.

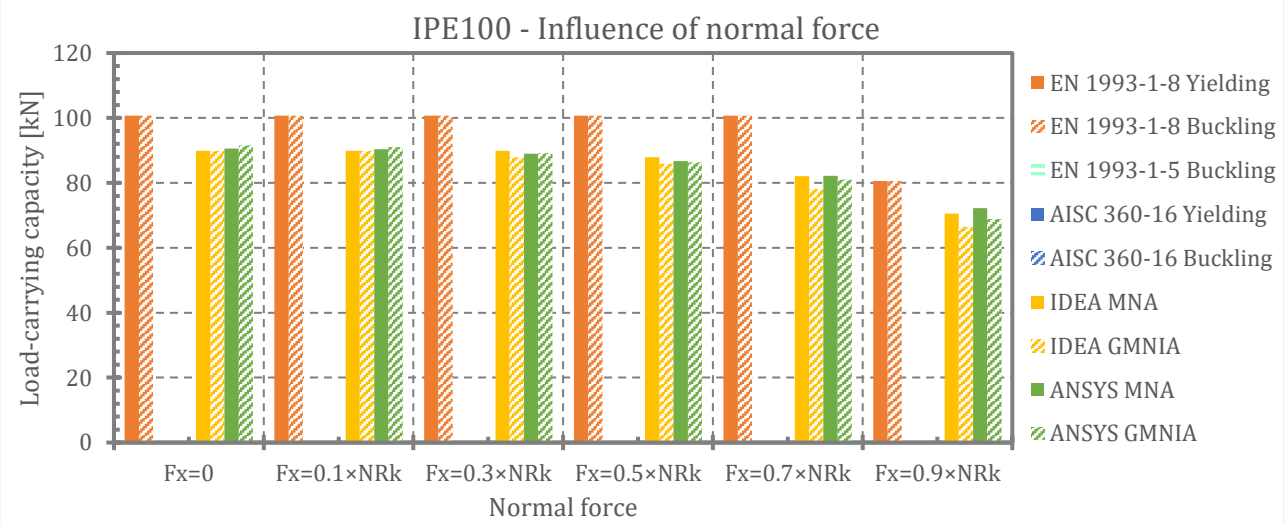


*Fig. 131 Influence of normal force in transversally compressed member IPE 100 – Load-carrying capacity*

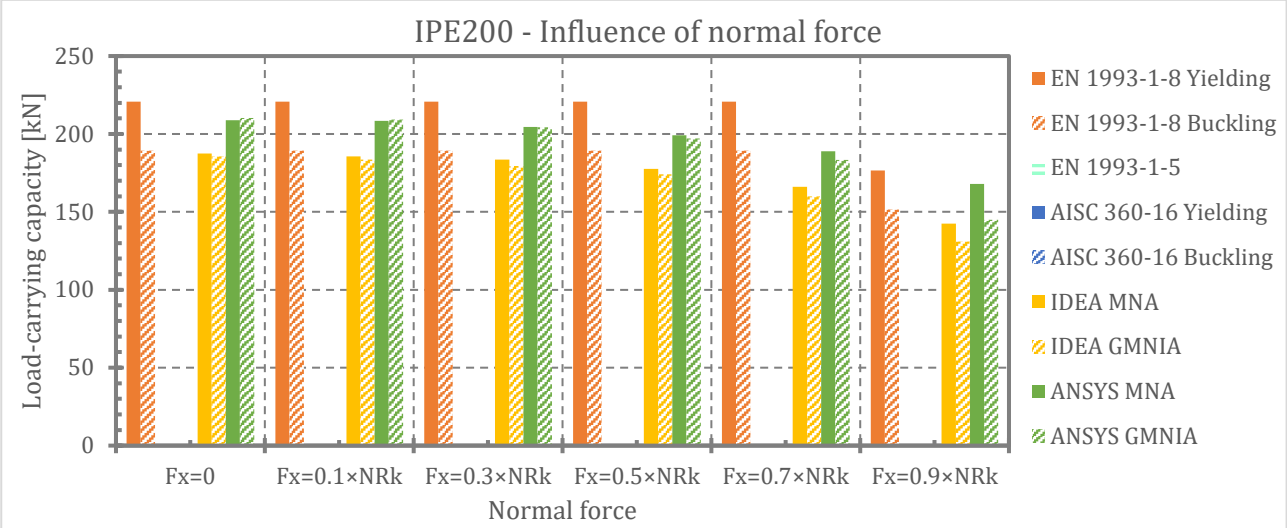


*Fig. 132 Influence of normal force in transversally compressed member IPE 200 – Load-carrying capacity*

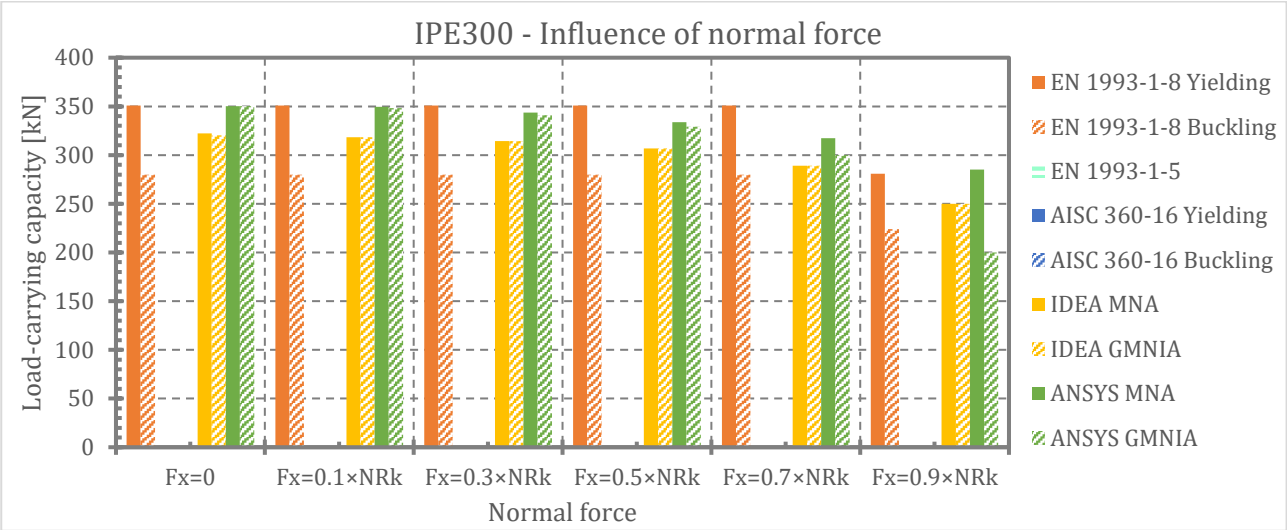


*Fig. 133 Influence of normal force in transversally compressed member IPE 300 – Load-carrying capacity*

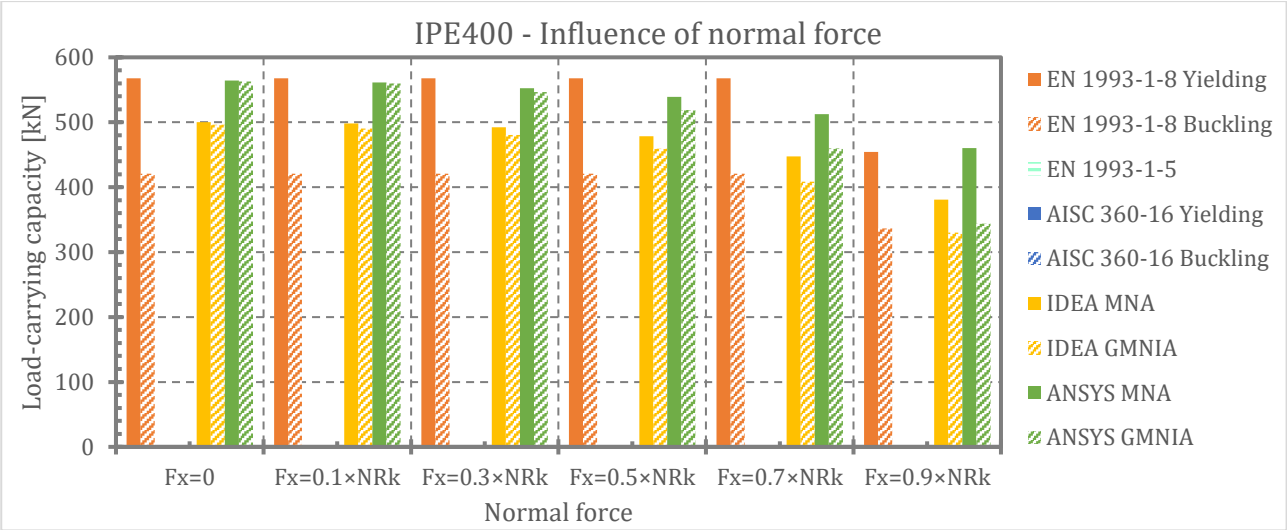


*Fig. 134 Influence of normal force in transversally compressed member IPE 400 – Load-carrying capacity*

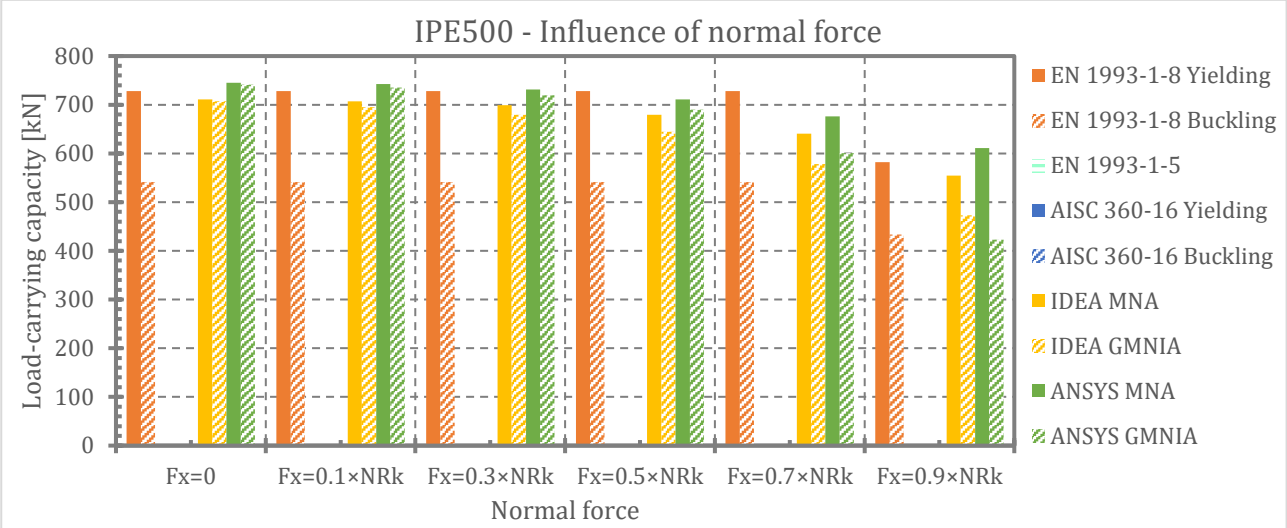


*Fig. 135 Influence of normal force in transversally compressed member IPE 500 – Load-carrying capacity*

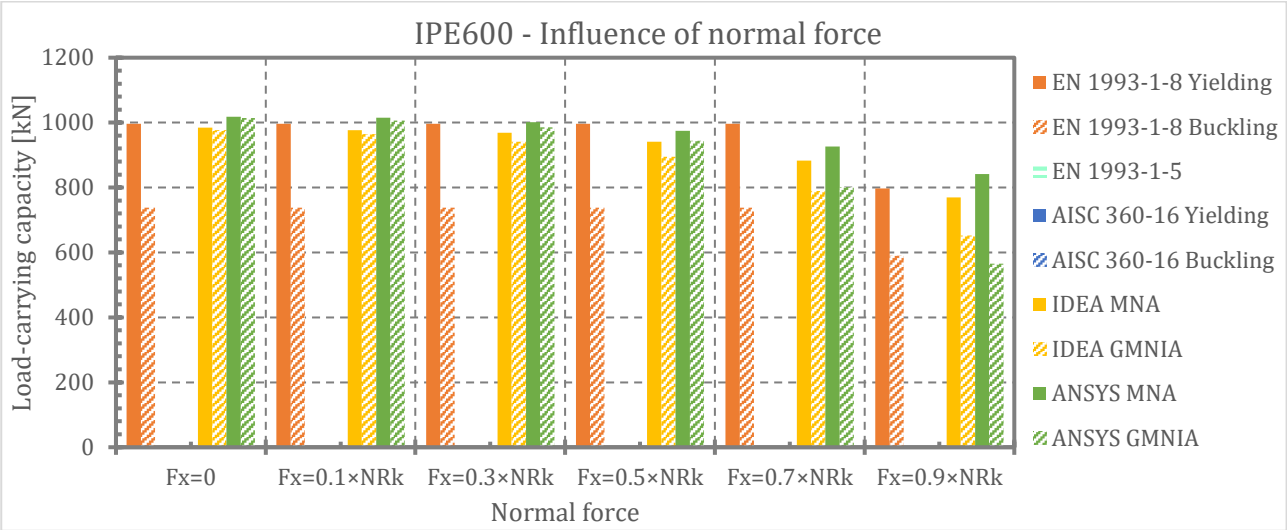


*Fig. 136 Influence of normal force in transversally compressed member IPE 600 – Load-carrying capacity*

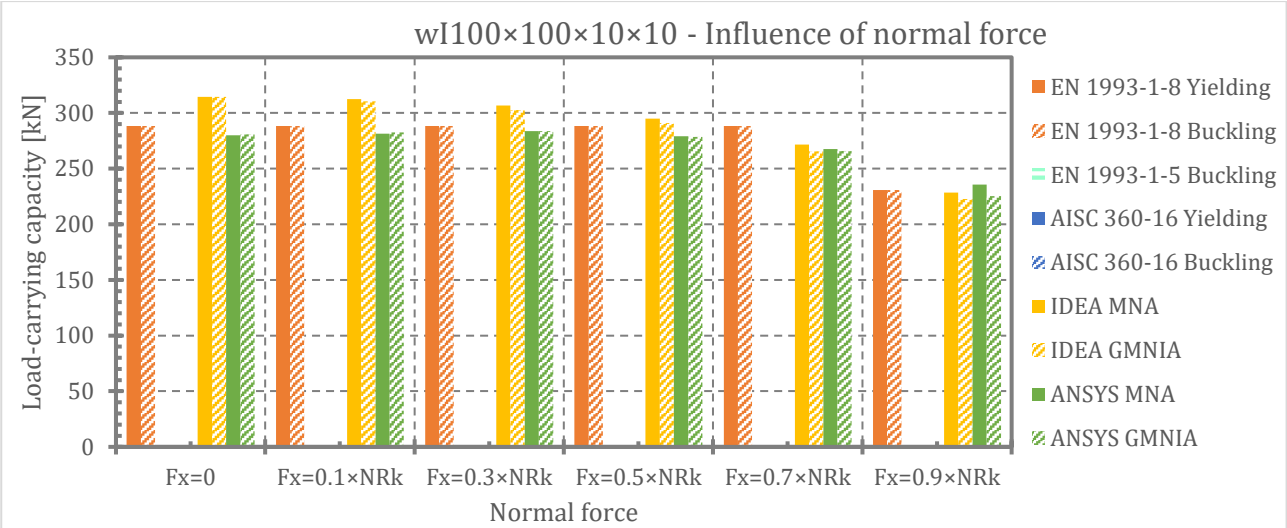


*Fig. 137 Influence of normal force in trans. compr. member wI100×100×10×10 – Load-carrying capacity*

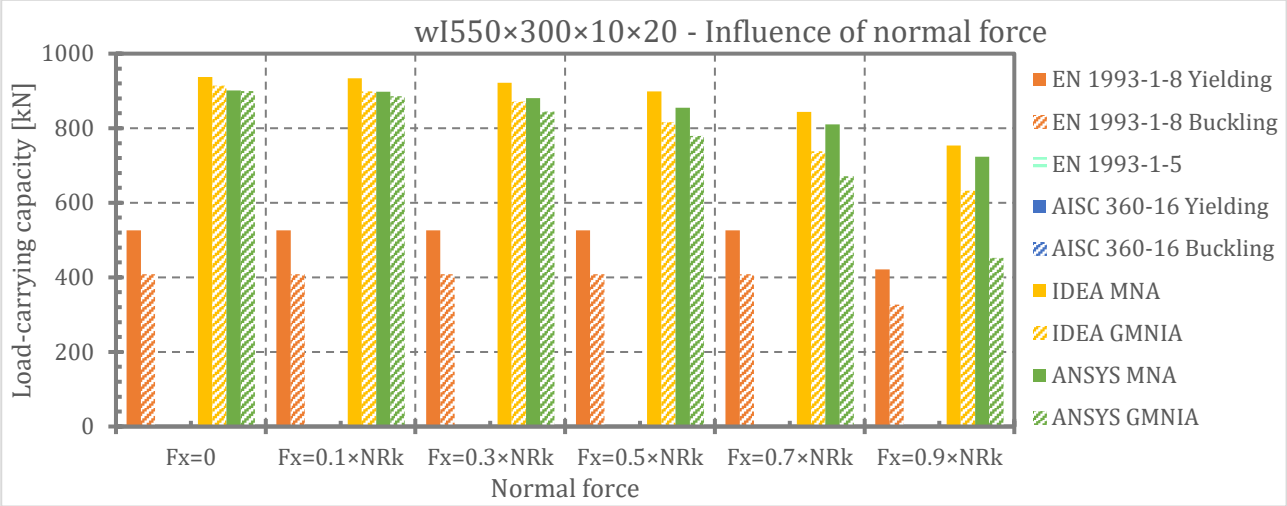


*Fig. 138 Influence of normal force in trans. compr. member wI550×300×10×20 – Load-carrying capacity*

Influence of normal force $F_x$ (axial load) on transversal load-carrying capacity is clearly shown in Fig. 139 to Fig. 146 where ratio of load-carrying capacities related to zero normal force ($F_x = 0$) is on vertical axis.

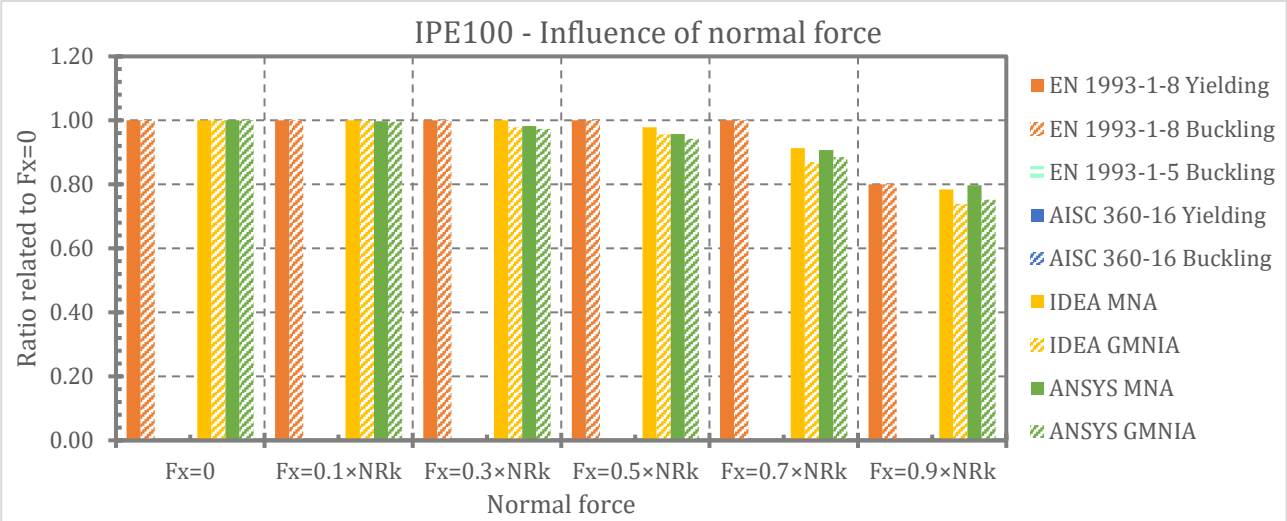


*Fig. 139 Influence of normal force in IPE 100 – relative influence of axial force on load-carrying capacity*

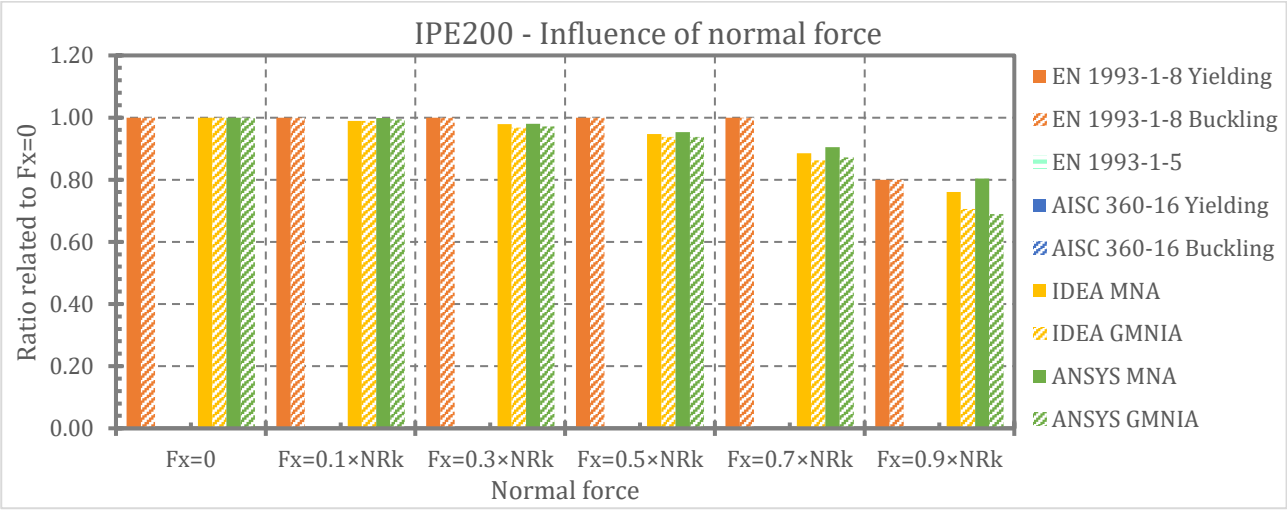


*Fig. 140 Influence of normal force in IPE 200 – relative influence of axial force on load-carrying capacity*

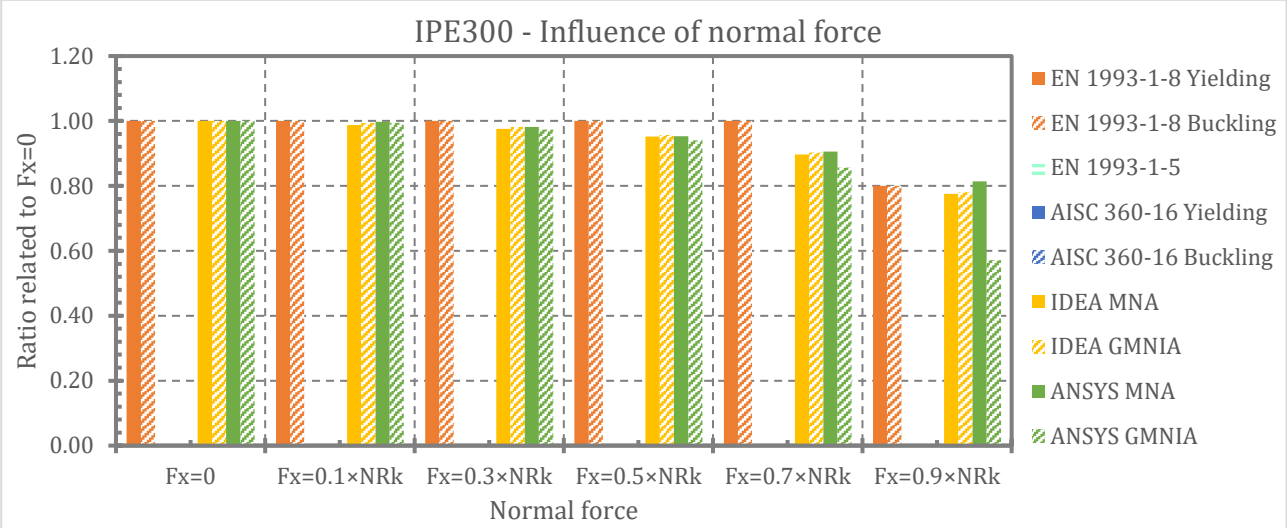


*Fig. 141 Influence of normal force in IPE 300 – relative influence of axial force on load-carrying capacity*

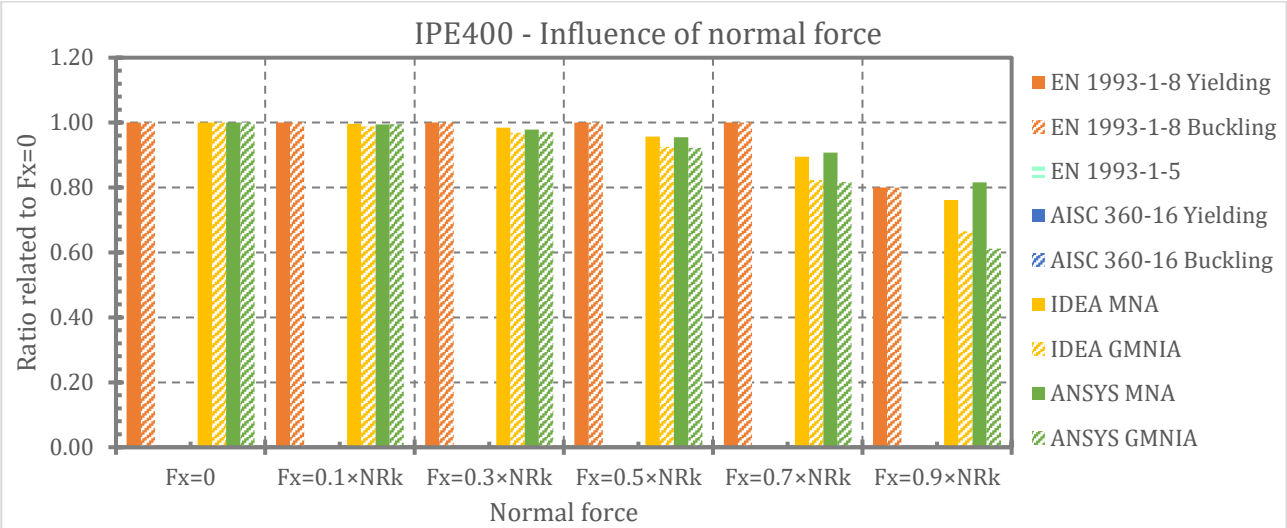


*Fig. 142 Influence of normal force in IPE 400 – relative influence of axial force on load-carrying capacity*

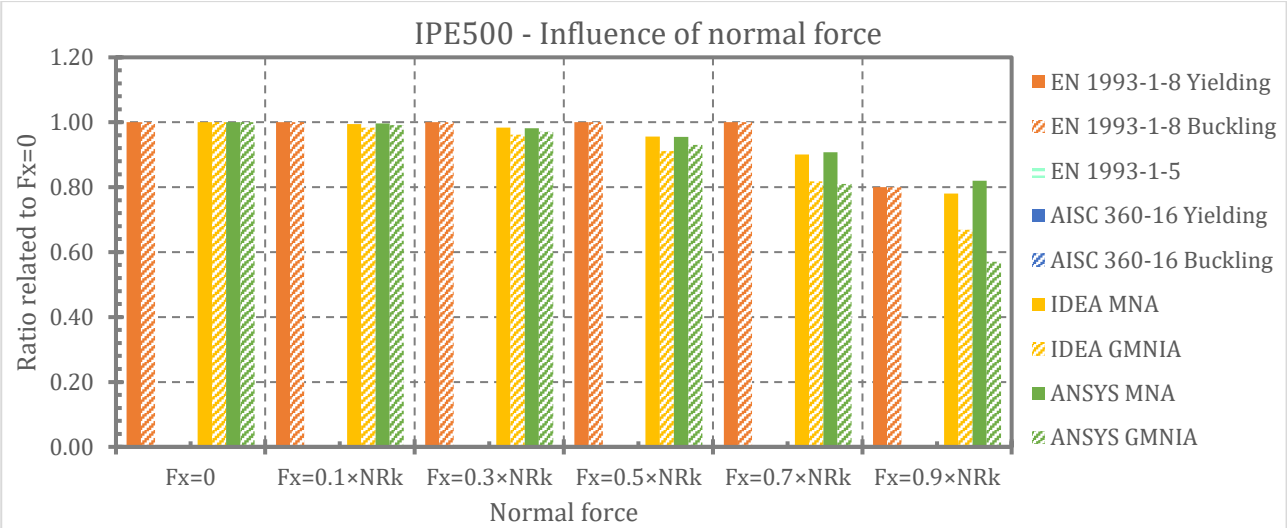


*Fig. 143 Influence of normal force in IPE 500 – relative influence of axial force on load-carrying capacity*

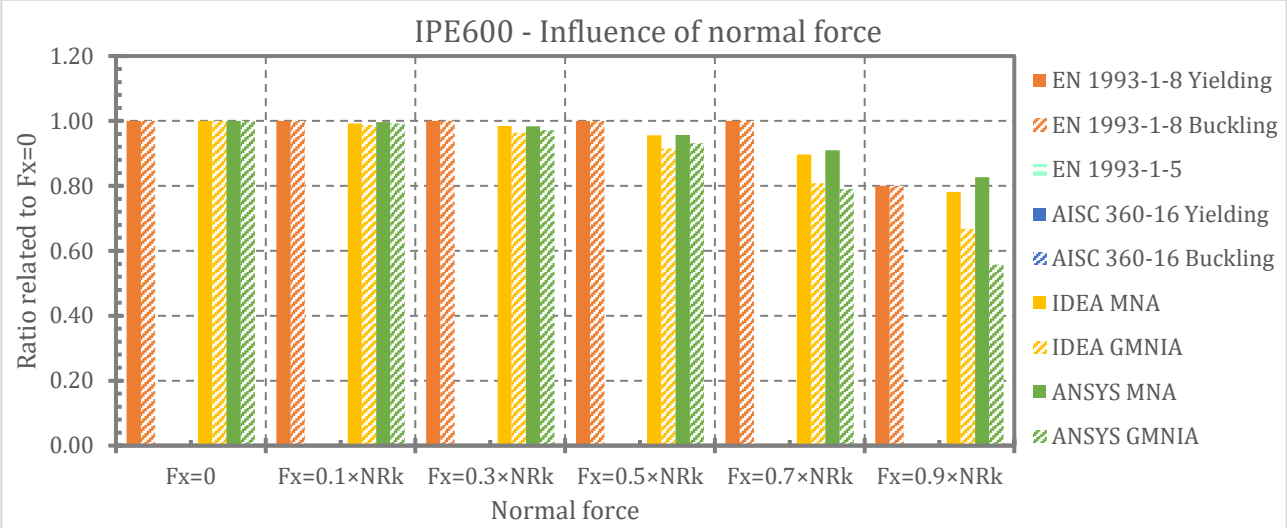


*Fig. 144 Influence of normal force in IPE 600 – relative influence of axial force on load-carrying capacity*

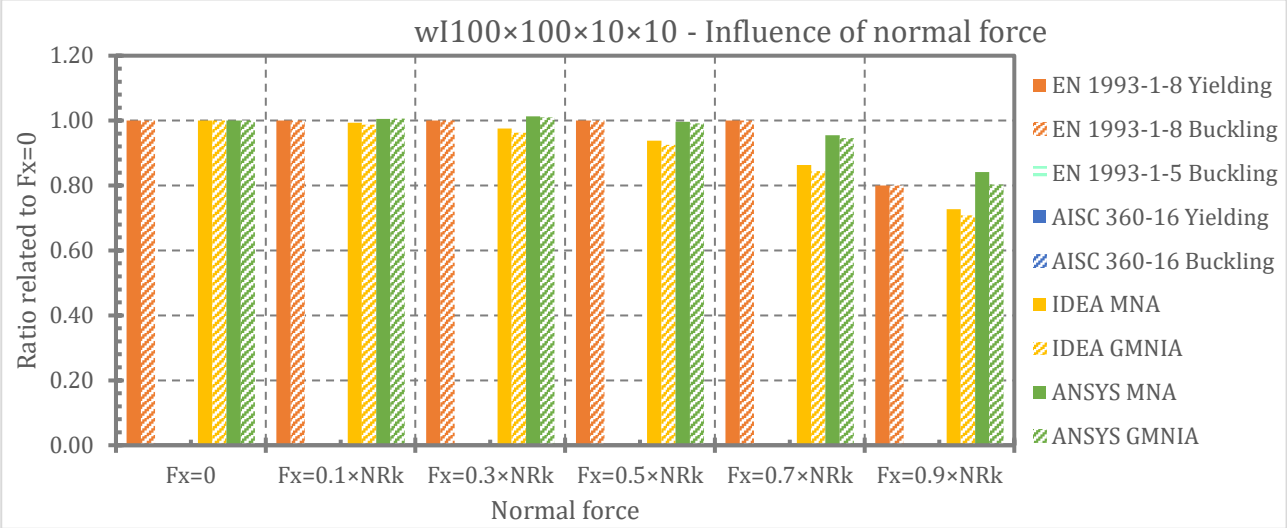


*Fig. 145 Influence of normal force in wI100×100×10×10 – relative influence of axial force on load-carrying capacity*

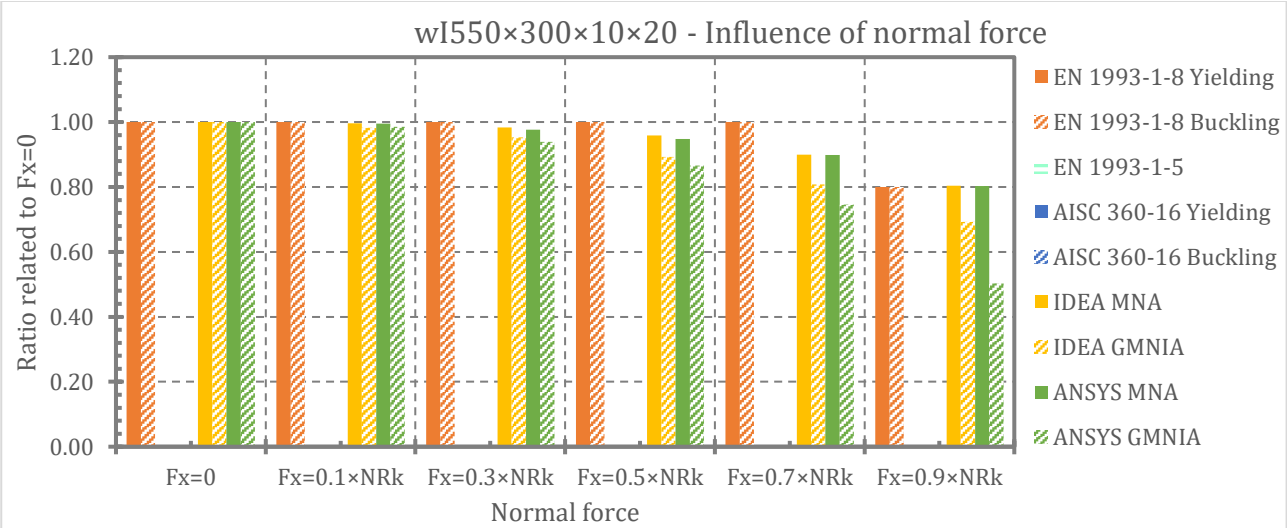


*Fig. 146 Influence of normal force in wI550×300×10×20 – relative influence of axial force on load-carrying capacity*

Influence of buckling on transversal load-carrying capacity is clearly shown in Fig. 147 and Fig. 154 where ratio of load-carrying capacities resulting from Buckling/Yielding resistances according to the EN 1993-1-8 and AISC 360-16 or GMNIA/MNA resulting from numerical analysis performed in IDEA StatiCa and ANSYS are on vertical axis. Results for EN 1993-1-5 are not listed because this standard does not offer "Yielding" and "Buckling" resistances.

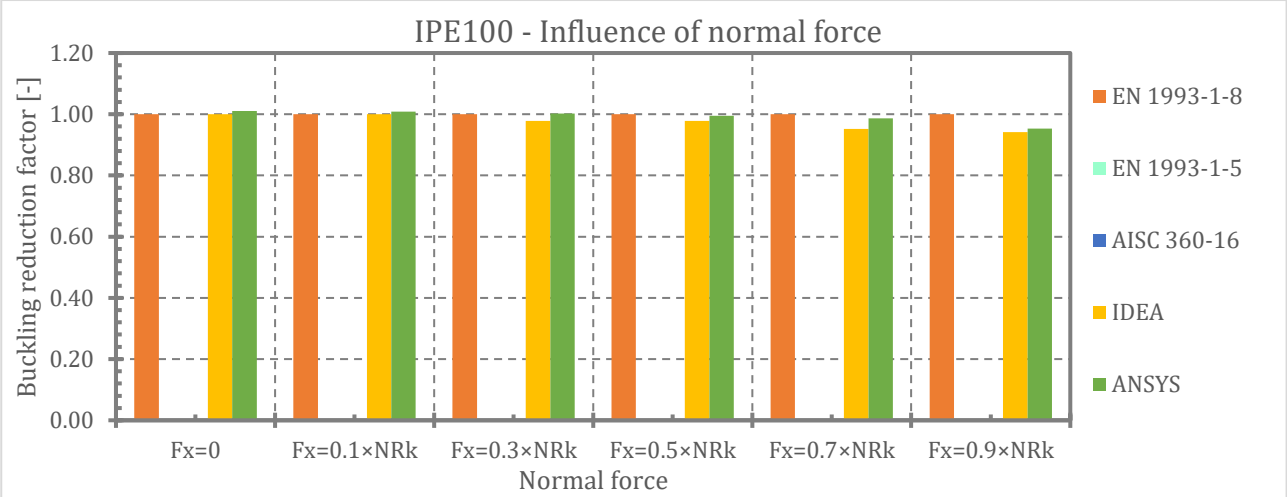


*Fig. 147 Influence of loading plates thickness at IPE 100 – reduction due to geometrical nonlinearity*

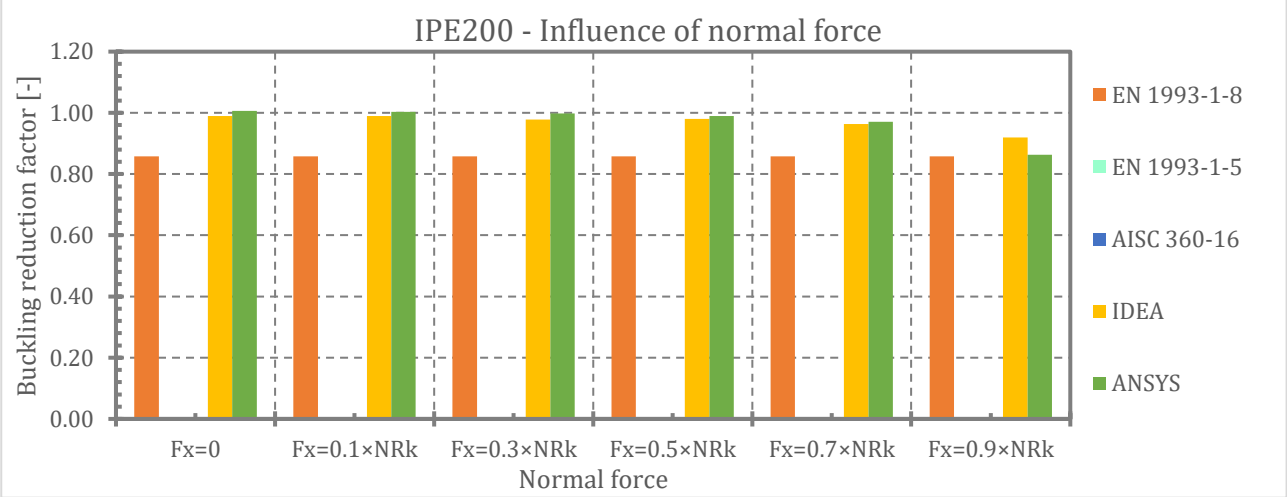


*Fig. 148 Influence of loading plates thickness at IPE 200 – reduction due to geometrical nonlinearity*

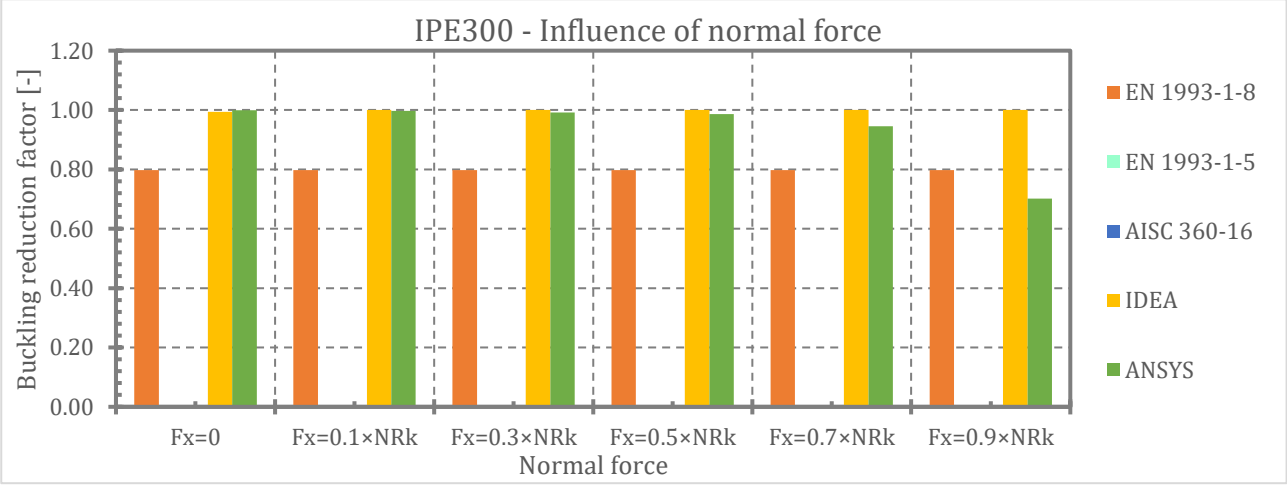


*Fig. 149 Influence of loading plates thickness at IPE 300 – reduction due to geometrical nonlinearity*

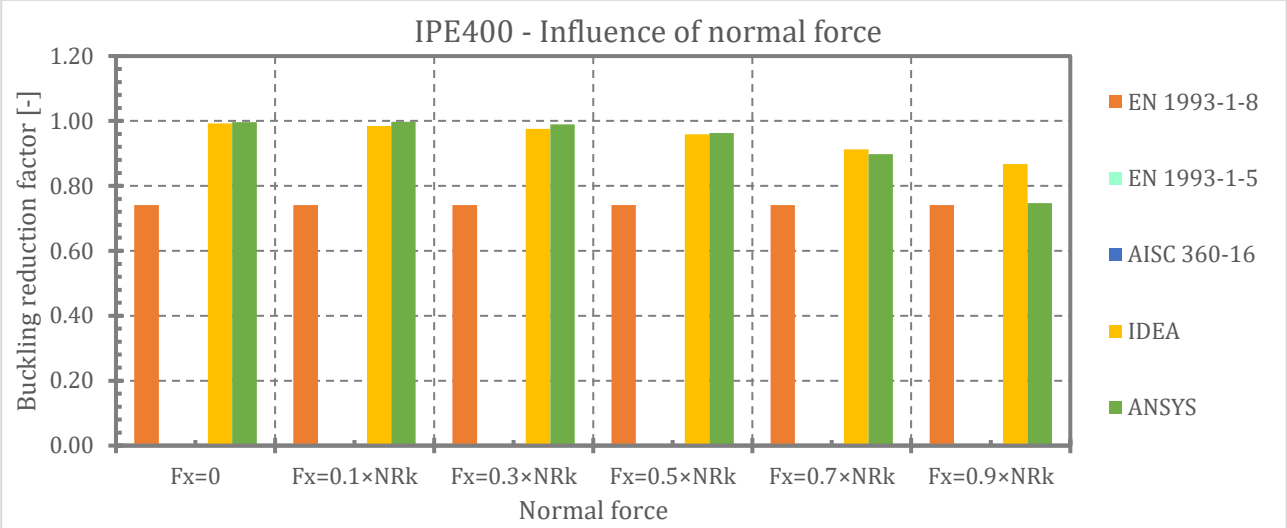


*Fig. 150 Influence of loading plates thickness at IPE 400 – reduction due to geometrical nonlinearity*

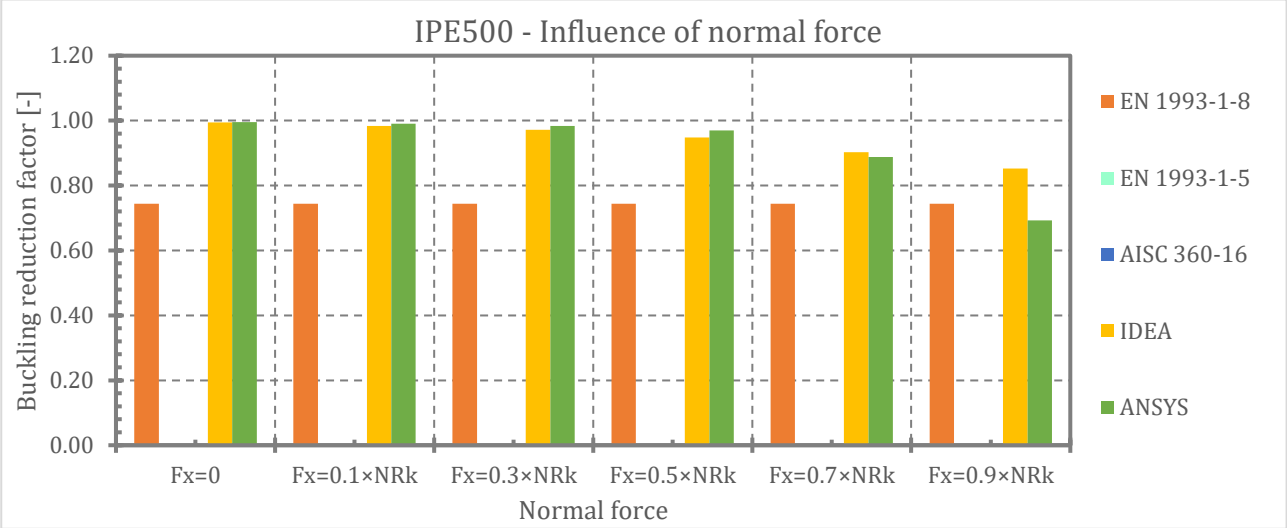


*Fig. 151 Influence of loading plates thickness at IPE 500 – reduction due to geometrical nonlinearity*

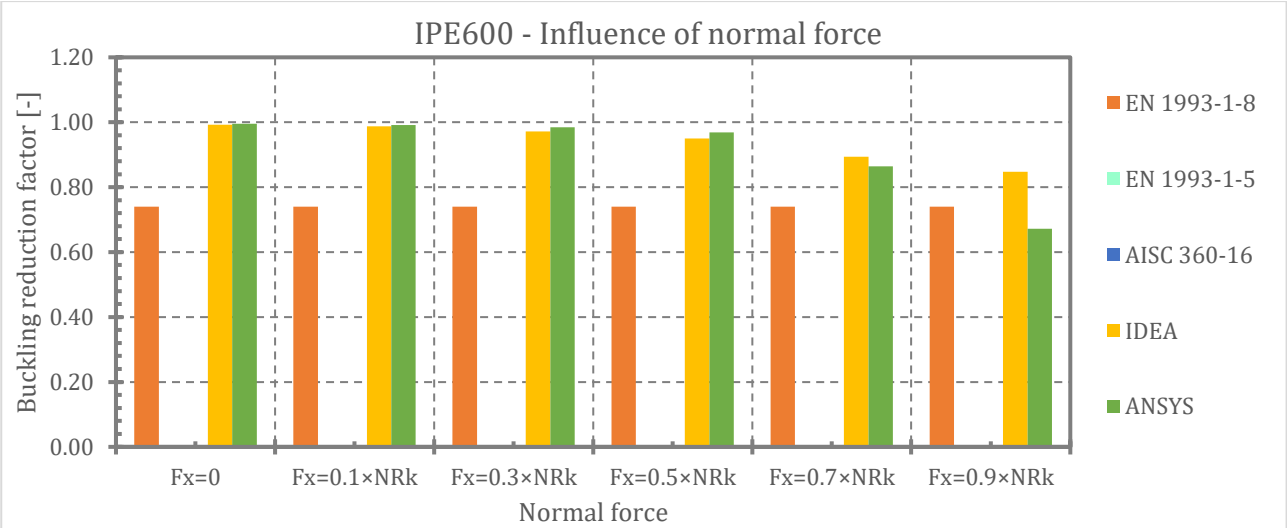


*Fig. 152 Influence of loading plates thickness at IPE 600 – reduction due to geometrical nonlinearity*

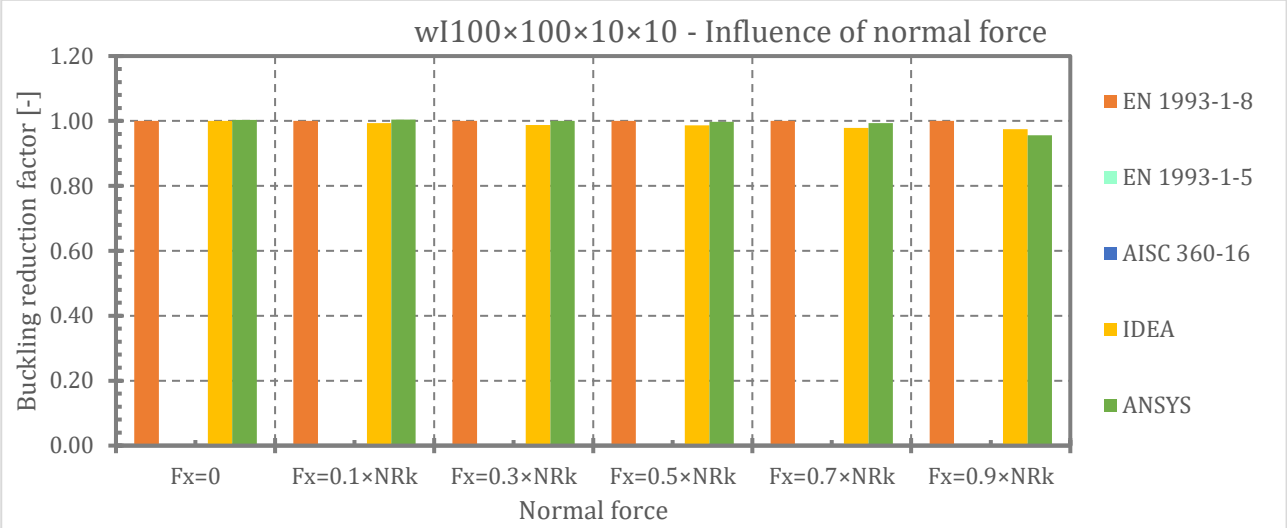


*Fig. 153 Influence of loading plates thickness at wI 100×100×10×10 – reduction due to geometrical nonlinearity*

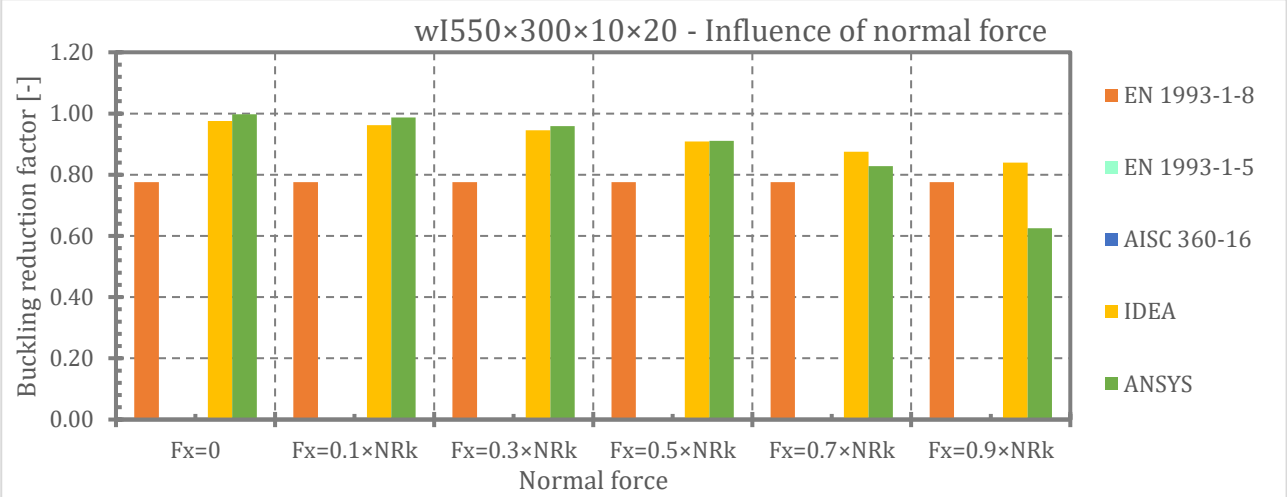


*Fig. 154 Influence of loading plates thickness at wI 550×300×10×20 – reduction due to geometrical nonlinearity*

Synthesis of all obtained data is plotted in Fig. 155 to Fig. 158, where level of reduction is on vertical axis - calculated according to the Eq. (4) for EN 1993-1-8 or as ratio of load-carrying capacities for any level of axial load and zero axial load.

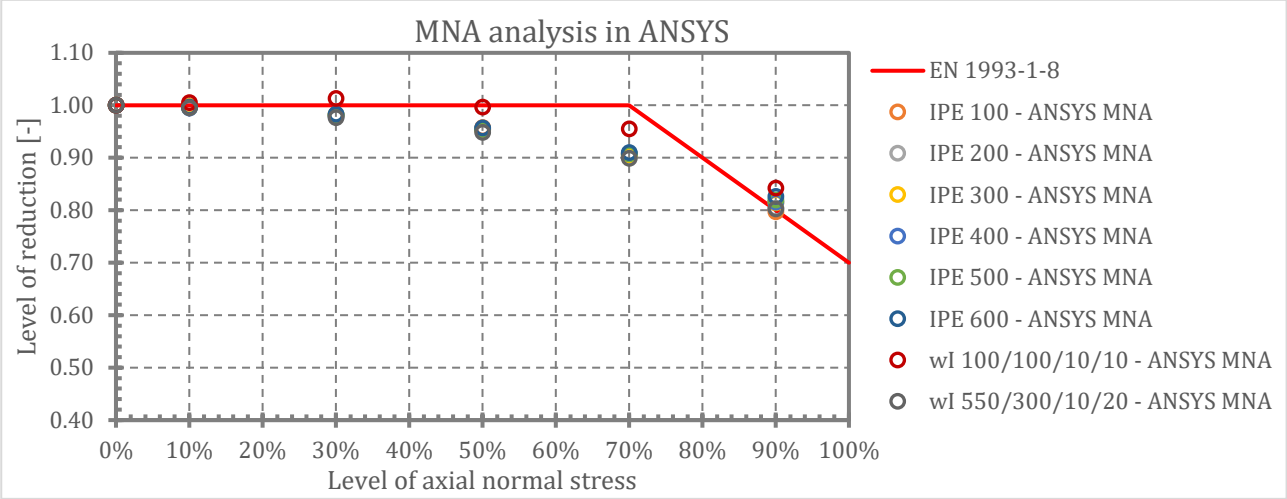


*Fig. 155 Influence of normal force – relative influence of axial force on load-carrying capacity*

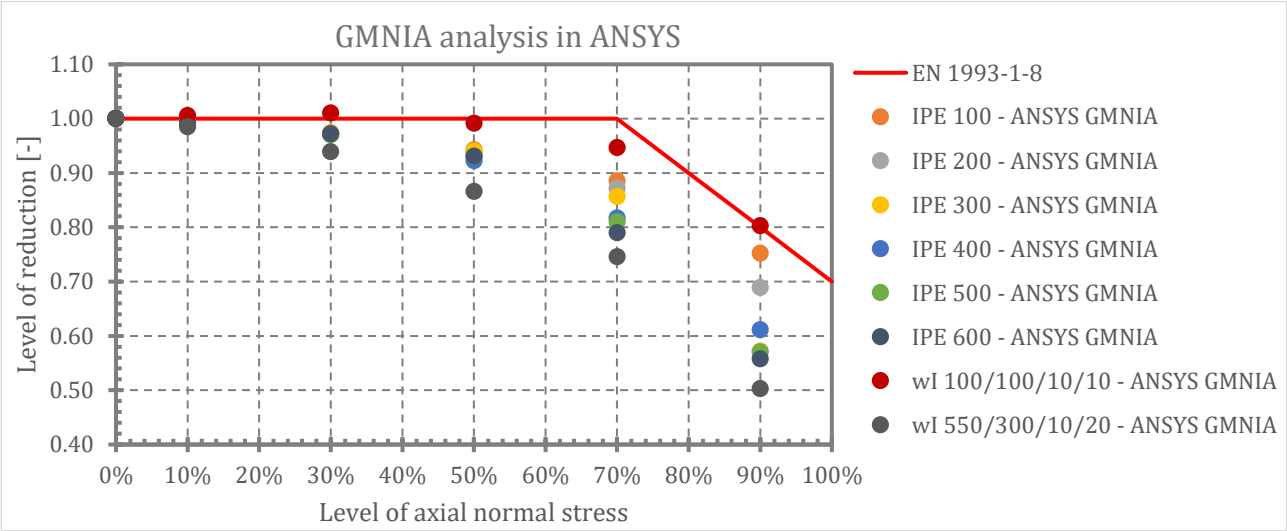


*Fig. 156 Influence of normal force – relative influence of axial force on load-carrying capacity*

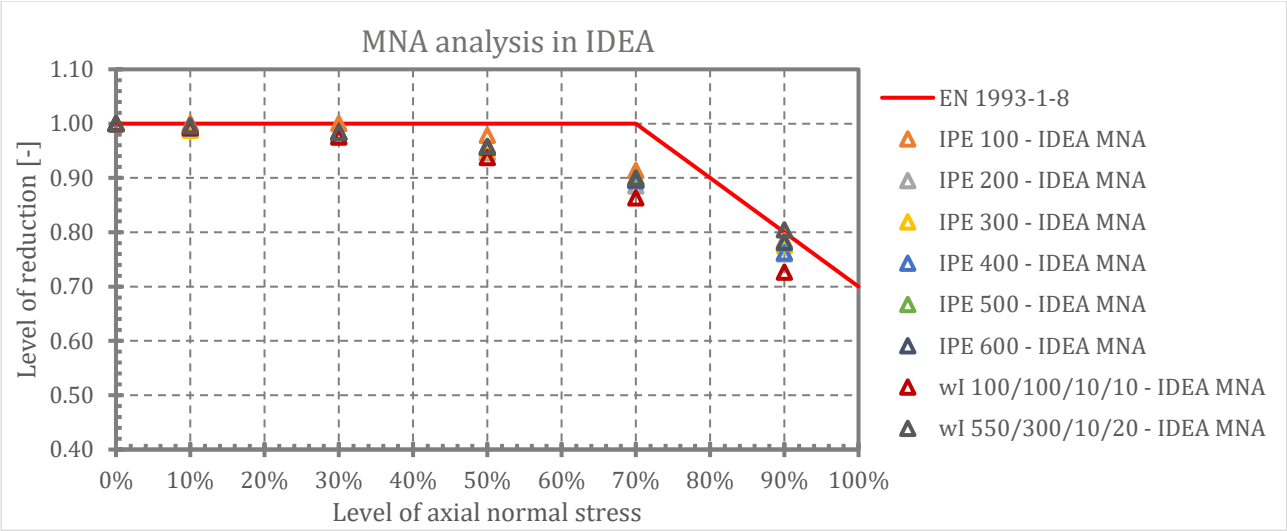


*Fig. 157 Influence of normal force – relative influence of axial force on load-carrying capacity*

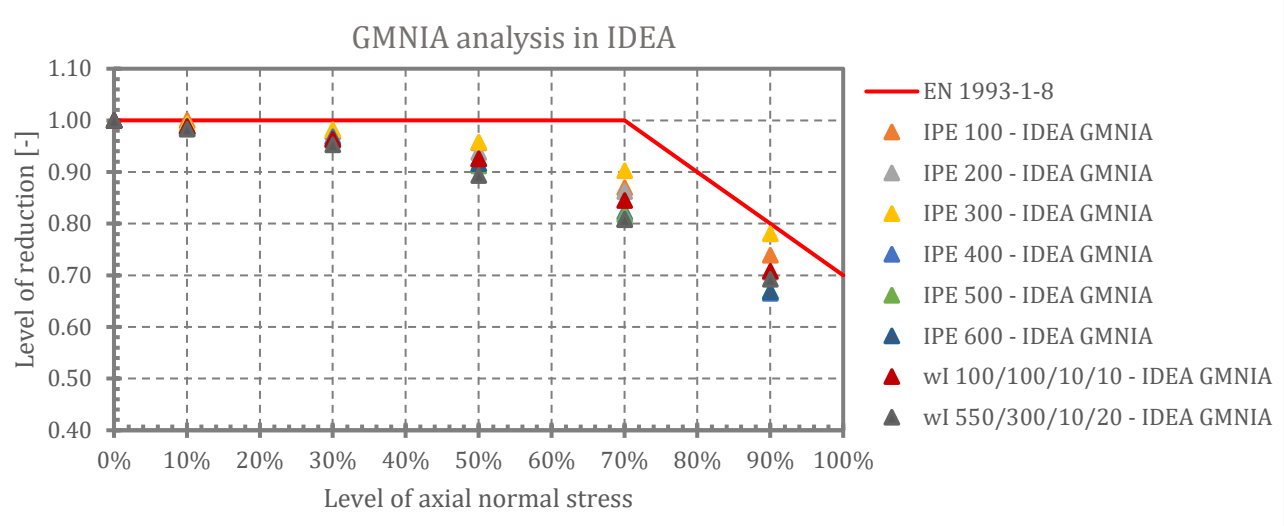


*Fig. 158 Influence of normal force – relative influence of axial force on load-carrying capacity*

All graphs (Fig. 155 to Fig. 158) putted together are plotted in Fig. 159.

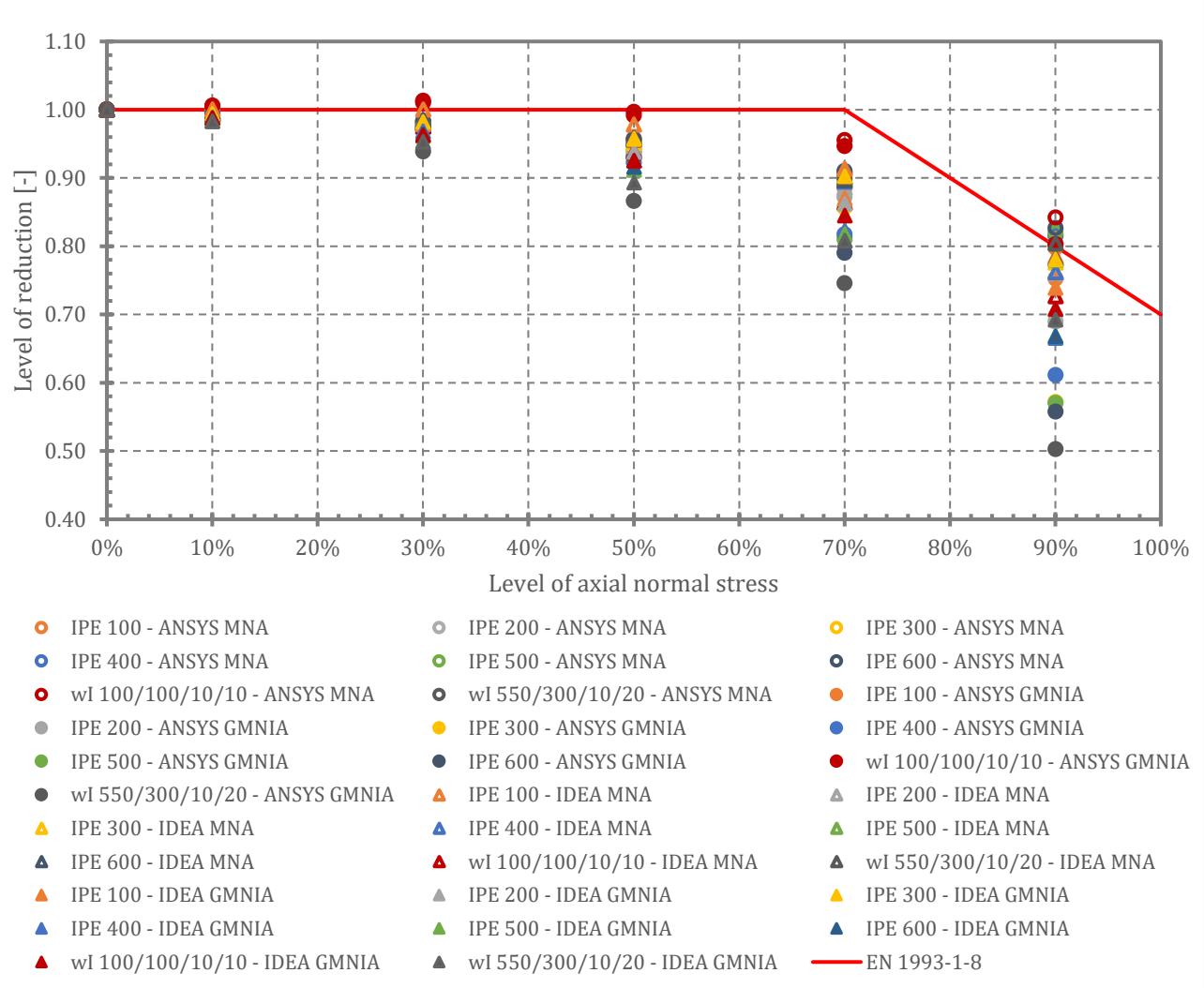


*Fig. 159 Influence of normal force – relative influence of axial force on load-carrying capacity*

The comparison of results with standard provisions was performed using ratios between yielding or buckling resistances in terms of the standard and resistances obtained using

numerical simulations in IDEA StatiCa or ANSYS (MNA or GMNIA). Fig. 160 to Fig. 163 shows ratio between yielding resistance according to the EN1993-1-8 and corresponding resistance obtained from numerical simulations.

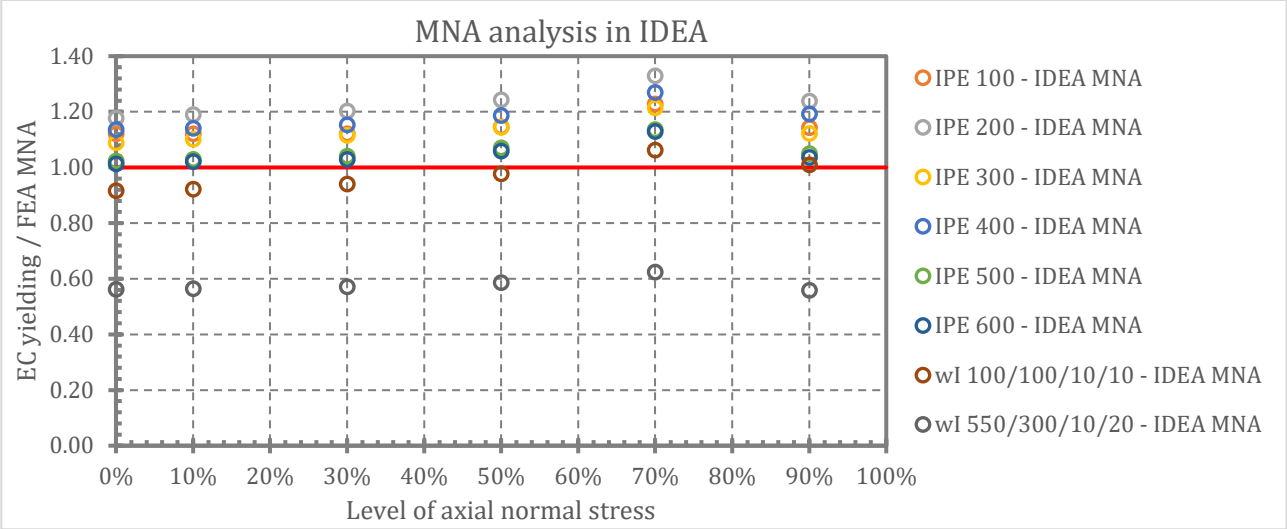


*Fig. 160 Influence of normal force – ratio between yielding resistance and resistance from MNA in IDEA*

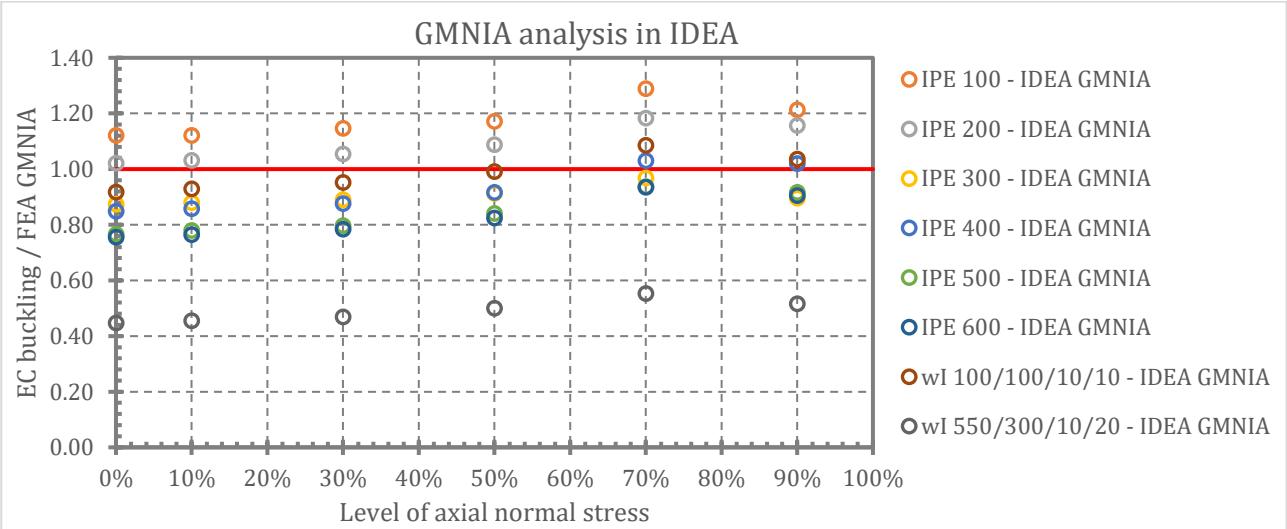


*Fig. 161 Influence of normal force – ratio between buckling resistance and resistance from GMNIA in IDEA*

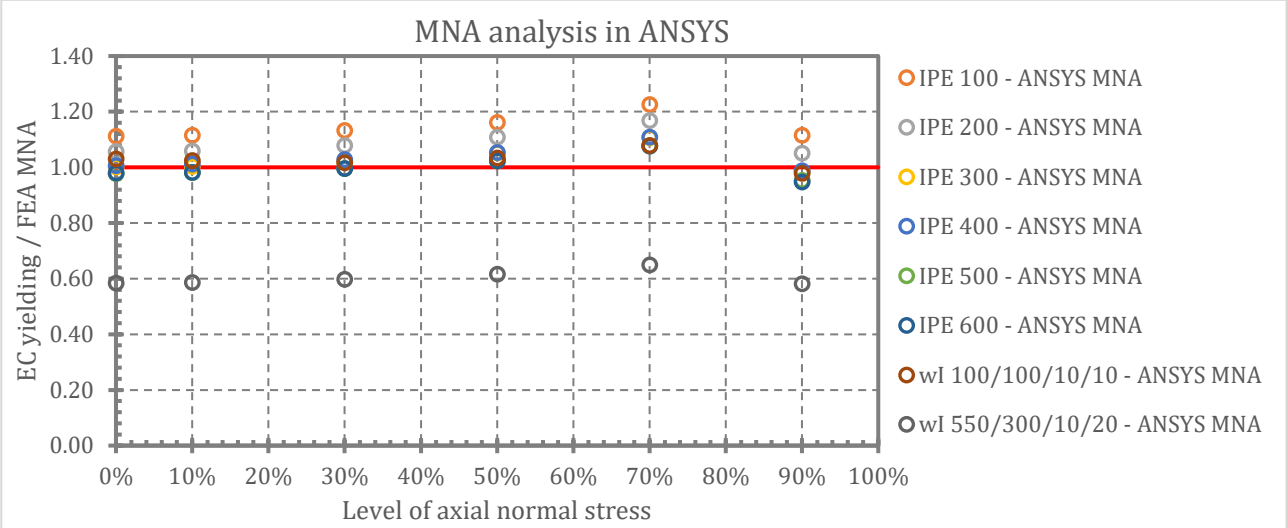


*Fig. 162 Influence of normal force – ratio between yielding resistance and resistance from MNA in ANSYS*

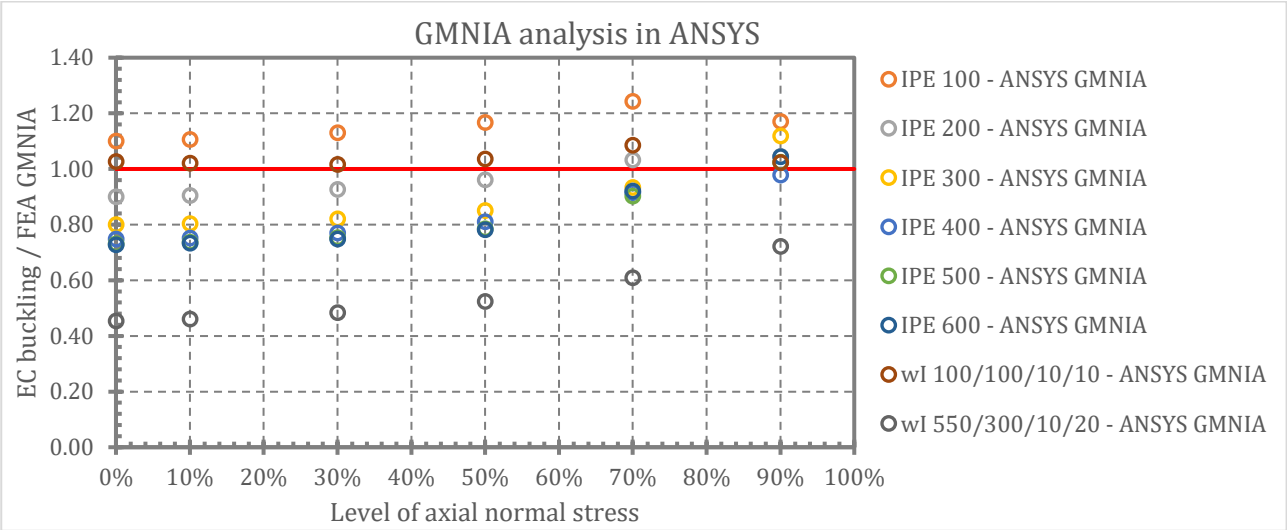


*Fig. 163 Influence of normal force – ratio between buckling resistance and resistance from GMNIA in ANSYS*

Influence of buckling represented by "buckling factor" is shown in Fig. 164 to Fig. 166. Buckling factors resulting from numerical analyses carried out in IDEA StatiCa and ANSYS were calculated as ratio of load-carrying capacity from GMNIA and MNA analysis. Buckling factor in standard EN 1993-1-8 is described in chapter 2.4.1.

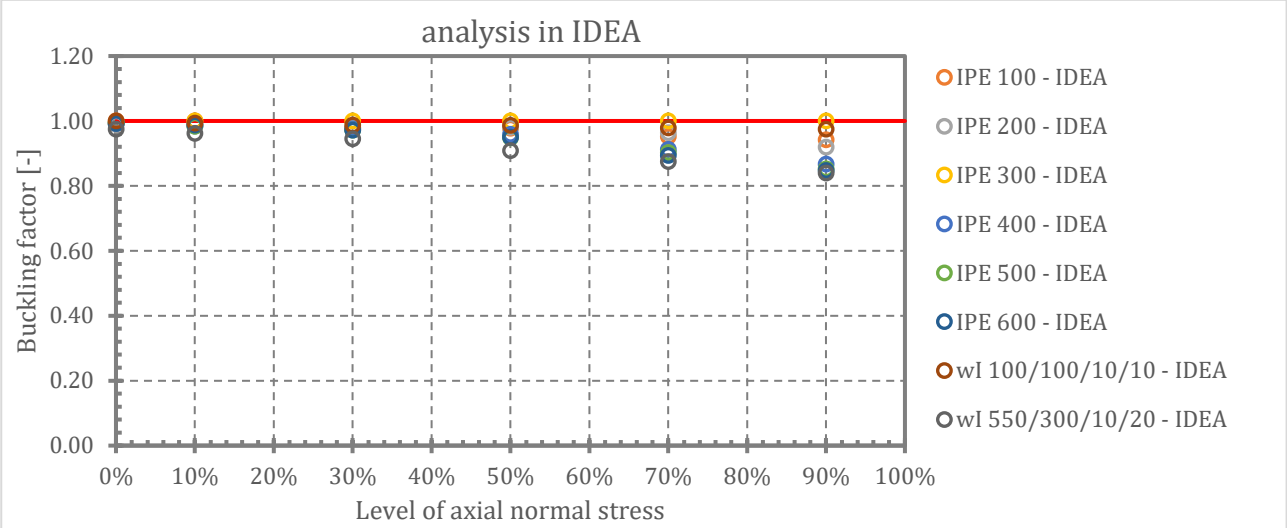


*Fig. 164 Influence of normal force in transversally compressed member – buckling factor*

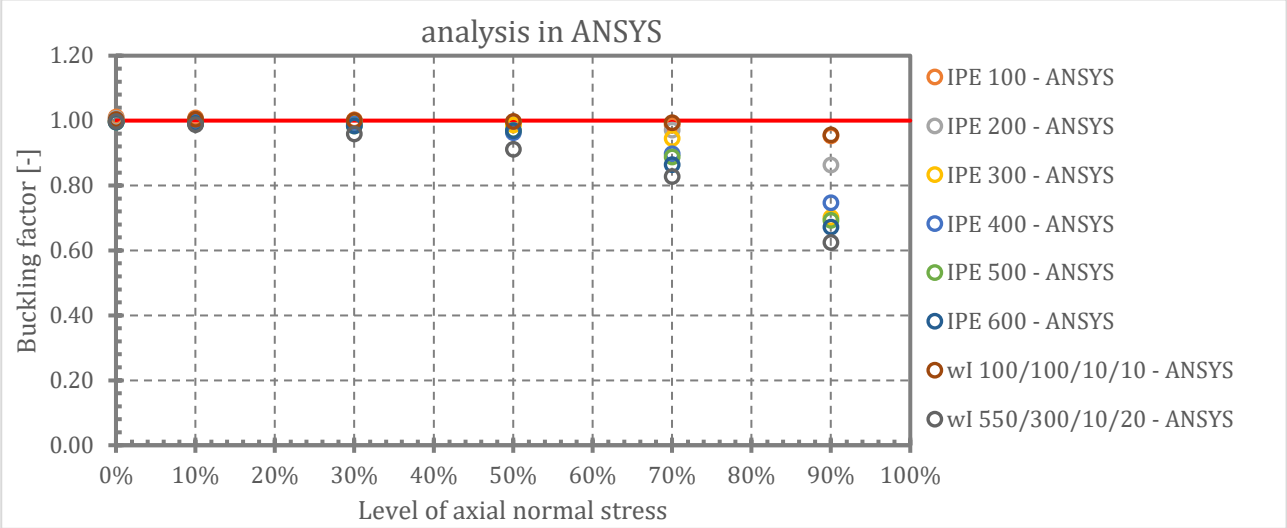


*Fig. 165 Influence of normal force in transversally compressed member – buckling factor*

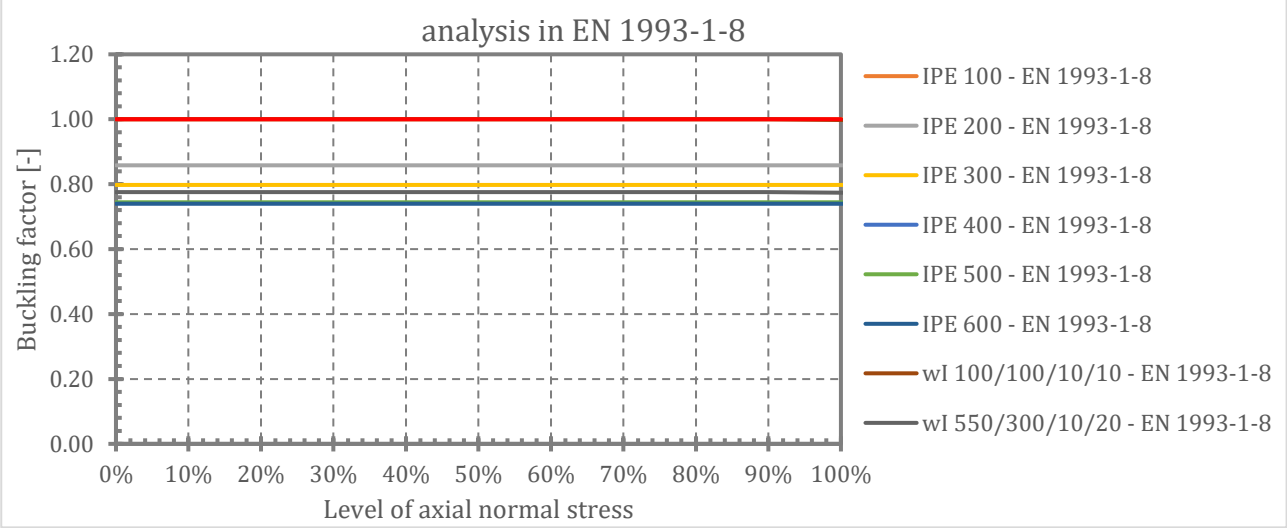


*Fig. 166 Influence of normal force in transversally compressed member – buckling factor*

Actual behaviour of axially and transversally compressed member is described in Fig. 167 to Fig. 172 for illustration for member of cross section IPE 400. For other analysed cross sections, the charts are similar.

Fig. 167 shows results of linear buckling analysis – critical forces $F_{cr}$ [kN] and critical load factor $\alpha_{cr}$ [-]. For increasing level of normal force in member both critical force and critical load factor decreasing.

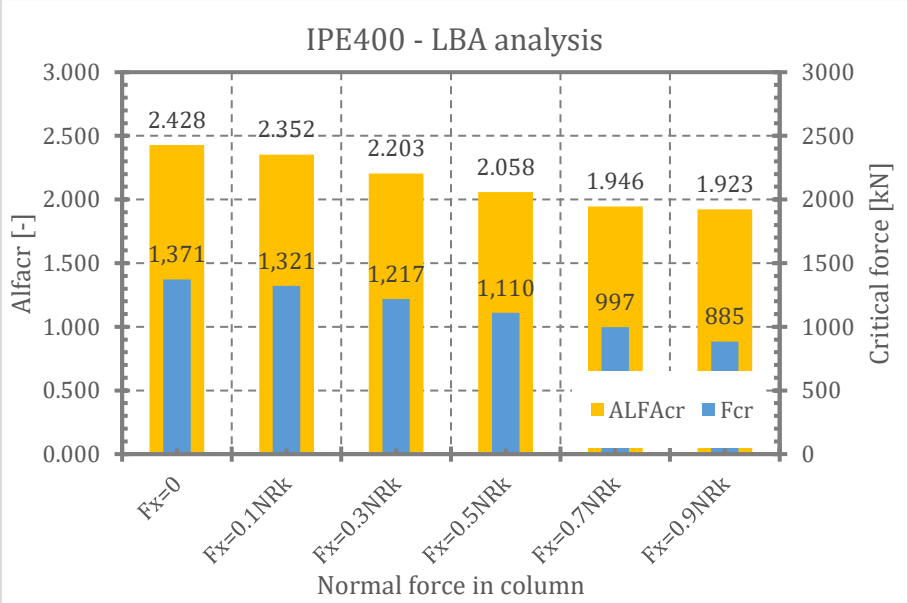


*Fig. 167 Influence of normal force in transversally compressed member – LBA results*

Fig. 168 illustrates relationship of vertical deformation and loading force for MNA and GMNIA. Fig. 169 describes dependency of lateral deformation in the middle of beam web on loading force for MNA and GMNIA. Dependency of maximal equivalent stress and equivalent stress in the middle of member web on loading force is plotted in Fig. 170 and Fig. 171. Fig. 172 shows developing of plastic strain with loading increasing.

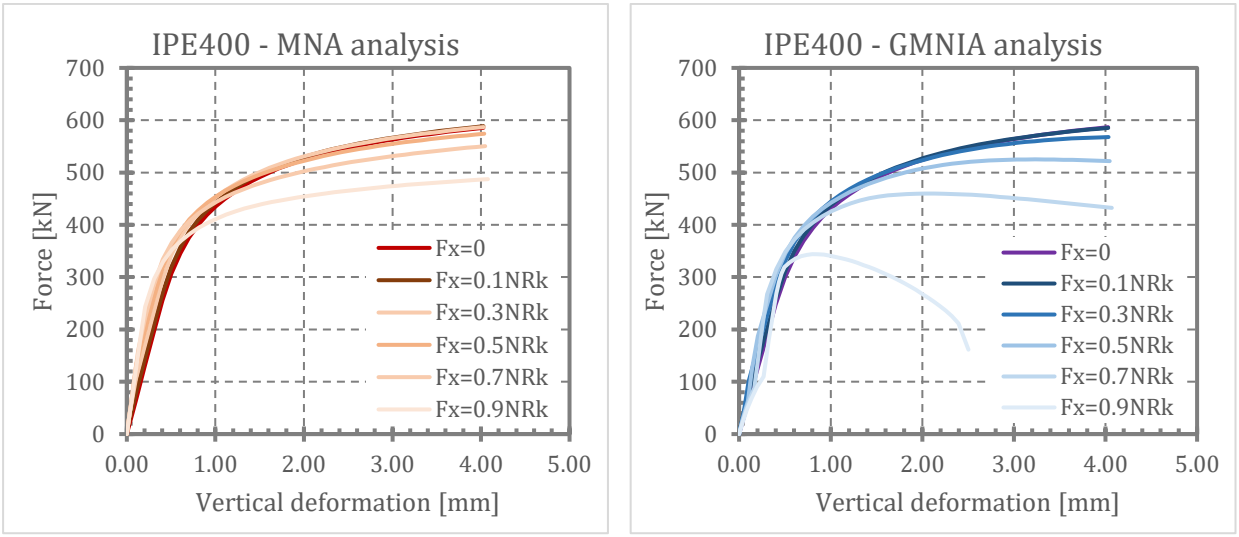


*Fig. 168 Influence of normal force in trans. compressed member – vertical deformation-force relationship*

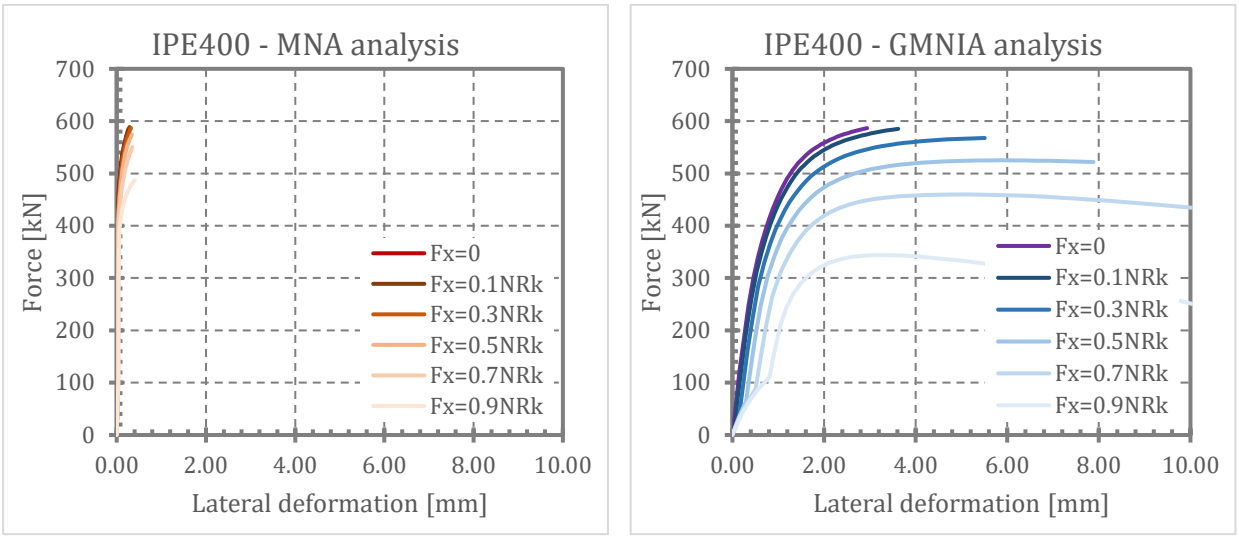


*Fig. 169 Influence of normal force in trans. compressed member – lateral deformation-force relationship*

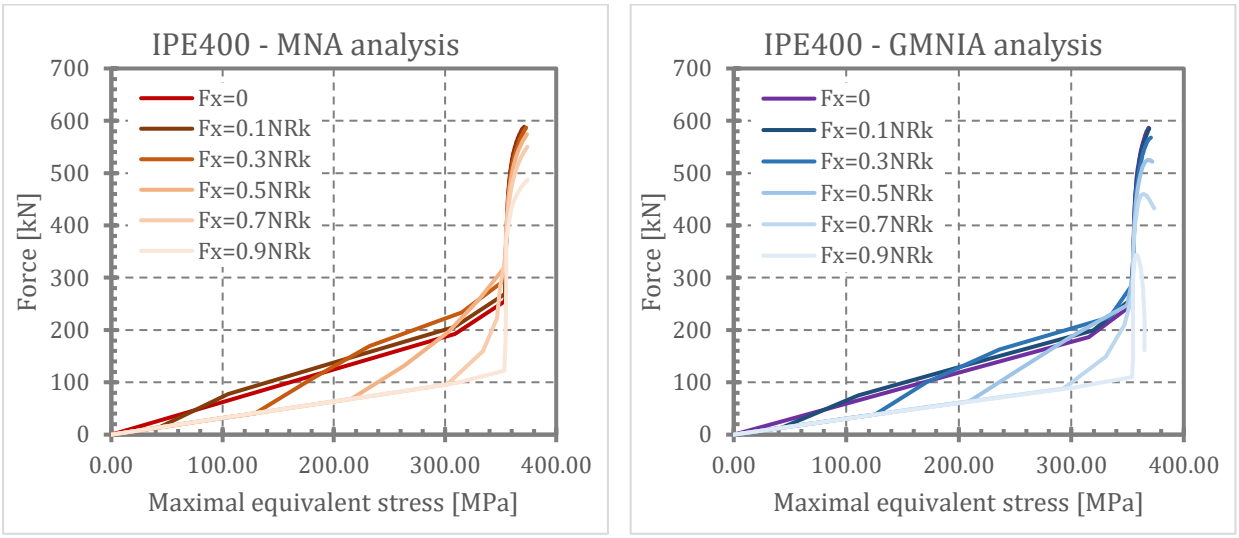


*Fig. 170 Influence of normal force in trans. compr. member – maximal equivalent stress-force relationship*

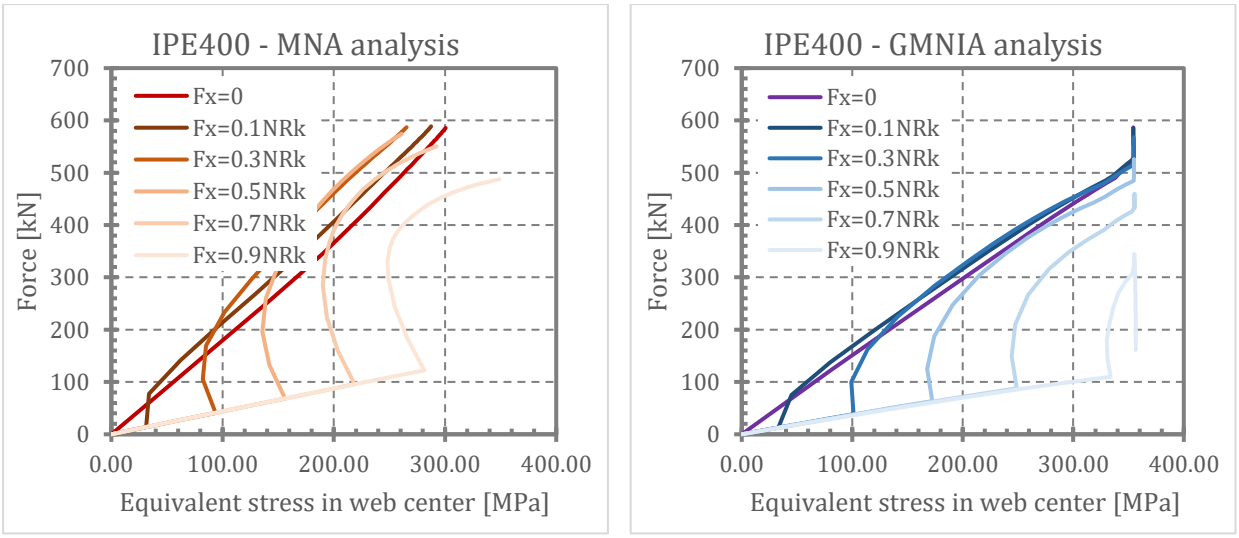


*Fig. 171 Influence of normal force in tr. compr. member – equivalent stress in web center-force relationship*

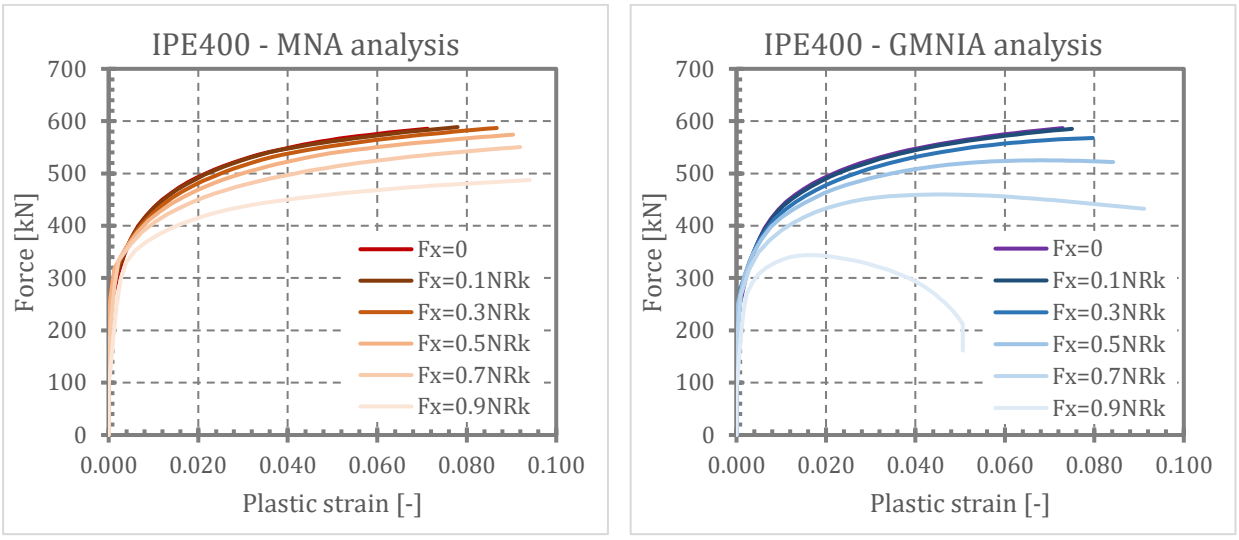


*Fig. 172 Influence of normal force in transversally compressed member – plastic strain-force relationship*

Fig. 173 to Fig. 180 shows comparison of load-carrying capacities obtained from all investigated cases and by all used methods related to the ANSYS results (i.e. ANSYS results are equal to 1.0).

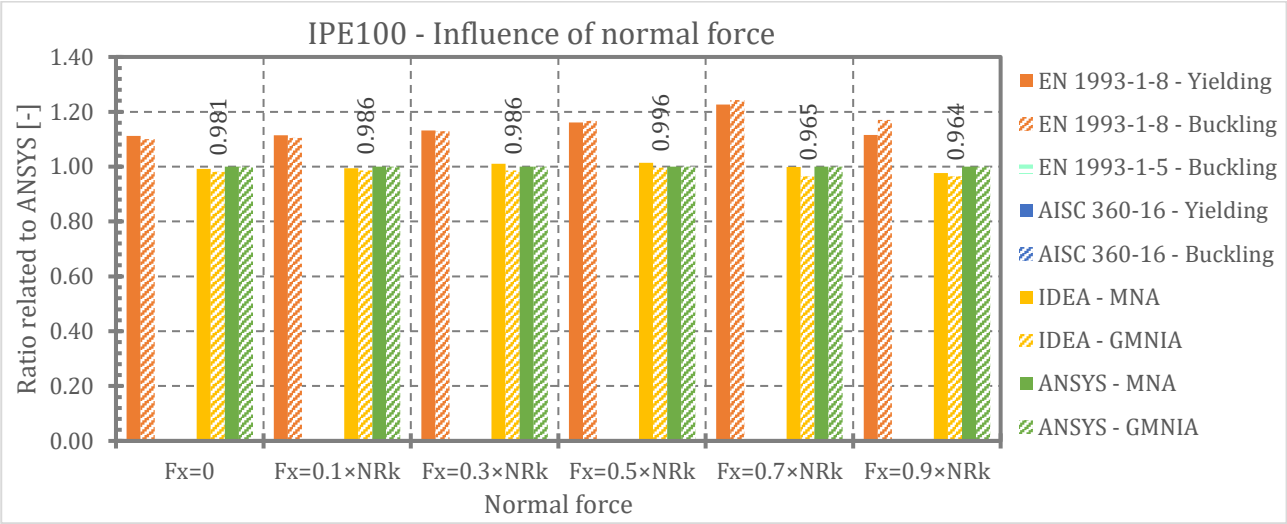


*Fig. 173 Influence of normal force – comparison of Load-carrying capacity related to the ANSYS results*

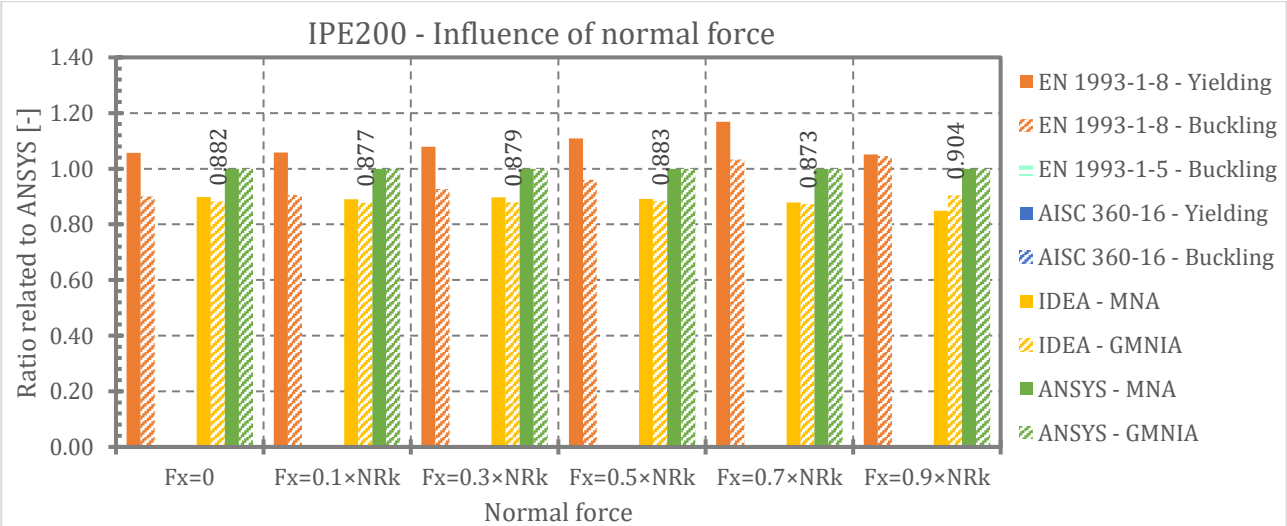


*Fig. 174 Influence of normal force – comparison of load-carrying capacity related to the ANSYS results*

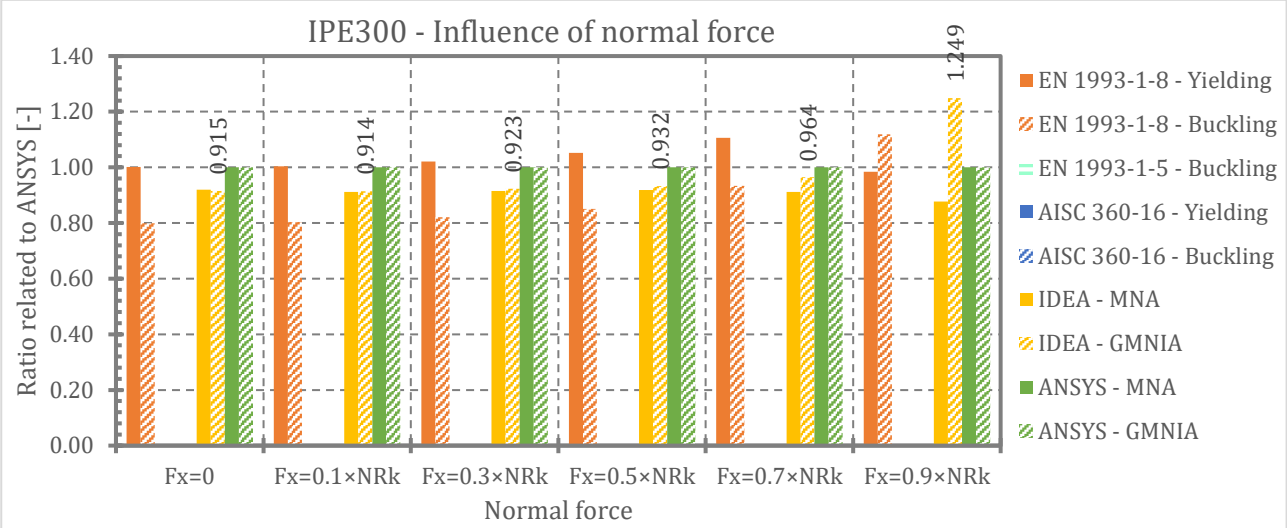


*Fig. 175 Influence of normal force – comparison of load-carrying capacity related to the ANSYS results*

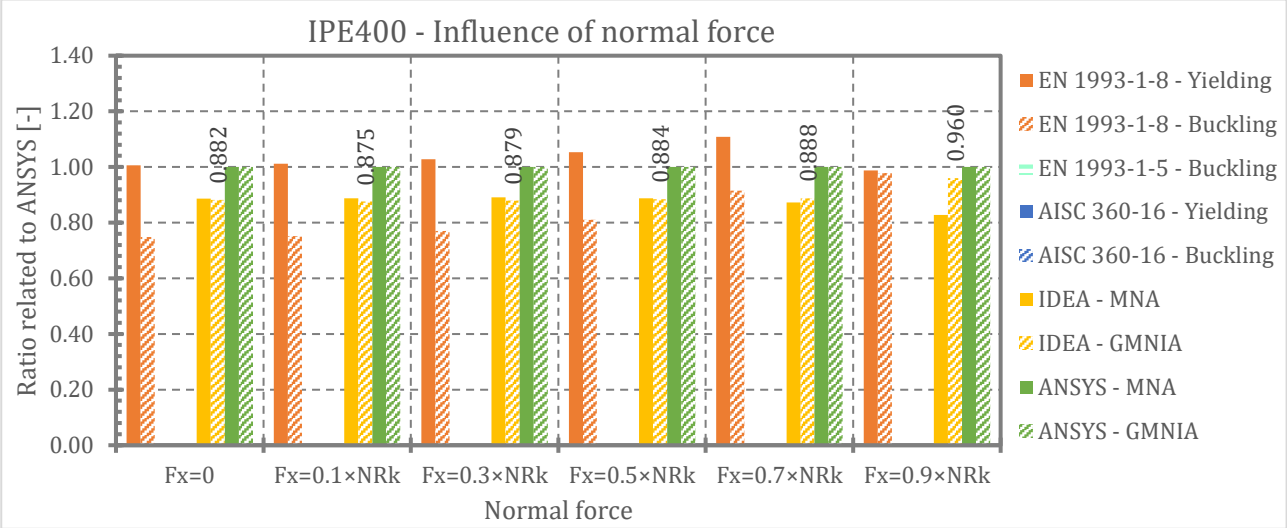


*Fig. 176 Influence of normal force – comparison of load-carrying capacity related to the ANSYS results*

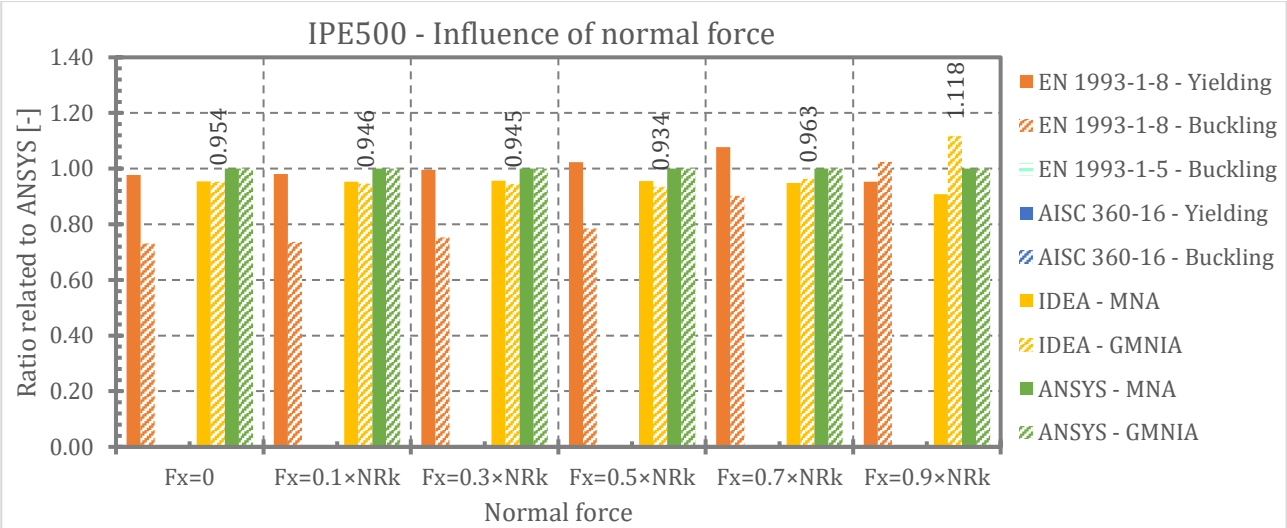


*Fig. 177 Influence of normal force – comparison of load-carrying capacity related to the ANSYS results*

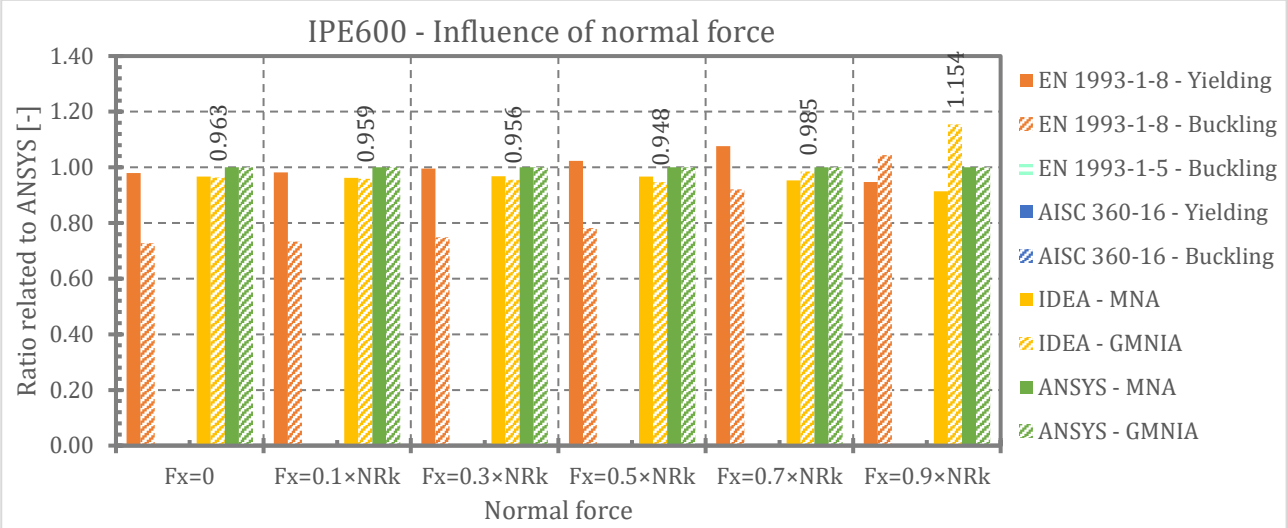


*Fig. 178 Influence of normal force – comparison of load-carrying capacity related to the ANSYS results*

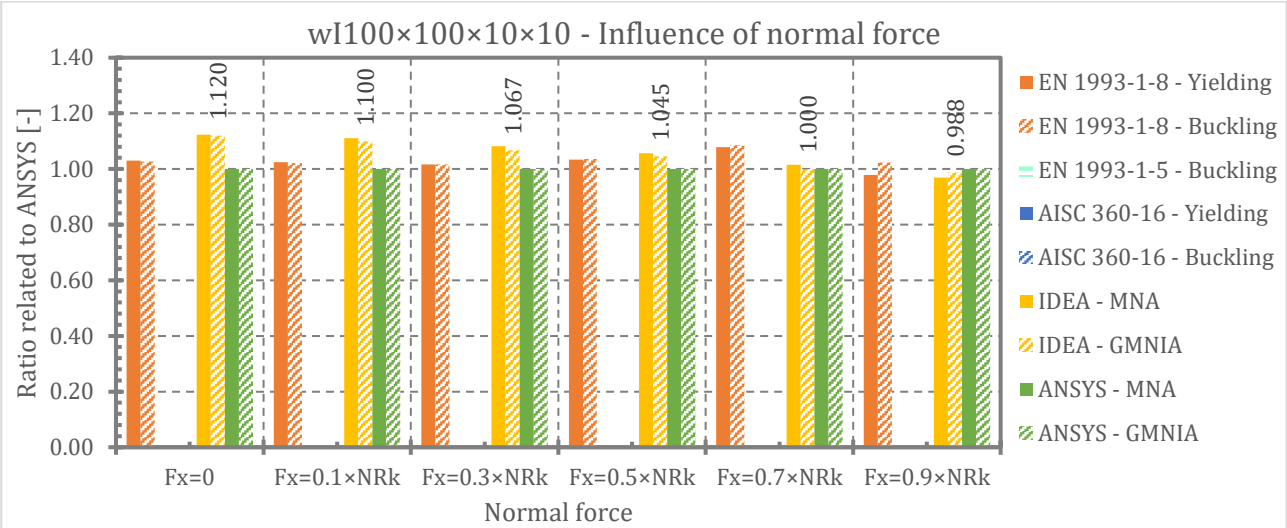


*Fig. 179 Influence of normal force – comparison of load-carrying capacity related to the ANSYS results*

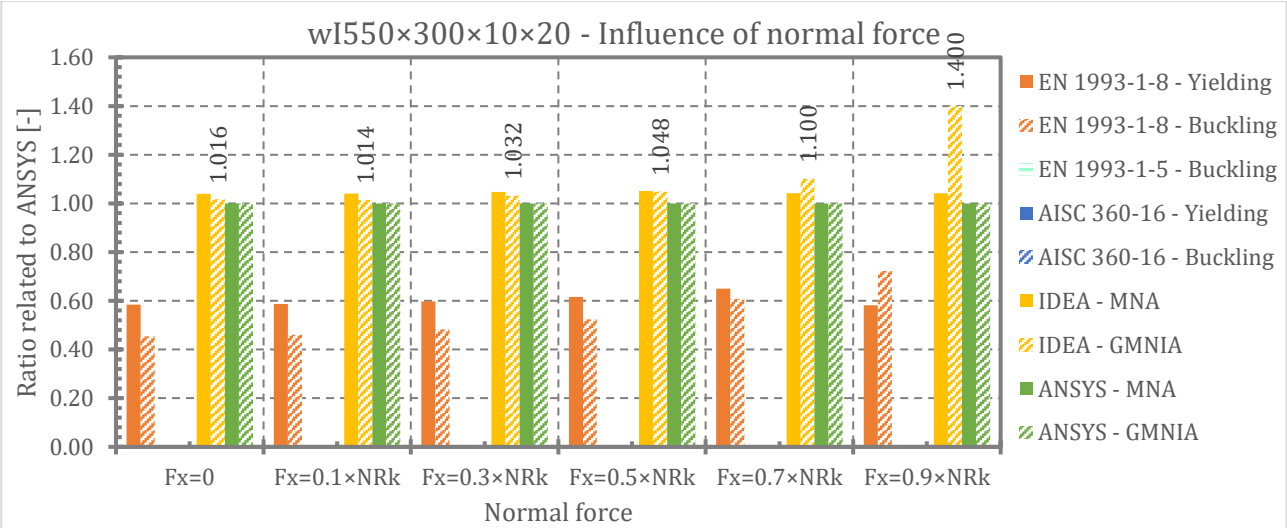


*Fig. 180 Influence of normal force – comparison of load-carrying capacity related to the ANSYS results*

### 4.6.3. Conclusion

As results of numerical simulations performed in IDEA StatiCa and ANSYS show, axial force in transversally compressed member influences resistance of that member. The influence is stronger for increasing axial load. The reduction of transversal strength due to axial force reach approximately 5%, 10% and 20% for axial force equal to 50%, 70% and 90% of compressive strength of member ($f_y \times A$) for materially nonlinear analysis MNA. But in the case of geometrically and materially analysis with imperfections (GMNIA) the reduction reaches approximately 10%, 20% and 35% (in some case up to 50%) for axial force equal to 50%, 70% and 90% of compressive strength of member. The reduction factor according to the EN 1993-1-8 is equal to 1.0 (no reduction) up to relative normal force 70% and for greater normal force there is linear formula which gives reduction 30% for 100% normal force. It means that design strength is in all case on the unsafe side, but for small normal forces the error could be neglected.

Comparison between results given by numerical simulations carried out in IDEA StatiCa and ANSYS software shows good agreement and conclusion that IDEA StatiCa gives results slightly on the safe side with exception of very low slender members (IPE 100) and both welded sections (wI 100×100×10×10 and wI 550×300×10×20). At all investigated sections of transversally compressed members there is bigger difference between IDEA StatiCa results and ANSYS software results for case of great axial force in the member ($F_x = 0.9 \times N_{rk}$), but this case is more theoretical than practical.

## 4.7. Influence of end-plate thickness

This part of study presents the influence of end-plate thickness (of loading member) on load-carrying capacity and other results. The goal is to evaluate actual behaviour and make comparison with design resistances according to the EN 1993-1-8 and EN 1993-1-5.

### 4.7.1. Methodology

The study was performed on transversally compressed member of rolled cross-sections IPE 100, 200, 300, 400, 500 and 600 and welded cross-sections wI 100×100×10×10 and wI 550×300×10×20 (section height × flange width × web thickness × flange thickness) with length on both side from loading plates $L = 2\times h$ (overall length is $L = 4\times h$). The member is made of structural steel S355. The imperfection amplitude for GMNIA was $d_w/200$, where $d_w$ is web height without rounded corners or fillet welds – see Fig. 4. Thickness of end-plate is variable in values: $t_{ep} = 0.50\times t_f$; $0.75\times t_f$; $1.00\times t_f$; $1.50\times t_f$ and $2.00\times t_f$ where $t_f$ is thickness of flange of transversally compressed member. All other geometrical properties are related to the flange thickness – see Fig. 182. For the clear determination the reference case with zero end-plate thickness was analysed ($t_{ep} = 0.00\times t_f$). The members were analysed using MNA, LBA and GMNIA in IDEA StatiCa and ANSYS. Load-carrying capacity was calculated according to the codes EN 1993-1-8 for "Yielding" and "Buckling" failure modes and according to the EN 1993-1-5. AISC 360-16 does not specify a calculation procedure applicable for this problem. Analysed member is illustrated in Fig. 231.

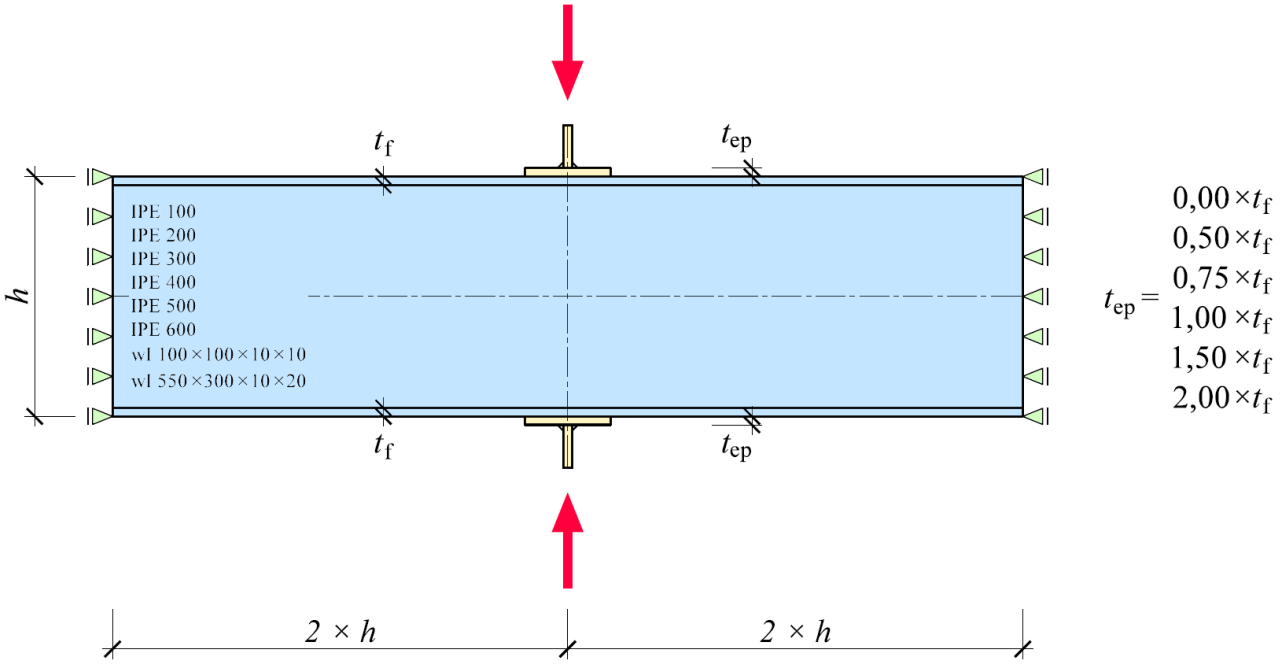


*Fig. 181 Influence of end-plate thickness – geometry amd boundary conditions*

In some cases, the resulting resistances obtained from IDEA StatiCa were related to the resistances of the fillet welds at the connection of the loading element to the end-plate (not to resistance of the web in transverse compression). As the study focuses to the specific problem of the member web, it was decided to model the connection of the loading element to the end-plate in IDEA StatiCa with butt weld instead of the fillet welds which resulted in elimination of this effect.

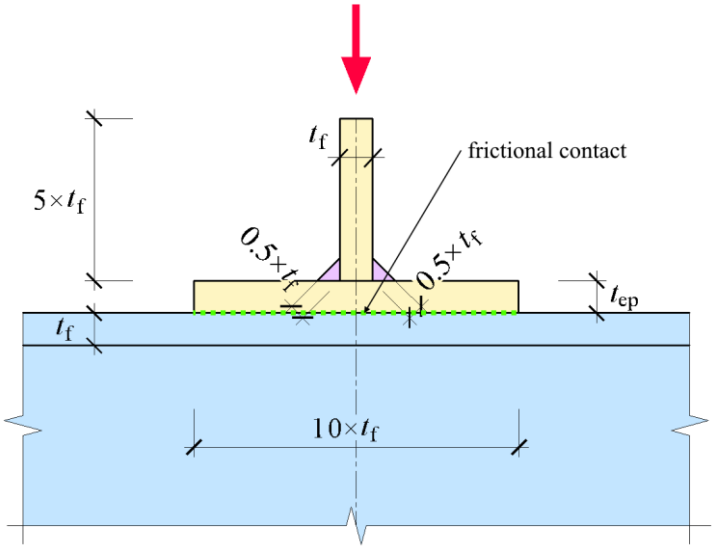


*Fig. 182 Influence of end-plate thickness – geometry detail*

In case of zero thickness of the end-plate ($0.00\times t_f$), minimum applicable thickness of the plate necessary to run the analysis was used in IDEA StatiCa models.

### 4.7.2. Results

Calculated load-carrying capacities are listed in Tab. 29 to Tab. 34 and Tab. 35 and Tab. 36 for all used methods for transversally compressed members of cross sections from IPE 100 to IPE 600 and welded sections.

*Tab. 29 Influence of end-plate thickness - IPE 100 - Load-carrying capacity [kN]*

| End-plate thickness $t_{ep}$ | EN 1993-1-8 | | EN 1993-1-5 | AISC 360-16 | | IDEA StatiCa | | ANSYS | |
|---|---|---|---|---|---|---|---|---|---|
| | Yielding | Buckling | | Yielding | Buckling | MNA | GMNIA | MNA | GMNIA |
| $0.00\times t_f$ | 112.45 | 112.45 | 97.39 | - | - | 85.95 | 85.95 | 94.10 | 95.56 |
| $0.50\times t_f$ | 120.75 | 119.56 | 105.69 | - | - | 93.75 | 93.75 | 100.45 | 102.69 |
| $0.75\times t_f$ | 124.90 | 122.35 | 109.84 | - | - | 101.55 | 101.55 | 104.93 | 107.24 |
| $1.00\times t_f$ | 129.05 | 125.10 | 113.99 | - | - | 109.40 | 109.40 | 112.23 | 114.95 |
| $1.50\times t_f$ | 137.34 | 130.48 | 132.32 | - | - | 126.95 | 125.00 | 128.03 | 129.23 |
| $2.00\times t_f$ | 145.64 | 135.69 | 136.40 | - | - | 146.50 | 140.65 | 146.48 | 141.09 |

*Tab. 30 Influence of end-plate thickness - IPE 200 - Load-carrying capacity [kN]*

| End-plate thickness $t_{ep}$ | EN 1993-1-8 | | EN 1993-1-5 | AISC 360-16 | | IDEA StatiCa | | ANSYS | |
|---|---|---|---|---|---|---|---|---|---|
| | Yielding | Buckling | | Yielding | Buckling | MNA | GMNIA | MNA | GMNIA |
| $0.00\times t_f$ | 244.57 | 202.14 | 202.39 | - | - | 177.75 | 177.75 | 212.77 | 214.47 |
| $0.50\times t_f$ | 261.46 | 210.83 | 209.10 | - | - | 193.35 | 193.35 | 227.49 | 230.53 |
| $0.75\times t_f$ | 269.91 | 215.06 | 212.38 | - | - | 209.00 | 209.00 | 238.88 | 241.10 |
| $1.00\times t_f$ | 278.36 | 219.23 | 215.61 | - | - | 230.45 | 228.50 | 253.28 | 252.94 |
| $1.50\times t_f$ | 295.26 | 227.38 | 221.92 | - | - | 271.50 | 269.55 | 288.53 | 273.21 |
| $2.00\times t_f$ | 312.16 | 235.31 | 228.06 | - | - | 316.40 | 291.00 | 331.19 | 287.90 |

*Tab. 31 Influence of end-plate thickness - IPE 300 - Load-carrying capacity [kN]*

| End-plate thickness $t_{ep}$ | EN 1993-1-8 | | EN 1993-1-5 | AISC 360-16 | | IDEA StatiCa | | ANSYS | |
|---|---|---|---|---|---|---|---|---|---|
| | Yielding | Buckling | | Yielding | Buckling | MNA | GMNIA | MNA | GMNIA |
| 0.00×$t_f$ | 388.99 | 298.35 | 309.26 | - | - | 304.70 | 302.75 | 352.95 | 351.53 |
| 0.50×$t_f$ | 415.96 | 310.89 | 318.66 | - | - | 330.10 | 328.15 | 373.57 | 374.52 |
| 0.75×$t_f$ | 429.45 | 317.01 | 323.26 | - | - | 361.35 | 359.40 | 392.59 | 393.16 |
| 1.00×$t_f$ | 442.93 | 323.03 | 327.80 | - | - | 394.55 | 390.65 | 416.75 | 413.67 |
| 1.50×$t_f$ | 469.90 | 334.81 | 336.69 | - | - | 462.90 | 455.10 | 478.42 | 445.04 |
| 2.00×$t_f$ | 496.87 | 346.25 | 345.35 | - | - | 541.38 | 482.82 | 549.86 | 464.36 |

*Tab. 32 Influence of end-plate thickness - IPE 400 - Load-carrying capacity [kN]*

| End-plate thickness $t_{ep}$ | EN 1993-1-8 | | EN 1993-1-5 | AISC 360-16 | | IDEA StatiCa | | ANSYS | |
|---|---|---|---|---|---|---|---|---|---|
| | Yielding | Buckling | | Yielding | Buckling | MNA | GMNIA | MNA | GMNIA |
| 0.00×$t_f$ | 626.15 | 446.43 | 443.96 | - | - | 480.50 | 476.60 | 562.66 | 559.86 |
| 0.50×$t_f$ | 667.36 | 463.90 | 457.26 | - | - | 515.60 | 515.60 | 594.11 | 587.45 |
| 0.75×$t_f$ | 687.97 | 472.43 | 463.76 | - | - | 558.60 | 554.70 | 622.61 | 610.30 |
| 1.00×$t_f$ | 708.58 | 480.83 | 470.18 | - | - | 605.50 | 597.70 | 657.24 | 634.56 |
| 1.50×$t_f$ | 749.79 | 497.28 | 482.76 | - | - | 707.00 | 679.70 | 747.61 | 669.90 |
| 2.00×$t_f$ | 791.01 | 513.29 | 495.01 | - | - | 824.20 | 722.70 | 851.15 | 696.89 |

*Tab. 33 Influence of end-plate thickness - IPE 500 - Load-carrying capacity [kN]*

| End-plate thickness $t_{ep}$ | EN 1993-1-8 | | EN 1993-1-5 | AISC 360-16 | | IDEA StatiCa | | ANSYS | |
|---|---|---|---|---|---|---|---|---|---|
| | Yielding | Buckling | | Yielding | Buckling | MNA | GMNIA | MNA | GMNIA |
| 0.00×$t_f$ | 809.75 | 577.89 | 608.64 | - | - | 672.00 | 668.00 | 745.67 | 727.15 |
| 0.50×$t_f$ | 867.69 | 602.44 | 626.77 | - | - | 723.00 | 715.00 | 788.39 | 773.55 |
| 0.75×$t_f$ | 896.66 | 614.41 | 635.65 | - | - | 777.00 | 770.00 | 828.27 | 812.71 |
| 1.00×$t_f$ | 925.63 | 626.18 | 644.40 | - | - | 840.00 | 828.00 | 878.54 | 855.25 |
| 1.50×$t_f$ | 983.56 | 649.19 | 661.56 | - | - | 977.00 | 949.00 | 1003.38 | 918.10 |
| 2.00×$t_f$ | 1041.50 | 671.54 | 678.28 | - | - | 1129.2 | 1008.0 | 1148.02 | 953.80 |

*Tab. 34 Influence of end-plate thickness - IPE 600 - Load-carrying capacity [kN]*

| End-plate thickness $t_{ep}$ | EN 1993-1-8 | | EN 1993-1-5 | AISC 360-16 | | IDEA StatiCa | | ANSYS | |
|---|---|---|---|---|---|---|---|---|---|
| | Yielding | Buckling | | Yielding | Buckling | MNA | GMNIA | MNA | GMNIA |
| 0.00×$t_f$ | 1111.3 | 787.83 | 833.98 | - | - | 922.00 | 914.00 | 1019.3 | 1001.7 |
| 0.50×$t_f$ | 1192.3 | 821.84 | 859.06 | - | - | 992.00 | 984.00 | 1088.2 | 1056.9 |
| 0.75×$t_f$ | 1232.7 | 838.40 | 871.32 | - | - | 1062.0 | 1054.0 | 1144.0 | 1100.2 |
| 1.00×$t_f$ | 1273.2 | 854.70 | 883.42 | - | - | 1148.0 | 1132.0 | 1211.0 | 1151.4 |
| 1.50×$t_f$ | 1354.1 | 886.54 | 907.12 | - | - | 1328.0 | 1296.0 | 1383.5 | 1239.9 |
| 2.00×$t_f$ | 1435.1 | 917.44 | 930.22 | - | - | 1532.0 | 1382.0 | 1580.0 | 1284.7 |

*Tab. 35 Influence of end-plate thickness - wI100×100×10×10 - Load-carrying capacity [kN]*

| End-plate thickness $t_{ep}$ | EN 1993-1-8 | | EN 1993-1-5 | AISC 360-16 | | IDEA StatiCa | | ANSYS | |
|---|---|---|---|---|---|---|---|---|---|
| | Yielding | Buckling | | Yielding | Buckling | MNA | GMNIA | MNA | GMNIA |
| 0.00×$t_f$ | 343.53 | 343.53 | 381.23 | - | - | 300.80 | 300.80 | 313.87 | 315.62 |
| 0.50×$t_f$ | 379.03 | 379.03 | 416.73 | - | - | 324.20 | 324.20 | 342.57 | 353.12 |
| 0.75×$t_f$ | 396.78 | 396.78 | 434.48 | - | - | 351.60 | 347.70 | 370.36 | 377.27 |
| 1.00×$t_f$ | 414.53 | 414.53 | 452.23 | - | - | 378.90 | 378.90 | 398.87 | 403.14 |
| 1.50×$t_f$ | 450.03 | 450.03 | 487.73 | - | - | 449.20 | 449.20 | 457.25 | 462.67 |
| 2.00×$t_f$ | 485.53 | 485.53 | 523.23 | - | - | 527.30 | 523.40 | 525.77 | 531.33 |

*Tab. 36 Influence of end-plate thickness - wI550×300×10×20 - Load-carrying capacity [kN]*

| End-plate thickness $t_{ep}$ | EN 1993-1-8 | | EN 1993-1-5 | AISC 360-16 | | IDEA StatiCa | | ANSYS | |
|---|---|---|---|---|---|---|---|---|---|
| | Yielding | Buckling | | Yielding | Buckling | MNA | GMNIA | MNA | GMNIA |
| 0.00×$t_f$ | 636.86 | 458.69 | 644.96 | - | - | 921.80 | 898.40 | 904.77 | 871.35 |
| 0.50×$t_f$ | 707.86 | 488.85 | 663.11 | - | - | 976.60 | 937.60 | 984.27 | 914.59 |
| 0.75×$t_f$ | 743.36 | 503.36 | 671.99 | - | - | 1046.8 | 968.80 | 1035.34 | 934.24 |
| 1.00×$t_f$ | 778.86 | 517.52 | 680.76 | - | - | 1140.6 | 992.20 | 1112.24 | 953.94 |
| 1.50×$t_f$ | 849.86 | 544.92 | 697.97 | - | - | 1343.8 | 1031.2 | 1297.9 | 994.38 |
| 2.00×$t_f$ | 920.86 | 571.19 | 714.77 | - | - | 1523.4 | 1054.6 | 1494.8 | 1023.4 |

Load–carrying capacities are graphically displayed in Fig. 183 to Fig. 188 for all used methods for transversally compressed members of cross sections IPE 100 and IPE 600 and in Fig. 189 and Fig. 190 for welded sections.

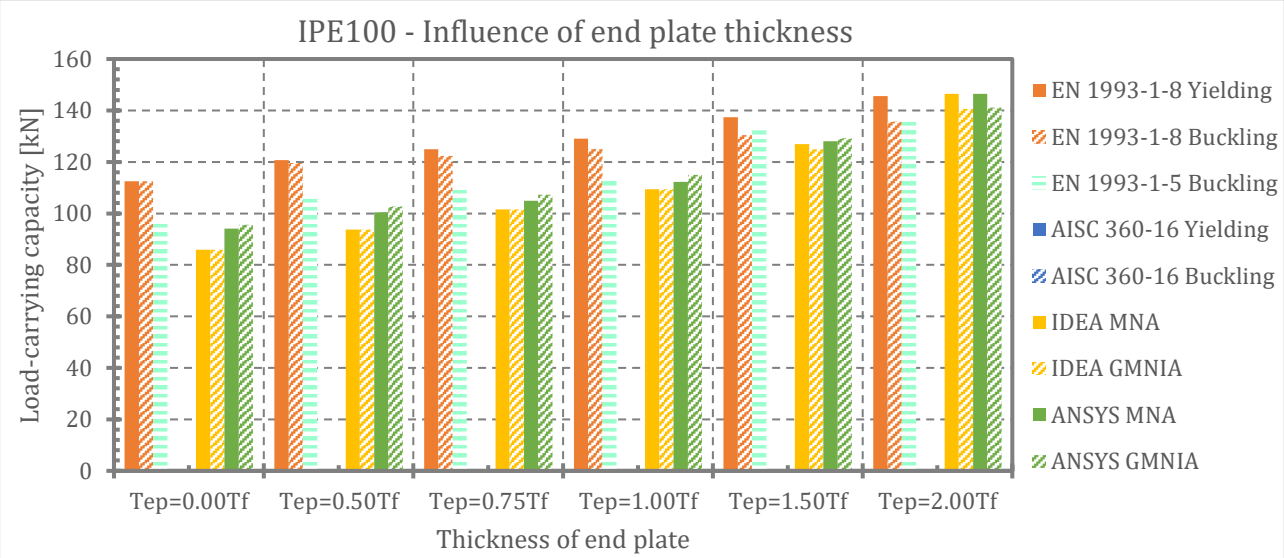


*Fig. 183 Influence of end-plate thickness - IPE 100 – Load-carrying capacity*

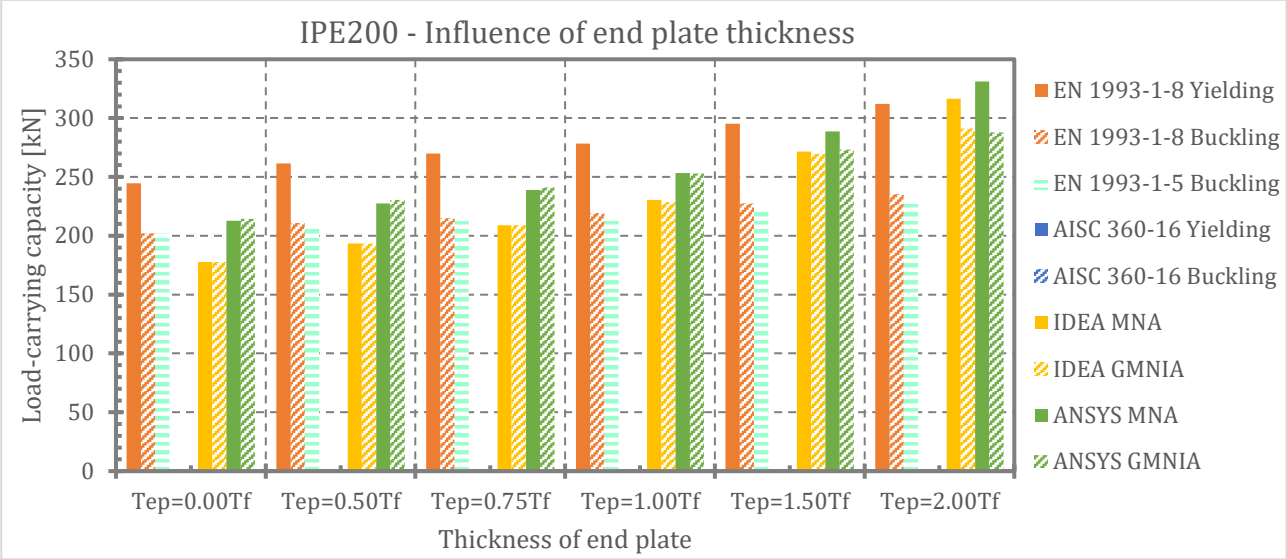


*Fig. 184 Influence of end-plate thickness - IPE 200 – Load-carrying capacity*

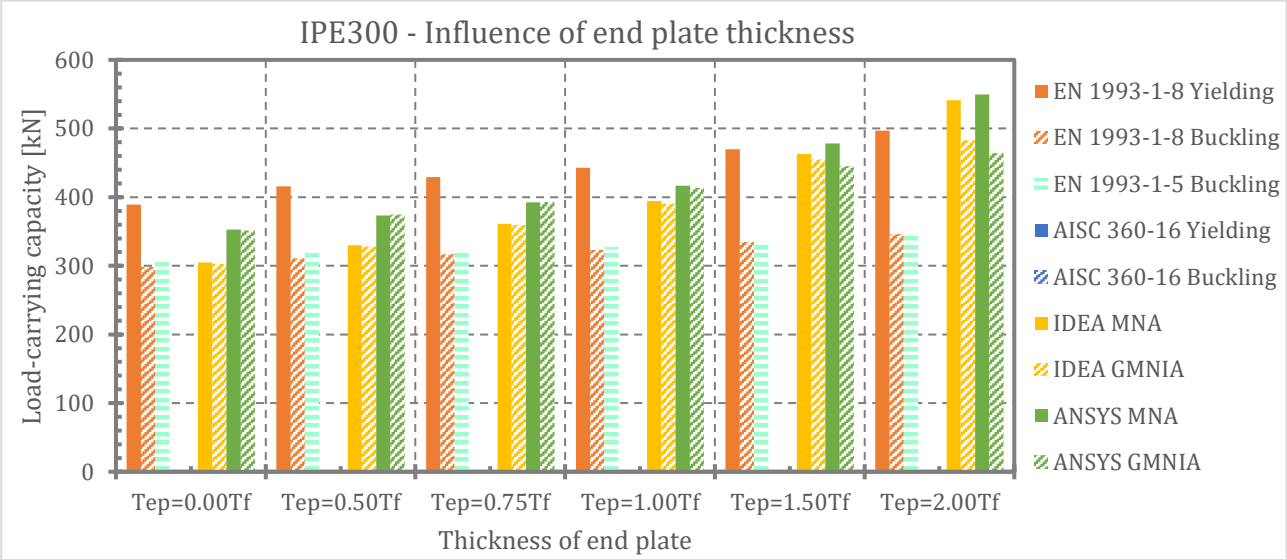


*Fig. 185 Influence of end-plate thickness - IPE 300 – Load-carrying capacity*

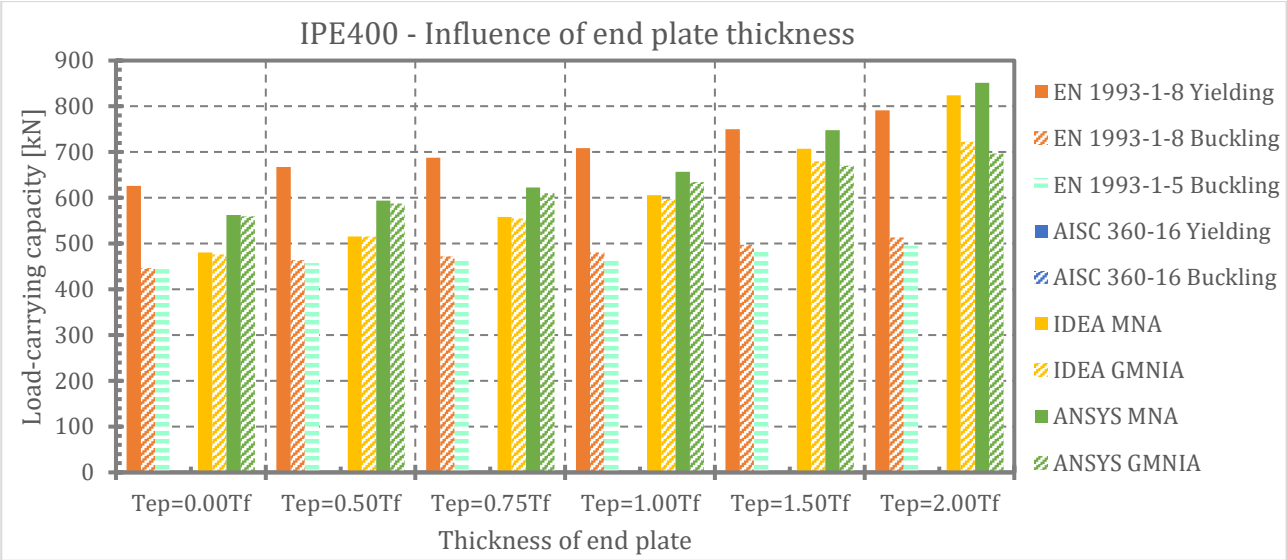


*Fig. 186 Influence of end-plate thickness - IPE 400 – Load-carrying capacity*

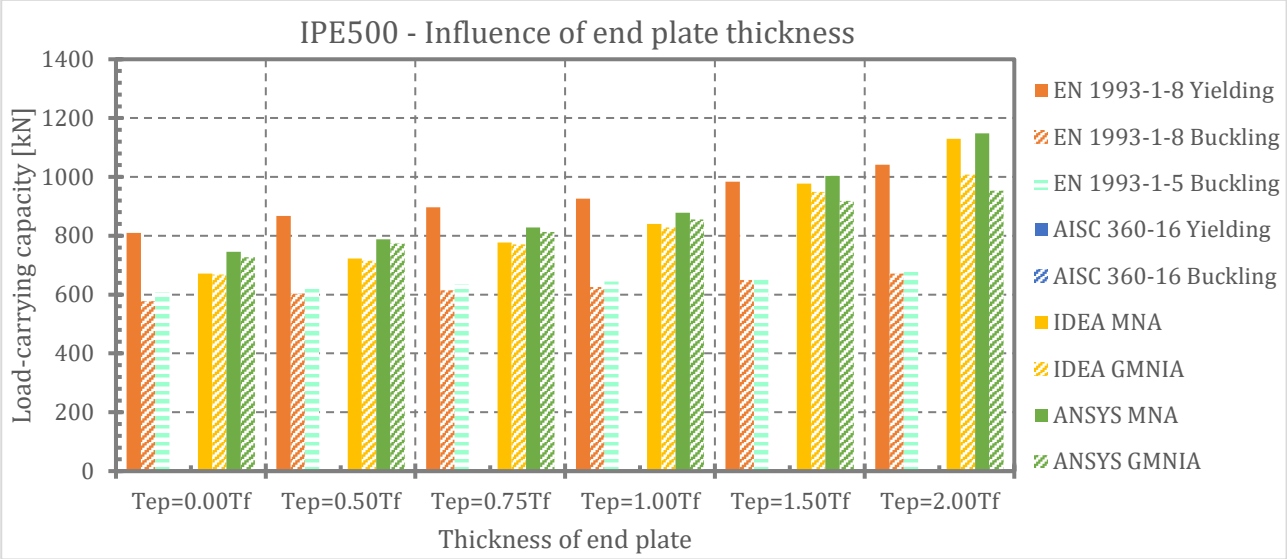


*Fig. 187 Influence of end-plate thickness - IPE 500 – Load-carrying capacity*

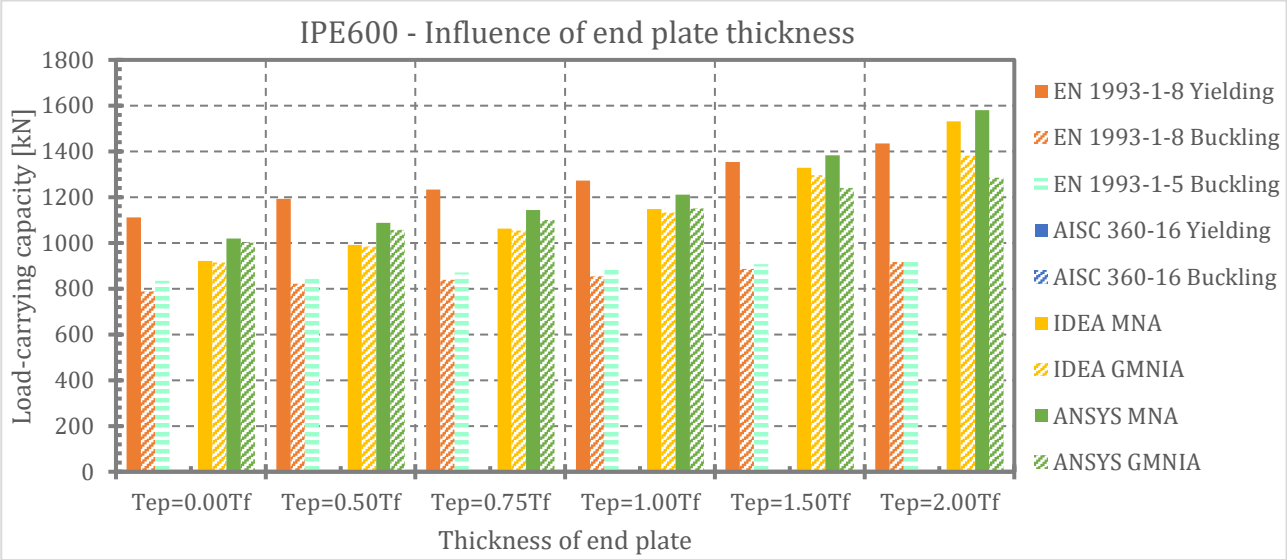


*Fig. 188 Influence of end-plate thickness - IPE 600 – Load-carrying capacity*

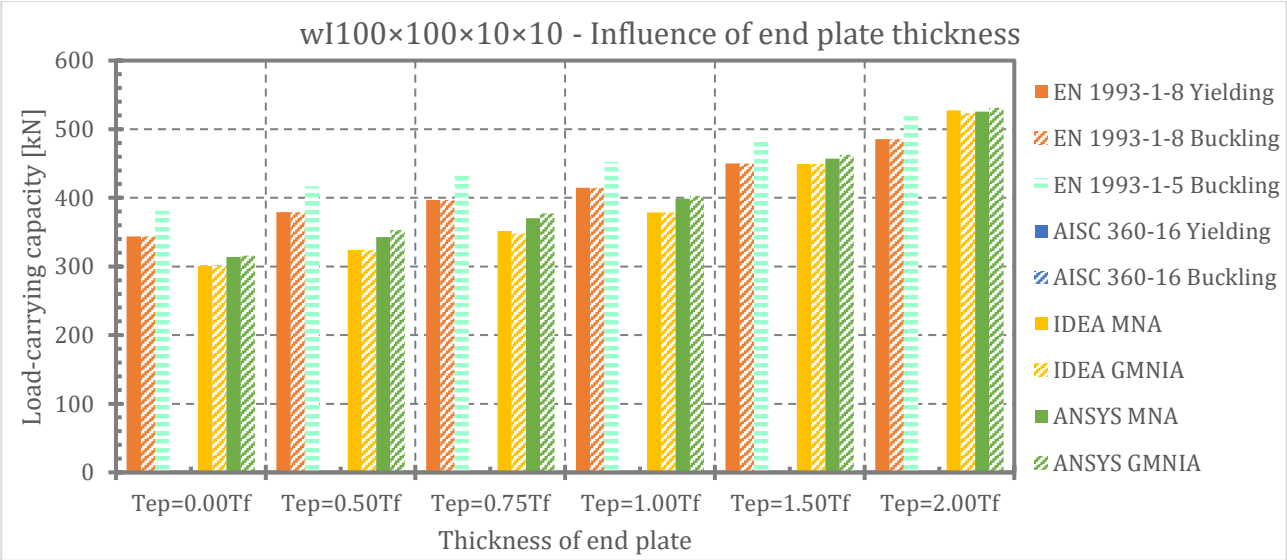


*Fig. 189 Influence of end-plate thickness – wI 100×100×10×10 – Load-carrying capacity*

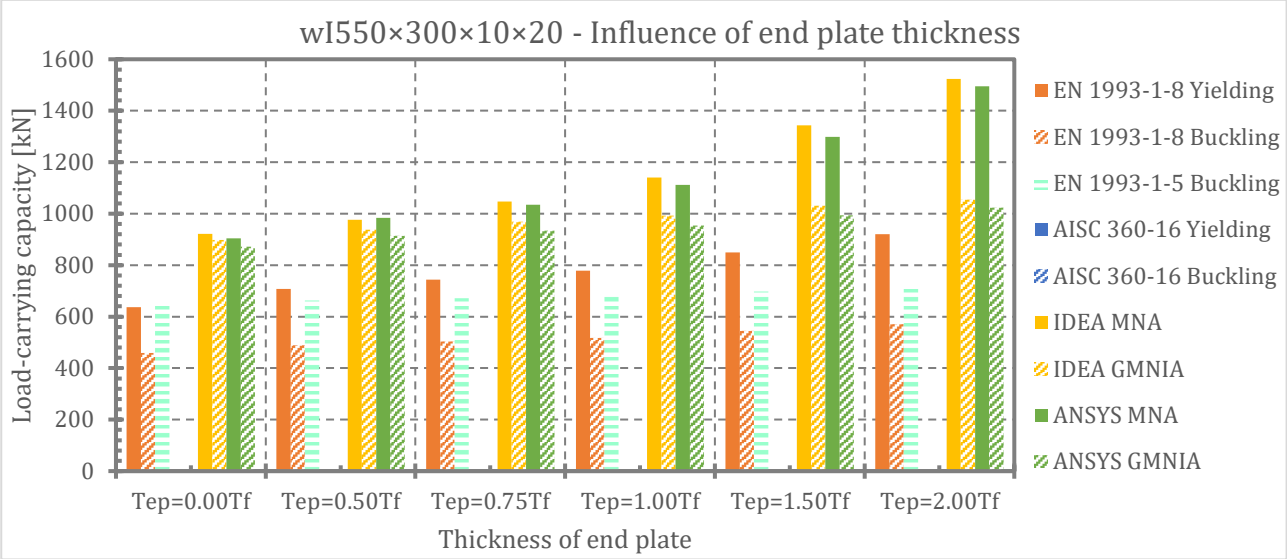


*Fig. 190 Influence of end-plate thickness – wI 550×300×10×20 – Load-carrying capacity*

Influence of end-plate thickness on transversal load-carrying capacity is clearly shown in Fig. 191 to Fig. 198 where ratio of load-carrying capacities related to case with zero end-plate thickness ($t_{ep}$ = 0.00×$t_f$) is on vertical axis.

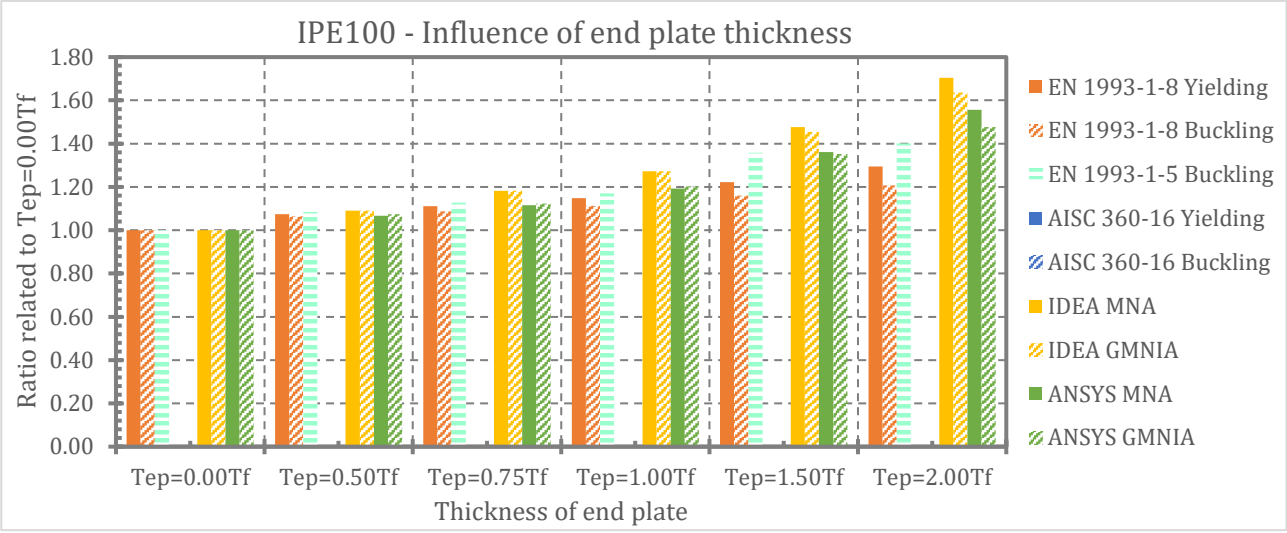


*Fig. 191 Influence of end-plate thickness - IPE 100 – relative influence of EP th. on load-carrying capacity*

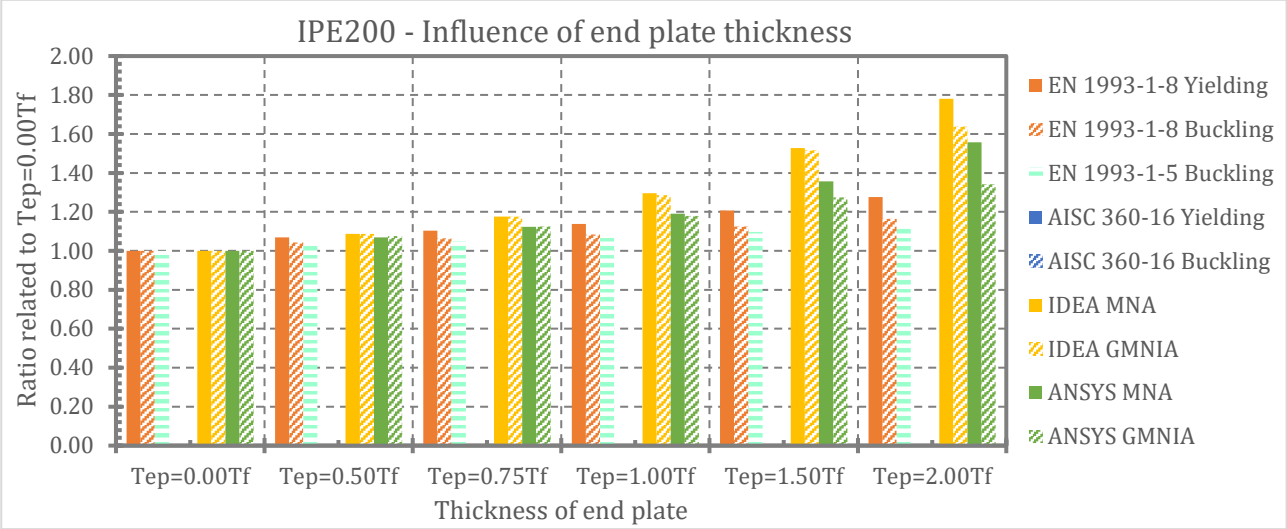


*Fig. 192 Influence of end-plate thickness - IPE 200 – relative influence of EP th. on load-carrying capacity*

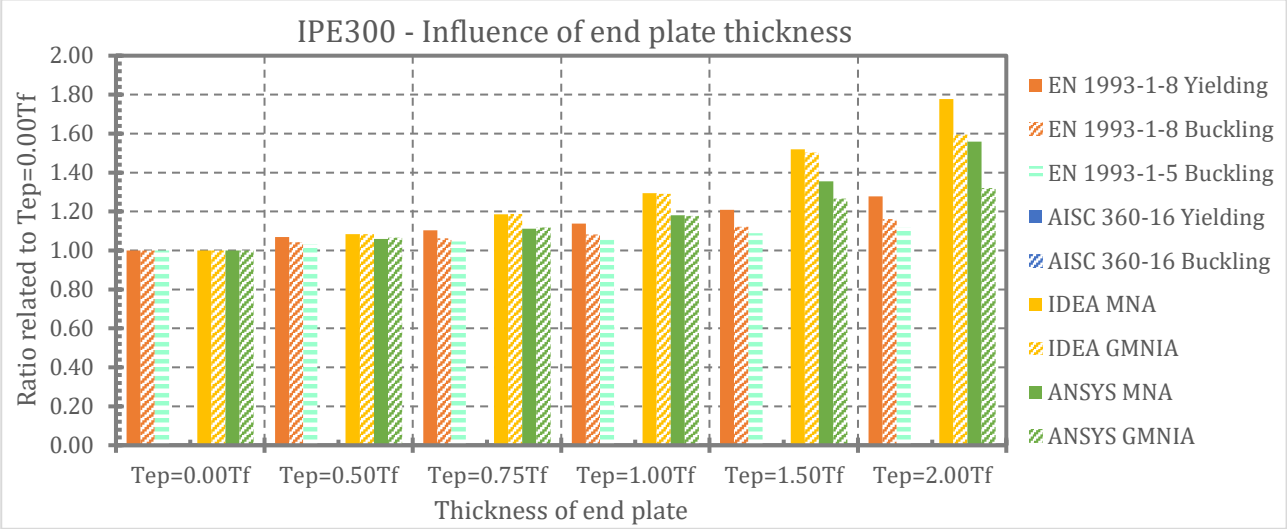


*Fig. 193 Influence of end-plate thickness - IPE 300 – relative influence of EP th. on load-carrying capacity*

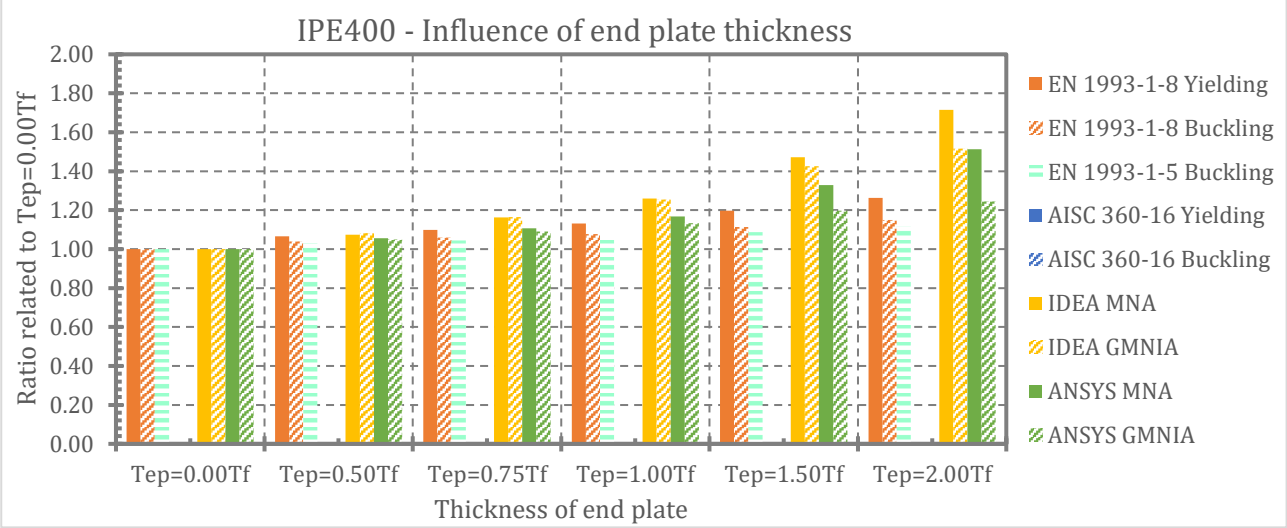


*Fig. 194 Influence of end-plate thickness - IPE 400 – relative influence of EP th. on load-carrying capacity*

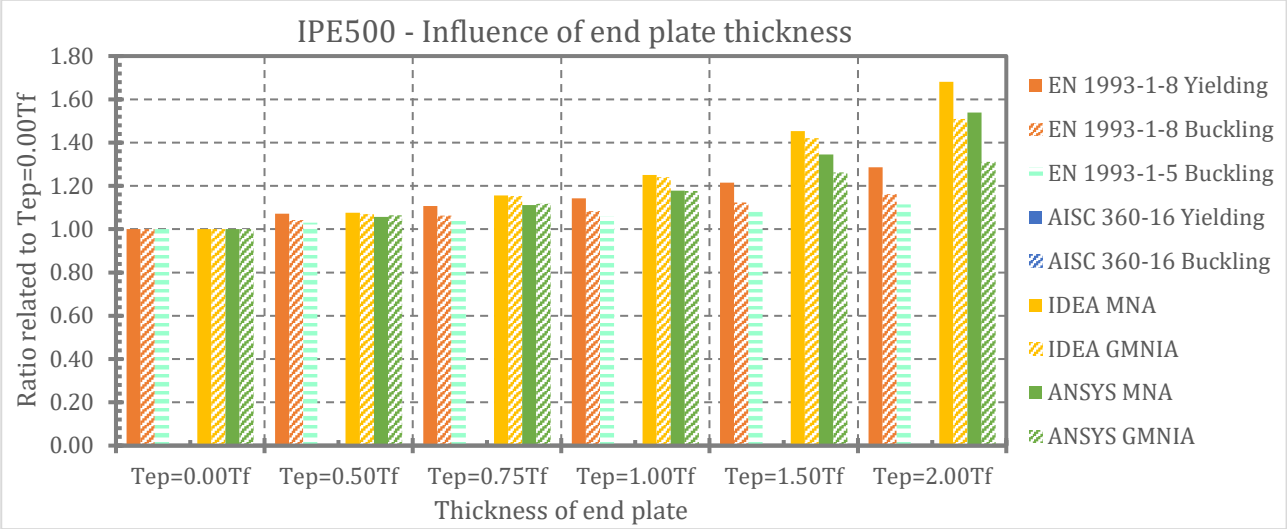


*Fig. 195 Influence of end-plate thickness - IPE 500 – relative influence of EP th. on load-carrying capacity*

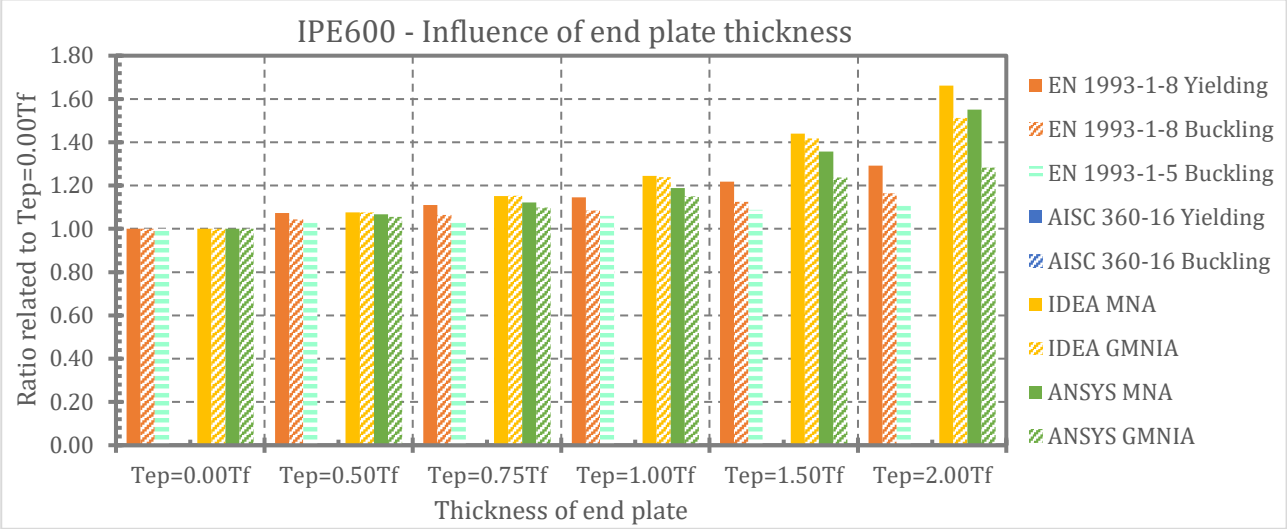


*Fig. 196 Influence of end-plate thickness - IPE 600 – relative influence of EP th. on load-carrying capacity*

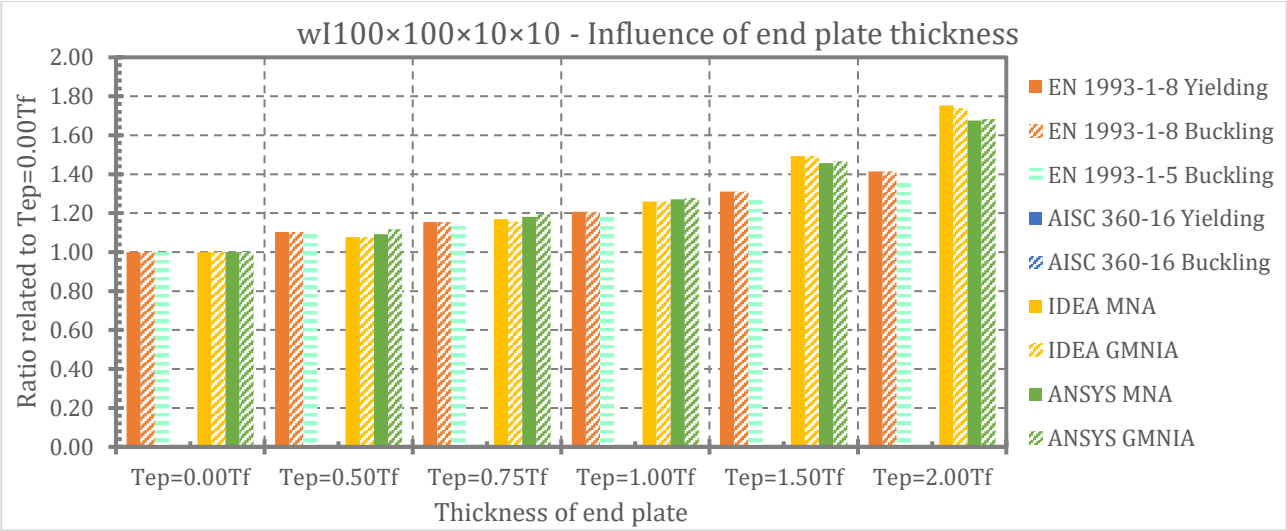


*Fig. 197 Influence of end-plate thickness - wI 100×100×10×10 – relative influence of EP th. on load-carrying capacity*

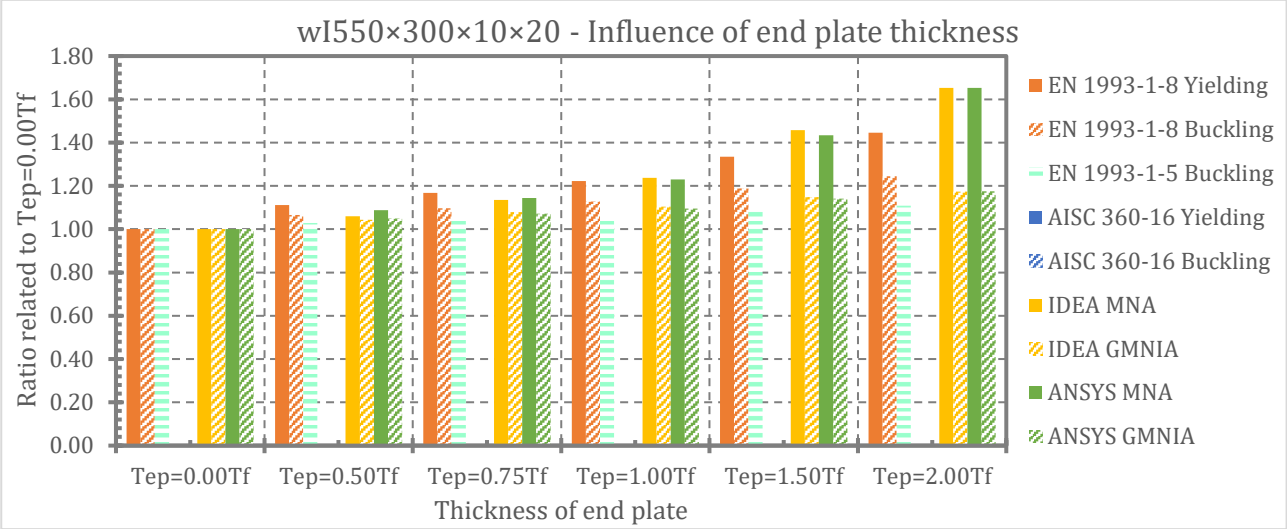


*Fig. 198 Influence of end-plate thickness - wI 550×300×10×20 – relative influence of EP th. on load-carrying capacity*

Influence of buckling on load-carrying capacity is clearly shown in Fig. 199 to Fig. 206 where ratio of load-carrying capacities resulting from Buckling/Yielding resistances according to the EN 1993-1-8 and EN 1993-1-5 or GMNIA/MNA resulting from numerical analysis performed in IDEA StatiCa and ANSYS are on vertical axis.


*Fig. 199 Influence of end-plate thickness - IPE 100 – reduction due to geometrical nonlinearity*

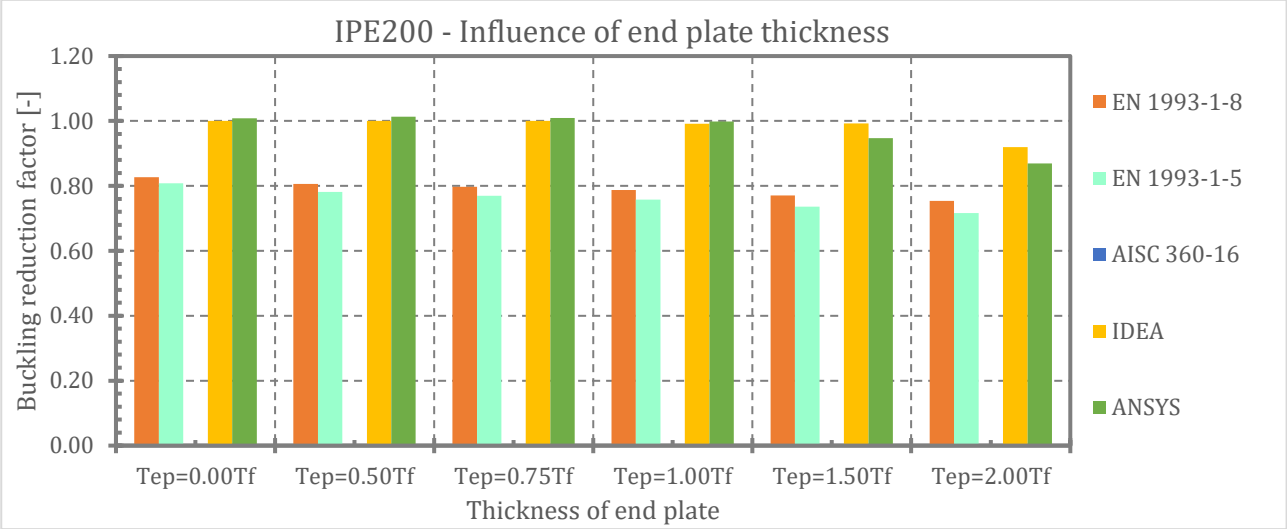


*Fig. 200 Influence of end-plate thickness - IPE 200 – reduction due to geometrical nonlinearity*

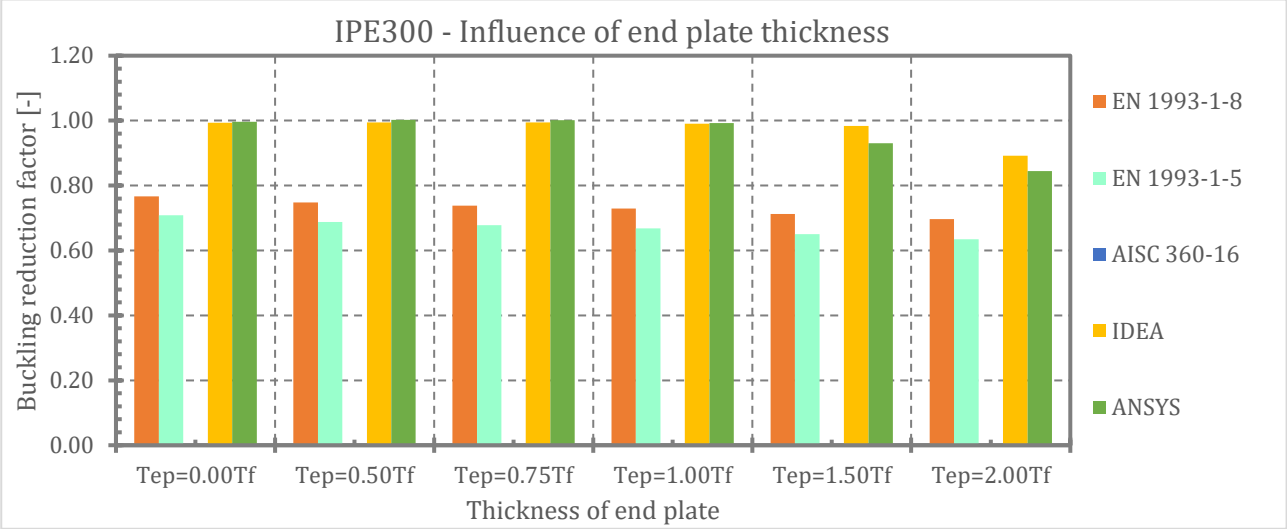


*Fig. 201 Influence of end-plate thickness - IPE 300 – reduction due to geometrical nonlinearity*

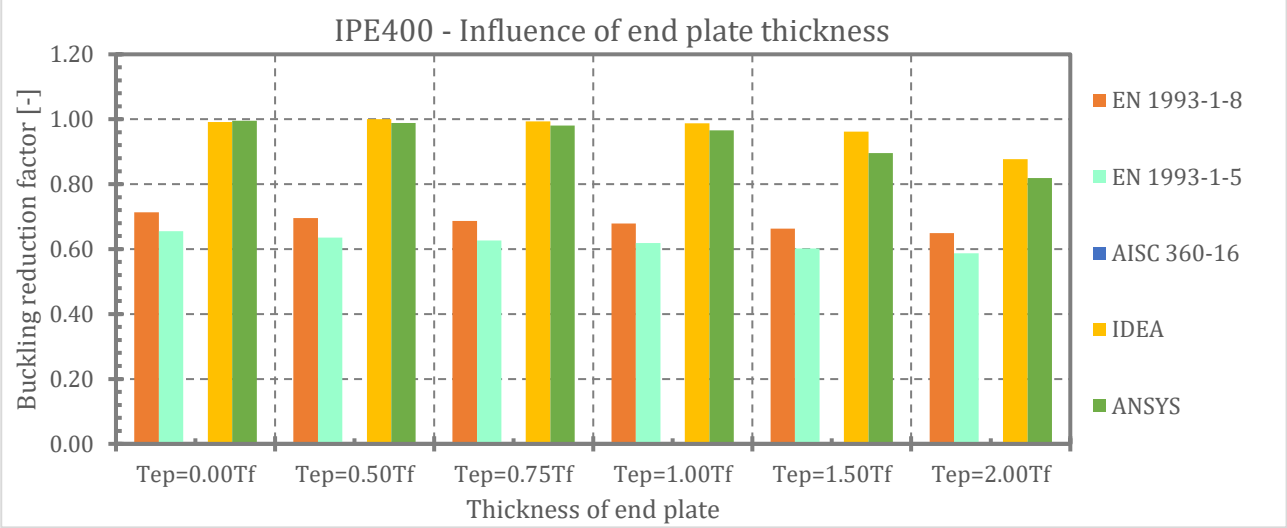


*Fig. 202 Influence of end-plate thickness - IPE 400 – reduction due to geometrical nonlinearity*

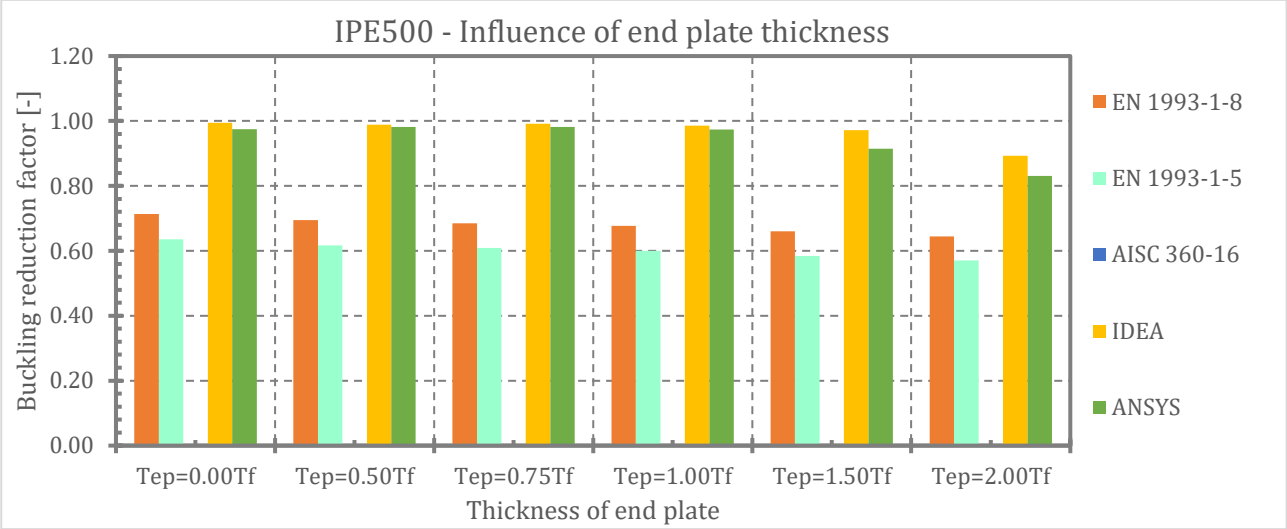


*Fig. 203 Influence of end-plate thickness - IPE 500 – reduction due to geometrical nonlinearity*

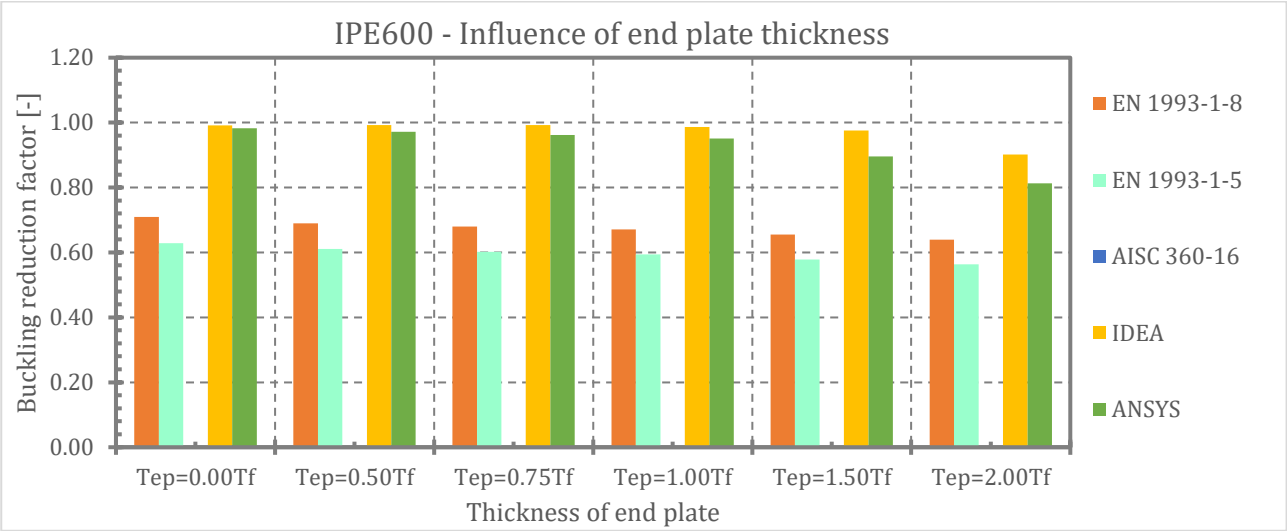


*Fig. 204 Influence of end-plate thickness - IPE 600 – reduction due to geometrical nonlinearity*

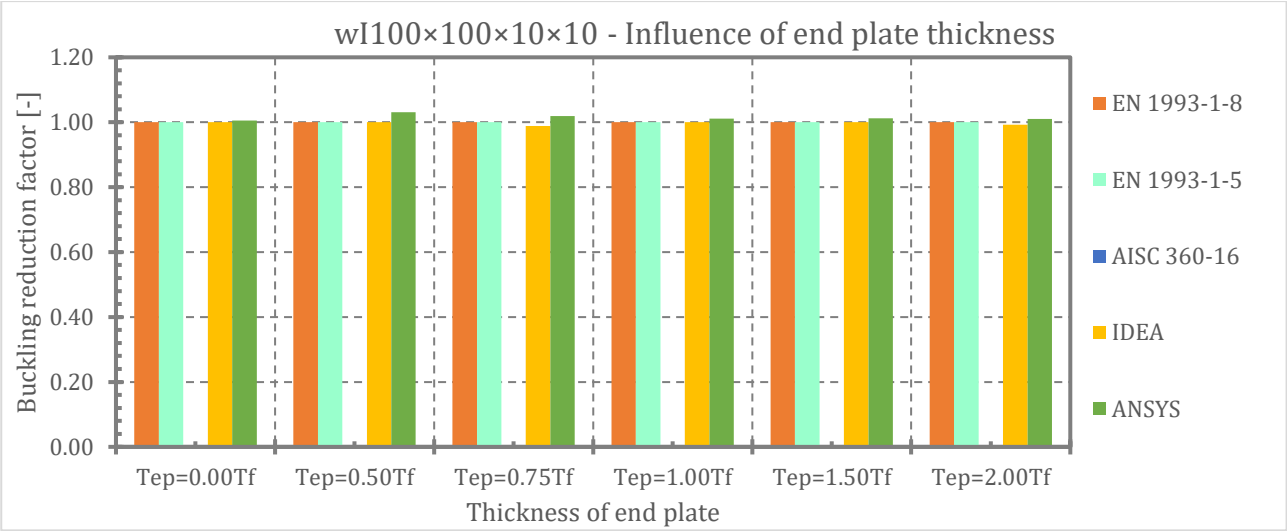


*Fig. 205 Influence of end-plate thickness - wI 100×100×10×10 – reduction due to geometrical nonlinearity*

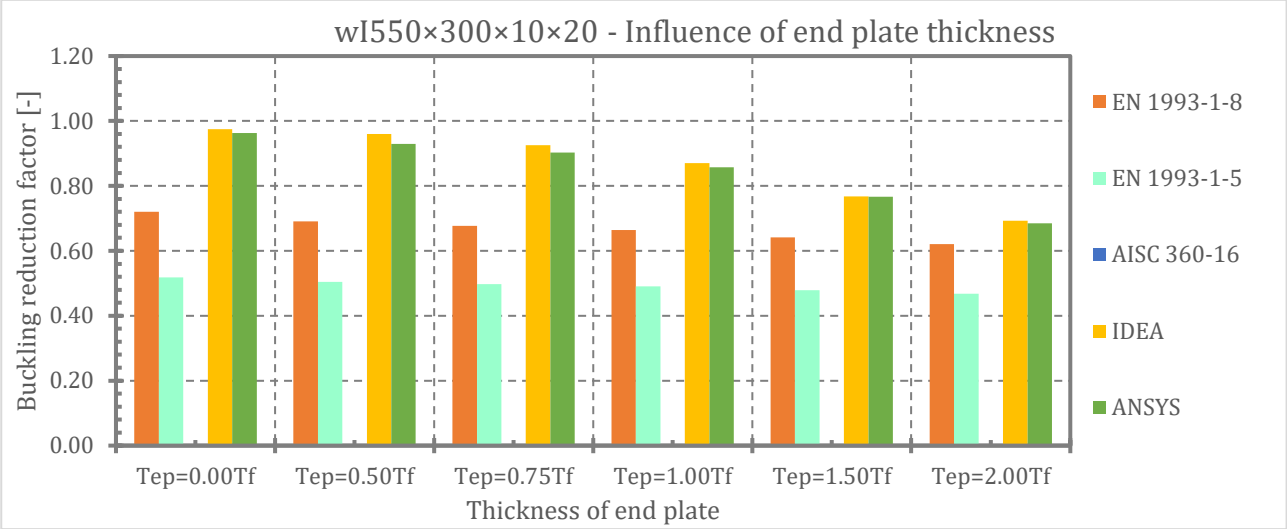


*Fig. 206 Influence of end-plate thickness - wI 550×300×10×20 – reduction due to geometrical nonlinearity*

Behaviour of members in transverse compression applied through end-plates is displayed in Fig. 207 to Fig. 212 for illustration for member of cross section IPE 400. For other analysed cross sections, the charts are similar.

Fig. 207 shows results of linear buckling analysis – critical forces $F_{cr}$ [kN] and critical load factor $\alpha_{cr}$ [-]. The critical force is increasing with increasing end-plate thickness. Critical load factor decreases with increasing thickness.

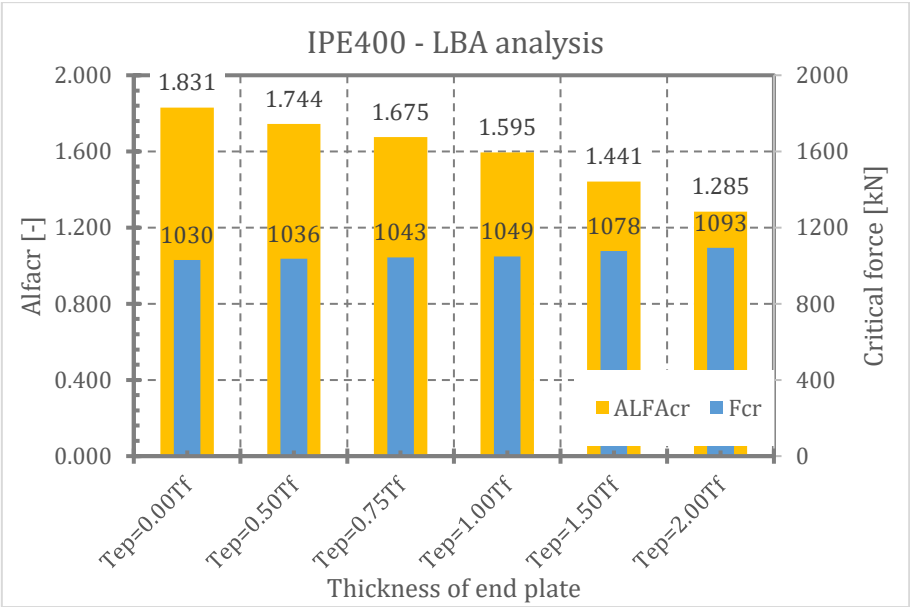


*Fig. 207 Influence of end.plate thickness – LBA results*

Fig. 208 illustrates relationship of vertical deformation and loading force for MNA and GMNIA. Fig. 209 describes relationship between lateral deformation in the middle of beam web and loading force for MNA and GMNIA. Dependency of maximal equivalent stress and equivalent stress in the middle of member web on loading force is plotted in Fig. 210 and Fig. 211. Fig. 212 shows developing of plastic strain with increasing load.

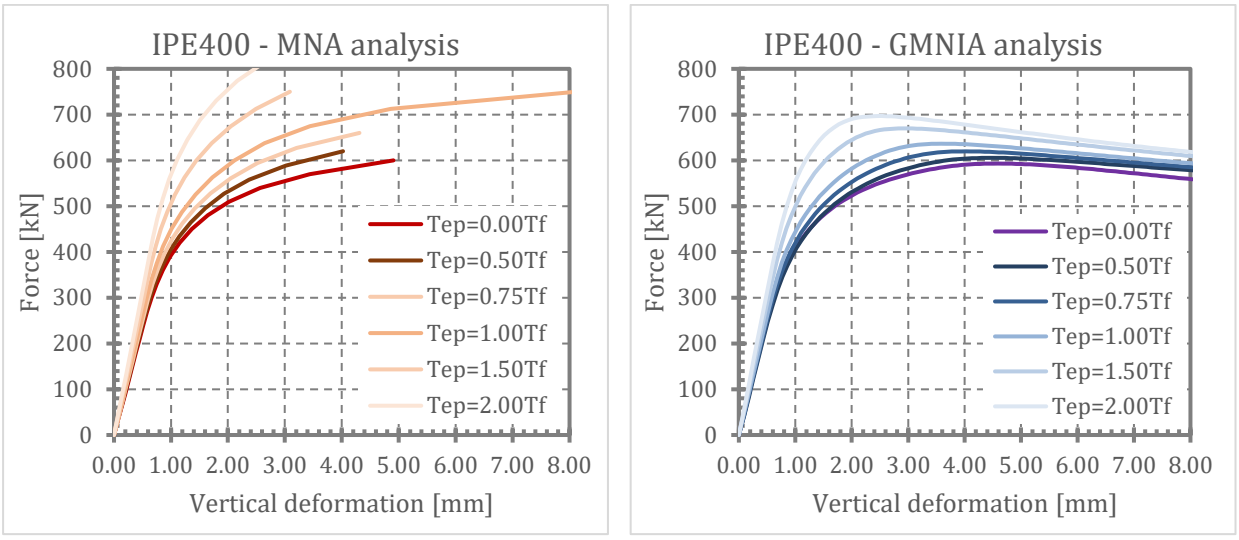


*Fig. 208 Influence of end-plate thickness – vertical deformation-force relationship*

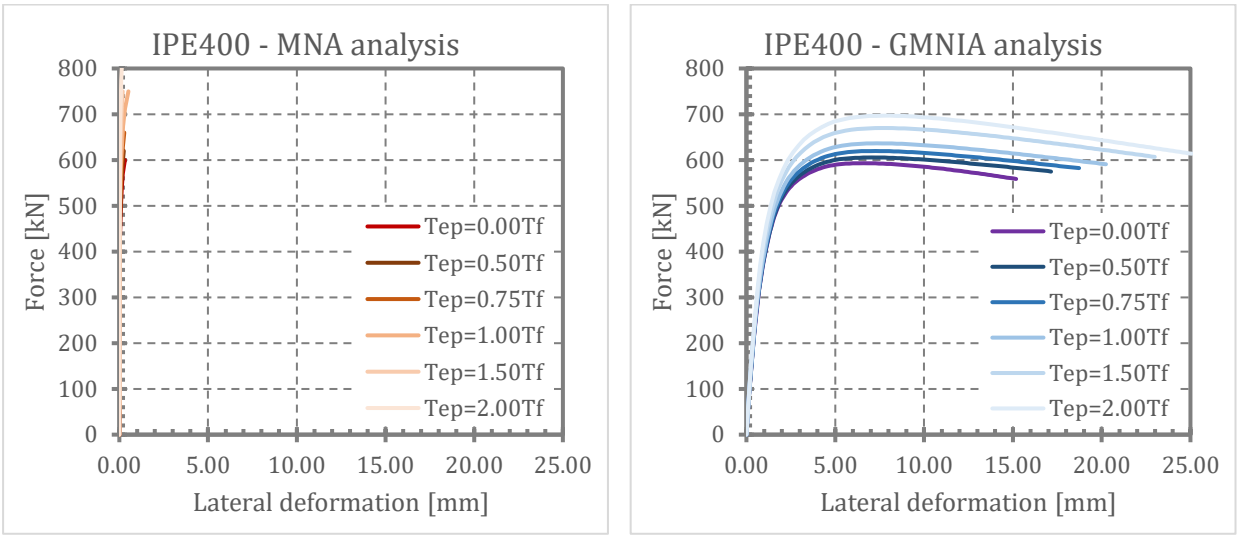


*Fig. 209 Influence of end-plate thickness – lateral deformation-force relationship*

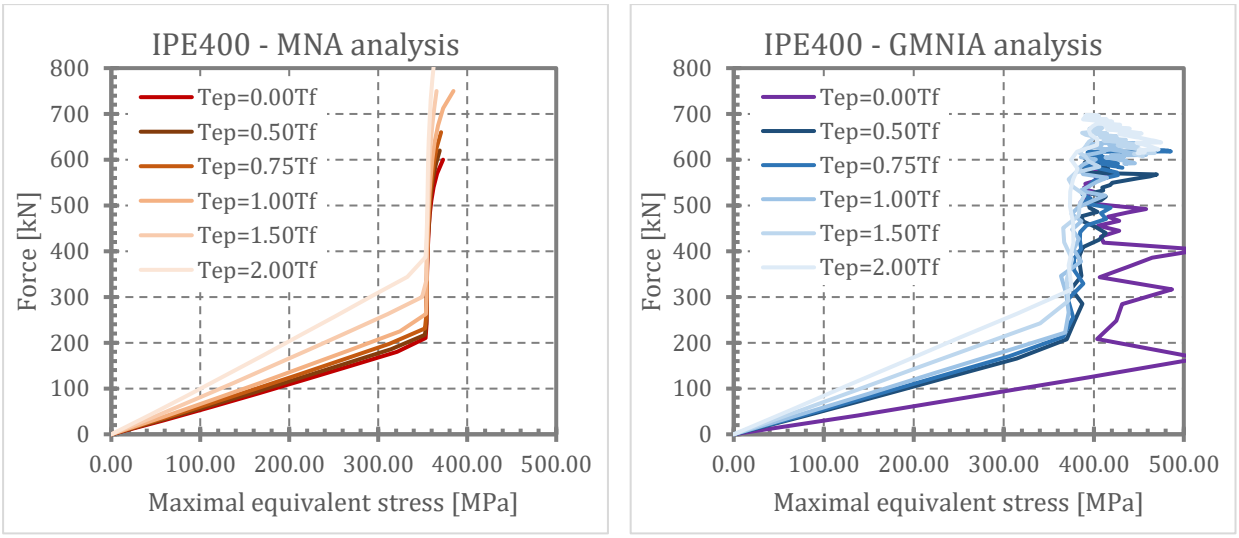


*Fig. 210 Influence of end-plate thickness – maximal equivalent stress-force relationship*

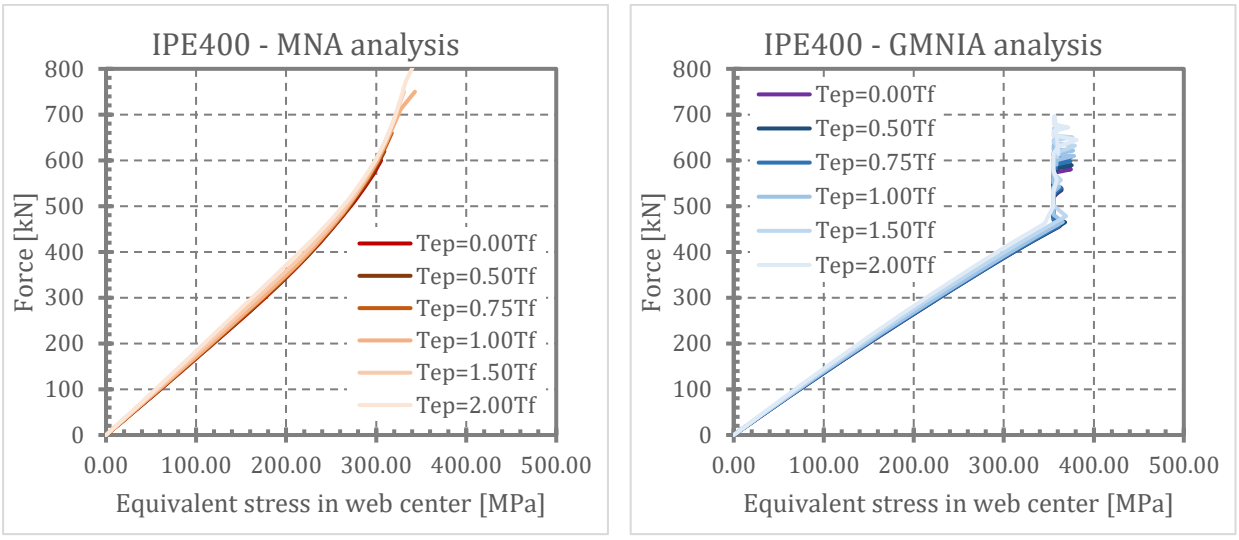


*Fig. 211 Influence of end-plate thickness – equivalent stress in web center-force relationship*

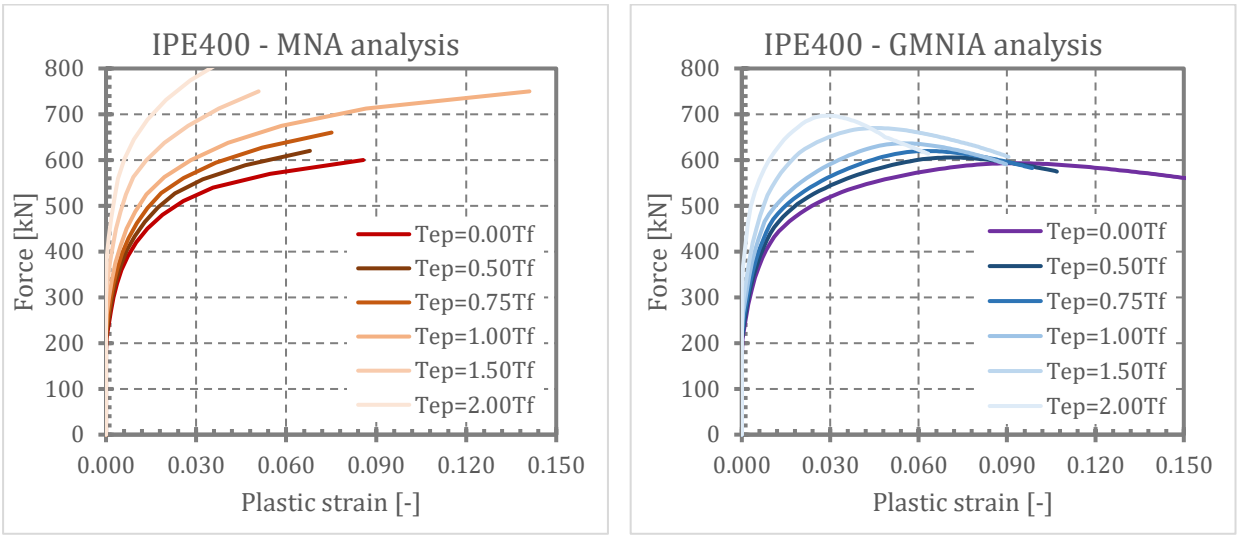


*Fig. 212 Influence of end-plate thickness – plastic strain-force relationship*

Fig. 213 to Fig. 220 show comparison of load-carrying capacities obtained from all investigated cases and by all used methods related to the ANSYS results (i.e. ANSYS results are equal to 1.0).

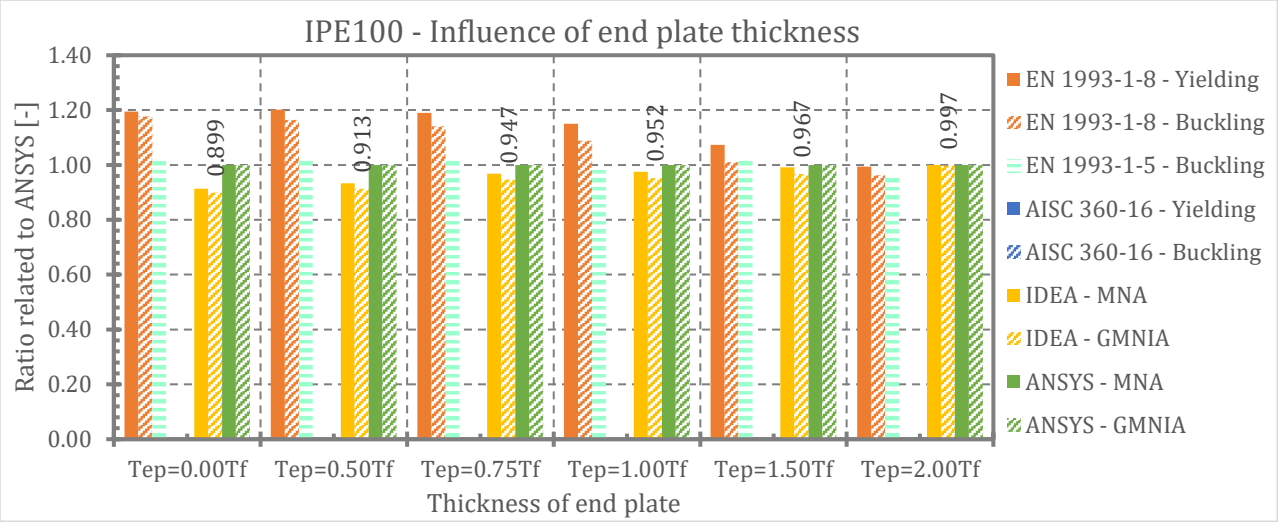


*Fig. 213 Influence of end-plate thickness – IPE 100 – comparison of Load-carrying capacity related to the ANSYS results*

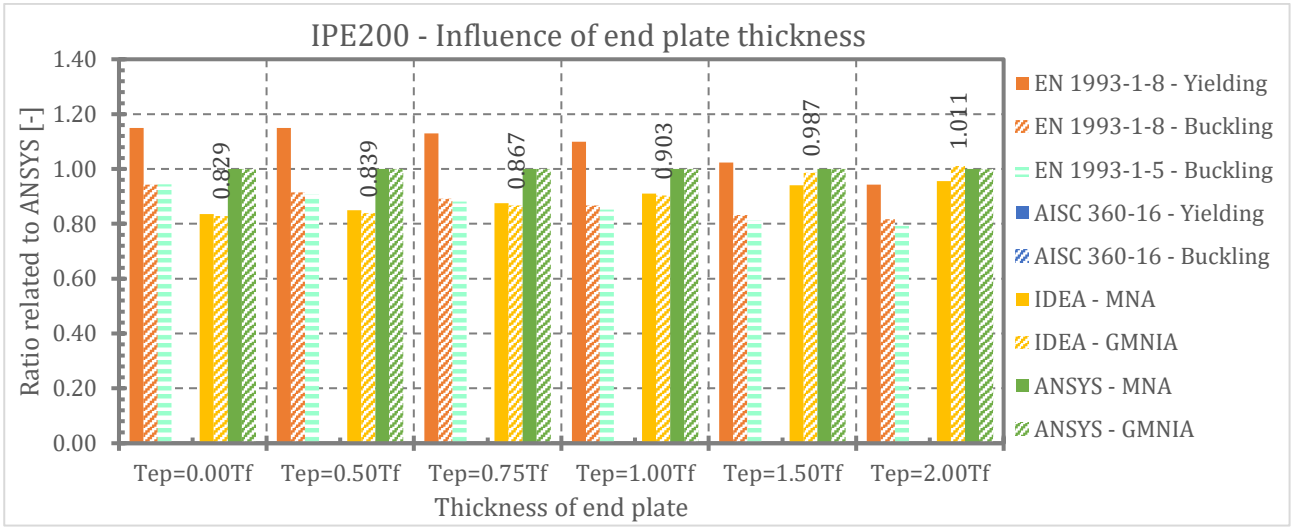


*Fig. 214 Influence of end-plate thickness – IPE 200 – comparison of load-carrying capacity related to the ANSYS results*

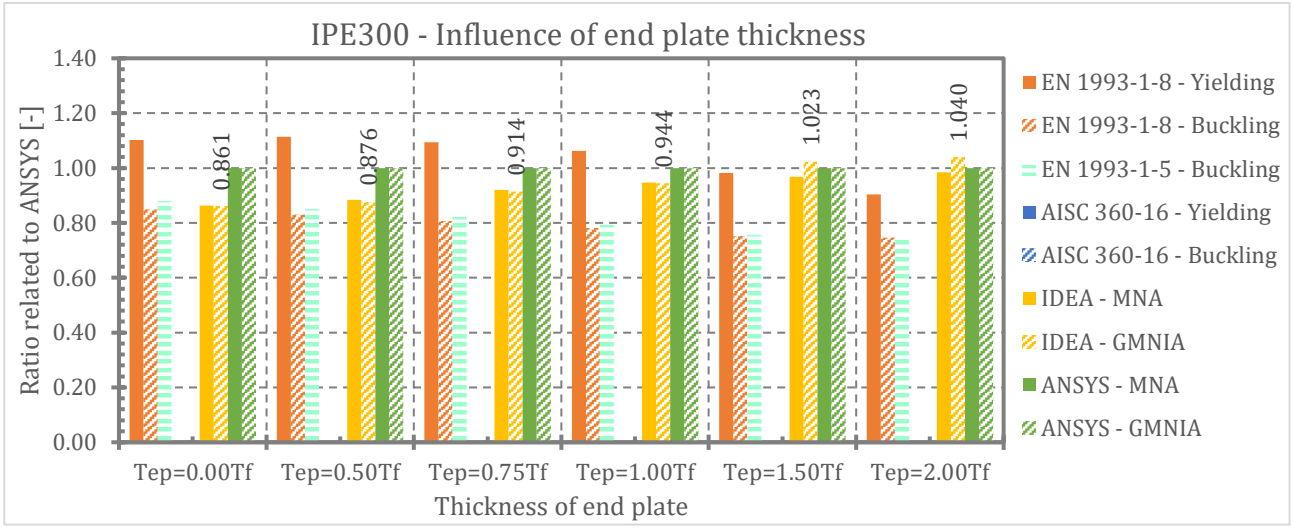


*Fig. 215 Influence of end-plate thickness – IPE 300 – comparison of load-carrying capacity related to the ANSYS results*

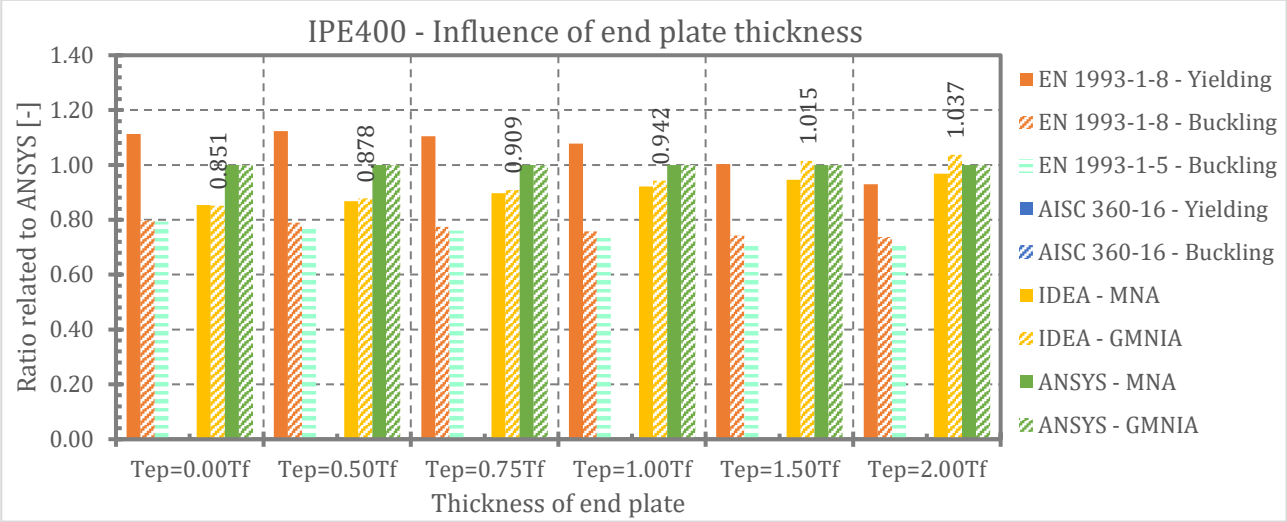


*Fig. 216 Influence of end-plate thickness – IPE 400 – comparison of load-carrying capacity related to the ANSYS results*

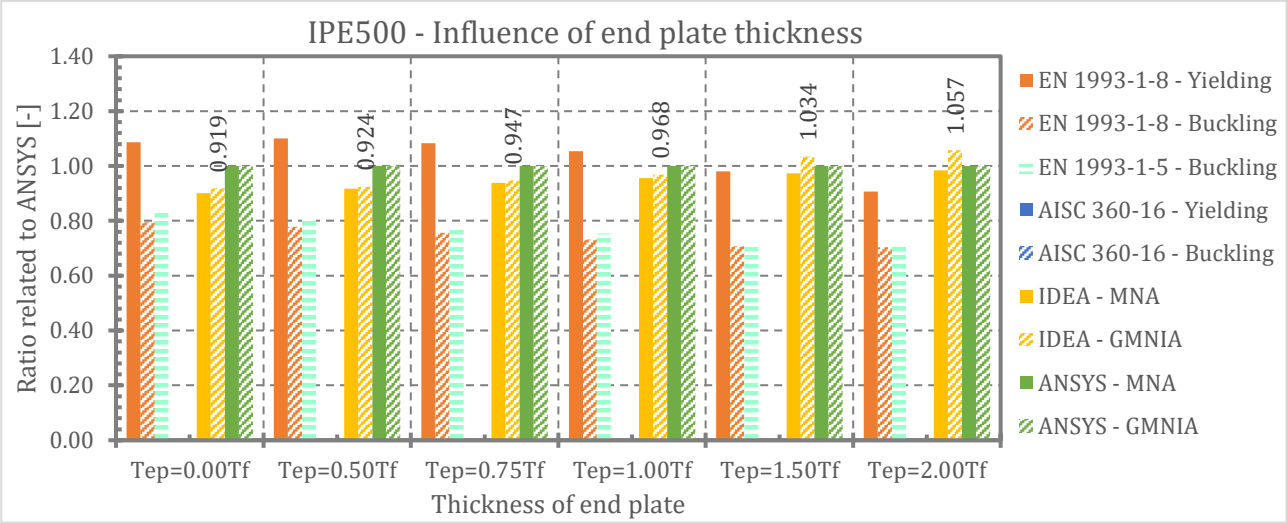


*Fig. 217 Influence of end-plate thickness – IPE 500 – comparison of load-carrying capacity related to the ANSYS results*

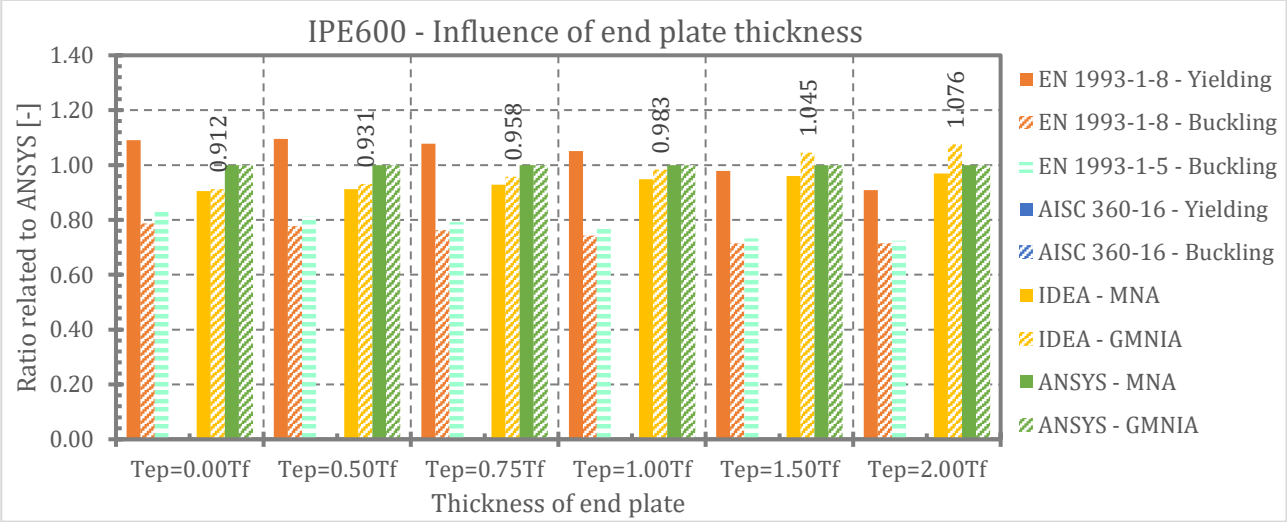


*Fig. 218 Influence of end-plate thickness – IPE 600 – comparison of load-carrying capacity related to the ANSYS results*

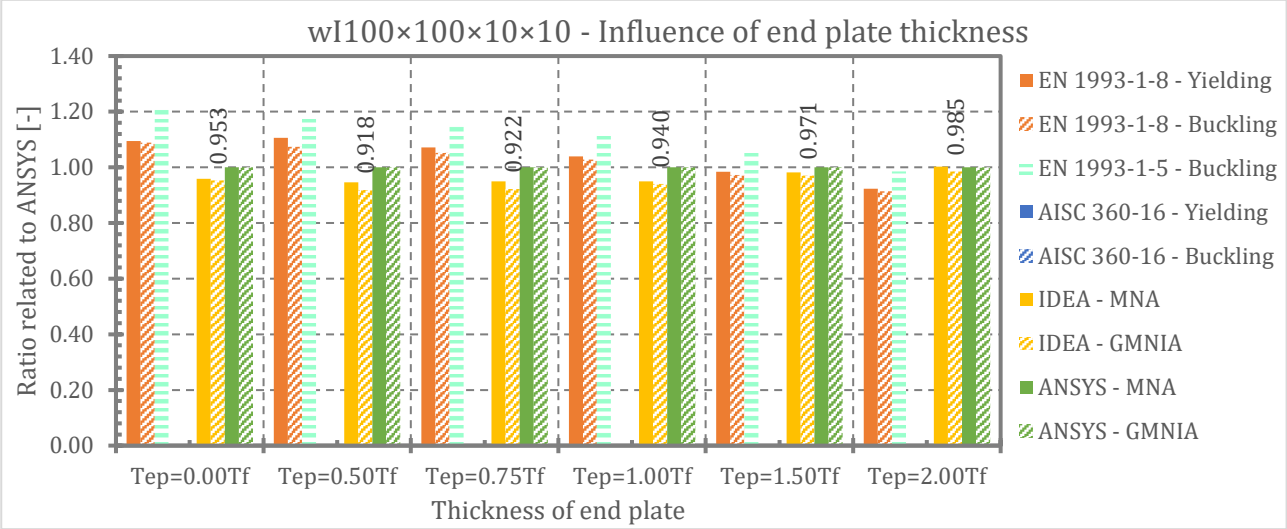


*Fig. 219 Influence of end-plate thickness – wI 100×100×10×10 – comparison of load-carrying capacity related to the ANSYS results*

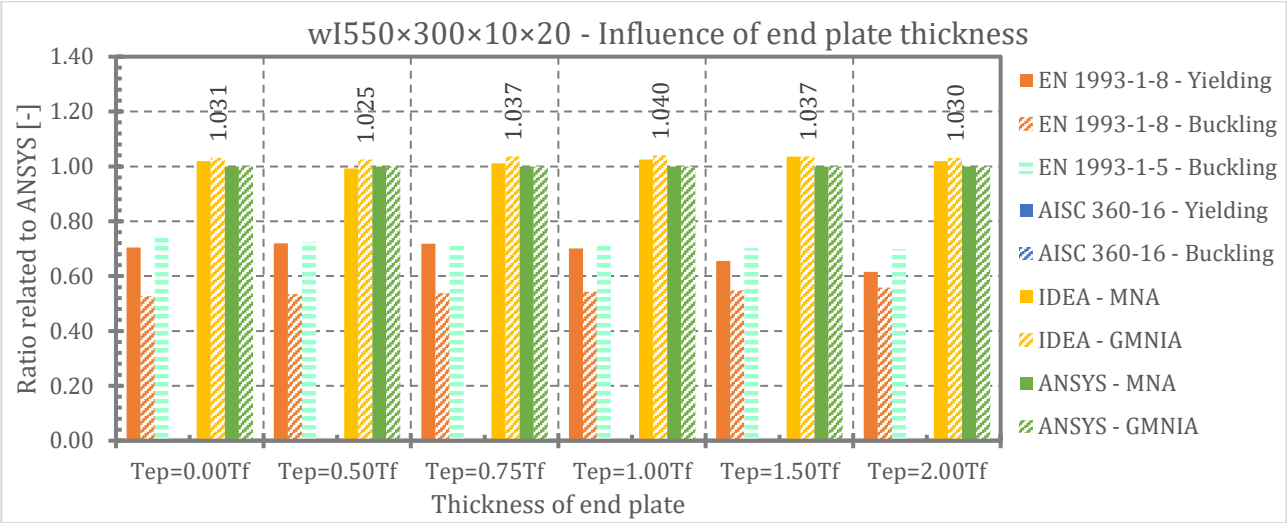


*Fig. 220 Influence of end-plate thickness – wI 550×300×10×20 – comparison of load-carrying capacity related to the ANSYS results*

### 4.7.3. Conclusion

As results of numerical simulations performed in IDEA StatiCa and ANSYS show, the thickness of the end-plate noticeably influences resistance of the member in transverse compression. Greater thickness of the end-plate results in higher resistance in transverse compression. In the design codes, it is generally assumed that the thickness of the end-plate influences certain breadth over which the transverse load is distributed to the member web and therefore the resistance is affected accordingly. The results obtained from the analysis are in compliance with this principle.

The results of the numerical analysis indicate that if the end-plate thickness is equal to the thickness of the member flange, the resistance is about 20% higher in comparison with the case with no end-plate for most investigated cases.

In some cases (especially smaller thicknesses of the end-plate) the codes EN 1993-1-8 and EN 1993-1-8 provide higher resistances than resistances obtained from the numerical analysis.

Comparison between results given by numerical simulations carried out in IDEA StatiCa and ANSYS software shows good agreement between the results. In most cases the resistances obtained from IDEA StatiCa are on the safe side except for some cases with relatively great thickness of the end-plate and for welded cross-section with relatively high slenderness. In the investigated cases (maximum end-plate thickness 2.00×$t_f$) the maximum difference was approximately 8%.

## 4.8. Transverse load at one flange

This part of study presents the influence of transverse load applied at one flange of the member. The goal is to evaluate actual behaviour and make comparison with design resistances according to the EN 1993-1-5 and AISC 360-16.

### 4.8.1. Methodology

The study was performed on transversally compressed member of rolled cross-sections IPE 100, 200, 300, 400, 500 and 600 and welded cross-sections wI 100×100×10×10 and wI 550×300×10×20 (section height × flange width × web thickness × flange thickness) with length on both side from loading plates $L = 2\times h$ (overall length is $L = 4\times h$). The member is made of structural steel S355. The imperfection amplitude for GMNIA was $d_w/200$, where $d_w$ is web height without rounded corners or fillet welds – see Fig. 4. Thickness of the loading plate is equal to thickness of the flange of the member. When the member is loaded only at one flange at mid-span and the supporting boundary conditions are as for simple beam, bending moment and resulting normal stresses due to bending are present in the analysed member. To eliminate the effect of bending the end-moments were applied on both ends of the member. The magnitudes of end-moments were equal to bending moment due to transverse load at mid-span, therefore the normal stress at mid-span is equal to zero. The members were analysed using MNA, LBA and GMNIA in IDEA StatiCa and ANSYS. Load-carrying capacity was calculated according to the codes EN 1993-1-5 and AISC 360-16 for local web crippling. EN 1993-1-8 does not specify a calculation procedure applicable for this problem. Analysed member is illustrated in Fig. 231.

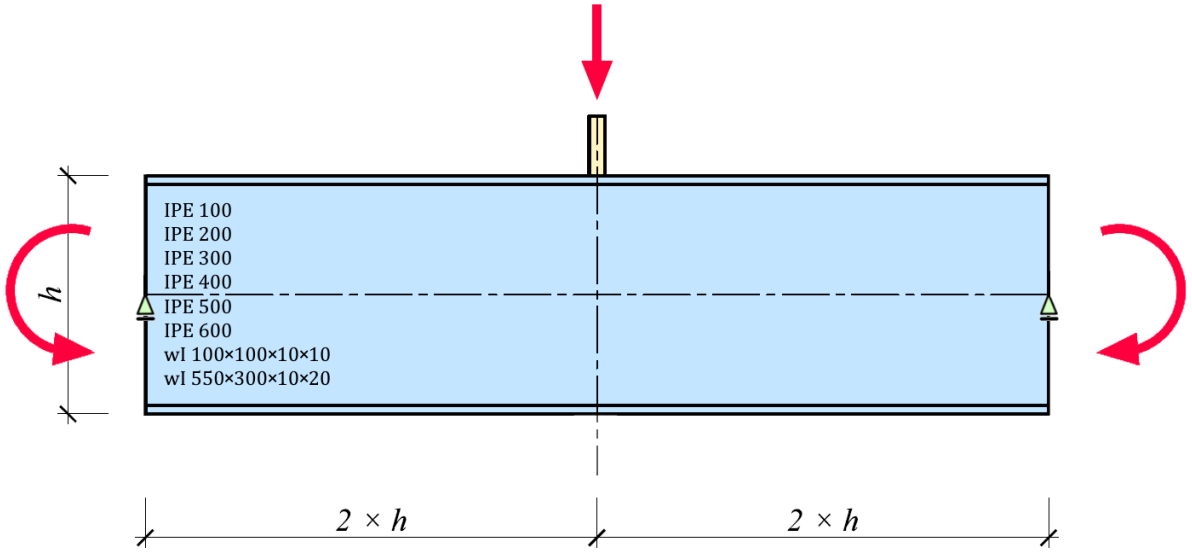


*Fig. 221 Influence of transverse load at one flange – geometry amd boundary conditions*

### 4.8.2. Results

Calculated load-carrying capacities are listed in Tab. 37 for all used methods for transversally compressed members of rolled sections and welded sections (in case of AISC 360-16, unfactored values of resistances are listed).

*Tab. 37 Influence of transverse load at one flange - Load-carrying capacity [kN]*

| Section | EN 1993-1-5 | AISC 360-16 | IDEA StatiCa | | ANSYS | |
|---|---|---|---|---|---|---|
| | Buckling | Crippling | MNA | GMNIA | MNA | GMNIA |
| IPE100 | 85.66 | 151.19 | 89.80 | 89.80 | 90.67 | 90.93 |
| IPE200 | 193.51 | 285.07 | 180.00 | 176.00 | 206.62 | 210.38 |
| IPE300 | 384.41 | 452.18 | 320.00 | 320.00 | 347.51 | 350.28 |
| IPE400 | 552.23 | 673.02 | 500.00 | 500.00 | 559.65 | 570.00 |
| IPE500 | 757.22 | 944.05 | 711.00 | 711.00 | 739.69 | 740.00 |
| IPE600 | 1037.13 | 1311.3 | 980.00 | 980.00 | 1008.7 | 1010.93 |
| wI 100×100×10×10 | 331.02 | 897.96 | 305.00 | 305.00 | 272.45 | 274.66 |
| wI 550×300×10×20 | 804.64 | 1014.5 | 934.00 | 930.00 | 906.46 | 950.00 |

Load–carrying capacities are graphically displayed in Fig. 222 for all used methods for transversally compressed members of rolled sections and welded sections.

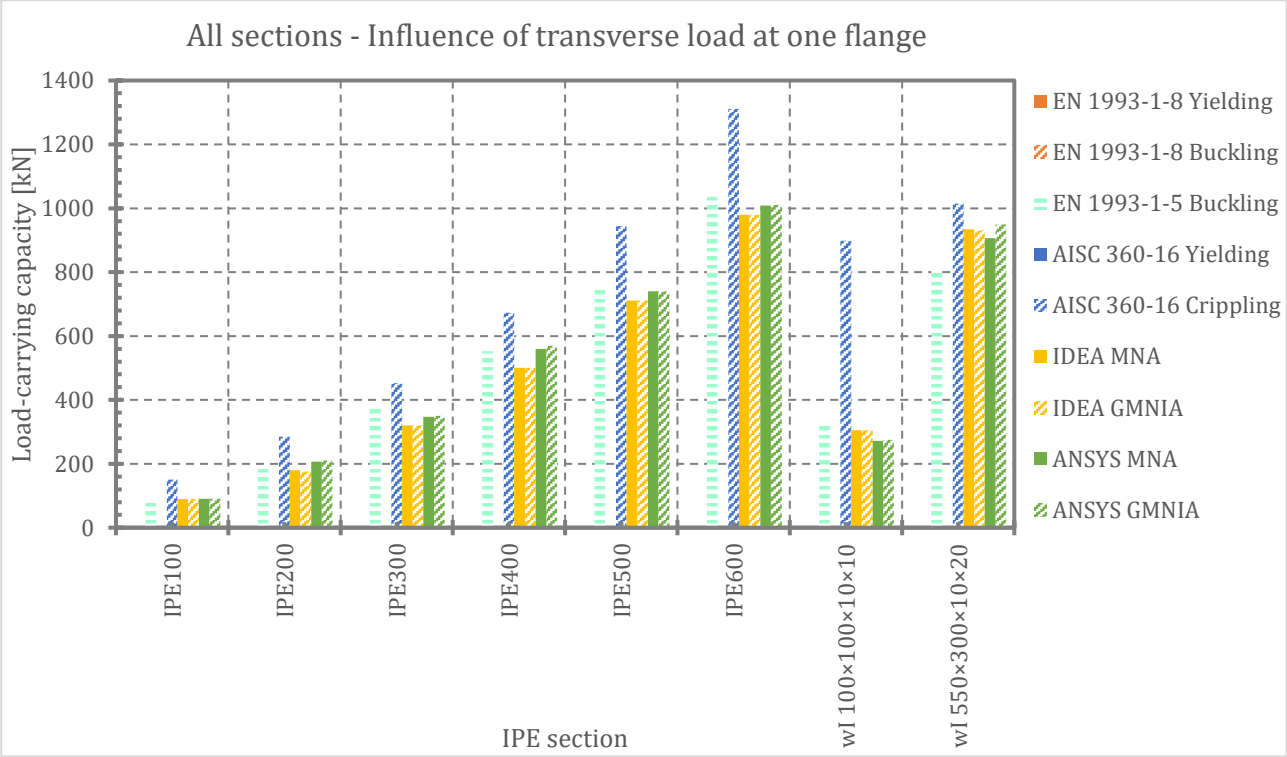


*Fig. 222 Influence of transverse load at one flange – Load-carrying capacity*

Influence of buckling on load-carrying capacity is clearly shown in Fig. 223 where ratio of load-carrying capacities resulting from Buckling/Yielding resistances according to the EN 1993-1-5 or GMNIA/MNA resulting from numerical analysis performed in IDEA StatiCa and ANSYS are on vertical axis.

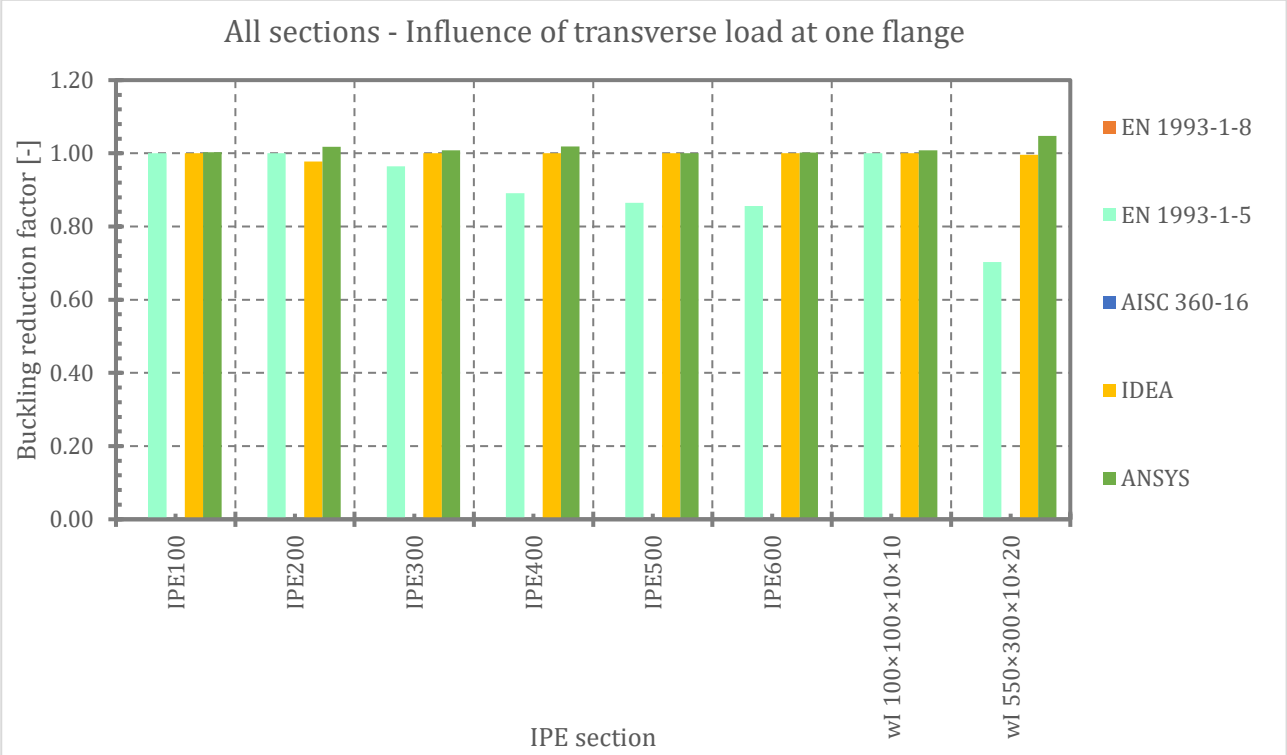


*Fig. 223 Influence of transverse load at one flange – reduction due to geometrical nonlinearity*

Fig. 224 shows results of linear buckling analysis – critical forces $F_{cr}$ [kN] and critical load factor $\alpha_{cr}$ [-]. The critical force is increasing with increasing IPE section. Critical load factor decreases with increasing IPE section.

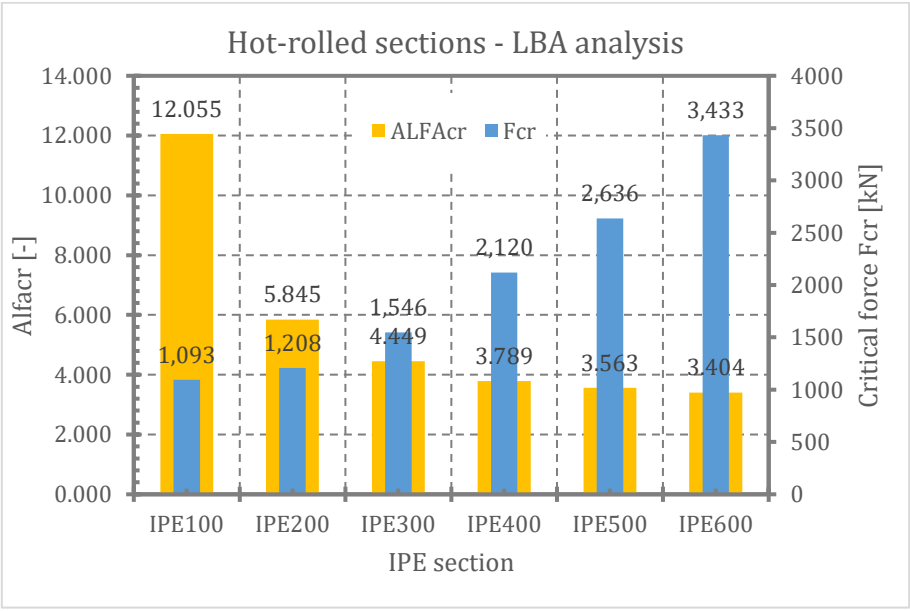


*Fig. 224 Influence of transverse load at one flange – LBA results*

Behaviour of members in transverse compression applied only at one flange is displayed in Fig. 225 to Fig. 229 for illustration for members of IPE cross sections.

Fig. 225 illustrates relationship of vertical deformation and loading force for MNA and GMNIA. Fig. 226 describes relationship between lateral deformation in the middle of beam web and loading force for MNA and GMNIA. Dependency of maximal equivalent stress and equivalent

stress in the middle of member web on loading force is plotted in Fig. 227 and Fig. 228. Fig. 229 shows developing of plastic strain with increasing load.

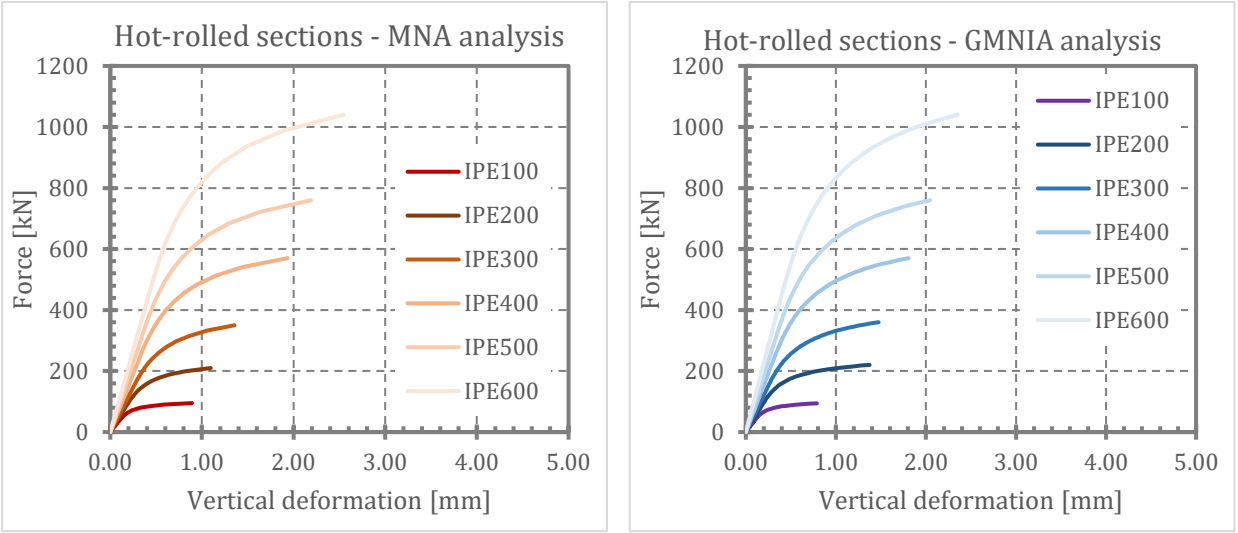


*Fig. 225 Influence of transverse load at one flange – vertical deformation-force relationship*

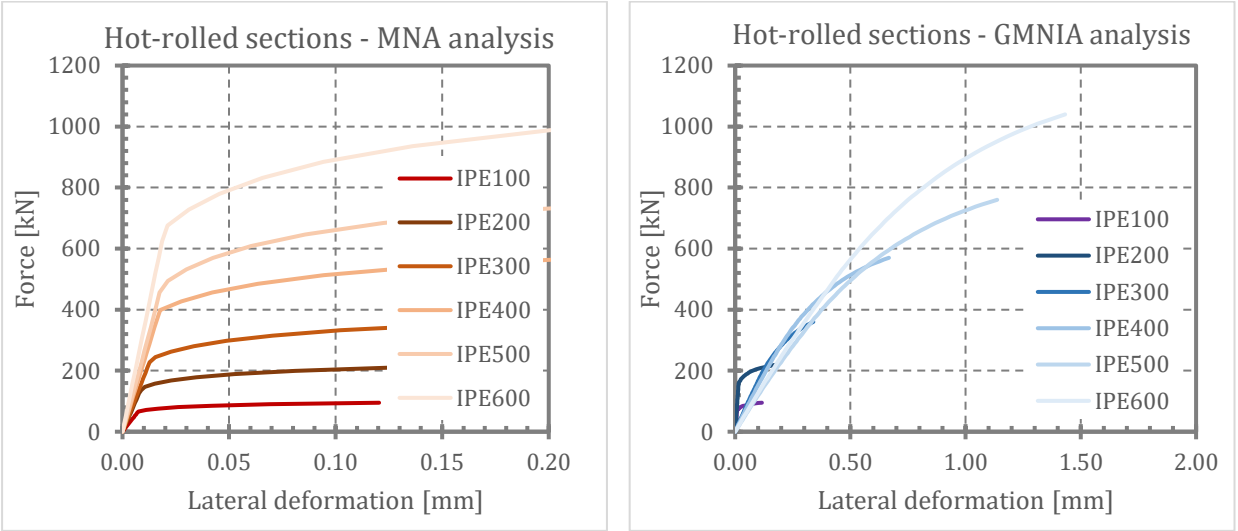


*Fig. 226 Influence of transverse load at one flange – lateral deformation-force relationship*

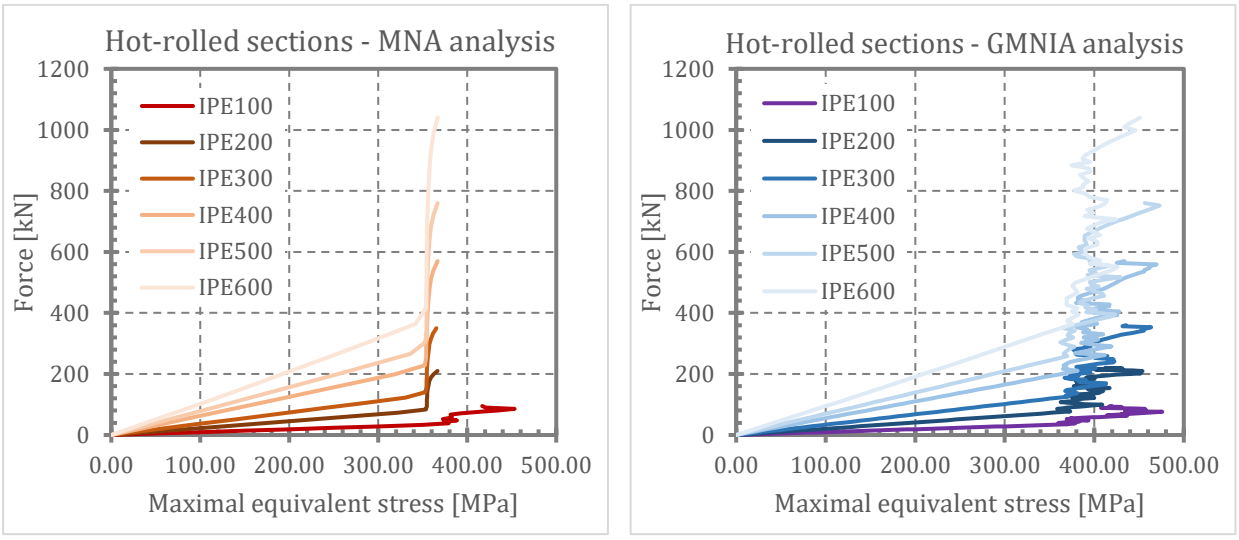


*Fig. 227 Influence of transverse load at one flange – maximal equivalent stress-force relationship*

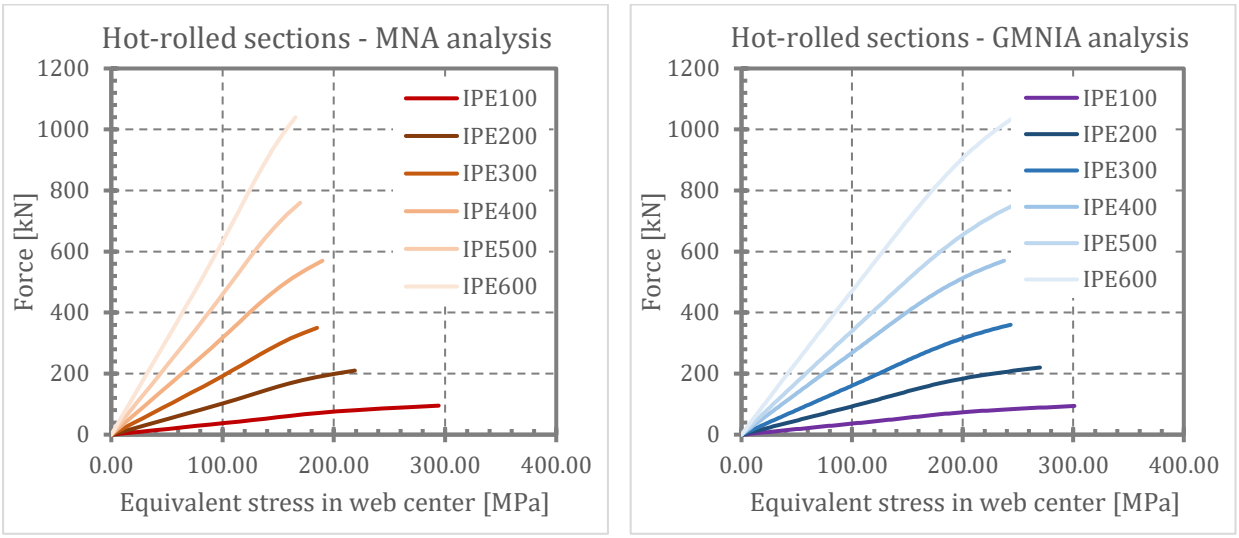


*Fig. 228 Influence of transverse load at one flange – equivalent stress in web center-force relationship*

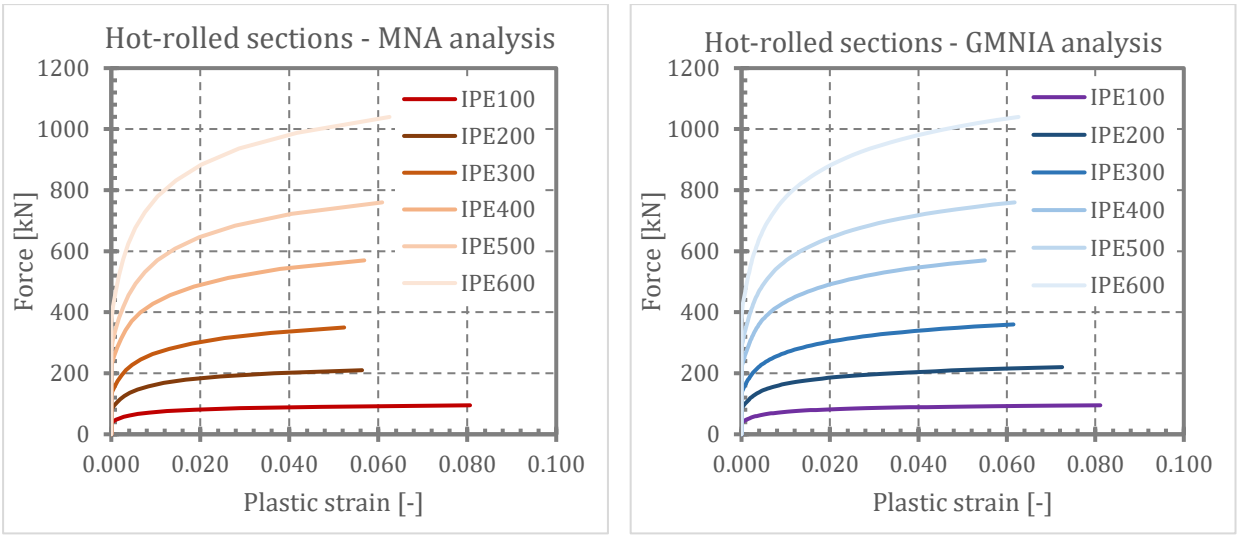


*Fig. 229 Influence of transverse load at one flange – plastic strain-force relationship*

Fig. 230 shows comparison of load-carrying capacities obtained from all investigated cases and by all used methods related to the ANSYS results (i.e. ANSYS results are equal to 1.0).

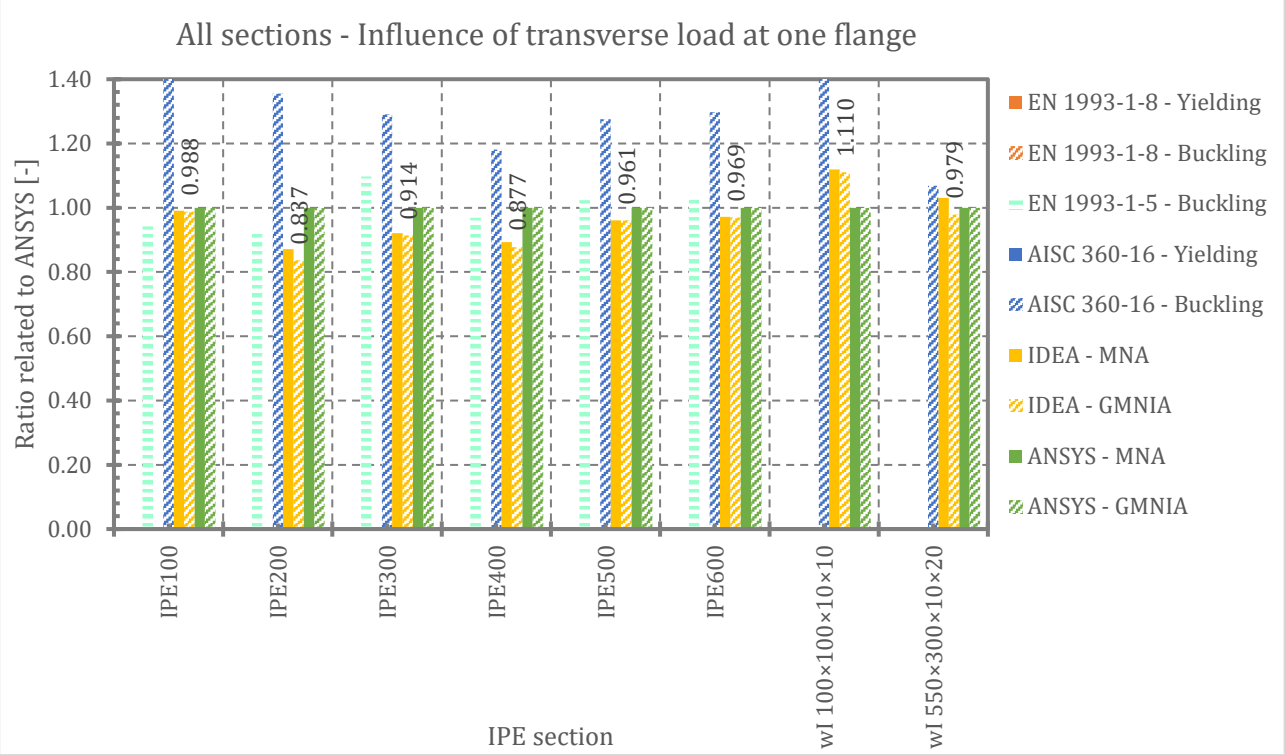


*Fig. 230 Influence of transverse load at one flange – comparison of Load-carrying capacity related to the ANSYS results*

### 4.8.3. Conclusion

The results of numerical analyses of members with transverse load applied at one flange only were, where possible, compared with results obtained from design codes calculations. This specific case of transverse compression is covered by EN 1993-1-5 and AISC 360-16 design codes. Relatively good agreement with results of numerical analysis was observed in case of EN 1993-1-5.

In case of rolled cross-sections investigated in the frame of this study the results obtained from IDEA StatiCa seem to be on the safe side. Differences on the unsafe side were found in case of welded cross-sections where for the section with relatively small slenderness of the web this difference was approx. 11%.

## 5. Statistical evaluation

Resistances of the cross-sections to transverse compression resulting from the numerical analyses listed in the previous chapters were in relevant cases summarized and statistically evaluated to quantify basic statistical parameters. Following cases investigated in this report were included in the statistical evaluation: influence of the yield strength, influence of the thickness of the loading plate, members subjected to transverse load at their mid-span only, members subjected to transverse load close to the unstiffened end, members subjected to transverse and axial load, members subjected to transverse load through end-plates at both flanges and members subjected to transverse load at one flange. The evaluation was based on

ratios between the resistances obtained from IDEA StatiCa and resistances obtained from ANSYS ($F_{R,IDEA}/F_{R,ANSYS}$). These ratios were calculated for all the above mentioned cases separately for MNA and for GMNIA analysis. Each group (MNA, GMNIA) consisted of 155 values to be evaluated. Results of this evaluation are listed in Tab. 38.

*Tab. 38 Summarization of the statistical evaluation – resistances*

| Parameter | Analysis | |
|---|---|---|
| | MNA | GMNIA |
| Minimum | 0.83 | 0.83 |
| Maximum | 1.15 | 1.40 |
| Average value | 0.98 | 0.98 |
| Standard deviation | 0.08 | 0.08 |

The resistances obtained from the numerical analyses are displayed in the graphical form in Fig. 231 (MNA) and Fig. 232 (GMNIA). The dashed red lines in the charts indicate levels of 10% deviation (positive and negative) from the theoretical full agreement (solid red line), i.e. the points representing the resistance ratios situated within the dashed lines are within these limits.

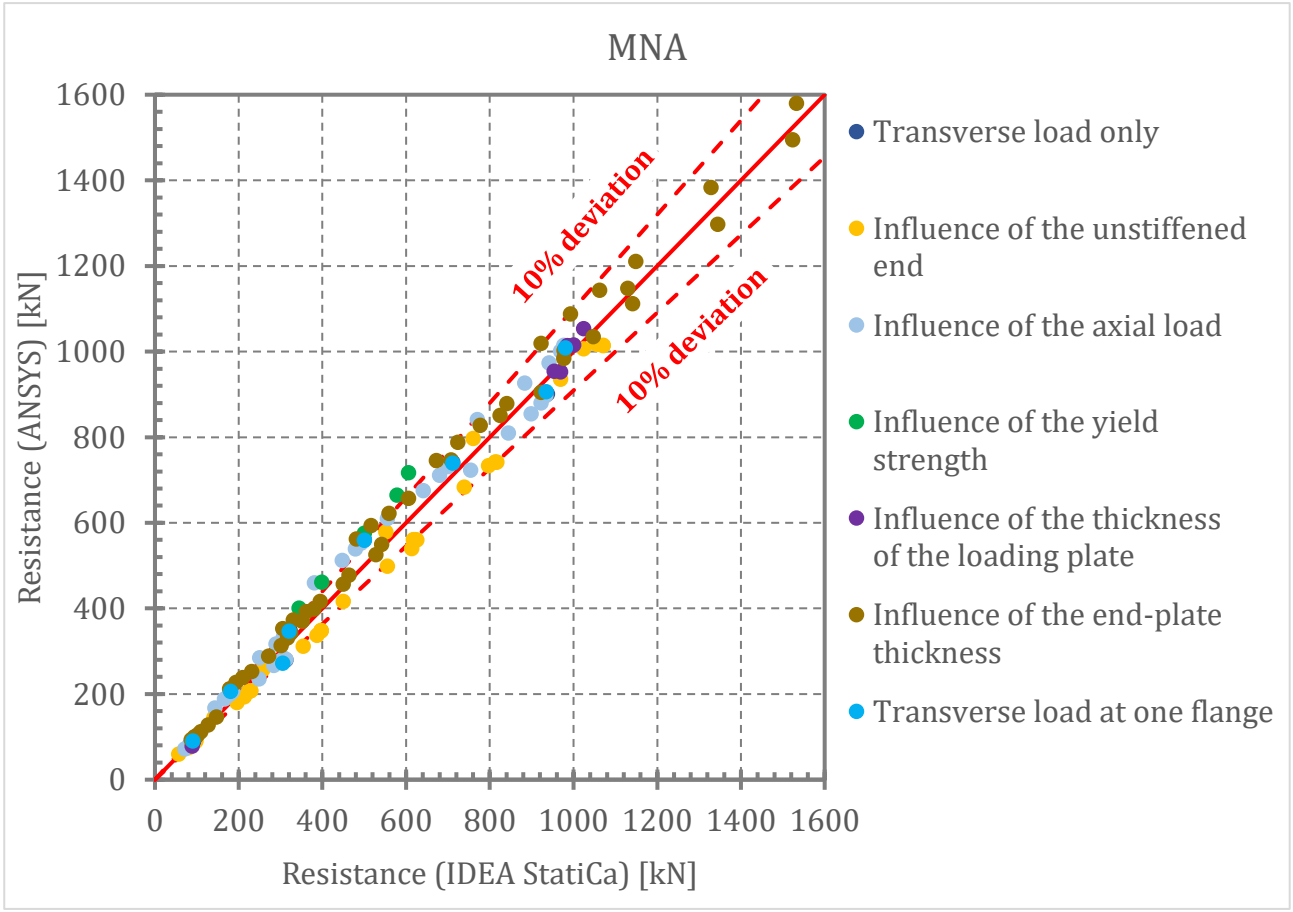


*Fig. 231 Summarization of results – MNA*

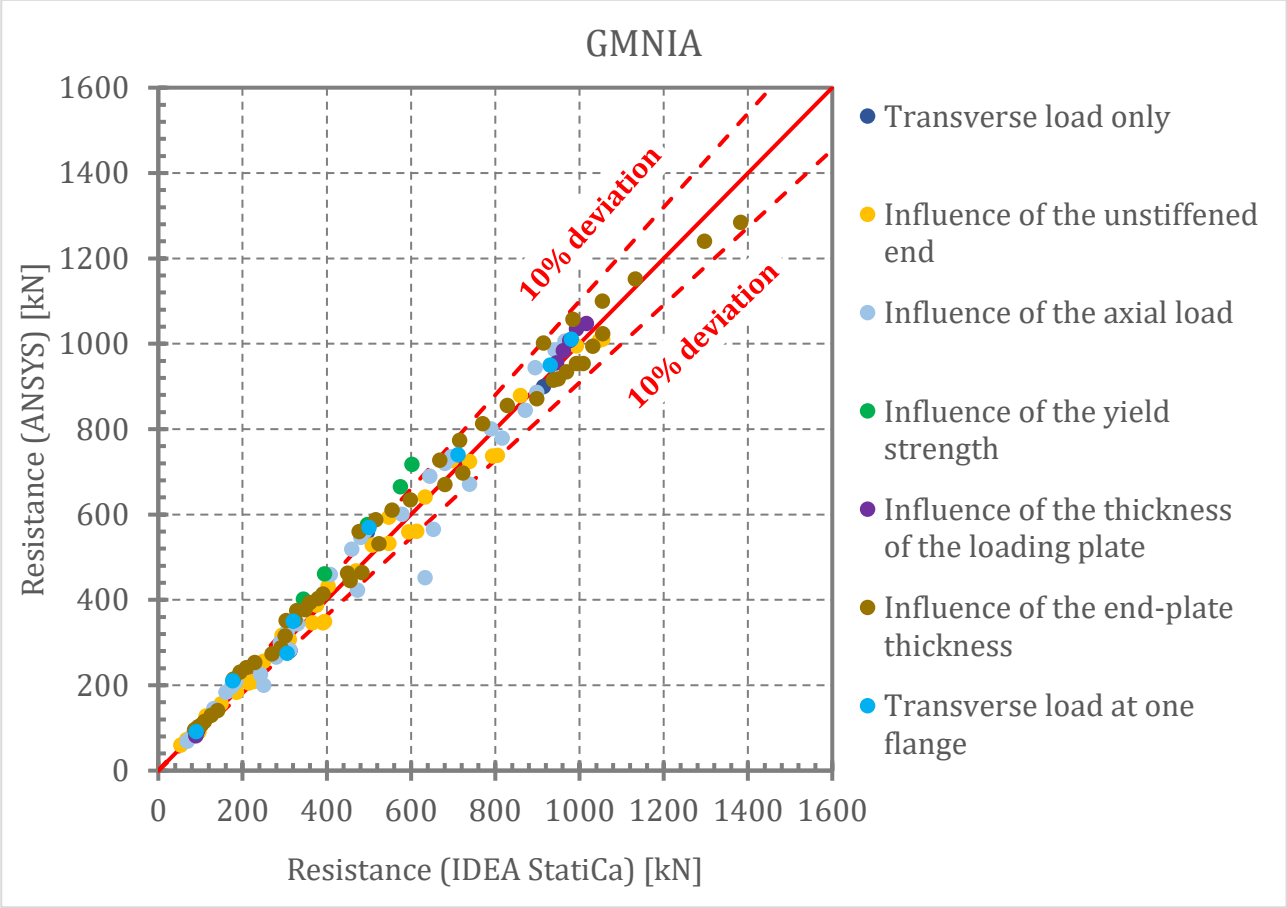


*Fig. 232 Summarization of results – GMNIA*

The results of statistical evaluation for critical loads are listed in Tab. 39.

*Tab. 39 Summarization of the statistical evaluation – critical loads*

| Parameter | Analysis |
|---|---|
| | LBA |
| Minimum | 0.68 |
| Maximum | 1.55 |
| Average value | 1.06 |
| Standard deviation | 0.21 |

## 6. Critical load factor to neglect geometrically nonlinear effects

The results obtained from IDEA StatiCa were evaluated to determine minimum critical load factor for which the effects resulting from geometrical nonlinearity could be neglected (i.e. GMNIA could be omitted). Critical load factor based on results of the numerical analysis in IDEA StatiCa determined using equation (20) and ratio of GMNIA and MNA resistance (which can be considered as level of reduction due to buckling) given as equation (21) were used.

$$\alpha_{cr} = \frac{F_{cr}}{F_{R,MNA}} \tag{20}$$

$$\rho_{FEA} = \frac{F_{R,GMNIA}}{F_{R,MNA}} \tag{21}$$

Considering a group of results for which the factor $\rho_{FEA}$ is equal or higher than specified value, it is possible to quantify the number of models (out of that group) with equal or higher value of the factor $\alpha_{cr}$. For this evaluation, the level of reduction $\rho_{FEA}$ was considered as 0.95 (this value is assumed to be sufficiently and acceptably high, i.e. the reduction due to buckling does not exceed 5%). Allowing max. 5% of models with lower value of $\rho_{FEA}$, the respective minimum $\alpha_{cr}$ factor was determined to be equal to 3. The respective value of relative slenderness is plotted in Fig. 233 and Fig. 234. These charts summarize the results of numerical analyses in form of the numerically determined relative slenderness given as equation (22) and respective buckling reduction factor given as equation (21).

$$\bar{\lambda} = \sqrt{\frac{F_{R,MNA}}{F_{cr}}} \tag{22}$$

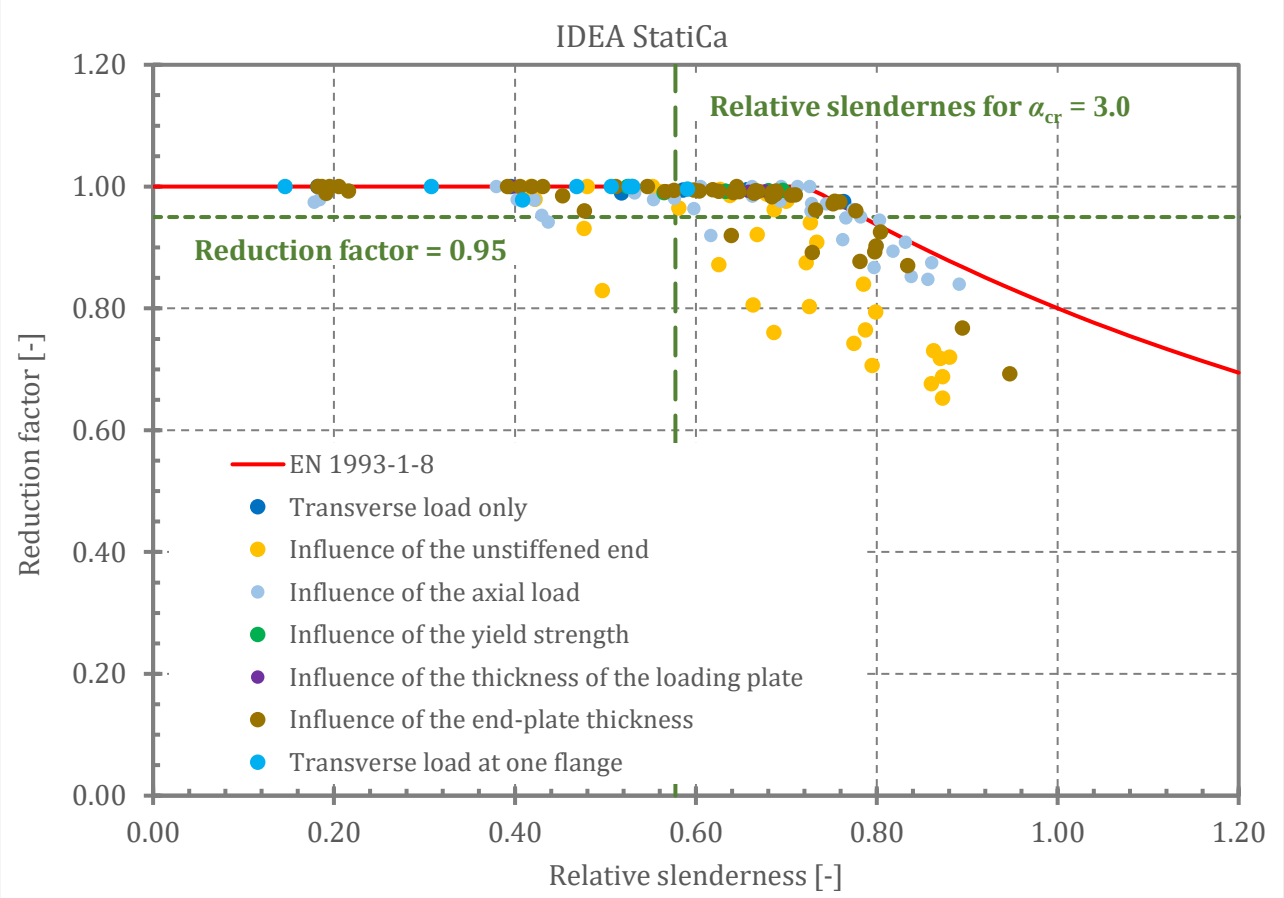


*Fig. 233 Relative slenderness and reduction factor – IDEA StatiCa*

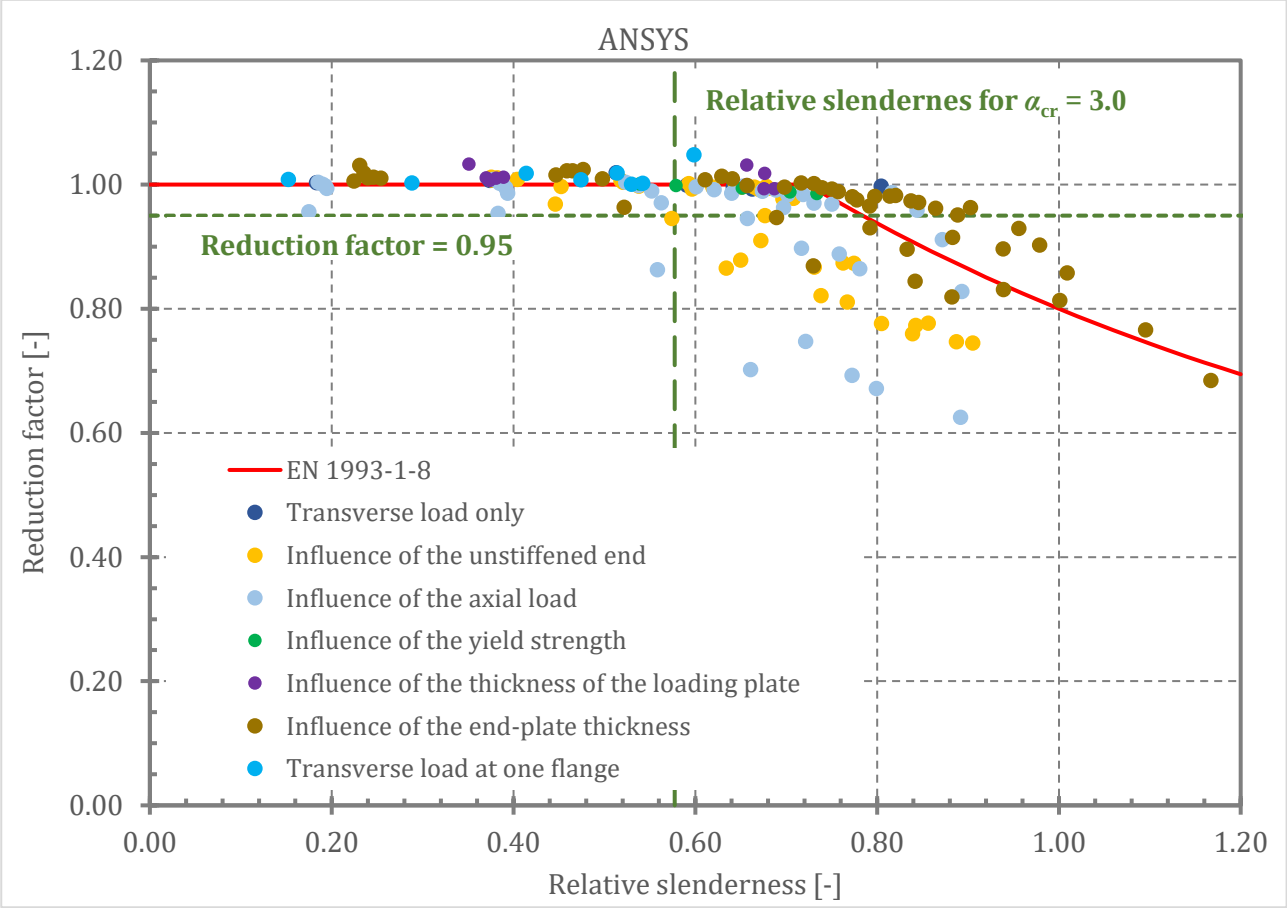


*Fig. 234 Relative slenderness and reduction factor – ANSYS*

In Fig. 235 and Fig. 236 percentages of cases (numerical models) for specific critical load factor and selected values of reduction factors are plotted.

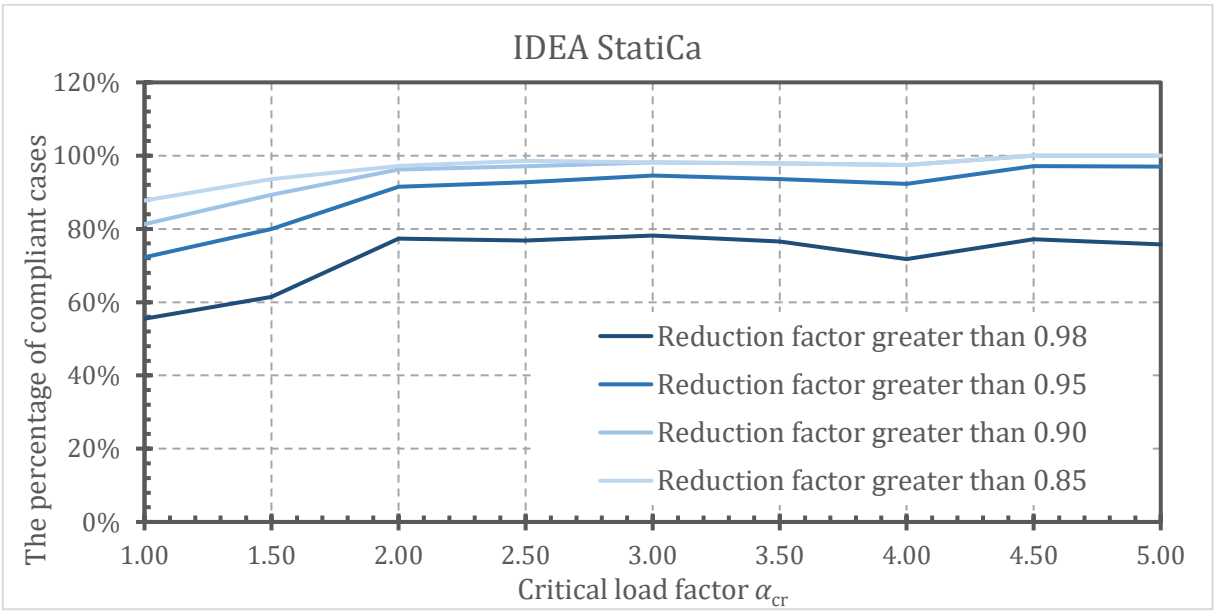


*Fig. 235 Percentage of cases for specific critical load factor and reduction factor – IDEA StatiCa*

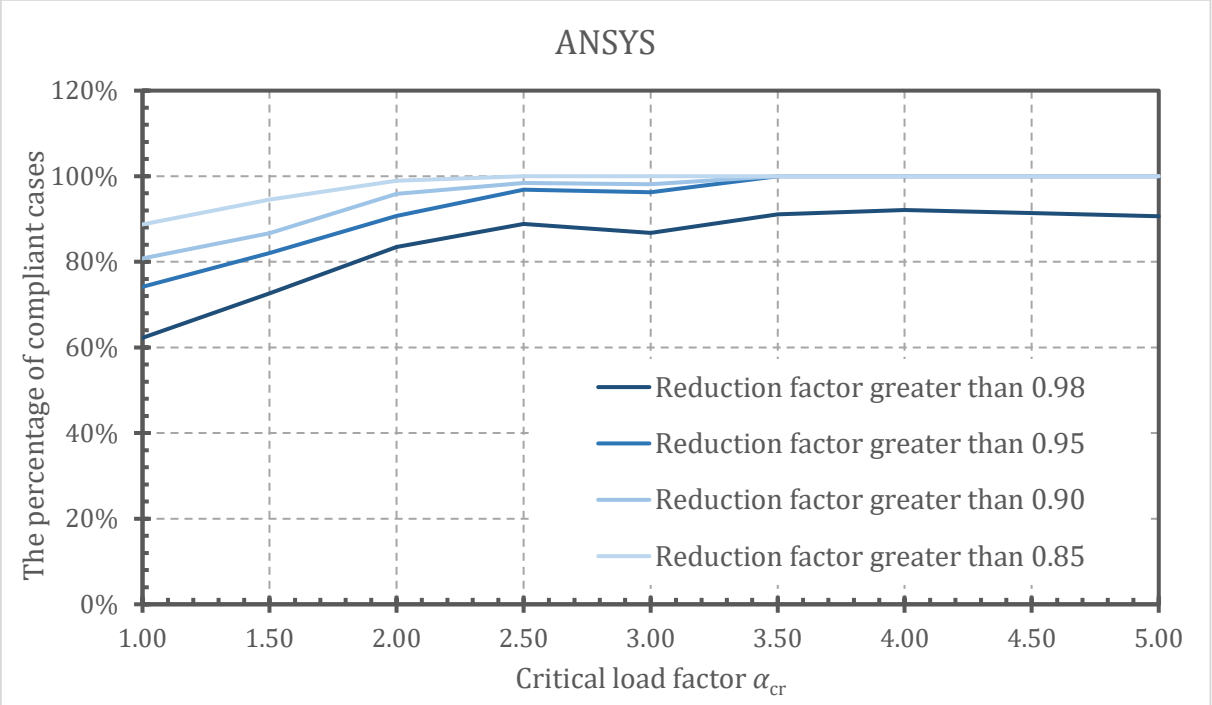


*Fig. 236 Percentage of cases for specific critical load factor and reduction factor – ANSYS*

## 7. Conclusions

Partial conclusions for investigated input parameters influencing resistance in transversal compression force subjected member made of hot-rolled or welded I-section or H-section are mentioned in the relevant chapters.

Main conclusion is that IDEA StatiCa provides (in most cases) very good agreement (from the point of view of resistance of modelled members – load-carrying capacities) with ANSYS software, whereas modelling steel structures and joints in IDEA is more usable, and computing time is much lower. On the other hand, sometimes it might seem on the unsafe side in comparison with resistances calculated according to the design standards EN 1993-1-5, EN 1993-1-8 and AISC 360-16, but this might be caused by low accuracy of proposed calculation procedures, from which lower resistances than from precise numerical simulations carried out in ANSYS software (with exception of basic cases) are resulting. In addition, design codes mentioned above do not offer calculation procedure for determination of design resistance for all cases which are common in praxis.

## References

[1] EN 1990 ed. 2 Eurocode: Basis of structural design. Brusseles: European Committee for Standardization, 2021.

[2] EN 1993-1-5 ed. 3 Eurocode 3: Design of steel structures – Part 1-5: Plated structural elements. Brusseles: European Committee for Standardization, 2020.

[3] EN 1993-1-8 ed. 2 Eurocode 3: Design of steel structures – Part 1-8: Design of Joints. Brusseles: European Committee for Standardization, 2013.

[4] EN 1993-6 Eurocode 3: Design of steel structures – Part 6: Crane supporting structures. Brusseles: European Committee for Standardization, 2008.

[5] ANSI/AISC 360-16 Specification for Structural Steel Buildings (American Institute of Steel Construction, Chicago, 2016).

[6] Commentary on ANSI/AISC 360-16 Specification for Structural Steel Buildings (American Institute of Steel Construction, Chicago, 2016).

[7] IDEA StatiCa®, Release 21.1.

[8] ANSYS® Multiphysics, Release 19.2.

Brno, June 3, 2022

**Ing. Ondřej Pešek, Ph.D.**

Main researcher

**Ing. Ivan Balázs, Ph.D.**

Co-researcher

**Ing. Martin Horáček, Ph.D.**

Co-researcher